PHOSPHA-ADAMANTANES: A NEW CLASS OF BULKY ALKYL PHOSPHINE LIGANDS

by

Robert Ian Pugh

A thesis submitted to the University of Bristol in accordance with the requirements for the degree of Doctor of Philosophy in the School of Chemistry, Faculty of Science.

April 2000

Abstract

The new cage phosphines 1,3-trifluoromethyl-5,7-methyl-4,6,8-trioxa-2-phenyl-2-phospha-adamantane and 1,3,5,7-tetramethyl-4,6,8-trioxa-2-isopropyl-2-phospha-adamantane have been synthesised. These ligands were complexed to platinum(II), palladium(II) and rhodium(I) to give species of the general formula *trans*-$[MCl_2(P)_2]$ (M – Pt or Pd) and *trans*-$[RhCl(CO)(P)_2]$ respectively. The cone angle of the trifluoromethyl cage ligand (167 °) was measured from the *X*-ray crystal structure of its palladium dichloride complex. 1,3,5,7-tetramethyl-4,6,8-trioxa-2-cyclohexyl-2-phospha-adamantane has been complexed to palladium(II) and platinum(II) to give the complexes *trans*-$[MCl_2(P)_2]$, whose *X*-ray crystal structures yielded an estimated cone angle of 180° for this ligand. The phosphines 2-chloro- and 2-bromo-1,3,5,7-tetramethyl-4,6,8-trioxa-2-phospha-adamantane were synthesised, and the phosphonium salt [1,3,5,7-tetramethyl-4,6,8-trioxa-2-phospha-*o*-xylene][BPh_4] fully characterised.

The diphosphines *meso/rac*-1,1'-bis(phospha-adamantyl)ferrocene and *meso/rac*-bis(phospha-adamantyl)-*o*-xylene have been prepared. These gave chelates of general formula $[PtCl_2(P\text{-}P)]$. Reaction of these ligands with palladium(II) gave chelates $[PdCl_2(P\text{-}P)]$ and oligomeric complexes. The separation of diastereomers *meso*- and *rac*-1,3-bis(phospha-adamantyl)propane was achieved. Resolution of the enantiomers of the *rac*-diastereomer with chiral palladium complexes was demonstrated by TLC.

The new diphospha-cages 1,2-(1,3,5,7-tetramethyl-6,8-dioxa-2,4-diphospha-adamantyl)benzene, 1,1'-(1,3,5,7-tetramethyl-6,8-dioxa-2,4-diphospha-adamantyl)-ferrocene, 1,3,5,7-tetramethyl-6,8-dioxa-2,4-diphospha-adamantyl-*o*-xylene and 1,8-(1,3,5,7-tetramethyl-6,8-dioxa-2,4-diphospha-adamantyl)methylnaphthalene have been synthesised. The first one reacted with two equivalents of gold(I) to give the first example of a binuclear gold complex $[(AuCl)_2(\mu\text{-}P\text{-}P)]$ with bridging diphospha-cage. The diphospha-cage 1,3,5,7-tetramethyl-4,6,8-trioxa-2,4-dicyclohexyl-2,4-diphospha-adamantane reacted with $[PtCl_2(cod)]$ to give a 4 membered chelate $[PtCl_2(P\text{-}P)]$.

The palladium(II)- and platinum(II)-catalysed carbonylation of olefins and acetylenes was compared with the diphosphines *meso*- and *rac*-enriched 1,3-bis(phospha-adamantyl)propane, *meso/rac*-1,1'-bis(phospha-adamantyl)ferrocene and *meso/rac*-1,2-bis(phospha-adamantyl)ethane. Palladium(II) complexes of these ligands catalyse the methoxycarbonylation of C_{11}/C_{12} internal olefins to linear esters, and the platinum(II) complex of *meso/rac*-1,3-bis(phospha-adamantyl)propane gives the highest activities to date for the Pt(II)-catalysed methoxycarbonylation of acetylene to methyl acrylate without tin chloride co-catalyst.

The stereoelectronics of the phospha-adamantane ligand have been investigated by *X*-ray crystallographic and IR studies. These show that the bulky rigid cage has a small C-P-C angle which confers π-acidity analogous to aryl phosphines.

This thesis is dedicated to my parents and sister
for their constant support,
and the memory of my Granddads.

Acknowledgements

The biggest thanks by far go to Paul Pringle. His enthusiasm, advice and ideas make him an exemplary boss - he is also a top bloke and very good friend.

I am indebted to Guy Orpen, Taya Phetmung, Charlie and Di Ellis for the crystal structure determinations (and cone angle calculations) and to Martin Murray for his NMR advice. Cheers to Adrian Stevenson and Tony Rogers for their assistance in synthetic matters and Andy Wood for carrying out the CV.

I am very grateful to Shell for financial support, and special thanks go to the inspirational Eite Drent for making my work in Amsterdam possible. I also appreciate the support and contributions of Jaqueline Suykerbuyk, Willem Jager, Pim Mul, Guido Batema (IR studies), Mike Doyle, Alexander van der Made (molecular modelling), J. F. K. Buijink and P. K. Maarson.

The Pringle lab have all made this work particularly pleasurable, especially Chris, Katie, Giles, E, Emily, Gayle, Charles, Shocker, Jim (Fleming and Dennett), Vicks, Gerry, Emma, Aina, Michael, Rich, Josie, Manuela, Liam and non-Prongles Carl, Sleggy and Elia. Cheers to all the people I've beaten at squash, and everyone I've played football with. Thanks also to Emma, Aina and Jim D for their thorough proof reading.

Entertaining extra-curricular activities have centred around various housemates over the last three and half years, namely Tom, Ceej, Emily, Fieldos, Parker, Filkin, Cove, Dunn, H, Lucy, Monkey, Greeves, Mark, Carter, Adkin and Muggz. Top Spot (by far the best snooker club in Bristol) has been a second home to me, mainly due to the green baize, Geoff, Mike, Dale, Shah, Matt, Mark, Neil, Greg, AP and Rob, among others. Finally I thank Ruth for her constant support and kindness.

Memorandum

The work described in this thesis was carried out at the University of Bristol between October 1996 and September 1999. Unless otherwise acknowledged in the text, it is the original work of the author and has not been submitted previously for a degree. In addition, any views expressed in this thesis are those of the author, and not of the University.

Robert Ian Pugh
University of Bristol
April 2000

Contents

Table of Contents

Chapter 1 Introduction

Chapter 2 Monodentate tetramethyl-trioxa-phospha-adamantanes

Appendices

Abbreviations

General

Ac		acetate
acac		acetylacetonato
BINAP		1,1'-bis(diphenylphosphino)binaphthalene
Bu^t		*tertiary*-Butyl
Cod		*cis,cis*-1,5-cyclooctadiene
CV		cyclic voltammogram
Cy		cyclohexyl
d		day(s)
dbpe		1,2-bis(di-*t*-butylphosphino)ethane
dbpp		1,3-bis(di-*t*-butylphosphino)propane
dbpf		1,1'-bis(di-*t*-butylphosphino)ferrocene
dcpe		1,2-bis(dicyclohexylphosphino)ethane
dcpp		1,3-bis(dicyclohexylphosphino)propane
dppf		1,1'-bis(diphenylphosphino)ferrocene
dppp		1,3-bis(diphenylphosphino)propane
EI		electron ionisation
equiv.		equivalents
Et		ethyl
FAB		fast atom bombardment
Fc		ferrocene
ΔG		Gibbs Free Energy
h		hour(s)
$h\upsilon$		photochemical excitation
IR		infrared
	cm^{-1}	wavenumbers
	υ	stretching frequency
L		ligand
L_2		bidentate ligand
M		metal
MEP		methyl propionate
m/z		mass/charge
min		minute(s)

nb	norbornene
Ph	phenyl
Pr^i	*iso*-propyl
R	alkyl (or aryl)
thf	tetrahydrofuran
tht	tetrahydrothiophene
TLC	thin layer chromatography
UV	ultraviolet
V65	$[CH_3(CH_3)CHCH_2(CN)(CH_3)CN{=}NC(CH_3)(CN)CH_2CH(CH_3)CH_3]$

NMR data

NMR	nuclear magnetic resonance
δ	chemical shift (in p.p.m.)
$\Delta\delta$	coordination chemical shift
p.p.m.	parts per million
s	singlet
d	doublet
dd	doublet of doublets
dt	doublet of triplets
t	triplet
q	quartet
quin	quintet
sept	septet
m	multiplet
bm	broad multiplet
bs	broad singlet
Hz	hertz
MHz	megahertz
J	coupling constant
$\{^1H\}$	proton decoupled
COSY	correlated spectroscopy
DEPT	distortionless enhancement by polarisation transfer

Chapter 1

Introduction

1.1 Introduction

Phosphine ligands have found wide-ranging applications in organometallic chemistry,[1] coordination chemistry[2] and homogeneous catalysis.[3] Until the 1970's, it was generally difficult to gauge the relative importance of the electronic and steric effects of a tertiary phosphine on the chemistry of its complexes.[4] Work by many groups over the last thirty years has clarified the field, and the purpose of this chapter is to give a general review of the role of sterically demanding alkyl phosphines in key developments in transition metal chemistry and homogeneous catalysis.

The work described in this thesis concerns the synthesis and characterisation of a range of adamantane-like bulky alkyl cage phosphines, their coordination chemistry and applications in homogeneous catalysis. To put this work into context, this introduction covers (i) the steric effect in organic chemistry, (ii) the quantification of steric and electronic effects in inorganic chemistry, (iii) a review of steric, conformation and entropy effects of bulky alkyl phosphines in the 1970's, and (iv) the coordination chemistry and homogeneous catalysis of sterically demanding alkyl phosphines since 1980, concentrating on the platinum group metals, with particular focus on group 10.

1.2 The steric effect in organic chemistry

The effect of sterically demanding substituents has been well documented in organic chemistry for over a century.[5-11] In the early 1920's, Thorpe and Ingold[12] investigated the formation of small rings and found that replacement of CH_2 by CMe_2 increased the stability of the cyclic product and the rate at which it was formed. This was called the Thorpe-Ingold or *gem*-dialkyl effect and is an established phenomenon whereby promotion of ring formation is achieved by increasing the steric bulk of the acyclic precursor. Ingold also noted that the *gem*-dialkyl effect was found in nature;[12] a *gem*-dialkyl group was present in essential oils that possessed a cyclopropane or cyclobutane ring.

The Thorpe-Ingold effect has since been demonstrated to be general in carbocyclic chemistry[13-15] and it has been shown that entropic and enthalpic factors are responsible. The loss of rotational entropy upon ring formation will be reduced if rotation about the bonds is already inhibited by the presence of other groups in the acyclic precursor,[16] and Allinger and Zalkow demonstrated an enthalpic barrier to ring closure.[17] For a straight chain compound, the preferred conformation about any particular bond will be *anti* (see Figure 1.1). For the compound to cyclise, the

conformation must be *gauche*. The presence of a *gem*-dialkyl susbstituent reduces the number of *gauche-gauche* interactions introduced upon cyclisation.

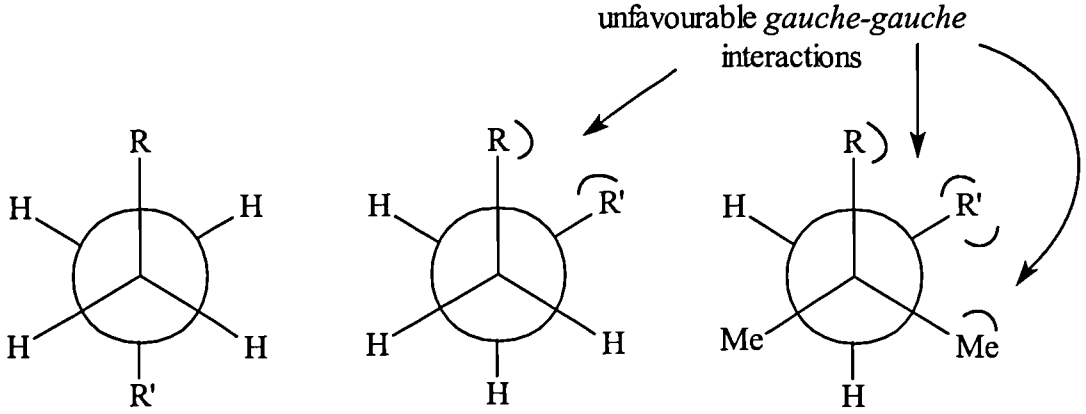

anti *gauche* *gauche* with *gem*-dimethyl

Figure 1.1

The nature of the steric effect in organic systems was reviewed by Anshutz in 1928[18], Newman in 1956[19] and Mosher and Tidwell in 1990.[20]

1.3 Steric, conformation and entropy effects of bulky alkyl phosphine ligands

Shaw *et al.* and Otsuka *et al.* were the first to explore comprehensively the effect of sterically encumbering tertiary alkyl phosphines on transition metal complexes. Their work in the 1970's has been reviewed[21] and it is summarised below. The *t*-butyl substituent on phosphorus was employed, as this group is very bulky and provided a valuable ^{1}H NMR probe for the chemistry undertaken.[22,23] The conclusions drawn by Shaw are highlighted by statements (1)-(9) below.

(1) PBu^t_2R ligands (R = alkyl or aryl) will not coordinate in mutually cis-positions

The large cone angles[24,25] (see Section 1.4) of ligands PBu^t_2R generally preclude them from coordinating in mutually *cis*-positions,[22] whilst less sterically demanding ligands (*e.g.* PMe_3, PEt_3, PPh_3) will coordinate in either mutually *cis*- or *trans*-orientations.

(2) Strong non-bonding interactions between PBu^t_2R and other ligands on the metal

Variable temperature ^{31}P NMR spectroscopy showed that complexes of the type *trans*-$[MCl(CO)(PBu^t_2R)_2]$ (M = Rh, Ir; R = Me, Et, Pr^n) exist as rotational conformers (**1.1a-c**). This showed that there was a significant energy barrier to rotation about the M-P bond due to eclipsing of a P-Bu^t and Rh-Cl or Rh-CO bond.

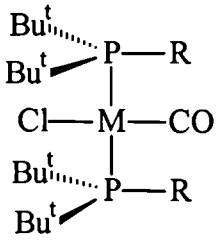

(1.1a)

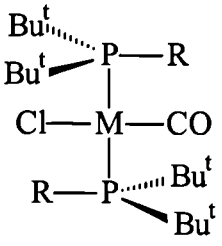

(1.1b)

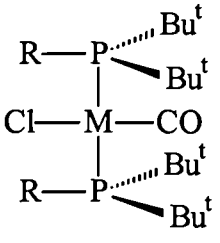

(1.1c)

(3) Formation of coordinatively unsaturated species reduces steric strain

Rhodium(III) and iridium(III) complexes usually favour octahedral coordination (*e.g.* $[RhCl_3(PEt_3)_3]$ from $RhCl_3$ and PEt_3). However, treatment of MCl_3 with PBu^tR_2 or PBu^t_2R afforded the five coordinate, square pyramidal hydrides $[MHCl_2L_2]$, such as (**1.2**) and (**1.3**).[22]

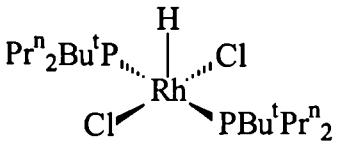

(1.2)

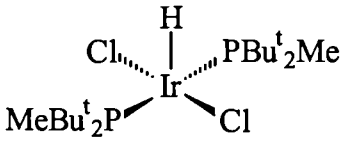

(1.3)

A propan-2-ol solution of rhodium complex (**1.2**) in the presence of isopropoxide gives a catalyst for the hydrogenation of olefins and acetylenes (as a catalyst for the hydrogenation of hex-1-ene it is as active as $[RhCl(PPh_3)_3]$). To our knowledge, this was the first example of a bulky phosphine-containing transition metal catalyst (see Sections 1.5.1 and 4.1 for more recent examples).

Other groups in the 1970's also used bulky alkyl phosphines to stabilise coordinatively unsaturated complexes of nickel(0),[25] rhodium(I) and rhodium(III),[26,27] palladium(0)[28-30] and platinum(0).[28,31]

(4) The other associated ligands are preferably small

The formation of hydrides is particularly favoured with bulky alkyl phosphines as steric strain is reduced. The first examples of stable *trans*-dihydrides were reported using bulky tertiary phosphines.[31-33] *Trans*-$[PtH_2L_2]$ are unstable when L = PEt_3 or PPh_3, but stable, crystalline derivatives can be prepared with bulkier alkyl phosphine ligands (L = PBu^t_2Et **(1.4)**[33] or PCy_3 **(1.5)**[31]). The first examples of *cis*-dihydridoplatinum(II) complexes were made using chelating bulky diphosphines, *e.g.* **(1.6a)**[34] and **(1.6b)**.[35] It is interesting to note that both of these bulky diphosphines were employed more recently as very active homogeneous catalysts for the palladium(II) catalysed methoxycarbonylation of ethylene to methyl propionate (see Section 4.1).[36-38]

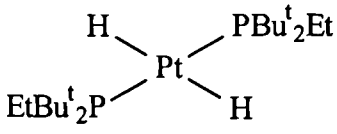

(1.4)

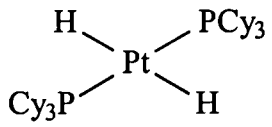

(1.5)

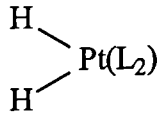

(1.6a) $L_2 = o\text{-}C_6H_4(CH_2PBu^t_2)_2$

(1.6b) $L_2 = Bu^t_2P(CH_2)_3PBu^t_2$

Polyhydride complexes are also kinetically stabilised with bulky alkyl phosphines. The iridium pentahydrides $[IrH_5L_2]$ are robust and easily handled with PBu^t_2R ligands compared to their labile analogues with less sterically protecting phosphines.[39] See Section 1.5.1 for more recent examples.

(5) The kinetic stabilisation of intermediates and unusual oxidation states

Bulky tertiary phosphines were shown to stabilize compounds that are not normally observed but which might have a transient existence with smaller phosphines. Thus, treatment of the iridium(III) hydride $[IrHCl_2(PBu^t_2Me)_2]$ **(1.3)** with $NaBH_4$ afforded the unusual tetrahydroborate complex **(1.7)** (Equation 1.1), the first example of a non-fluxional metal tetrahydroborate. This slowly decomposes to give the iridium pentahydride $[IrH_5(PBu^t_2Me)_2]$ even in benzene. The very bulky analogue $[IrH_2(BH_2)(PBu^t_3)_2]$ is stable in benzene.[39,40]

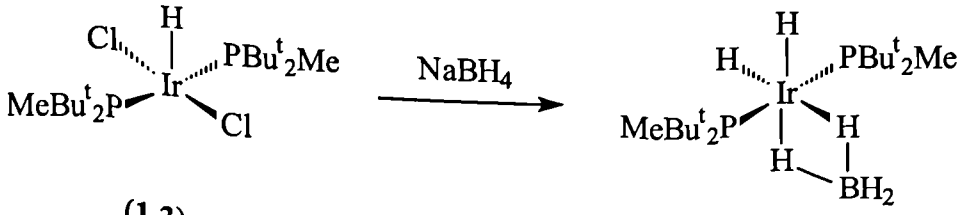

(1.3) **(1.7)**

Equation 1.1

Bulky tertiary phosphines were used to trap unusual oxidation states. Thus the first examples of a stable rhodium(II) and iridium(II)[41-43] complexes were achieved, *e.g.* addition of PBu^t_2Et to an ethanolic solution of $RhCl_3$ at 0 °C gave complex (**1.8**).[44]

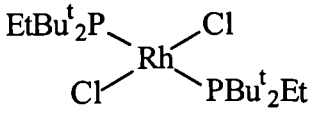

(1.8)

(6) The decarbonylation of alcohols

The use of sterically demanding alkyl phosphines facilitates the reaction of alcohols with metal complexes to form transition metal hydrides, carbonyls and carbonyl hydrides. For example complexes of the type $[RhHCl_2(PBu^t_2R)_2]$ react in seconds with methoxide in methanol to afford *trans*-$[RhCl(CO)(PBu^t_2R)_2]$.[44] Similar chemistry was also observed with iridium[45] and ruthenium complexes.[46,47] The accelerated reaction with bulky phosphine metal complexes was attributed to (i) the vacant coordination site facilitating attack by alcohol/alkoxide and (ii) the decrease of steric congestion in the transition metal complex upon decarbonylation of the coordinated alkoxide.

(7) Metal-metal bond formation

When an alcoholic solution of $RuCl_3$ is treated with CO and then a tertiary phosphine is added, the octahedral Ru(II) complexes $[RuCl_2(CO)_2L_2]$ are formed if L is a small phosphine such as PEt_3. Markedly different chemistry is observed if a bulky phosphine is added, producing binuclear Ru(I) complexes $[Ru_2Cl_2(CO)_4L_2]$ (**1.9**) where only one phosphine is complexed per ruthenium (see Equation 1.2).[48,49]

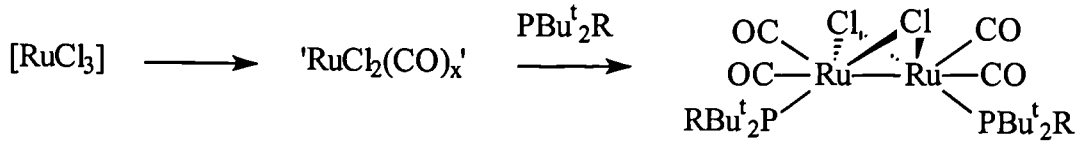

(1.9)

Equation 1.2

(8) Cyclometallation

The chemistry described here provided the basis for many more recent advances in homogeneous catalysis involving sterically demanding phosphines (see Section 1.5). Cyclometallation is the process whereby the carbon atom on an organic group attached to the donor atom (phosphorus in the following examples) is metallated. The hydrogen of a C-H bond is replaced by a metal and a cyclic system is formed (see Equation 1.3).[50,51] There were many examples of internal transition metal-carbon bond formation involving phosphine ligands before the 1970's,[52] but Shaw *et al.* were the first to probe the factors that effect this cyclometallation.

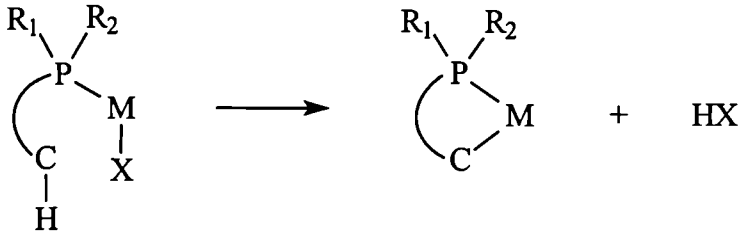

Equation 1.3

Cyclometallation with a wide variety of organic groups attached to phosphorus was achieved,[53-59] and in all these cases, the tendency to cyclometallate was found to increase in the order (R_1 or R_2) Me < Ph < Bu^t, demonstrating that steric effects are dominant over electronic effects. Two examples of cyclometallated products are shown below. The ring-closed complexes (**1.10**) and (**1.11**) are both formed by heating their corresponding *trans*-[$PtCl_2(PBu^t_2R)_2$] complexes in 2-methoxyethanol.[60] An unusual example of cyclometallation is the iridium-carbene complex (**1.12**).

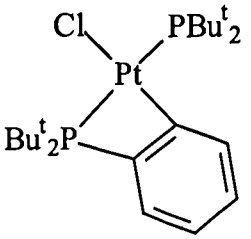

(1.10)

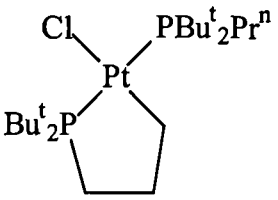

(1.11)

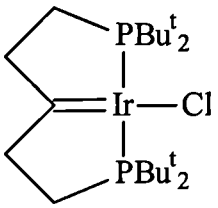

(1.12)

The promotion of cyclometallation by bulky substituents on phosphorus is related to the Thorpe-Ingold effect. The sterically demanding Bu^t substituents on the phosphines restricts rotation around several bonds, reducing the loss of entropy on cyclisation and the preferred torsion angle of the backbone is 60° (*cf.* 180° with smaller groups) to the metal facilitating cyclometallation (see Figure 1.2).

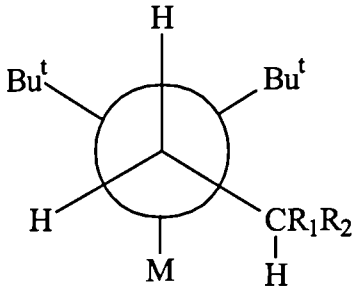

Figure 1.2 Newman projection of view down CH_2-P bond

(9) Formation of large chelate rings

It was thought that large chelate rings would be unstable with respect to their open chain precursors and polymeric species, exemplified by compounds that undergo slow polymerisation when concentrated (*e.g.* $[PtCl_2\{CH_2{=}CH(CH_2)_mCO_2(CH_2)_nC_5H_2Me_2N\}]$)[61] or dissociate in solution (*e.g.* $[Rh_2Cl_2(CO)_2\{Ph_2P(CH_2)_2O(CH_2)_2PPh_2\}_2]$).[62,63] However, it was shown that whilst $Me_2P(CH_2)_{12}PMe_2$ and $Ph_2P(CH_2)_{10}PPh_2$ give polymeric species when complexed to transition metals, ligands of the type $Bu^t_2P(CH_2)_nPBu^t_2$ (n = 5-10), $Bu^t_2P(CH_2)_4C{\equiv}C(CH_2)_4PBu^t_2$ and $Bu^t_2PC{\equiv}C(CH_2)_nC{\equiv}CPBu^t_2$ (n = 4 or 5) gave large chelate rings of Pt(II), Pd(II), Rh(I), Ir(I), Ir(III) and Ru(II) which were indefinitely stable, even in solution.[53,64]

The reaction of $Bu^t_2P(CH_2)_7PBu^t_2$ with $[PdCl_2(NCPh)_2]$ demonstrates the influence of the bulky phosphine on the formation of the product, *trans*-$[Pd_2Cl_4\{Bu^t_2P(CH_2)_7PBu^t_2\}_2]$ (**1.13**).

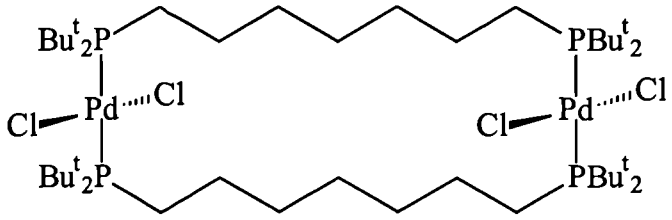

(1.13)

Comparison can be drawn again with the *gem*-dialkyl effect with the steric factors that influence the formation of this stable, large chelate. Restricted rotation about the Pd-P and P-C bonds induced by the *t*-butyl groups reduces loss of rotational entropy upon cyclisation. Furthermore, torsional strain is reduced for chelate formation as the preferred torsion angles of the open ring compound precursor (*e.g.* $PdCl_2\{Bu^t_2P(CH_2)_7PBu^t_2\}$-$PdCl_2\{Bu^t_2P(CH_2)_7PBu^t_2\}$) are similar to those observed in the crystal structure of the 20 membered ring product.[53] Shaw also noted[21] that nature uses sterically demanding groups to stabilise large macrolide rings.[65]

1.4 Measurement of steric and electronic effects of bulky phosphines

1.4.1 Ligand cone angle

Although the steric and electronic effects of a phosphorus(III) ligands are related, a useful separation can be made and the steric effect of a ligand measured by its "cone angle". This invaluable concept was first introduced by Tolman in 1970,[24,66] and reviewed in 1977.[25] It is still the most widely used and accepted steric measure for inorganic chemists, and has provided insight into complex reactivity and selectivity observed in catalysis.

To obtain the cone angle, a symmetrical ligand (PR_3) is positioned 2.28 Å from a metal and the linear angle, θ, between the vectors tangential to the outermost van der Waals radii of the atoms on the ligand is measured. For asymmetric ligands, $PR_1R_2R_3$, the total cone angle is defined as the average sum of the semivertex angles for each PR_i group (Figure 1.3).

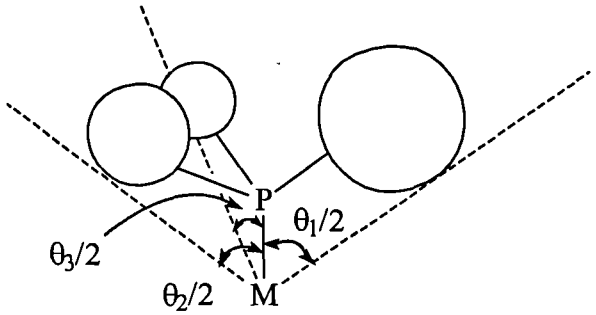

$$\text{Cone angle, } \theta = (2/3)\sum_{i=1}^{3} \theta_i/2.$$

Figure 1.3 Measurement of the average cone angle (θ) for a ligand $PR_1R_2R_3$.

The M-P value of 2.28 Å was chosen as it is typical of a Ni-P bond distance and the original data were generated for $[Ni(CO)_3L]$ complexes. It is assumed that this arbitrary set of data can be used for all metals bound to phosphorus. This method is easy to apply to ligands with few conformational degrees of freedom (*e.g.* PH_3). However, for ligands that are more conformationally flexible (*e.g.* PBu^t_3), the cone angle was originally measured with the ligand in its minimum conformation. This is a significant assumption, and when in doubt, Tolman based his final calculation on the position of the equilibrium in the reaction showed in Equation 1.4.

$$Ni(CO)_4 + 8L \rightleftharpoons Ni(CO)_{4-n}L_n$$

Equation 1.4

For a bidentate diphosphine, the cone angle for each phosphorus atom (θ) is defined as the sum of the angle between one M-P bond and the vector bisecting the P-M-P bite angle (β) and the cone angle of the nonbridging substituents (see Figure 1.4).

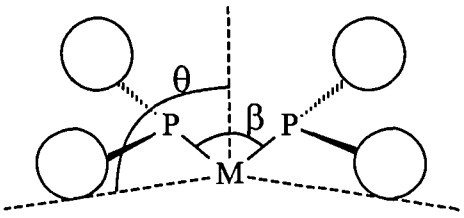

Figure 1.4

A variety of new procedures for evaluating steric bulk in inorganic chemistry have been reported since Tolman's work, including solid angles[67-70] and ligand repulsive energy.[71-73] Clark and Hampden-Smith reviewed steric effects in bulky phosphines in

1987[74] and the quantification of steric effects in organometallic chemistry was comprehensively reviewed in 1994 by White and Coville.[75]

1.4.2 Bonding in phosphorus(III) ligand metal complexes

Stromeier[76] showed that phosphorus ligands can be ranked in an electronic series based on the CO stretching frequencies of a variety of monosubstituted transition metal carbonyls. Tolman[25] based his electronic parameter on the frequency of the A_1 carbonyl mode of $Ni(CO)_3PR_3$ and reviewed the correlation between various spectroscopic properties and the phosphine-metal bonding in transition metal complexes (*e.g.* NMR chemical shifts and coupling constants).

Phosphorus ligands are able to stabilise high and low oxidation states, and this versatility is attributed to varying degrees of σ-donation and π-acceptance in the M-P bond.[77] A new description of the orbitals involved in π-acceptance was proposed by Orpen and Connelly[78] who presented evidence for P-X σ^* orbital involvement using bond length arguments. The σ^* orbitals retain some phosphorus 3*d* character *via* hybridisation of the σ^* and 3*d* orbitals, forming better π-acceptor orbitals (see Figure 1.5)

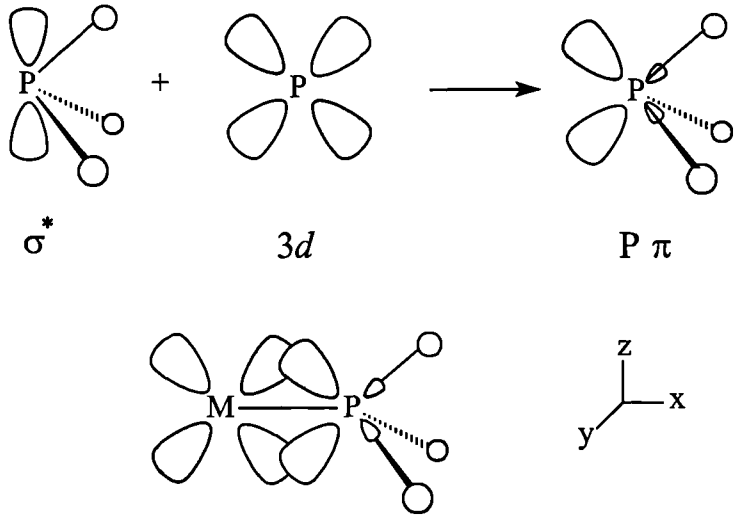

Figure 1.5 Hybridisation of σ^* orbital with $3d_{zx}$ orbital to form P π-accepting orbital and the back bonding form filled metal d_{zx} orbitals to empty P π acceptor orbitals

Further experimental evidence supporting this bonding theory was reported in the crystal structure database study of coordinated PPh_3 fragments.[79] Strong correlations were found between the mean C-P-C bond angle and the P-C bond length (*i.e.* as the mean bond angle decreases, the bond length increases), rationalised by qualitative molecular orbital arguments based on Walsh diagrams for the deformations of PX_3 orbital model (see Figure 1.6).

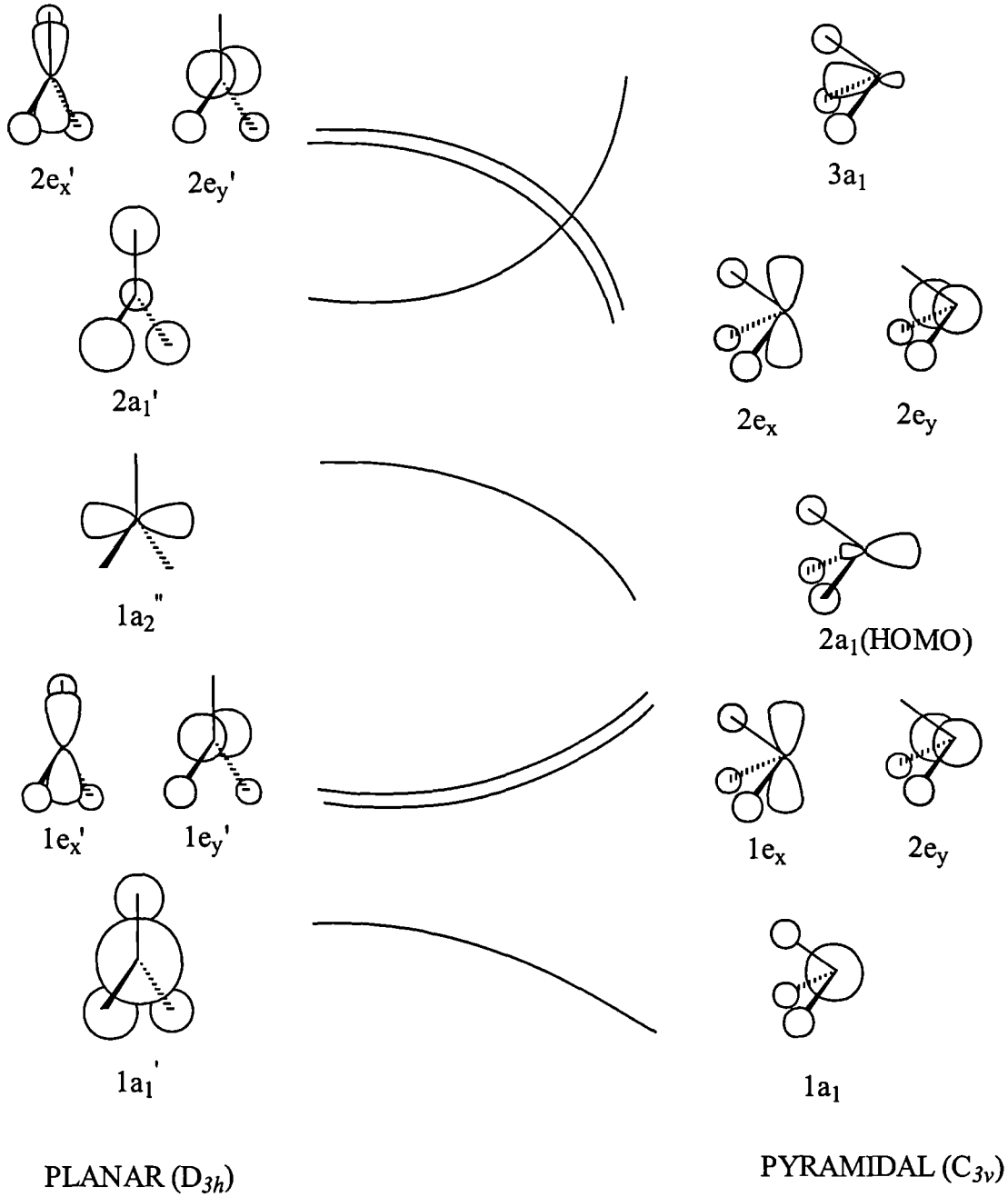

Figure 1.6 Walsh diagram for the deformation of a PX_3 species, showing rehybridisation of the phosphine lone pair $2a_1$, and π-acceptor function 2e, on pyramidalisation at phosphorus

The pyramidal structure for PPh_3 was accounted for by the lowering of the HOMO energy from the planar $2a_1'$ to pyramidal $2a_1$ level, the $2a_1$ orbital becoming the lone pair of the PPh_3 ligand. The distortion destabilises the P-X σ-bonding orbitals, since the $1e$ pair of orbitals rise in energy. Upon coordination, the electron density of the lone pair orbital ($2a_1$) is reduced. This has the effect of removing the stabilisation of the pyramidal geometry, due to the $1e$ orbitals requiring that they obtain their lowest energy level, *i.e.* planar geometry. Therefore, the X-P-X angles increase and the P-A bond lengths shorten with σ-donation. The π-back donation populates the P-X σ^* orbitals ($2e$) which achieves stabilisation by moving towards pyramidal geometry, thereby decreasing the mean X-P-X bond angles and increasing the mean P-X bond lengths.

1.5 Coordination chemistry of bulky alkyl phosphines with late transition metals

There has been a tremendous amount of development of transition metal chemistry with bulky alkyl phosphines since the work of Shaw *et al.*[21,56,80-86] For its relevance to this thesis, the bulky phosphine chemistry with the platinum group metals is reviewed below, with a concentration on the Ni, Pd and Pt subgroup. Whilst this review is not exhaustive, it gives an indication of the huge amount of research in bulky phosphine-transition metal complexes.

1.5.1 Chemistry of group 10 metal complexes with bulky alkyl phosphines

1.5.1.1 Metal hydrides, polyhydrides, hydrido-metal clusters and β-agostic interactions

Various groups in the 1970's showed that metal hydride species were stabilised by bulky alkyl phosphines as ancillary ligands (see Section 1.3).[21] This was extended to polynuclear, bulky phosphine-stabilised complexes of nickel(0)[87] and platinum(II)[88-90] containing terminal and bridging hydrides.

Spencer *et al.* showed that by use of tertiary bulky monophosphines, hydrido-platinum clusters could be synthesised in which the ratio Pt : H exceeds unity (see Scheme 1.1).[91,92] Treatment of $[Pt(C_2H_4)_2PR_3]$[89] with H_2 (300 atm) afforded the platinum clusters (**1.14**)-(**1.16**). Trinuclear cluster (**1.16**) was treated with ethylene to yield the new cluster $[Pt_4H_2(PBu^t_3)_4]$ (**1.17**).

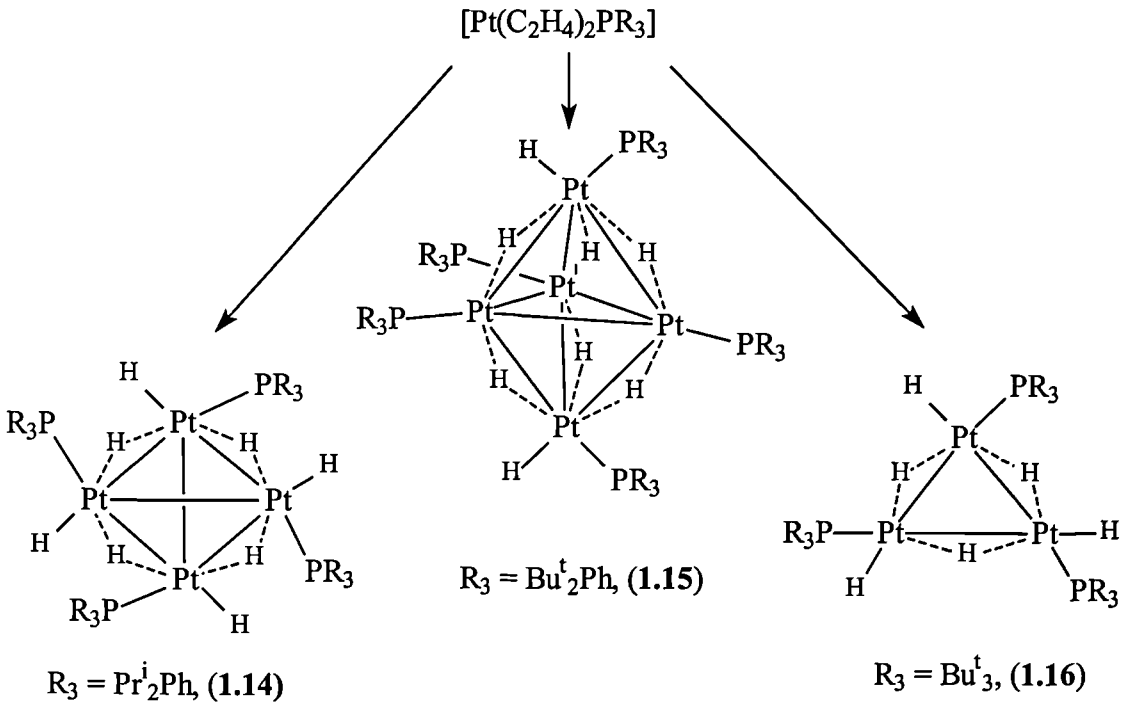

Scheme 1.1

Treatment of dihydride (**1.17**) with strong acid affords the dicationic hydrido cluster (**1.18**) which slowly deprotonates in acetone to give monocation (**1.19**) (see Scheme 1.2).[93] Both (**1.18**) and (**1.19**) react rapidly with H_2 to give the heptahydrido cluster (**1.20**) which has a 'butterfly' core of platinum atoms. Cation (**1.20**) reacts with ethylene to regenerate (**1.19**) or with atmospheric oxygen to afford the non-hydride cluster (**1.21**) in which one of the *t*-butyl groups has been metallated.

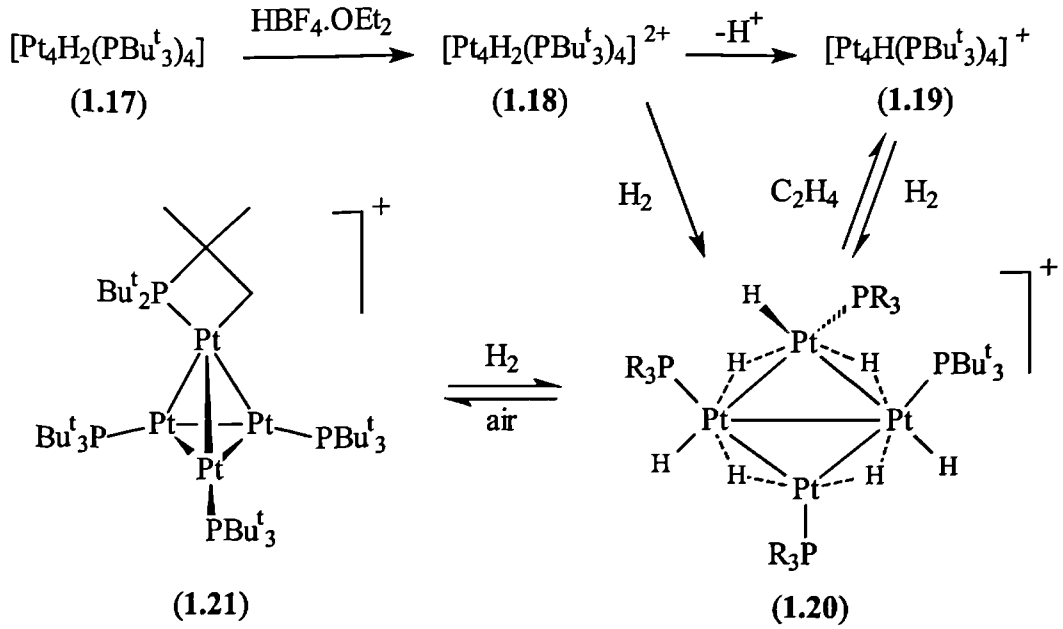

Scheme 1.2

The 1980's saw the development of agostic complexes in which a ligand's α- or β-C-H bonds act as two electron donors to otherwise unsaturated metals,[94,95] mainly with Groups 4-7 transition metals. In 1988, Spencer *et al.* reported β-agostic complexes with a late transition metal,[96] and later studied the strength of the agostic interaction as a function of the ligand set at platinum and palladium in a series of complexes.[97] Treatment of [Pt(norbornene)$_3$] or [Pd(η-C_3H_5)(η-C_5H_5)] with chelating bulky alkyl diphosphines afforded the neutral, zero-valent, η^2-norbornene complexes (**1.22a-h**). Protonation with strong acid yielded the 14-electron, cationic complexes (**1.23a-h**) (see Scheme 1.3).

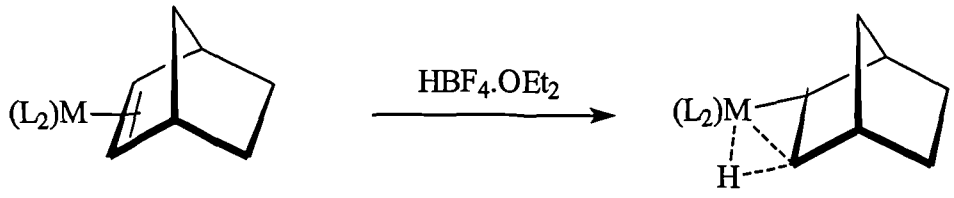

	M	L_2
(1.22a)	Pt	$Cy_2P(CH_2)_2PCy_2$
(1.22b)	Pt	$Bu^t{}_2P(CH_2)_2PBu^t{}_2$
(1.22c)	Pt	$Cy_2P(CH_2)_3PCy_2$
(1.22d)	Pt	$Bu^t{}_2P(CH_2)_3PBu^t{}_2$
(1.22e)	Pt	*o*-$C_6H_4(CH_2PBu^t{}_2)_2$
(1.22f)	Pd	$Cy_2P(CH_2)_2PCy_2$
(1.22g)	Pd	$Bu^t{}_2P(CH_2)_2PBu^t{}_2$
(1.22h)	Pd	*o*-$C_6H_4(CH_2PBu^t{}_2)_2$

(1.23a)-(1.23h)

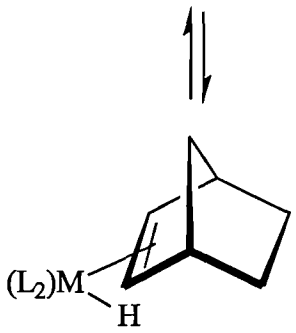

Scheme 1.3

The IR, NMR and *X*-ray crystallographic (for **(1.22b)** and **(1.23b)**) data were used to assess the influence of the ancillary ligands on the equilibrium between the alkene hydride and agostic alkyl. The more sterically demanding diphosphines (*e.g.* *o*-$C_6H_4(CH_2PBu^t{}_2)_2$) tended to promote insertion of alkene into the M-H (M = Pt or Pd) bond, and thus favouring the alkyl over the alkene hydride.

This work was extended to nickel(II), palladium(II)[98] and platinum(II)[99] β-agostic ethyl cations. The ethene-hydride/ethyl equilibrium (see Equation 1.5) was shown to be very sensitive to the bulky diphosphine ligand. For the platinum systems, the NMR data were consistent with ethyl ligands bound to platinum through σ-alkyl and β-agostic C-H-M bonds with the *o*-xylyl **(1.24a)** and the C_3 **(1.25a)** diphosphines,

whereas the ethene hydride was the dominant species with the C_2-*t*-butyl ligand (**1.26b**). Thus, a larger bite-angle of the diphosphine favours the agostic form.

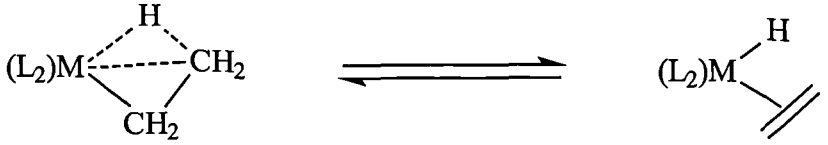

(1.24a)	$L_2 = o\text{-}C_6H_4(CH_2PBu^t_2)_2$	**(1.24b)**	$L_2 = o\text{-}C_6H_4(CH_2PBu^t_2)_2$
(1.25a)	$L_2 = Bu^t_2P(CH_2)_3PBu^t_2$	**(1.25b)**	$L_2 = Bu^t_2P(CH_2)_3PBu^t_2$
(1.26a)	$L_2 = Bu^t_2P(CH_2)_2PBu^t_2$	**(1.26b)**	$L_2 = Bu^t_2P(CH_2)_2PBu^t_2$

Equation 1.5

The β-agostic structure was thermodynamically favoured with all three diphosphines for palladium and nickel complexes ((**1.24a**)-(**1.26a**), M = Pd or Ni). Furthermore, Spencer *et al.* showed that β-hydrogen migration was sensitive to small perturbations in ancillary diphosphine structure, and highlighted the subtle differences between the platinum group metals with respect to some of the fundamental processes of organometallic chemistry.

Spencer and Mhinzi reported the preparation and properties of alkyl platinum complexes bearing bulky substituents on the β-carbon.[100] The cationic complexes (**1.27a-c**) were synthesised *via* protonation of their platinum(0) alkene precursors. Complex (**1.27a**) could also be prepared by reaction of the diplatinum complex $[Pt_2(\mu\text{-}H_2)_2(dbpp)_2][BF_4]_2$[101] with an excess of 3,3-dimethylbut-1-ene.

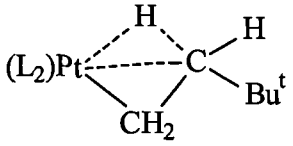

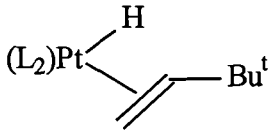

	L_2
(1.27a)	dbpp
(1.27b)	dbpx

	L_2
(1.27c)	dbpe

The balance between agostic and alkene-hydride isomers was generally similar to the previously described ethyl/ethene complexes,[99] though the bulky substituents appeared to promote the alkene hydride tautomer.

Spencer and Crascall prepared a series of η^3-benzyl platinum(II) ((**1.28a-c**) and (**1.29a-f**)) and palladium(II) (**1.28d-f**) complexes by protonation of their Pt(0) pr Pd(0) styrene analogues.[102,103] Complexes (**1.28a-f**) were shown to be fluxional on the NMR

timescale, and mechanisms were proposed for this dynamic behaviour. The activation energies for these internal rearrangements were dependent on both the metal centre (Pd > Pt) and on the steric effect of the diphosphine (ΔG was larger for smaller bite angle and less bulky substituents, *e.g.* Cy-substituted diphosphine complexes were not fluxional).

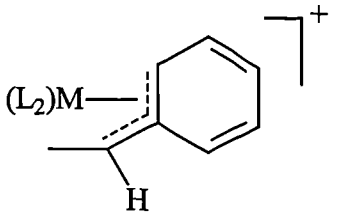

	M	L_2
(1.28a)	Pt	$Bu^t_2P(CH_2)_2PBu^t_2$
(1.28b)	Pt	$Bu^t_2P(CH_2)_3PBu^t_2$
(1.28c)	Pt	o-$C_6H_4(CH_2PBu^t_2)_2$
(1.28d)	Pd	$Bu^t_2P(CH_2)_2PBu^t_2$
(1.28e)	Pd	$Bu^t_2P(CH_2)_3PBu^t_2$
(1.28f)	Pd	o-$C_6H_4(CH_2PBu^t_2)_2$

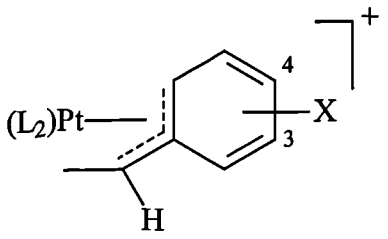

L_2 = $Bu^t_2P(CH_2)_3PBu^t_2$

	X
(1.29a)	Br-3
(1.29b)	Br-4
(1.29c)	Me-4
(1.29d)	F-4
(1.29e)	F-3
(1.29f)	MeO-4

The effect of phenyl substitution on η^3-benzyl bonding in the platinum complexes (**1.29a-f**) was also investigated.[102,104] Although phenyl substitution did not affect the ground-state structure or mechanism of dynamic behaviour in fluxional complexes (**1.29**), the asymmetry of the Pt-η^3-$MeCHC_6H_4X$ interaction and elimination of styrene varied with the substituent. Thus the more electron donating the substituent (*e.g.* X = MeO-4 (**1.29f**)) the more asymmetric was the bond and the more facile the loss of styrene. The ease with which complexes (**1.29d**) and (**1.29f**) lost styrene led to a convenient route to new platinum(II) complexes; for instance bulky alkyl β-agostic complex (**1.27a**) was prepared by reaction of η^3-benzyl complex (**1.29d**) with 3,3-dimethylbut-1-ene.

This methodology was extended to the synthesis of platinum(II) complexes containing cyclic ligands with Pt-C and Pt-O bonds.[105] Thus the reaction of complexes (**1.28b**) or (**1.29d**) with olefins methyl acrylate, methyl vinyl ketone or dimethylmaleate (or dimethylfumarate) afforded the complexes (**1.30a-c**) respectively (see Scheme 1.4, L_2 = dbpp).

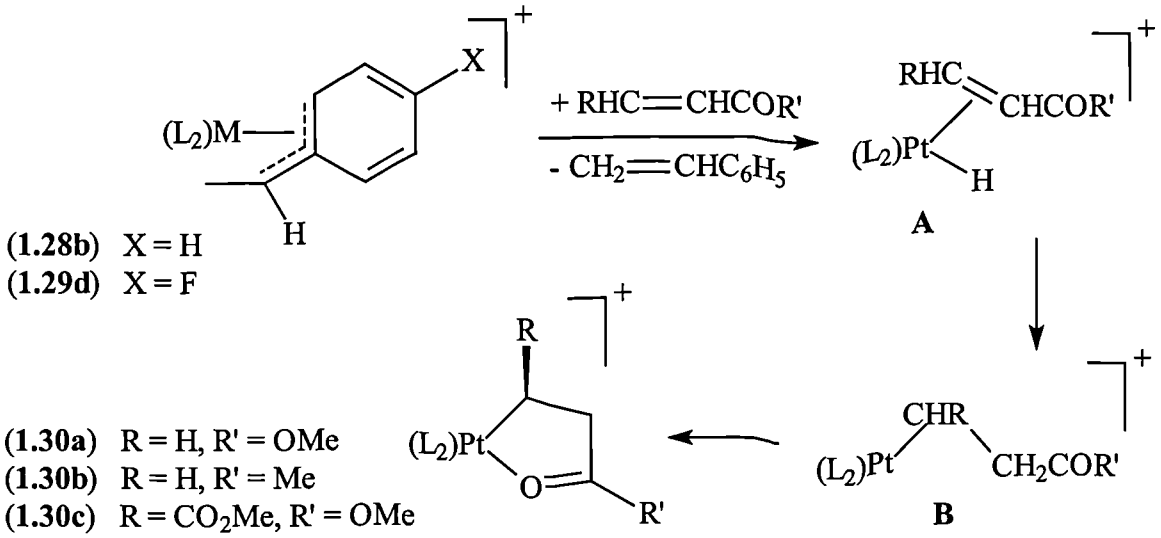

(1.28b) X = H
(1.29d) X = F

(1.30a) R = H, R' = OMe
(1.30b) R = H, R' = Me
(1.30c) R = CO_2Me, R' = OMe

Scheme 1.4

Taken with the results from the η^3-benzyl complexes,[102-104] an approximate order of stability is evident: intramolecular Pt-O > η^3-benzyl ~ Pt-H-C.

There are many bulky alkyl phosphine-stabilised diplatinum complexes with two or more hydride ligands, both neutral[88,106] and cationic.[90] Binuclear palladium complexes with bridging hydrides have also been reported.[107,108] During the study by Spencer on platinum alkyl complexes stabilised by β-agostic interactions described above, formation of diplatinum complexes as the decomposition products of the mononuclear alkyls was observed. The synthesis, structure and spectroscopic properties of a new series of bridging dihydroplatinum cations (**1.31a-d**) was subsequently reported (see Scheme 1.5).[109] Complexes (**1.31b**) and (**1.31d**) were also available *via* protonation of the corresponding mononuclear dihydride.

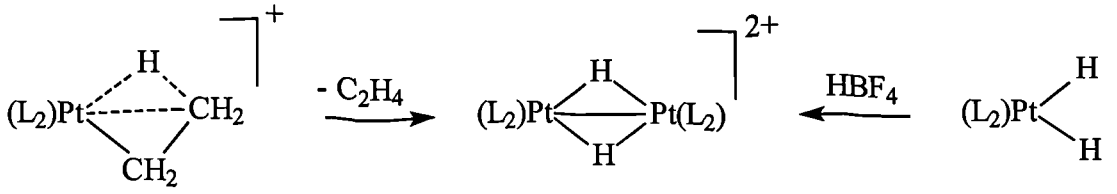

L_2
(1.31a) dcpe
(1.31b) dbpe
(1.31c) dcpp
(1.31d) dbpp

Scheme 1.5

The chemical and spectroscopic properties of complexes (**1.31a-d**) were dictated by the steric demands of the diphosphine ligand. For example, complex (**1.31d**) which contains the bulkiest diphosphine is destabilised to the extent that it serves as a useful source of the $[PtH(L_2)]^+$ fragment in a variety of reactions with electron donors.

1.5.1.2 C-C, C-H, C-O and C-Si bond activation via cyclometallation

Since the early 1990's Milstein *et al.* have investigated cyclometallation with the platinum group metals. This work is reviewed below, concentrating on the group 10 metals with bulky alkyl phosphines.

Reaction of the bidentate phosphine (**1.32**) with $[PtCl_2(cod)]$ afforded the kinetically favoured C-H activation product (**1.33**) (see Scheme 1.6).[110,111] The thermodynamically preferred C-C activation was then induced by heating the thermally stable (**1.33**) in the presence of HCl to generate the Ar-Pt complex (**1.34**) and methyl chloride. Overall retention of the metal oxidation state and functionalisation of the C-C bond by a polar substrate in this transformation can be essentially viewed as 'methylene transfer'.[112]

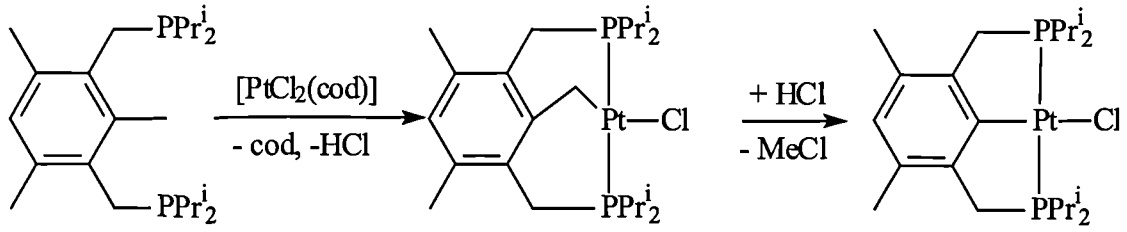

(1.32) **(1.33)** **(1.34)**

Scheme 1.6

Consecutive cyclometallation by platinum(II) and the monophosphine (**1.35**) was also reported.[113] Activation of two benzylic C-H bonds resulted in formation of two new M-C σ-bonds, *via* selective loss of 2 equiv of CH_4 with retention of the metal oxidation state (see Equation 1.6)

$$2R\text{-}CH_3 + Pt^{II}(CH_3)_2 \longrightarrow (R\text{-}CH_2)_2Pt^{II} + 2CH_4$$

Equation 1.6

The first C-H activation proceeds at room temperature to afford monometallated *cis* complex (**1.36a**). Isomerisation of *cis*-(**1.36a**) to *trans*-(**1.36b**) is kinetically

preferred over the second cyclometallation for electronic reasons. However heating (**1.36a**) leads to the second C-H activation to generate (**1.37**) (see Scheme 1.7).

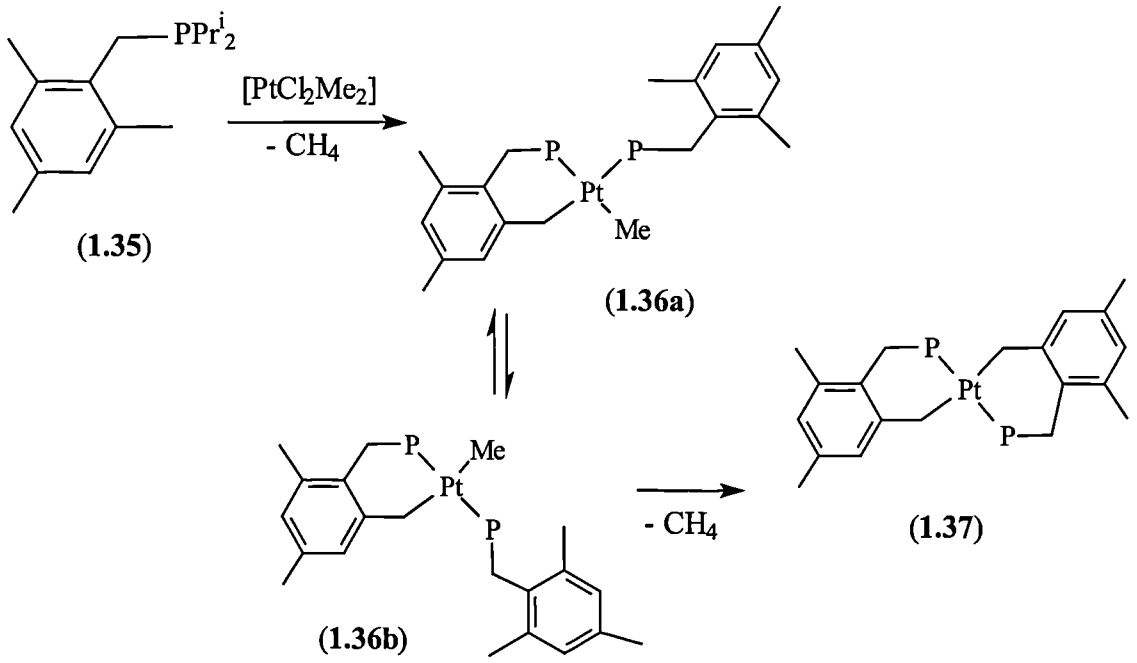

Scheme 1.7

Mechanistic studies showed that both cyclometallations involved a coordinatively unsaturated 14-electron complex which undergoes oxidative addition to form alkylhydridoplatinum(IV) intermediates. These reductively eliminate CH_4 to generate the ring-closed platinum(II) products. The overall process shows that the σ-bonded methylene group has a major electronic effect on the course of the reaction, but that steric demands eventually prevail in forming (**1.37**).

The C-Si bond formation upon reaction of platinum(II) alkyl (**1.36a**) with various primary silanes has been described (see Scheme 1.8).[114] The formation of platinum(II) hydride (**1.39**) was promoted by bulky phosphine (**1.35**). The *cis*-geometry of complex (**1.36a**) was also shown to be required for selective C-Si bond formation, reaction of the *trans* isomer (**1.36b**) with silanes resulted in CH_4 elimination and formation of (**1.37**). Complex (**1.39**) was also available *via* thermolysis of *trans*-dihydride (**1.38**), which was generated by treatment of (**1.36a**) with H_2.

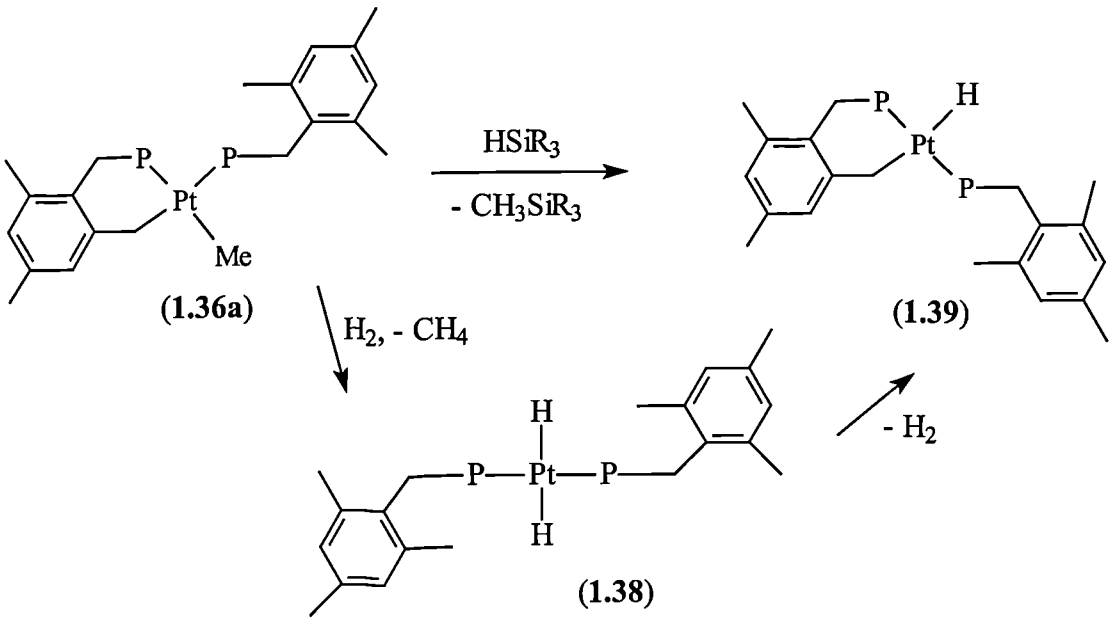

Scheme 1.8

Late transition metal complexes with NCN pincer ligands have been extensively studied by van Koten *et al.*[115] Milstein *et al.* recently reported a PCN ligand system (**1.40**) which promotes C-C activation with rhodium(I) and C-H activation with platinum(II).[116] The C-C activated product (**1.41**) (see Scheme 1.9) is the only one observed with platinum(II) even after prolonged heating, and is assisted by the non-coordinating internal amine which drives the reaction by deprotonation of a platinum(IV) intermediate.

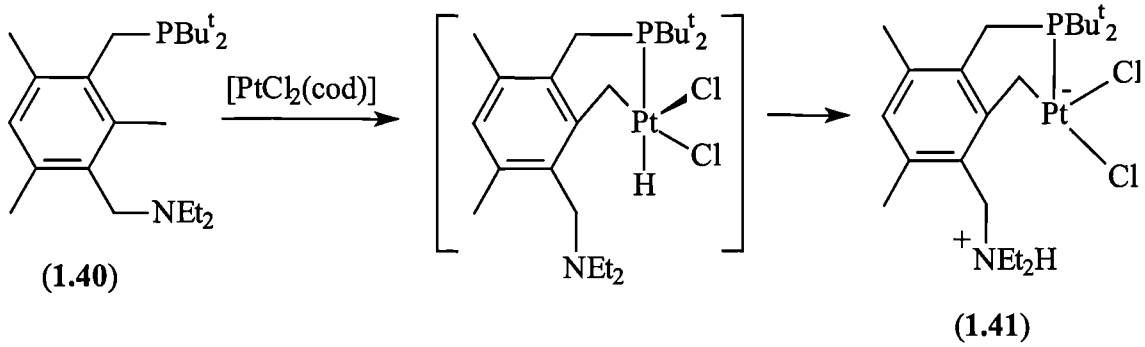

Scheme 1.9

Pincer ligand systems have also been used to investigate alkyl- and aryl-oxygen bond activation by rhodium(I), palladium(II) and nickel(II).[117,118] Transition metal-based selectivity was observed, with the first example of metal insertion into the strong aryl-oxygen bond of an aromatic ether or phenol under mild conditions by rhodium. Conversely, the more electrophilic palladium(II) and nickel(II) centres favoured sp^3-sp^3 alkyl-oxygen bond activation. Thus reaction of aryl ether diphosphine (**1.42**) and phenol

diphosphine (**1.43**) with palladium(II) or nickel(II) afforded the phenoxy M(II) complexes (**1.44**) and (**1.45**) as a result of alkyl C-O and O-H activation processes respectively (see Scheme 1.10). The aryl C-O activated product (**1.46**) (available from diphosphine (**1.45**)) was not observed for any of the reactions shown, demonstrating the thermodynamic preference for sp^3-sp^3 C-O activation in this system.

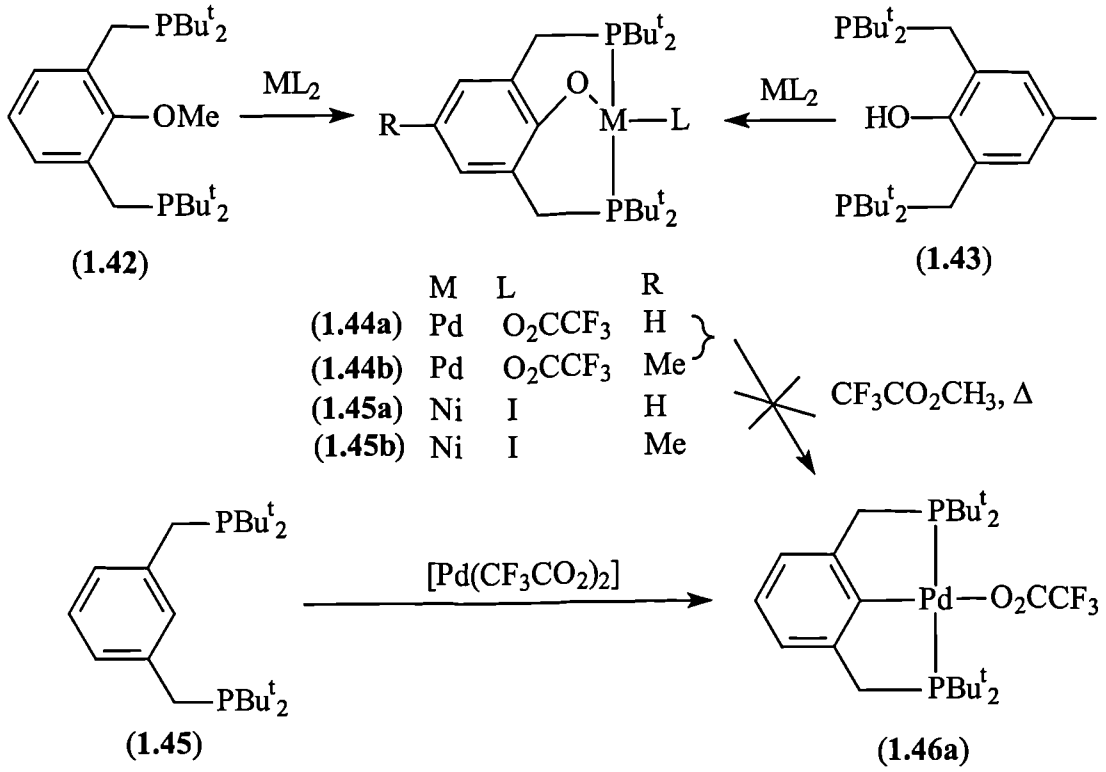

Scheme 1.10

Remarkably, heating complexes (**1.44a,b**) under H_2 pressure afforded the aryl-Pd(II) complexes (**1.46a,b**), *via* unprecedented hydrodeoxygenation of a strong ArO-transition metal bond in solution (see Equation 1.7).

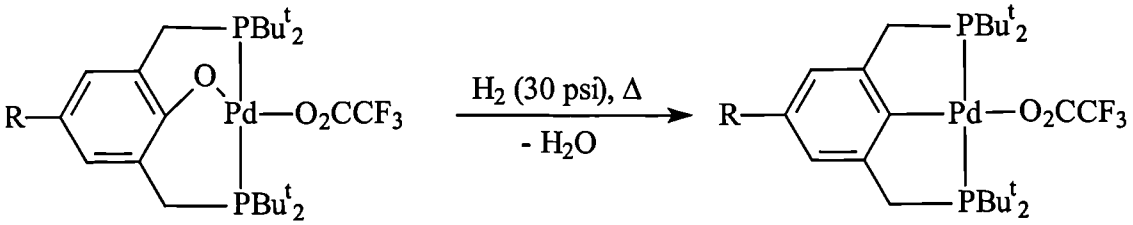

Equation 1.7

Competitive alkyl- and aryl-oxygen bond activation was observed in the reaction of aryl ether diphosphine (**1.47**) with palladium(II), forming complexes (**1.44a**) and (**1.46a**) respectively (see Scheme 1.11). Prolonged heating of the reaction mixture did

not change the product distribution, suggesting complexes (**1.44a**) and (**1.46a**) are formed independently and do not interconvert. Moreover, both C-O bonds are accessible to the metal centre, and the overall bond activation is probably kinetically controlled.

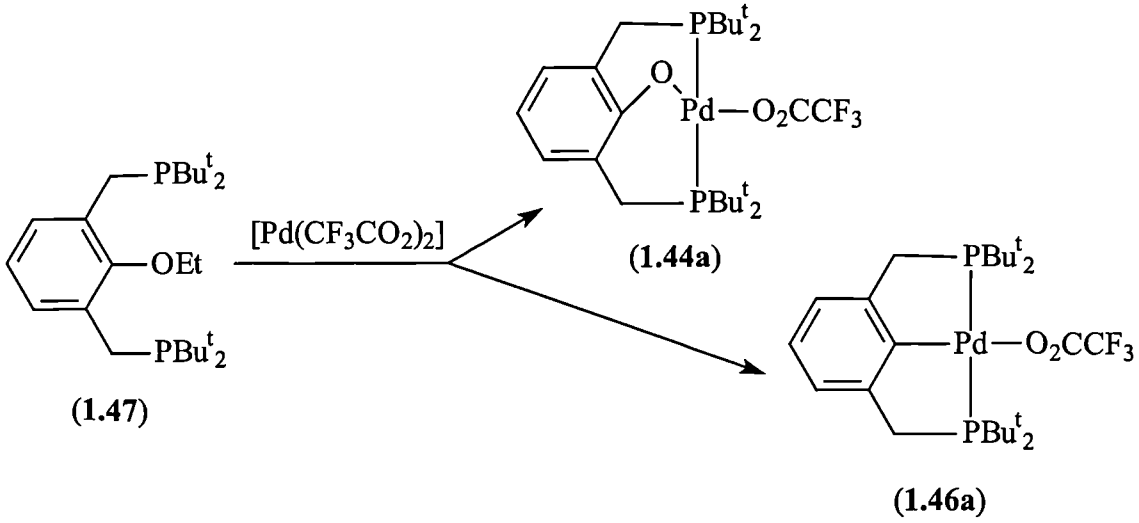

(**1.47**) (**1.44a**) (**1.46a**)

Scheme 1.11

The palladium-catalysed vinylation of aryl halides (the 'Heck Reaction') is a very useful synthetic method for the generation of C-C bonds (see Equation 1.8).[119,120] Milstein *et al.* recently reported thermally stable palladium complexes with PCP-type ligands (**1.48**) and (**1.49**) that give extremely high activites and yields for the Heck reaction.[121]

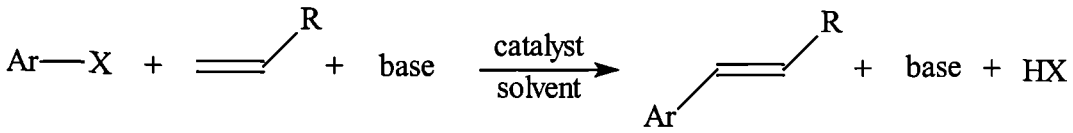

Equation 1.8

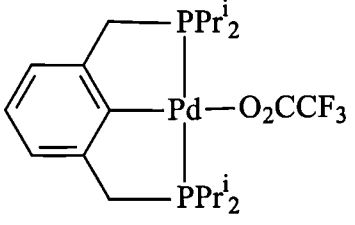

(**1.48**)

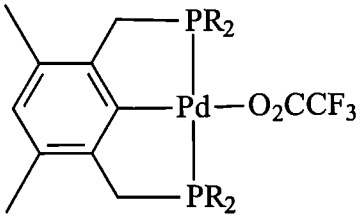

(**1.49a**) R = *i*-Pr
(**1.49b**) R = *t*-Bu

The catalyst system shown is currently, to our knowledge, the most active and stable known. Turnover numbers of up to 500 000 were reported for the coupling of

iodobenzene and methyl acrylate and 100 000 for reactions of non-activated aryl bromides. Complex (**1.49a**) gives the highest turnover rates, attributed to the electron rich metal centre. The reduced efficiency of complex (**1.49b**) is a result of the higher steric bulk of the diphosphine, but it is the steric protection engendered by the diphosphines employed that gives rise to the very high stability of the catalysts.

1.5.1.3 Palladium-catalysed aromatic C-X bond formation (X = N, C, O)

The palladium-catalysed amination of aryl halides[122-127] (Equation 1.9) has become an important method for the synthesis of arylamines which have found use in pharmaceuticals,[128,129] materials with important electronic properties,[130-132] and ligands for early transition metal catalysis.[133]

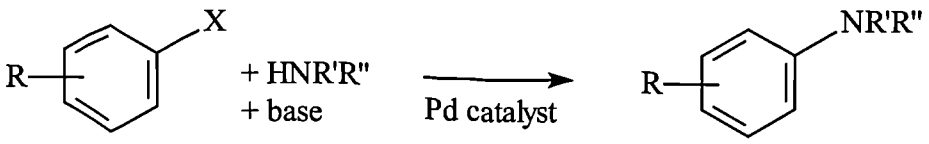

Equation 1.9

Originally, P(*o*-tolyl)$_3$-based palladium complexes were the only catalysts for intermolecular amination chemistry.[134-137] Studies showed that this ligand was unusually effective because each intermediate in the catalytic cycle was a highly unsaturated monophosphine complex, and the selectivity for amination over reduction was enhanced by steric bulk.[134,138] Chelating aryl diphosphines such as dppf and BINAP were then found to be more effective than P(*o*-tolyl)$_3$ in the amination chemistry with many amine and aromatic substrates,[122,126] and the systematic variation of bidentate ligands used highlighted some unusual effects of steric, electronic and geometric perturbations.[139]

These studies led Hartwig *et al.* to believe that bulky alkyl phosphines may accelerate reaction rates by increasing the electron density at the metal centre and favouring ligand dissociation.[140] For these reasons they tested the bulky alkyl diphosphines (**1.50**)-(**1.52**) in the reaction illustrated in Scheme 1.12. The purported catalytic cycle is also illustrated. The results obtained with a variety of substrates demonstrated (i) remarkable rate enhancements for reactions with sterically demanding alkyl diphosphines, (ii) mild conditions for aminations of aryl chlorides, (iii) the first amination of aryl tosylates, and (iv) the first preparation of mixed alkyl arylamines in

high yields by the metal catalysed amination of unactivated aryl chlorides with primary alkylamines.

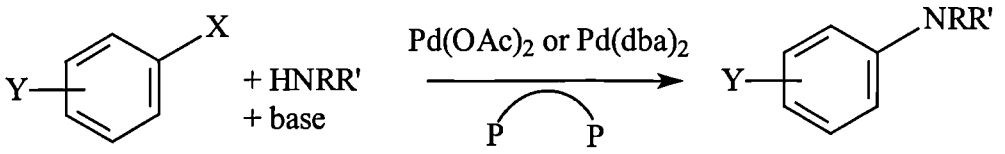

X = Cl, Br, I, OTs

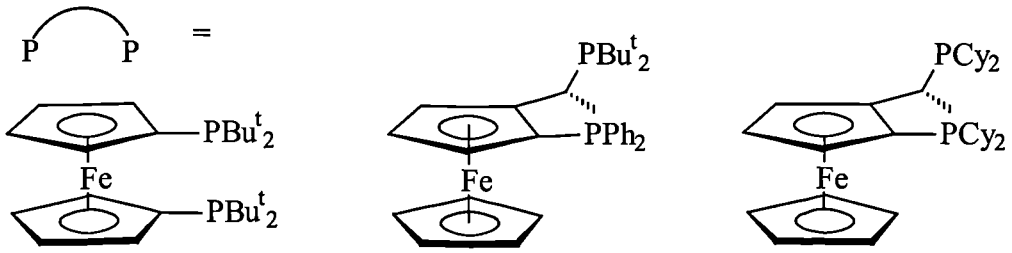

(1.50) **(1.51)** **(1.52)**

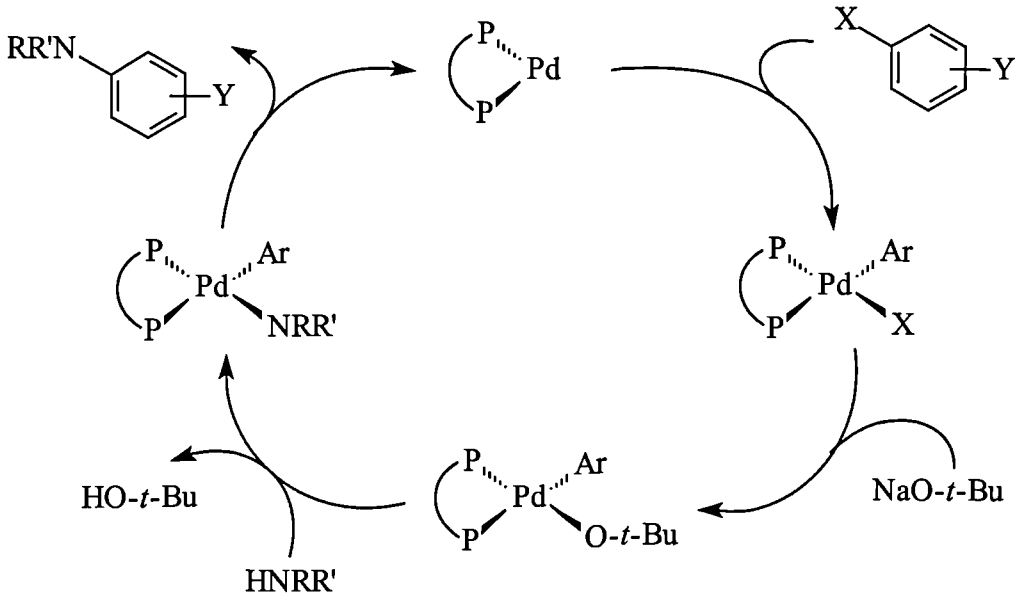

Scheme 1.12

The high activity observed with diphosphines **(1.50)**-**(1.52)** was attributed to their electron donating ability and steric bulk. Workers at Tosoh Co. reported that PBu^t_3 provided high turnover numbers for the Pd-catalysed C-N bond formation in the presence of excess ligand at high temperatures.[141] Hartwig *et al.* subsequently extended the scope of aromatic C-N bond formation with PBu^t_3 as ligand to assess the importance of chelation.[142] They reported room temperature Pd-catalysed amination of aryl bromides and chlorides with a large range of substrates by using PBu^t_3 and $Pd(dba)_2$ in

an approximate 1:1 ratio. Thus, the versatility of this bulky ligand was demonstrated, and the fact that a chelate was not a prerequisite for high activity.

The effect of chelation was also studied with palladium-catalysed C-C bond formation.[143] In this instance, the palladium-catalysed arylation of ketones was investigated with diphosphines (**1.50**) and (**1.51**) and monophosphines PBu^t_3 and PCy_3 (see Equation 1.10). High yields and turnover numbers were reported for the coupling of a variety of alkyl and aryl ketones or malonates with aryl bromides, chlorides and tosylates. These results and mechanistic studies showed that reductive elimination from the palladium-enolate intermediate to generate the coupled product was driven by steric congestion, not chelation. The activation of chloroarenes under mild conditions was also shown not to require chelation. Finally, the arylation of simple malonates was shown to be a convenient route to α-aryl carboxylic acids.

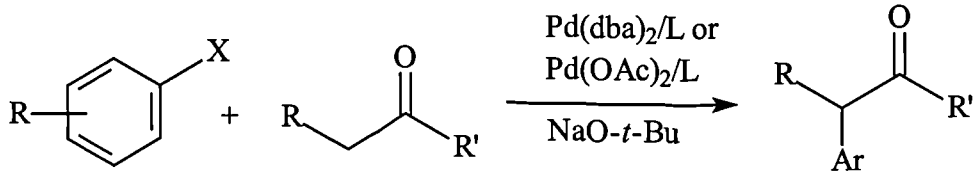

X = Cl, Br, OTs

R, R' = alkyl, aryl
R = C(O)OR, R' = OR'

L = (**1.50**), (**1.51**), PBu^t_3, PCy_3

Equation 1.10

Hartwig *et al.* also reported the use of sterically hindered alkyl phosphines in the Heck olefination of aryl halides.[144] Several readily available phosphines were screened for the palladium-catalysed coupling of an acrylate (with a tethered fluorophore) to an aryl halide (attached to a solid support). The bulky ligands PBu^t_3 and diphosphine (**1.50**) were found to produce the most active ligands reported to date for the olefination of unactivated aryl bromides, ligand (**1.50**) being the most efficient for olefination of unactivated aryl chlorides.

Palladium-catalysed C-O coupling involving unactivated aryl halides was explored recently.[145] High yields of diaryl ether were observed in Pd-catalysed aryl halide etherification with the bulky monophosphines PBu^t_3 and 1-(di-*t*-butyl)phosphinoferrocene (**1.53**) with a variety of substrates (see Equation 1.11).

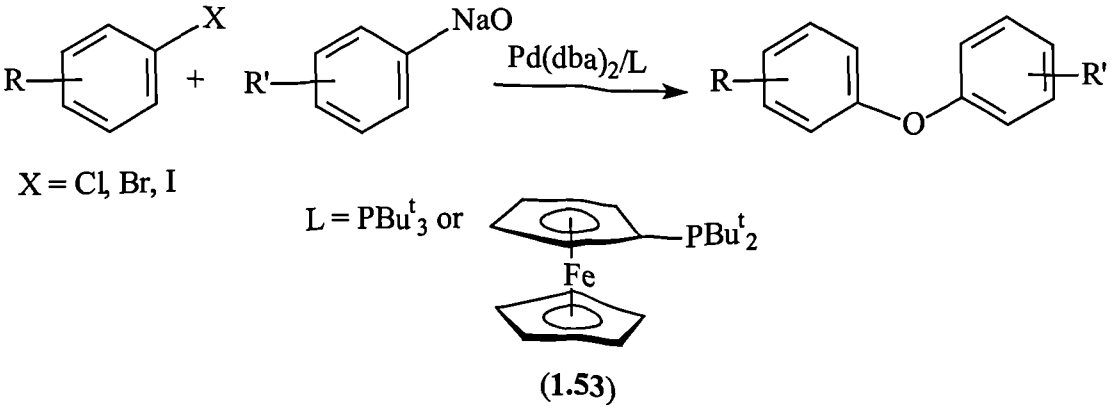

(1.53)

Equation 1.11

Complexes containing phosphines such as dppf, BINAP and P(*o*-tolyl)$_3$ as ligand gave no ether, and although DB^{t}PF (**1.50**) formed an active catalyst, it was shown to be due to ligand cleavage to the monophosphines PPhBu$^t_2$ and (**1.53**). These results contrast the more common C-C bond formation between aryl halides and phenoxides with conventional arylphosphines.[146-148] This is attributed to faster reductive elimination of ethers from arylpalladium phenoxides with the sterically encumbering phosphines PBu$^t_3$ and (**1.53**).

1.5.2 Chemistry of other late transition metal complexes with bulky alkyl phosphines

1.5.2.1 Group 9

Since the early 1980's the group of Werner has reported an enormous number of novel rhodium[149-220] and iridium[153,154,168,189,195,199,203,221-238] based organometallic chemistry, the vast majority of which employing isopropyl- and cyclohexyl-substituted tertiary monophosphine ligands. Caulton *et al.*[239-250] have also been active in this area of research since the early 1990's, focusing more on the application of *t*-butyl substituted tertiary monophosphines in iridium based organometallic chemistry.

Milstein *et al.* have reported the chemistry associated with cyclometallation of bulky phosphines by rhodium [112,118,251-263] and iridium.[253,254,261,264] The bulky diphosphines employed are shown below. Some of this work has recently been reviewed.[265]

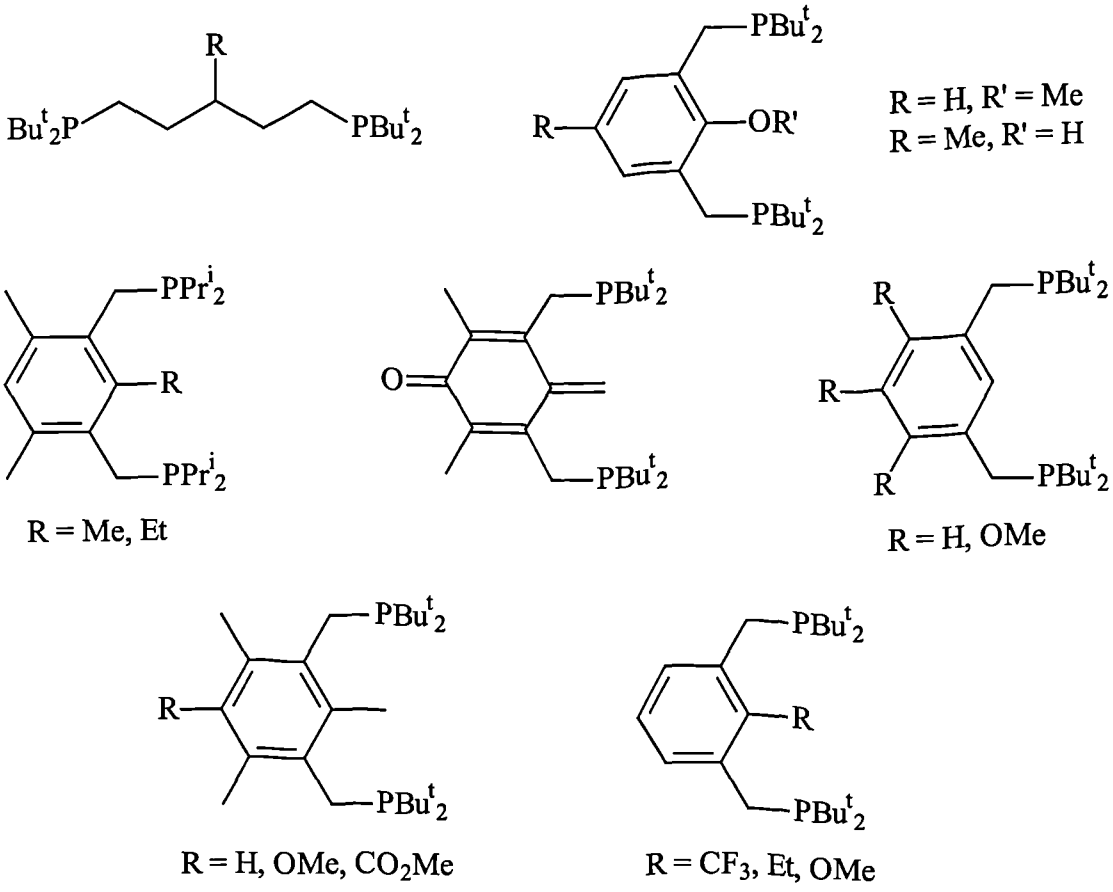

1.5.2.2 Group 8

Since 1985, the group of Werner has developed much bulky tertiary monophosphine chemistry with ruthenium[266-288] and osmium.[266-272,274,277,289-314]

Since 1992, the group of Caulton has added to this wealth of bulky phosphine-mediated chemistry with ruthenium[288,315-351] and osmium.[341,342,345,352-365] . Esteruelas *et al.* have also contributed to the understanding in this field.[366-370] There are also examples of bulky phosphine-stabilised iron complexes.[210,371,372] The vast majority of the phosphines used in the chemistry cited above were monodentate, tertiary phosphines based on *t*-butyl, isopropyl or cyclohexyl substituents.

1.5 Aims

Following the work by Gee (see Section 3.1), we set out to prepare a series of new bulky alkyl cage phosphines (phospha-adamantanes), investigating their synthesis, coordination chemistry and application in homogeneous catalysis. More detailed and relevant aims are described in the introductions to each of the following chapters.

Chapter 2

Monodentate tetramethyl-trioxa-phospha-adamantanes

2.1 Introduction

2.1.1 Synthesis of monodentate tetramethyl-trioxa-phospha-adamantanes

The first example of a 1,3,5,7-tetramethyl-4,6,8-trioxa-2-phospha-adamantane compound was reported in 1961 by Epstein and Buckler.[373] They found that solutions of 2,4-pentanedione in aqueous hydrochloric acid readily absorbed PH_3 and a white crystalline solid was precipitated, assigned to the cage secondary phosphine (**2.1**) (Equation 2.1) on the basis of chemical and spectroscopic evidence.

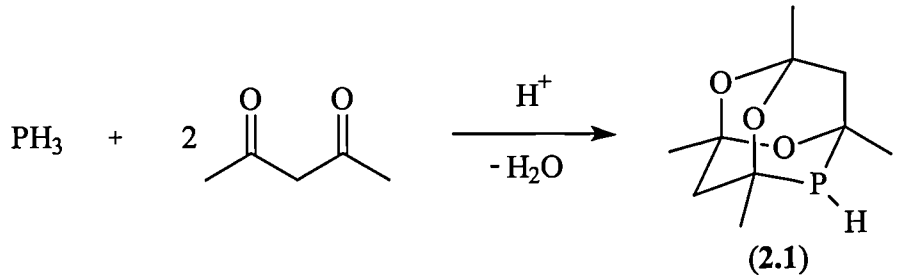

(**2.1**)

Equation 2.1

The acid-catalysed addition of PH_3 to hexafluoropentanedione and heptane-2,4-dione yielded similar secondary cage phosphines (**2.2**) and (**2.3**) respectively.[374] Furthermore, certain primary phosphines have been treated with 2,4-pentanedione to give crystalline tertiary derivatives (**2.4**)-(**2.6**).[373,374]

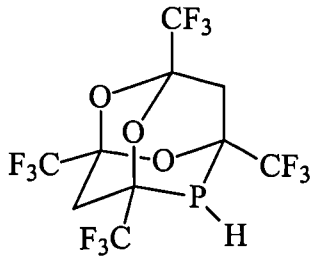

(**2.2**)

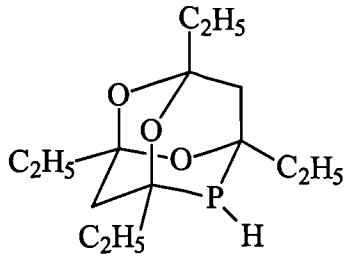

(**2.3**)

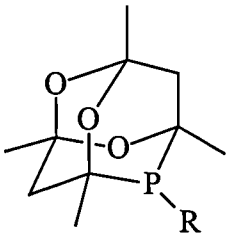

R = *n*-C_8H_{17} (**2.4**)
R = *i*-C_4H_9 (**2.5**)
R = Ph (**2.6**)

The addition of P-H containing compounds to carbonyls has recently been reviewed by Gee;[375] who named this phosphorus cage moiety "*adamphosphino*" based on Downing's naming of 1,3,5,7-tetramethyl-4,6,8-trioxa-2-phospha-adamantane (**2.1**) as "*adamphos*".[376] The formation of phospha-adamantanes (**2.1**)-(**2.6**) are examples of hydrophosphination/dehydration reactions.

2.1.2 Stereochemistry of tetramethyl-trioxa-phospha-adamantane cages

Closer inspection of adamphos shows that it is chiral; the molecule has four stereocentres at the 1,3,5 and 7 positions (Figure 2.1), resulting in two enantiomers for all phospha-adamantane cages. The enantiomers are arbitrarily labelled α and β. Structurally, interconversion between α and β is achieved simply by exchanging two oxygen atoms with two CH_2 groups.

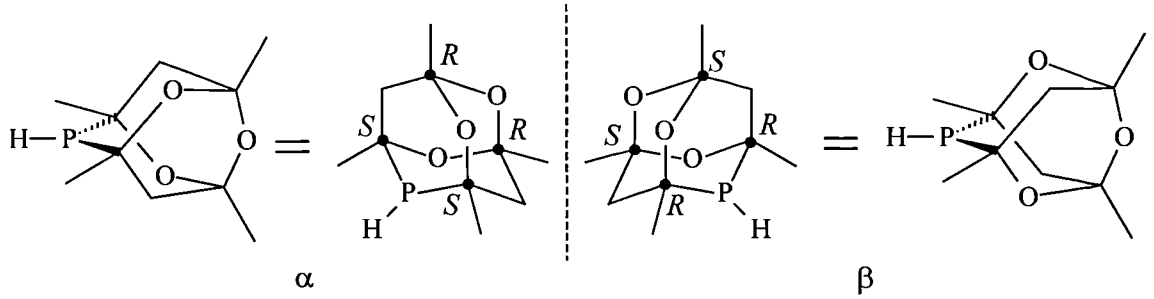

Figure 2.1 Stereochemistry of adamphos (**2.1**)

The secondary dodecafluoro-phospha-adamantane (**2.2**) similarly exists in two enantiomers, but the CF_3 substituents (and any group with higher priority than CH_3) reverse the *R* and *S* notation for the absolute stereochemistry of the 1,3,5 and 7-position carbon atoms (Figure 2.2). However, the position of the oxygen atoms, and the α and β assignments remain the same for all phospha-adamantane cages described in this thesis.

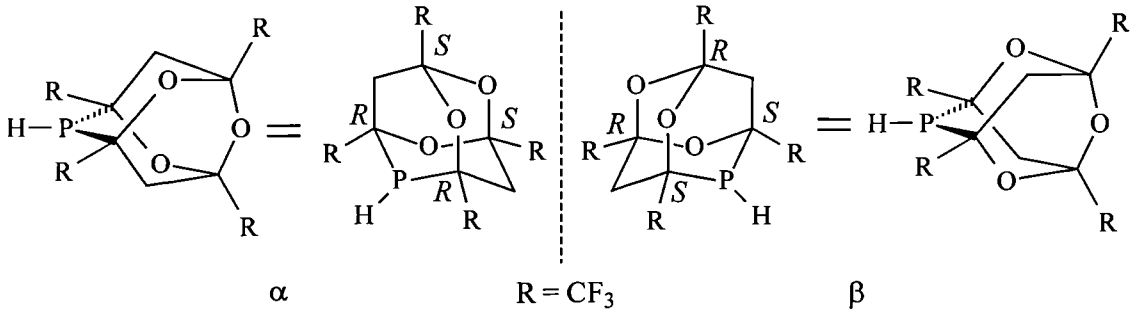

Figure 2.2 Stereochemistry of dodecafluoro-phospha-adamantane (**2.2**)

Epstein suggested a mechanism for the acid-catalysed formation of adamphos[373] that Gee extended to rationalise the formation of bis(phospha-adamantyl)alkanes (see Section 3.1) from bis(diphosphino)ethane and bis(diphosphino)propane with pentane-2,4-dione and 1,1,1-trifluoro-pentane-2,4-dione.[375,377] A truncated version of this mechanism is given in Scheme 2.1.

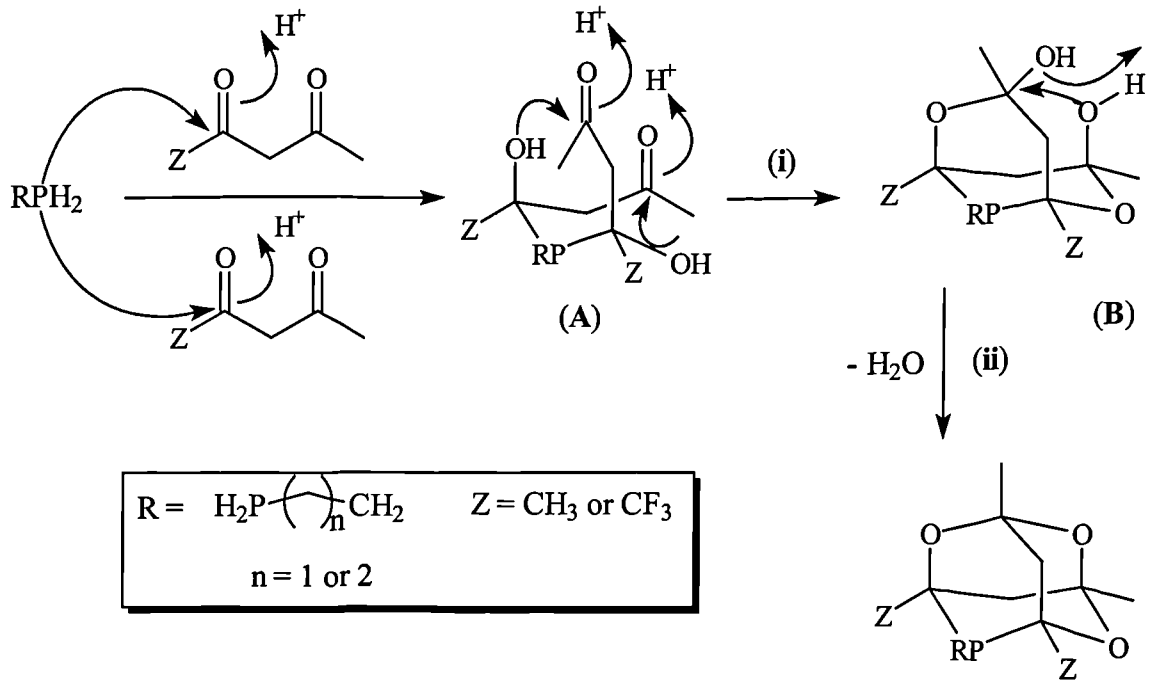

Scheme 2.1 Acid-catalysed mechanism of phospha-adamantane formation

The mechanism proceeds with two P-H additions to carbonyls to form bis(α-hydroxymethyl)phosphine (**A**). Subsequent double intramolecular nucleophilic attack of hydroxy on carbonyl (**i**) affords the cyclic hemiketal (**B**). The two generated hydroxy groups are in close proximity to one another due to the double chair conformation of the two rings, facilitating a condensation reaction (**ii**) to give the phospha-adamantane and water.

Roschenthaler *et al.*[378,379] investigated the reaction of PH_3 with 1,1,1-trifluoro-pentane-2,4-dione and 1,1,1,5,5,5-hexafluoro-pentane-2,4-dione, in the absence of acid catalyst or solvent. They found that the two 1,3-diketones used afforded different types of products, the hexafluoro-phospha-adamantane α/β-(**2.12**) from reaction with trifluoropentanedione, and the bicyclic compound (**2.11a**) from reaction with 1,1,1,5,5,5-hexafluoro-2,4-pentanedione. They postulated a mechanism for the formation of these two products using NMR spectroscopic evidence in support of some of the intermediates and addressed stereochemical features of cage formation. The erroneous assignments they made of absolute stereochemistry have been corrected in the mechanism illustrated in Scheme 2.2.

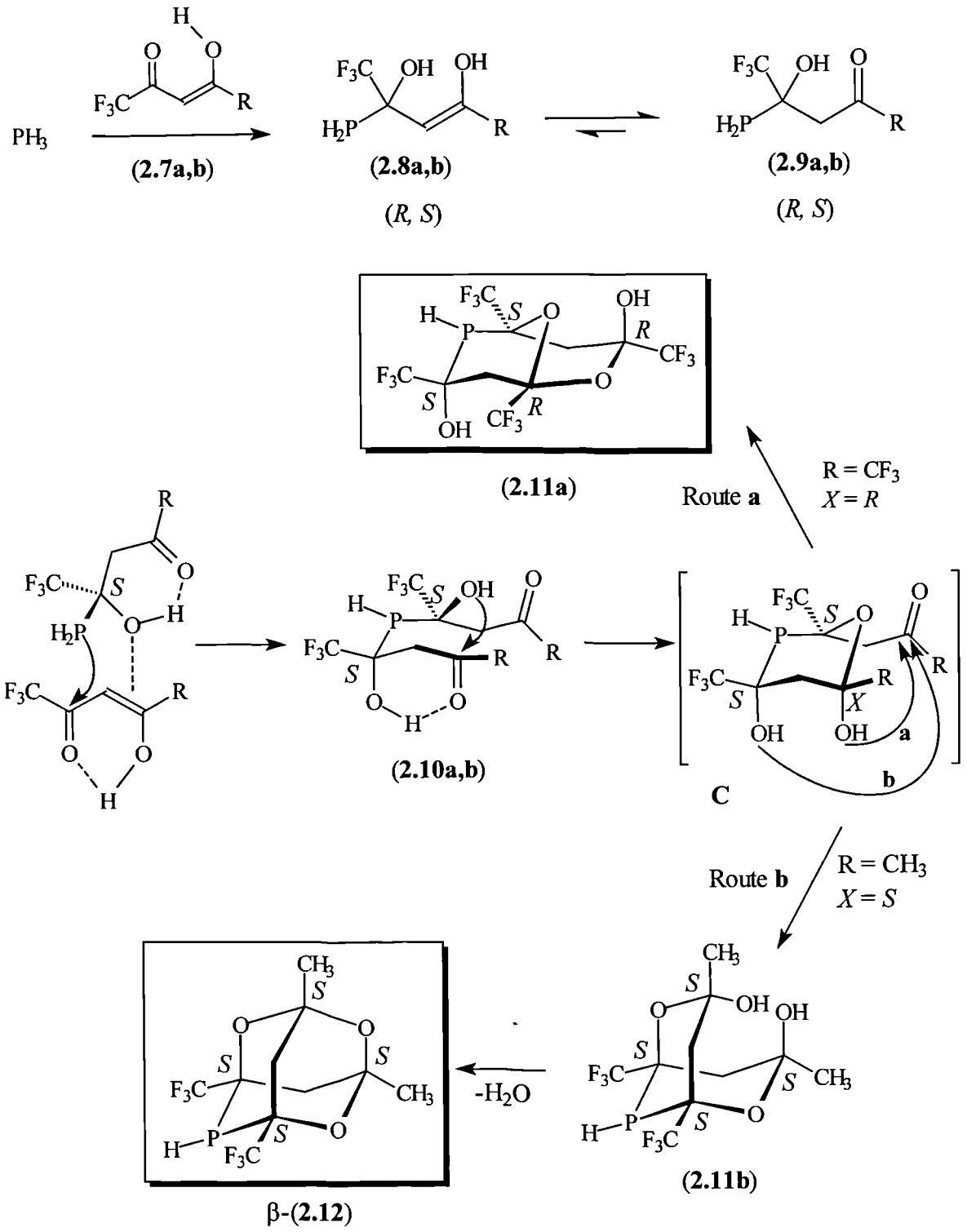

Scheme 2.2 "Diastereoselective" synthesis of phospha-adamantane (**2.12**) and bicyclic compound (**2.11a**).

Addition of PH_3 to the keto/enol tautomers (**2.7a,b**) affords the chiral (*R,S*)-α-hydroxyphosphine (**2.8a,b**), whose enol functions isomerise to the corresponding ketones (**2.9a,b**). The PH_2 group of (*R,S*)-(**2.9a,b**) then adds to another molecule of keto-(**2.7a,b**). This "diastereoselective" addition results in the two carbon atoms

adjacent to phosphorus having the same absolute stereochemistry, and the authors suggest that if the orientation of the approach is governed by an additional OH···π interaction,[380] (*S,S*)- and (*R,R*)-(**2.10a,b**) are exclusively formed (pathways are depicted for (*S*)-(**2.9a,b**)).

Subsequently the cyclic, chair-configured hemiketal intermediate (**C**) is formed, creating a new stereocentre whose *R* or *S* assignment depends on whether R = CH_3 or CF_3. The formation of bicyclic (**2.11a**) is achieved by intramolecular hemiketal cyclisation of the 6-OH group with the remaining keto-function (route **a**). The compound (**2.11a**) cannot undergo the intramolecular condensation reaction due to the orientation of OH groups conferred by the chair-boat conformation of the two rings.

The analogous acid mediated reaction to form phospha-adamantane α/β-(**2.2**)[374] presumably proceeds by 4-OH cyclisation with the free keto-function, enabling dehydration *via* the double chair conformation (see Scheme 2.1) to form the phospha-admantane cage. This pathway (route **b**) is also used to explain the formation of α/β-(**2.12**).

Both the mechanisms described (Scheme 2.1 and 2.2) have their value, but our work discussed in Chapter 3 (see Section 3.2.1) suggests that, especially in acid-catalysed phospha-adamantane cage formation, many possible intermediates (not just those that must form in order to generate the observed products) are in equilibria with each other, and the thermodynamic stability of the phospha-adamantane cage and/or its precipitation from solution results in moderate to excellent yields of the cages described. Hence, although the diastereoselective mechanism postulated by Roschenthaler *et al.*[378] is consistent with the observed products, it must be borne in mind that phospha-adamantanes can only exist if the carbon atoms adjacent to phosphorus have the same absolute stereochemistry.

2.1.3 Coordination chemistry of tetramethyl-trioxa-phospha-adamantanes

To our knowledge, the coordination chemistry of the ligands discussed in the previous section has been little studied. Downing[376] showed that the secondary cage phosphine (**2.1**), named "*adamphos*", forms stable complexes with a range of transition metals. This chemistry has recently been reviewed by Gee,[375] who also studied the synthesis and coordination chemistry of some bidentate bis(phospha-adamantyl)alkanes; this will be discussed in Section 3.1.

The aim of this work was to investigate the synthesis of tertiary derivatives of the phospha-adamantane (**2.1**) by the hydrophosphination of 1,3-dicarbonyls with some primary phosphines, and then study the metal chemistry of the new ligands.

2.2 Synthesis and characterisation of tertiary monodentate phospha-adamantanes

2.2.1 Reactions of 1,3-diketones with phenylphosphine

The reaction of $PhPH_2$ with acetylacetone has already been reported by Epstein, yielding the tertiary phospha-adamantane (**2.6**) and other products (discussed in Section 5.1). It was decided to extend this reaction to fluorinated 1,3-diketones. The reaction of 6 equivalents of hexafluoropentanedione with $PhPH_2$ in 5M HCl resulted in immediate precipitation of a white solid, but *ca.* 10 resonances were observed in the $^{31}P\{^1H\}$ NMR spectrum of this product. The analogous reaction with 1,1,1-trifluoropentanedione (Equation 2.2) afforded crystals of the phenyl hexafluoro-phospha-adamantane α/β-(**2.13**) in excellent yield.

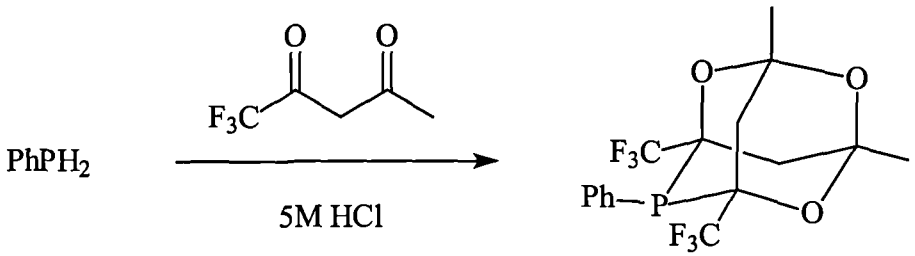

(2.13)

Equation 2.2

The product shows a broad singlet at δ -39.2 p.p.m. in the $^{31}P\{^1H\}$ NMR spectrum, due to unresolved coupling to fluorine. This coupling is resolved in the $^{19}F\{^1H\}$ NMR spectrum, which exhibits doublets at δ 98.15 p.p.m. (^3J(PF) = 14.6 Hz) and δ 99.96 p.p.m. (^3J(PF) = 16.4 Hz). The product was also characterised by ^1H and $^{13}C\{^1H\}$ NMR spectroscopy (Table 2.3), mass spectrometry, elemental analysis (see Experimental) and *X*-ray crystallography.

The β-enantiomer of phospha-adamantane (**2.13**) is illustrated in Equation 2.2, although the product is of course racemic. The crystal structure determination was carried out by Miss. H. Phetmung in this department. Single crystals were obtained from the crude product, and the structure determined showed a racemic mixture of α- and β-(**2.13**) and was solved in the monoclinic space group $P2_1/c$ with four formula

units per unit cell. The numbering scheme and molecular structure is shown in Figure 2.3. The salient features (Tables 2.1 and 2.2) are the small C(3)-P-C(6) angle and the corresponding[79] increase in P-C(3) and P-C(6) bond lengths characteristic of phospha-adamantane cages.[375,377,378]

Table 2.1 Selected bond lengths (Å) for β-(**2.13**)

Bond	length/ Å
P(1)-C(11)	1.834(2)
P(1)-C(1)	1.900(2)
P(1)-C(6)	1.911(2)

Table 2.2 Selected bond angles (°) for β-(**2.13**)

Bond	angle/°
C(11)-P(1)-C(1)	107.41(7)
C(11)-P(1)-C(6)	102.67(7)
C(1)-P(1)-C(6)	88.87(7)

The method of data collection, structure solution and refinement, the tables containing atomic coordinates, bond lengths and angles, isotropic and anisotropic displacement coefficients are all collected in the Appendix.

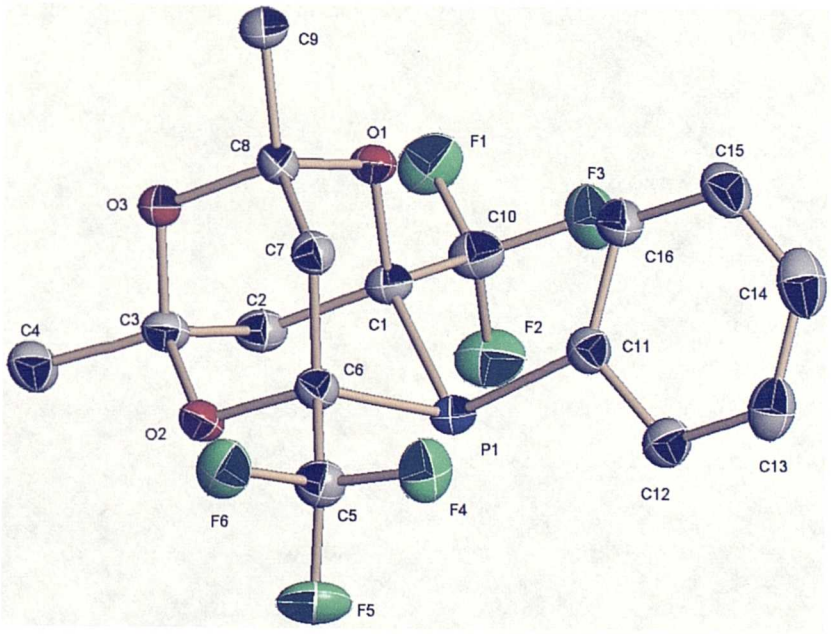

Figure 2.3 Molecular structure of phenyl hexaflouro-phospha-adamantane β-(2.13). All hydrogen atoms are omitted for clarity.

Table 2.3 $^{13}C\{^1H\}$ NMR[a] and ^1H NMR[b] data for hexaflouro-phospha-adamantane α/β-(**2.13**)

	$\delta(^{13}C)$[c]		$\delta(^1H)$[d]
C5 and C10	135.9 (br m), 128.4 – 131.3 (m)	7.86	(m, 2H, *o*-$H_2C_6H_3$)
C3 and C8	97.4 (s), 96.8 (s)	7.35 – 7.46	(m, 3H, *m,p*-$H_3C_6H_3$)
C1 and C6	77.6 – 79.1 (m)	2.16 – 2.39	(m, 3H, CH_2 + C*H*H)
C2 and C7	36.7 (d, ^2J(PC) 13.7) 28.5 (s)	1.97	(d,d, 1H, C*H*H, ^2J(PH) 2.2, ^2J(HH) 13.4)
C4 and C9	27.8 (s) 27.3 (s)	1.59 1.53	(s, 3H, CH_3) (s, 3H, CH_3)

[a] Spectra recorded at 100 MHz in $CDCl_3$ at 28 °C. Chemical shifts [$\delta(^{13}C)$] in p.p.m.(± 0.1) relative to $CDCl_3$ (77.0 p.p.m.). Coupling constants (*J*) in Hz (± 0.1).

[b] Spectra recorded at 300 MHz in $CDCl_3$ at 24 °C. Chemical shifts [$\delta(^1H)$] in p.p.m.(± 0.1) relative to residual solvent (7.26 p.p.m.). Coupling constants (*J*) in Hz (± 0.1).

[c] Assigned in parallel with $^{13}C\{^1H\}$ NMR DEPT spectrum.

[d] Detailed assignments made on the basis of ^1H COSY NMR.

2.2.2 Reaction of isopropyl phosphine with 2,4-pentanedione

Stirring isopropyl phosphine and 2,4-pentanedione in 10 M HCl for 11 days gave the white solid isopropyl phospha-adamantane α/β-(**2.14**) in moderate yield (Equation 2.3).

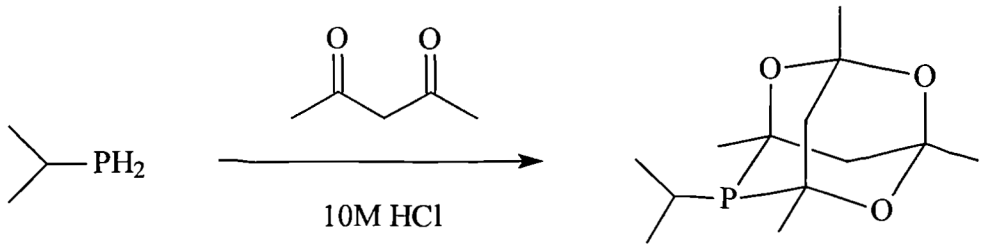

(**2.14**)

Equation 2.3

The ligand has been characterised by $^{31}P\{^1H\}$ (δ -7.9 p.p.m.), ^1H and $^{13}C\{^1H\}$ NMR spectroscopy (Table 2.4) and elemental analysis (see Experimental). Comparing the $^{13}C\{^1H\}$ NMR data for phospha-adamantanes (**2.13**) and (**2.14**), there is more resolved *J*(PC) coupling for the latter, probably a consequence of unresolved C-F

coupling broadening the resonances in the former. The NMR data shown in Tables 2.3 and 2.4 are consistent with those reported for the analogous secondary phosphines (**2.1**)[376] and (**2.12**).[378]

Table 2.4 $^{13}C\{^1H\}$ NMR[a] and ^1H NMR[b] data for phospha-adamantane α/β-(**2.14**)

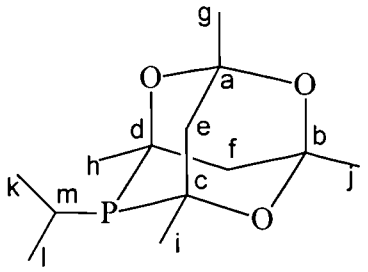

	$\delta(^{13}C)$[c]		$\delta(^1H)$[d]
a and b	96.3 (s), 95.8 (s)	1.06	(d of d, 3H, C*H*$_3$ (k or l), ^3J(PH) 10.6, ^3J(HH) 7.2)
c and d	73.4 (d, ^1J(PC) 24.7), 72.8 (d, ^1J(PC) 12.8)	1.21	(d of d, 3H, C*H*$_3$ (k or l), ^3J(PH) 16.4, ^3J(HH) 6.9)
e and f	45.7 (d, ^2J(PC) 14.7), 38.2 (s)	1.34	(s, 3H, C*H*$_3$ (g or j))
g and j	28.3 (s), 28.0 (s)	1.36	(s, 3H, C*H*$_3$ (g or j))
h and i	29.9 (d, ^2J(PC) 21.1), 28.6 (d, ^2J(PC) 11.9)	1.37	(s, 3H, C*H*$_3$ (h or i))
		1.41	(s, 3H, C*H*$_3$ (h or i))
m	23.8 (d, ^1J(PC) 23.8)	1.60 – 1.82	(m, 3H, C*H*$_2$ + C*H*H (e, f))
k and l	21.3 (d, ^2J(PC) 21.1) 21.1 (d, ^2J(PC) 9.2)	1.86 – 2.04	(m, 2H, C*H* (m) + C*H*H (e or f))

[a] Spectra recorded at 100 MHz in $CDCl_3$ at 28 °C. Chemical shifts [$\delta(^{13}C)$] in p.p.m.(± 0.1) relative to $CDCl_3$ (77.0 p.p.m.). Coupling constants (*J*) in Hz (± 0.1).

[b] Spectra recorded at 300 MHz in $CDCl_3$ at 24 °C. Chemical shifts [$\delta(^1H)$] in p.p.m.(± 0.1) relative to residual solvent (7.26 p.p.m.). Coupling constants (*J*) in Hz (± 0.1).

[c] Assigned in parallel with $^{13}C\{^1H\}$ NMR DEPT spectrum.

[d] Detailed assignments made on the basis of ^1H COSY NMR.

2.2.3 Reaction of cyclohexylphosphine with 2,4-pentanedione

This work was carried out by Dr. Charles Carraz at the University of Windsor, Canada, who kindly donated a sample for studying the coordination chemistry with platinum(II) and palladium(II) (Section 2.3.3 and 5.5). He reacted (see Experimental) cyclohexylphosphine with 2,4-pentanedione in 5 M HCl to form the phospha-

adamantane α/β-(**2.15**) (Equation 2.4). However, the sample provided consisted of *ca.* 85 % (**2.15**) by $^{31}P\{^{1}H\}$ NMR spectroscopy, and the remaining 15 % was unassigned (see Section 5.5)

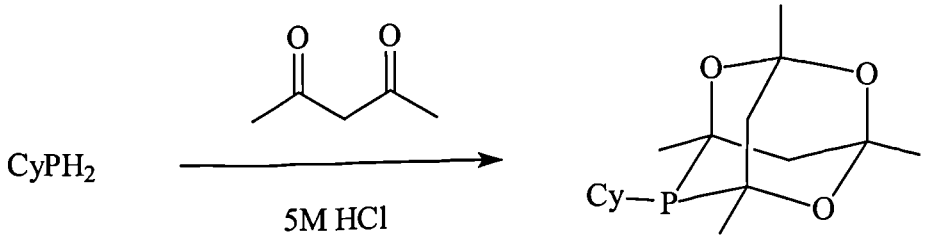

2.15

Equation 2.4

2.3.1 Coordination chemistry of phenyl hexafluorophospha-adamantane α/β-(2.13)

Addition of 2.2 equiv. of (**2.13**) to $[PdCl_2(NCPh)_2]$ in dichloromethane afforded the diastereomeric mixture *meso/rac*-(**2.16**) as a yellow solid.

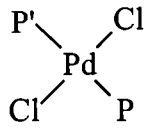

rac-(**2.16**): P = P' = α-(**2.13**) or β-(**2.13**)

meso-(**2.16**): P = α-(**2.13**); P' = β-(**2.13**)

Characterisation by NMR spectroscopy was difficult due to the insolubility of the product, and only a very weak $^{31}P\{^{1}H\}$ NMR spectrum of the product was obtained, showing two singlets at δ 4.61 and 4.83 p.p.m. corresponding to the two diastereomers. Further characterisation was obtained by mass spectrometry, elemental analysis (see Experimental) and *X*-ray crystallography. Single crystals were grown by slow evaporation of solvent from a weak dichloromethane solution of the complex and the structure determination was carried out by Miss H. Phetmung of this department, confirming the *trans*-orientation of the ligands around the palladium(II) centre. The structure was solved in the monoclinic space group C2/c with four formula units per unit cell, and the crystal was shown to be exclusively the *rac*-diastereomer (equal number of enantiomers (αα and ββ), so racemic overall). The molecular structure and selected numbering scheme is shown in Figure 2.4.

The molecular structure demonstrates the sterically encumbering nature of this ligand, the CF_3 groups encroaching on the Pd(II) centre. In order to determine the steric bulk of the ligand (**2.13**), a ligand cone angle[25] was measured from the crystal structure

of the metal complex *rac*-(**2.16**). The calculation of the cone angle (θ) was carried out following methods reported by Tolman[24] and found to be 167° (*cf.* 145° for PPh_3[25]).

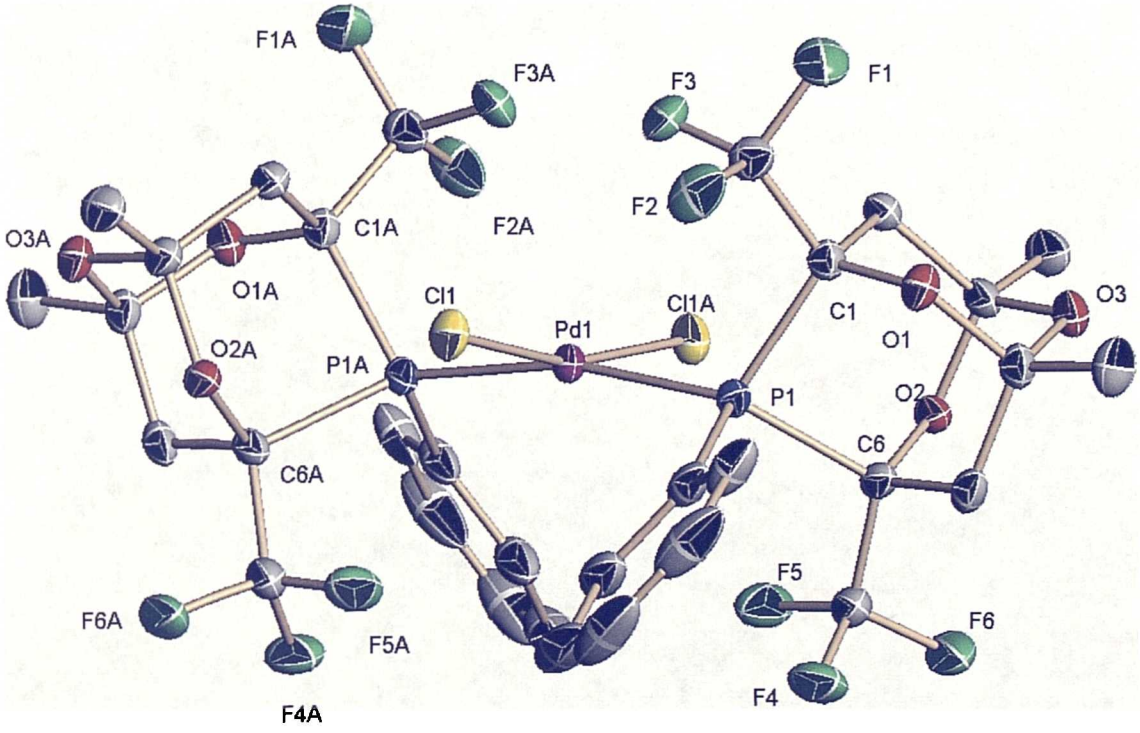

Figure 2.4 Molecular structure and selected numbering scheme for *rac*-(**2.16**). Hydrogen atoms are omitted for clarity.

Clearly, *cis*-orientation of the two hexafluoro-phospha-adamantanes is precluded on steric grounds, and even in *rac-trans*-(**2.16**), there is significant distortion from square planar as a result of these bulky ligands. The method of data collection, structure solution and refinement, the tables containing atomic coordinates, bond lengths and angles, isotropic and anisotropic displacement coefficients are all collected in the Appendix.

The reactions between 2.2 equiv. of (**2.13**) with $[PtCl_2(cod)]$ in CH_2Cl_2 and 2.1 equiv. of (**2.13**) with $[PtCl_2(SMe_2)_2]$ were followed by $^{31}P\{^1H\}$ NMR spectroscopy. After 1 day, the $^{31}P\{^1H\}$ NMR spectrum of the $[PtCl_2(cod)]$ reaction showed only unreacted (**2.13**), even upon heating the solution to reflux. The $^{31}P\{^1H\}$ NMR spectrum of the $[PtCl_2(SMe_2)_2]$ reaction showed *ca.* 70% unreacted (**2.13**) and resonances at δ -

15.15 and -15.26 p.p.m. with platinum satellites (^1J(PtP) 3959 Hz) consistent with the formation of the diastereomeric mixture *meso/rac-trans*-[$PtCl_2$(**2.13**)$_2$]. This coupling constant is very high for a *trans*-coordinated monodentate phosphine, but analogous weakly coordinated fluorocarbylphosphines[389] show similar values. To achieve complete reaction between (**2.13**) and platinum(II), more forcing conditions *e.g.* refluxing in toluene may be required. The fact that the reaction is slow is probably a reflection of the steric bulk of this phospha-adamantane, inhibiting reaction with the relative kinetically inert platinum(II).

Addition of 4.2 equiv. of (**2.13**) to [$Rh_2Cl_2(CO)_4$] in dichloromethane yielded the yellow solid *meso/rac*-(**2.17**) in excellent yield.

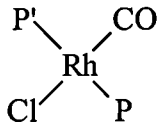

rac-(**2.17**): P = P' = α-(**2.13**) or β-(**2.13**)

meso-(**2.17**): P = α-(**2.13**); P' = β-(**2.13**)

The $^{31}P\{^1H\}$ NMR spectrum of the product showed a broad resonance at δ 14.9 p.p.m. (d, J(RhP) 150 Hz). The diastereoisomerism is not resolved, tentatively assigned to CO exchange in solution or unresolved P-F coupling rendering the resonance broad. *Meso/rac*-(**2.17**) was also characterised by mass spectrometry, elemental analysis (see Experimental) and *X*-ray crystallography. Single crystals were grown by slow evaporation of solvent from a weak dichloromethane solution of complex *meso/rac*-(**2.17**). The structure determination was carried out by Miss H. Phetmung of this department, confirming the *trans*-orientation of the ligands around the rhodium(I) metal. The structure was solved in the monoclinic space group $P2_1/c$ with four formula units per unit cell, and the crystal was shown to be exclusively the *rac*-diastereomer (equal number of enantiomers (αα and ββ)). The selected numbering scheme and molecular structure is shown in Figure 2.5. The method of data collection, structure solution and refinement, the tables containing atomic coordinates, bond lengths and angles, isotropic and anisotropic displacement coefficients are all collected in the Appendix.

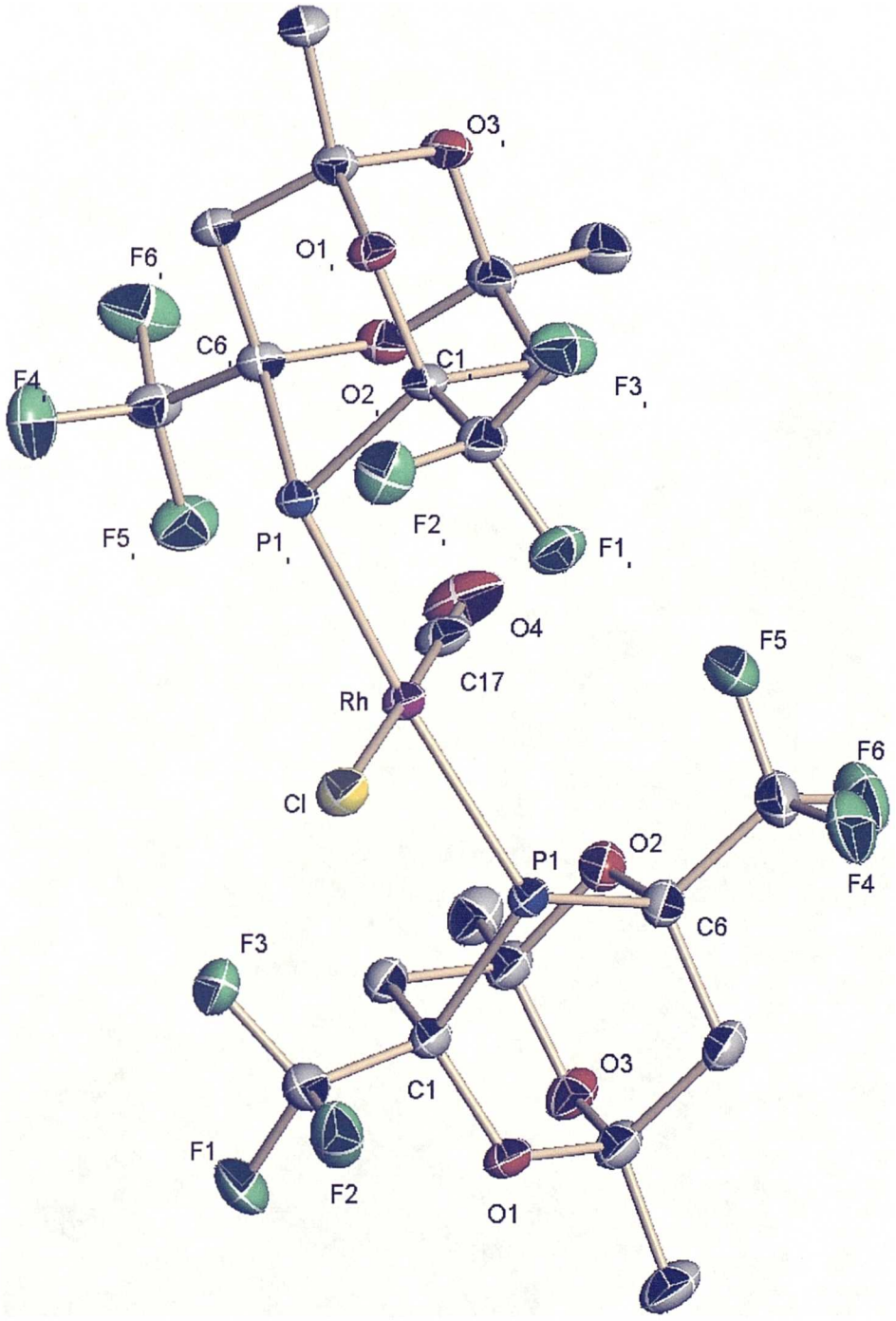

Figure 2.5 Molecular structure of rhodium complex *trans-rac*-(**2.17**). Phenyl rings and all hydrogen atoms have been omitted for clarity

2.3.2 Coordination chemistry of isopropyl phospha-adamantane α/β-(2.14)

Addition of 2.1 equiv. of (**2.14**) to $[PtCl_2(cod)]$ in dichloromethane afforded the diastereomeric mixture *meso/rac*-(**2.18**) as a white solid.

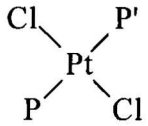

rac-(**2.18**): P = P' = α-(**2.14**) or β-(**2.14**)

meso-(**2.18**): P = α-(**2.14**); P' = β-(**2.14**)

The $^{31}P\{^1H\}$ NMR spectrum of the product showed two resonances at δ 3.08 and 3.16 p.p.m. corresponding to the two diastereomers with platinum satellites (^1J(PtP) 2600 and 2610 Hz respectively). The ^1J(PtP) coupling constant is indicative of *trans*-orientation of the phospha-adamantane to platinum(II). The $^{195}Pt\{^1H\}$ NMR spectrum exhibited two triplets (^1J(PtP) 2600 and 2610 Hz) at δ 868 and 871 p.p.m. corresponding to the two diastereomers (Figure 2.6). *Meso/rac*-(**2.18**) was further characterised by ^1H NMR spectroscopy, mass spectrometry and elemental analysis (see Experimental).

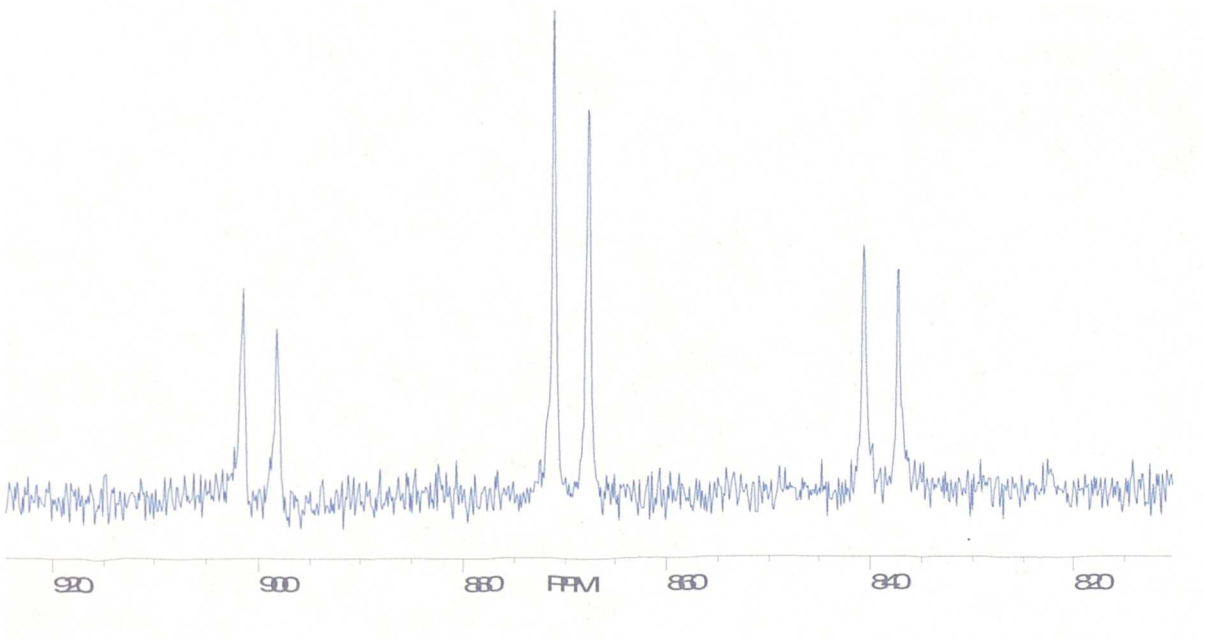

Figure 2.6 $^{195}Pt\{^1H\}$ NMR spectrum of *meso/rac*-(**2.18**)

The reaction between 2.1 equiv. of (**2.14**) and $[PdCl_2(NCPh)_2]$ was followed by $^{31}P\{^1H\}$ NMR spectroscopy. Two singlets were observed at δ 13.1 and 13.3 p.p.m. corresponding to two diastereomers. A yellow solid was isolated, but further NMR characterisation proved difficult due to insolubility. Mass spectrometry and satisfactory

elemental analysis data were obtained (see Experimental), and the product is tentatively assigned to *meso/rac*-(**2.19**).

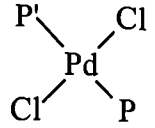

rac-(**2.19**): P = P' = α-(**2.14**) or β-(**2.14**)
meso-(**2.19**): P = α-(**2.14**); P' = β-(**2.14**)

The reaction of 4.1 equiv. of (**2.14**) and $[Rh_2Cl_2(CO)_4]$ was followed by $^{31}P\{^1H\}$ NMR spectroscopy, which exhibited two doublets (^1J(RhP) 130 Hz) tentatively assigned to the mixture *meso/rac*-(**2.20**).

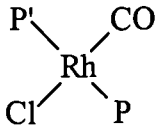

rac-(**2.20**): P = P' = α-(**2.14**) or β-(**2.14**)
meso-(**2.20**): P = α-(**2.14**); P' = β-(**2.14**)

2.3.3 Coordination chemistry of cyclohexylphospha-adamantane α/β-(2.15)

Addition of 2.0 equiv. of (**2.15**) to $[PtCl_2(cod)]$ in dichloromethane afforded the diastereomeric mixture *meso/rac*-(**2.21**) as a pale yellow solid, characterised by $^{31}P\{^1H\}$, ^1H and $^{13}C\{^1H\}$ NMR spectroscopy, mass spectrometry (see Experimental) and *X*-ray crystallography (see Appendix).

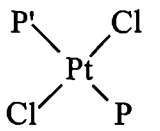

rac-(**2.21**): P = P' = α-(**2.15**) or β-(**2.15**)
meso-(**2.21**): P = α-(**2.15**); P' = β-(**2.15**)

The $^{31}P\{^1H\}$ NMR spectrum of the product showed two singlets at δ -0.03 and -0.11 p.p.m. corresponding to the two diastereomers, with platinum satellites (J(PtP) 2599 Hz). Two separate coupling constants were not observed due to chemical shift anisotropy rendering the satellite resonances broad. Another resonance was observed at -33.9 p.p.m., the assignment of which is discussed in Section 5.5.

Addition of 2.0 equiv. of (**2.15**) to $[PdCl_2(NCPh)_2]$ in dichloromethane afforded the diastereomeric mixture *meso/rac*-(**2.22**) as an orange solid, characterised by $^{31}P\{^1H\}$, ^1H and $^{13}C\{^1H\}$ NMR spectroscopy, mass spectrometry (see Experimental) and *X*-ray crystallography (see Appendix).

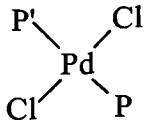

rac-(**2.22**): P = P' = α-(**2.15**) or β-(**2.15**)
meso-(**2.22**): P = α-(**2.15**); P' = β-(**2.15**)

The $^{31}P\{^{1}H\}$ NMR spectrum of the product showed the expected two singlets at δ 9.20 and 9.36 p.p.m., and the *X*-ray structure confirmed the *trans*-configuration of the ligand around palladium(II). Single crystals were grown from dichloromethane/hexane and the structure determination was carried out by Miss H. Phetmung of this department. The structure was solved in the triclinic space group P1 with four formula units per unit cell, and the crystal was shown to be exclusively the -*rac*-diastereomer (equal number of enantiomers (αα and ββ)). The numbering scheme and molecular structure is shown in Figure 2.7. The method of data collection, structure solution and refinement, the tables containing atomic coordinates, bond lengths and angles, isotropic and anisotropic displacement coefficients are all collected in the

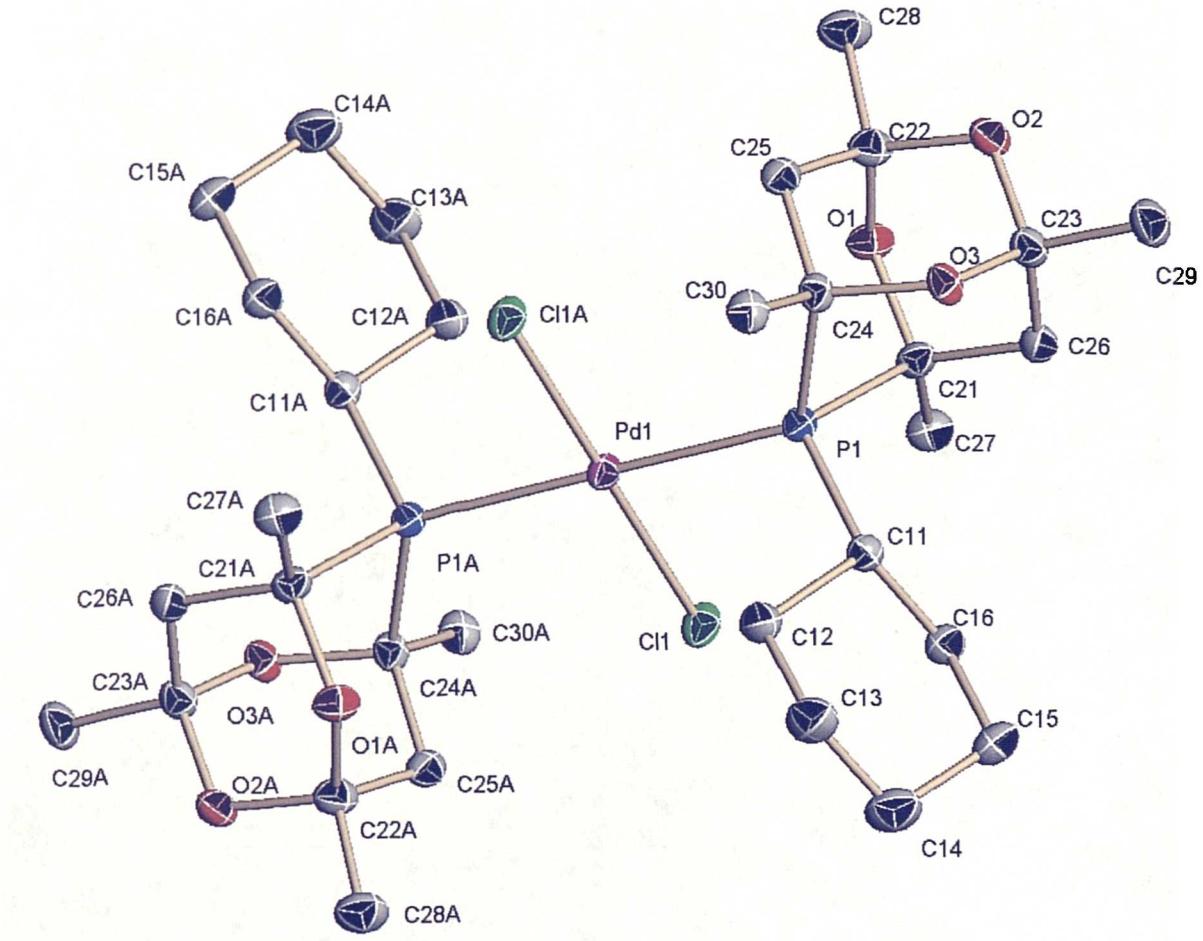

Appendix.

Figure 2.7 Molecular structure of palladium complex *trans-rac*-(**2.22**). All hydrogen atoms have been omitted for clarity.

The cone angle for ligand (**2.15**) was measured from the crystal structures of *rac*-(**2.21**) and *rac*-(**2.22**) and found to be 180°.

Chapter 3

Bidentate tetramethyl-trioxa-phospha-adamantanes

3.1 Introduction

The first example of a bis(phospha-adamantyl) diphosphine was recently reported by Gee.[375] She extended the work of Epstein *et al.* by reacting diprimary phosphines 1,2-diphosphinoethane and 1,3-diphosphinopropane with 2,4-pentanedione and 1,1,1-trifluoro-2,4-pentanedione in aqueous hydrochloric acid to form the bis(phospha-adamantyl)alkanes (**3.1**)-(**3.4**) (Scheme 3.1).

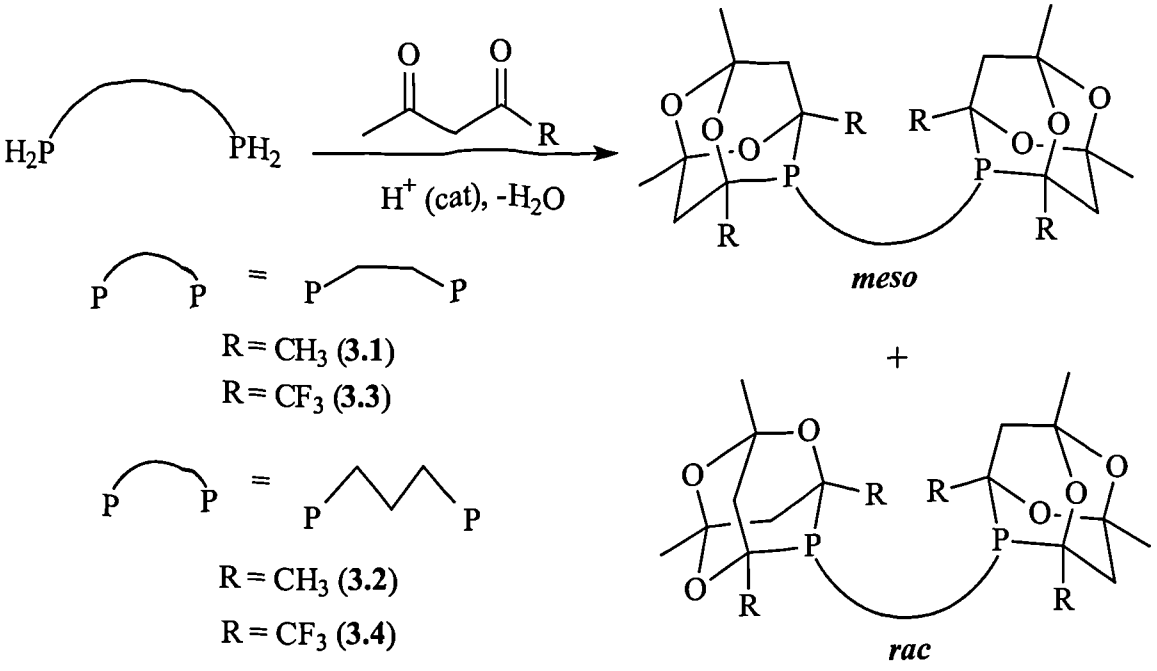

Scheme 3.1 C_2 and C_3 bis(phospha-adamantyl)alkanes

The stereochemistry of the phospha-adamantane cage (see Section 2.1.2) renders bis(phospha-adamantanes) diastereomeric, resulting in two resonances of similar intensity in the $^{31}P\{^1H\}$ NMR spectra of the four diphosphines shown. *Meso*-(**3.1**)-(**3.4**) are C_S-symmetric, with one phospha-adamantane cage α and the other β. *Rac*-(**3.1**)-(**3.4**) are C_2-symmetric, with the phospha-adamantane moieties either αα or ββ. For the purposes of the work in this chapter, it is notable that recrystallisation of the phospha-adamantanes described generally yielded a product which deviated significantly from the *ca.* 1:1 ratio of diastereomers observed in the crude products.

The coordination chemistry of these four diphosphines was thoroughly explored by Gee.[375,377] Phospha-adamantanes (**3.1**) and (**3.2**) were shown to be excellent ligands forming stable complexes with a range of transition metals. The complexes (**3.5**)-(**3.12**) were synthesised by the addition of 1.0 equiv. of (**3.1**) or (**3.2**) to the appropriate Pt(II),

Pd(II) and Rh(I) precursors. For each complex, the $^{31}P\{^{1}H\}$ NMR spectra showed the expected two signals for the diastereomers.

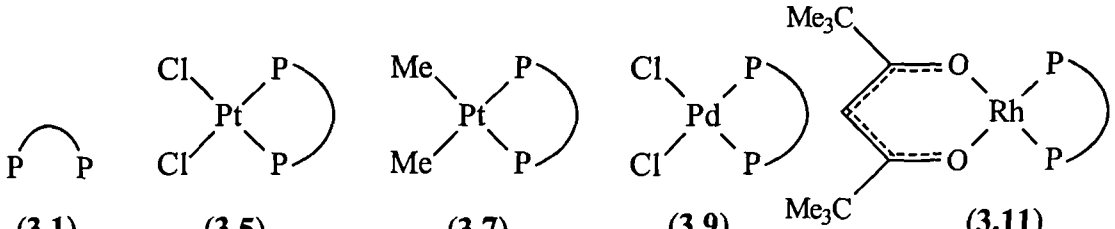

(3.1) (3.5) (3.7) (3.9) (3.11)

(3.2) (3.6) (3.8) (3.10) (3.12)

Addition of 2.0 equiv. of C_3-diphosphine (**3.2**) to $[PtCl_2(cod)]$ gave only the mono-chelate species, with no evidence for bis-chelate formation or diastereoselectivity. In contrast to this, the reactions of phospha-adamantanes (**3.1**) and (**3.2**) with $[Pt(norbornene)_3]$ showed that bis-chelates could be formed and diastereoselectivity was observed in the monochelate formation.

In the case of 1.0 equiv. of diphosphines (**3.1**) or (**3.2**), the $^{31}P\{^{1}H\}$ NMR spectra showed an AB pattern and two singlets all with ^{195}Pt satellites tentatively assigned to the complexes (**3.13**)-(**3.18**).

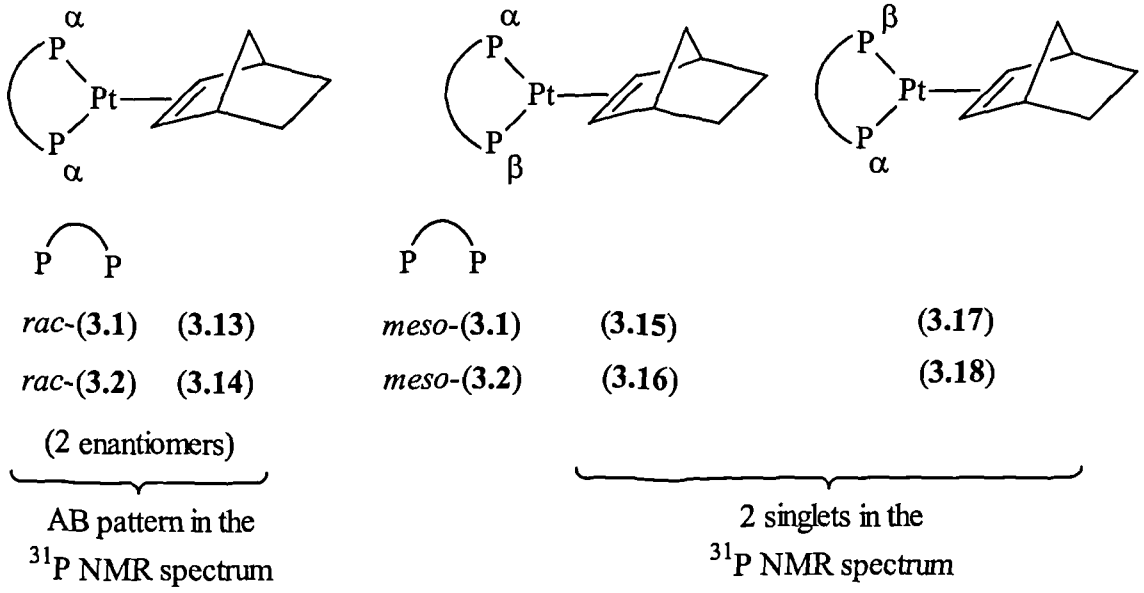

rac-(**3.1**) (**3.13**) *meso*-(**3.1**) (**3.15**) (**3.17**)

rac-(**3.2**) (**3.14**) *meso*-(**3.2**) (**3.16**) (**3.18**)

(2 enantiomers)

AB pattern in the ^{31}P NMR spectrum

2 singlets in the ^{31}P NMR spectrum

For the *rac*-phospha-adamantanes (αα and ββ), the Pt(0) complex has C_1 symmetry, and hence the phosphorus atoms are inequivalent, giving rise to the AB pattern. The two singlets arise because *meso*-(**3.1**) and (**3.2**) form two C_S-symmetric diastereomeric complexes (αβ and βα).

When 2.0 equiv. of C_2-diphosphine (**3.1**) was reacted with [Pt(norbornene)$_3$], a prominent singlet was observed in the $^{31}P\{^1H\}$ NMR spectrum, tentatively assigned to the bis-chelate (**3.19**).

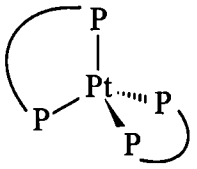

(**3.19**)

= *rac*-(**3.1**)

The $^{31}P\{^1H\}$ NMR spectrum of the analogous reaction with 1,3-bis(phospha-adamantyl)propane (**3.2**) exhibited the two diastereomers (**3.16**) and (**3.18**) and unreacted (**3.2**), but no (**3.14**) or bis-chelate, suggesting that the *meso* diastereomer reacted selectively with [Pt(norbornene)$_3$].

The coordination chemistry of the hexafluoro-phospha-adamantanes (**3.3**) and (**3.4**) was also studied by Gee.[375] No reaction was observed with platinum(II) with these ligands, probably due to the kinetic inertness of Pt(II) and steric bulk of these ligands. However, addition of (**3.3**) and (**3.4**) to the appropriate Pd(II) and Rh(I) precursors afforded the complexes (**3.20**)-(**3.23**).

(**3.3**)
(**3.4**)

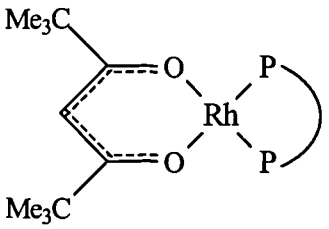

(**3.20**)

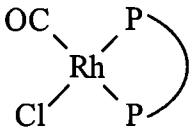

(**3.21**)
(**3.22**)

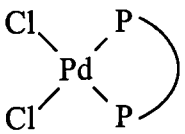

(**3.23**)

The cone angle (θ)[25] for phospha-adamantanes (**3.2**) and (**3.4**) were measured following methods reported by Tolman[24] from the crystal structures of complexes (**3.10**) and (**3.23**) and found to be 173° and 192° respectively. Compared to other chelating diphosphine ligands (see Table 3.1) they are even larger than the archetypal bulky diphosphines based on the *tert*-butyl substituent.[381] It is worth noting that the phospha-adamantane moiety is very rigid. Consequently, the cone angle values obtained for phospha-adamantanes are more realistic than aryl and alkyl phosphine analogues because aryl and alkyl groups can "mesh". Hence, conformations are adopted in which the cone angle is significantly less than the maximum values in Table 3.1.

Table 3.1 Comparing cone angles (θ) for phospha-adamantanes (**3.2**) and (**3.4**) with a range of simple diphosphines

Ligand	Cone Angle (θ)/°
$Me_2PCH_2CH_2PMe_2$	107
$Et_2PCH_2CH_2PEt_2$	115
$Ph_2PCH_2CH_2PPh_2$	125
$Ph_2PCH_2CH_2CH_2PPh_2$	127
$Cy_2PCH_2CH_2PCy_2$	142
$Bu^t_2PCH_2CH_2CH_2PBu^t_2$	155
(**3.2**)	173
(**3.3**)	192

The aim of this work was to extend the work described above to the synthesis and characterisation of new bis(phospha-adamantanes), with a view to investigating new synthetic pathways to these ligands. Some of Gee's work also suggested that the separation of *meso* and *rac* (**3.2**) might be possible. This was to be investigated alongside coordination chemistry studies of phospha-adamantanes.

Diphosphines (**3.1**) and (**3.2**) have recently found application in the palladium-catalysed carbonylation of olefins.[382,383] This work and catalysis resulting from the work described in this chapter are found in Chapter 4.

3.2 Synthesis and characterisation of bis(phospha-adamantane) diphosphines

3.2.1 Attempted synthesis of bis(1,3,5,7-tetramethyl-4,6,8-trioxa-2-phospha-adamantane)-*o*-xylene from adamphos

The bulky diphosphine bis(di-*t*-butylphosphino)-*o*-xylene (**3.25**) was prepared[34] *via* the reaction illustrated below.

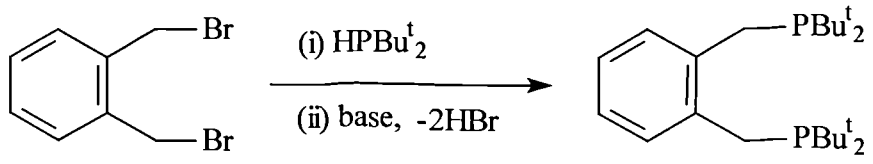

(**3.24**) (**3.25**)

Equation 3.1

A similar synthesis of bis(phospha-adamantyl)-*o*-xylene required the secondary phospha-adamantane (**3.26**). As mentioned earlier (see Section 2.1.1), (**3.26**) was first prepared by Epstein and Buckler[373,374] who found that solutions of 2,4-pentanedione in aqueous hydrochloric acid under pressure of PH_3 precipitated phospha-adamantane (**3.26**) in up to 80 % yield (see Equation 3.2).

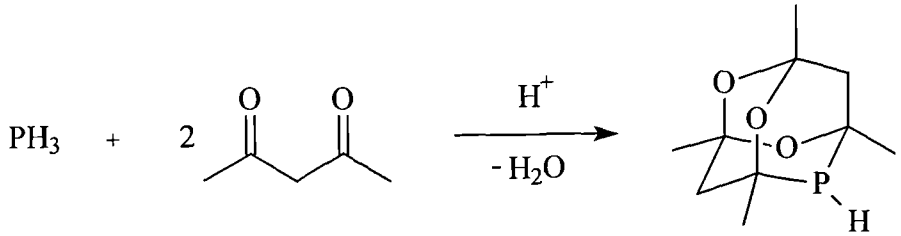

(**3.26**)

Equation 3.2

Downing[376] repeated the reaction under ambient pressure but did not quote a yield for the product, which she named "adamphos". We repeated this reaction, and obtained (**3.26**) in 15 % yield. A study of the effect of temperature on this reaction was undertaken, the results of which are shown below (see Table 3.2). The best yield was obtained at the lowest temperature, where precipitation of the product and dissolution of PH_3 are facilitated. The reaction at 80 °C gave no adamphos (**3.26**), and the $^{31}P\{^1H\}$ NMR spectrum of the reaction solution showed more than 10 resonances in the region δ -40 to 20 p.p.m. and no signal corresponding to the desired product. It seems that many intermediates are in equilibria in solution, and at elevated temperatures the final dehydration step (see Section 2.1.2) is prevented. In contrast, at low temperature the reaction equilibria are driven by the precipitation of adamphos (**3.26**) from solution.

Table 3.2 The effect of temperature on the yield of adamphos formation

Temperature/°C	Yield/%
80	0
60	8
40	12
25	15
0	50

Slow cooling of a methanol solution of (**3.26**) afforded single crystals, and Miss H. Phetmung of this department carried out the structure determination. The structure was solved in the monoclinic space group $P2_1/c$ with four formula units per unit cell. The method of data collection, structure solution and refinement, the tables containing atomic coordinates, bond lengths and angles, isotropic and anisotropic displacement coefficients are all collected in the Appendix. The numbering scheme and molecular structure is shown in Figure 3.1.

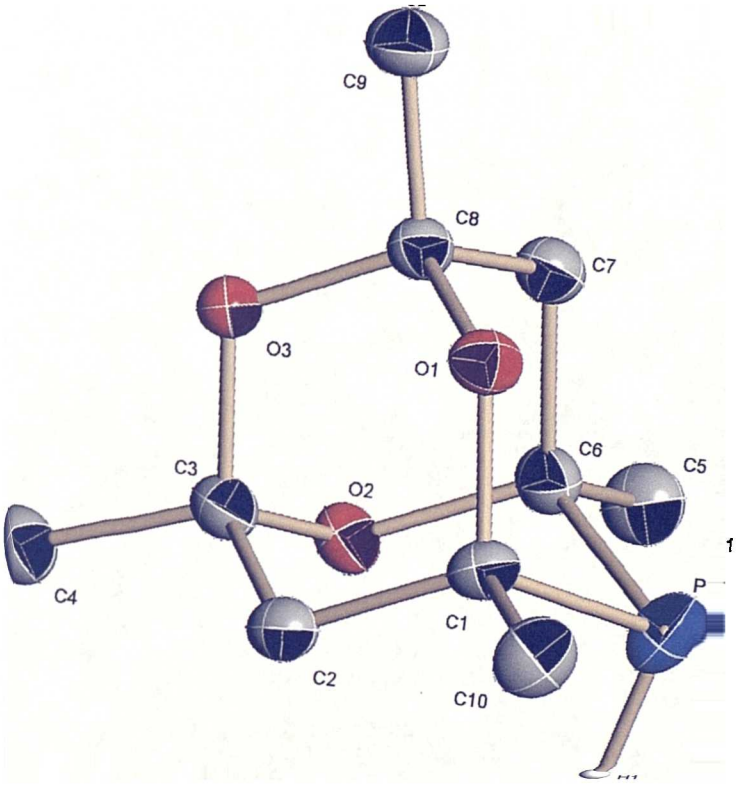

Figure 3.1 Molecular structure of adamphos (**3.26**). All hydrogens except P-H are omitted for clarity.

The P-H bond is positioned pseudo-axially, and in this way the lone pair on phosphorus is situated pseudo-equatorially and thus sterically protected by the methyl groups (C_5 and C_{10}). This explains why crystalline (**3.26**) is a rare example of a secondary phosphine that is stable to oxidation in air.

Reaction of adamphos (**3.26**) with α,α-dibromo-*o*-xylene (**3.24**) in acetonitrile, followed by addition of $NaBPh_4$ resulted in precipitation of a white crystalline solid. The $^{31}P\{^1H\}$ NMR spectrum of this product showed a singlet at δ -36.5 p.p.m., consistent with the formation of a phosphonium salt, but the highly symmetric ^1H NMR

spectrum (see Figure 3.2a, Table 3.3) showed that the cyclic phospha-adamantane phosphonium salt (**3.27**) had been formed (see Scheme 3.3), rather than the desired diphosphine product. Salt (**3.27**) was further characterised by $^{13}C\{^1H\}$ NMR spectroscopy (Table 3.2), mass spectrometry, elemental analysis (see Experimental) and *X*-ray crystallography.

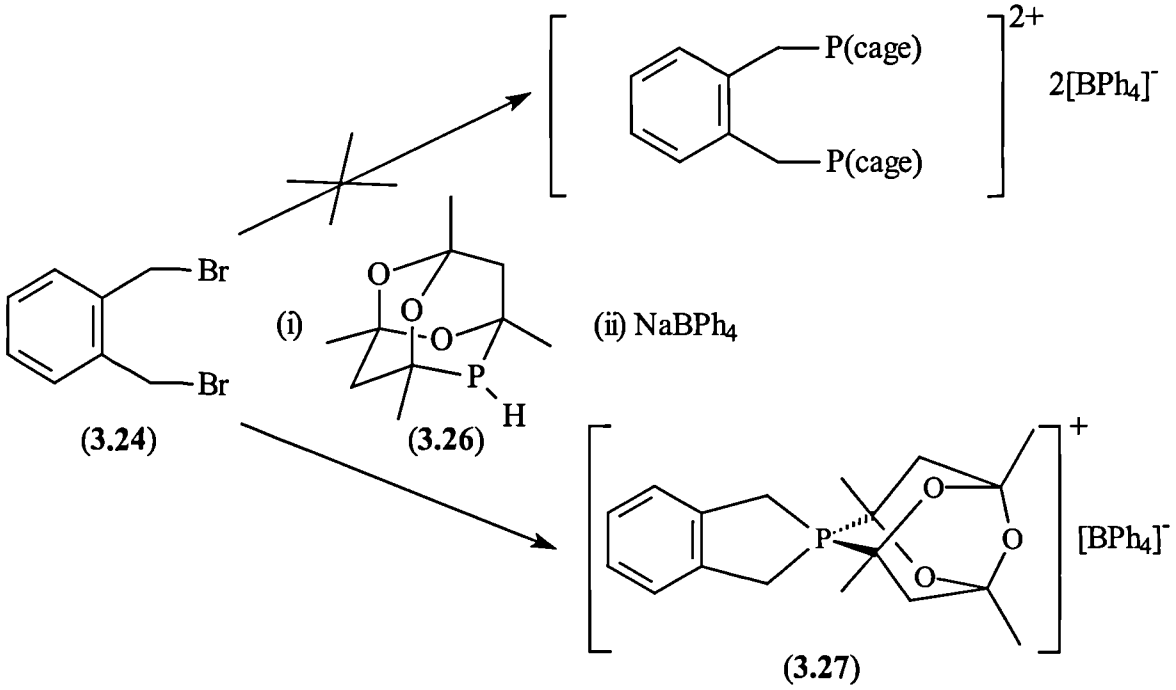

Scheme 3.2

Formation of cyclic salt (**3.27**) can be attributed to the great steric bulk of adamphos (**3.26**).

The benzylic protons give a well resolved [ABX] pattern in the ^1H NMR spectrum (Figure 3.2b) which agrees well with the simulation illustrated in Figure 3.2c.

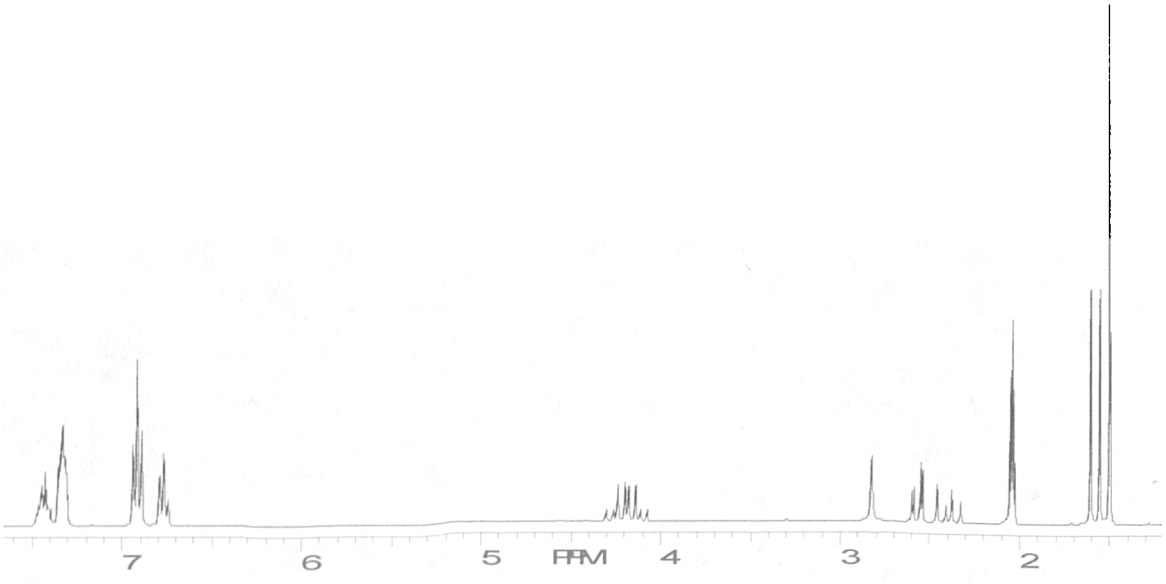

Figure 3.2a ^{1}H NMR spectrum of cyclic adamphosponium (**3.27**)

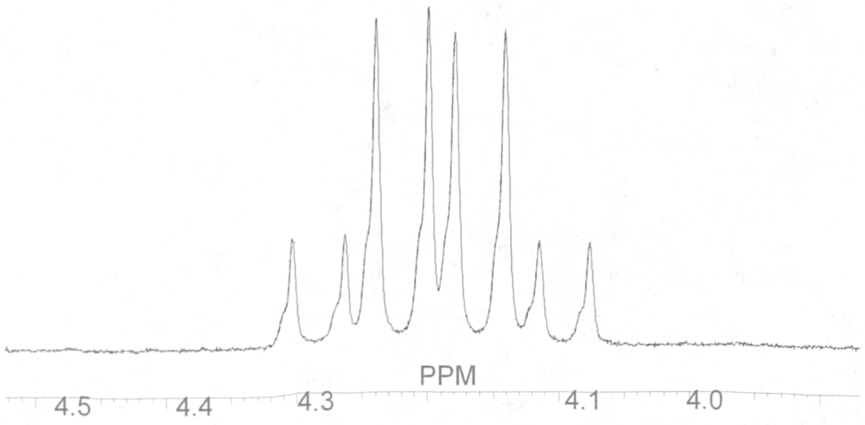

Figure 3.2b [ABX] spin system for benzylic protons in (**3.27**)

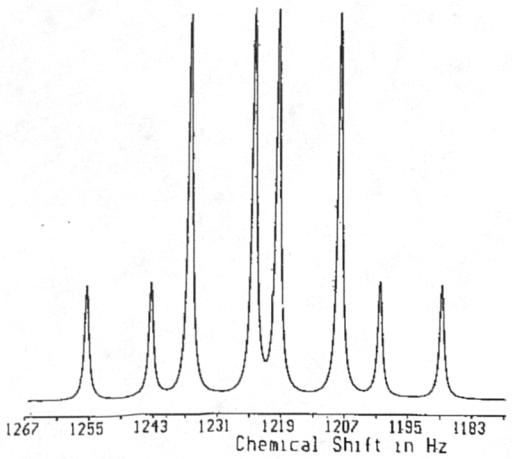

Figure 3.2c Simulated [ABX] spin system for benzylic region of (**3.27**)

Table 3.3 $^{13}C\{^1H\}$ NMR[a] and ^1H NMR[b] data for phospha-adamantane salt (**3.27**)

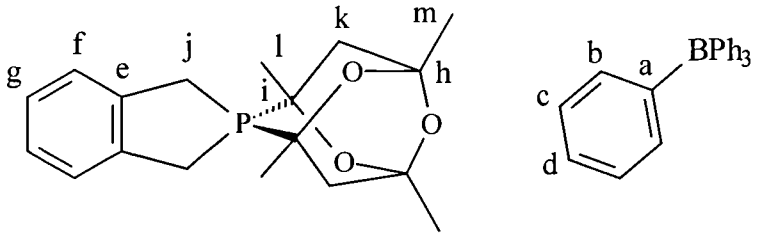

$\delta(^{13}C)$[c]		$\delta(^1H)$[d]	
a, b, c, d, e, f, g	136.8 (m), 129.8 (d, *J*(PC) 1.6 Hz), 128.2 (d, *J*(PC) 14.3 Hz), 125.9 (m), 122.1 (s)	6.73–7.51	(m, 24H, $4C_6H_5 + C_6H_4$)
		3.96 and 4.17	(ABX, 4H, benzyl $2CH_2$; $^2J(H^AH^B)$ 19.3 Hz, $^2J(PH^A)$ 11.6 Hz, $^2J(PH^B)$ 12.1 Hz)
h	98.1 (m)	2.58	(ABX, 2H, CH_2; $^2J(H^AH^B)$ 3.3 Hz, $^2J(PH^A)$ 12.3 Hz, $^2J(PH^B)$ 14.9 Hz)
i	71.6 (d, ^1J(PC) 41.6 Hz)		
j	40.8 (d, ^2J(PC) 3.7 Hz)	2.40	(ABX, 2H, CH_2; $^2J(H^AH^B)$ 24.5 Hz, $^2J(PH^A)$ 14.7 Hz, $^2J(PH^B)$ 14.9 Hz)
k	21.3 (d, ^2J(PC) 39.8 Hz)		
	27.0 (s)	1.59	(d, 6H, $2CH_3$; ^3J(PH) 15.2 Hz
	22.1 (s)	1.51	(s, 6H, $2CH_3$)

[a] Spectra recorded at 100 MHz in $CDCl_3$ at 24 °C. Chemical shifts [$\delta(^{13}C)$] in p.p.m.(± 0.1) relative to d^6-acetone (206.0 p.p.m.). Coupling constants (*J*) in Hz (± 0.1).

[b] Spectra recorded at 300 MHz in d^6-acetone at 22 °C. Chemical shifts [$\delta(^1H)$] in p.p.m.(± 0.1) relative to residual solvent (2.09 p.p.m.). Coupling constants (*J*) in Hz (± 0.1).

[c] Assignments aided by $^{13}C\{^1H\}$ NMR DEPT spectrum.

[d] Detailed assignments made on the basis of ^1H COSY NMR.

Single crystals of (**3.27**) suitable for *X*-ray diffraction were present in the crude product, and Miss H. Phetmung of this department carried out the structure determination. The structure was solved in the monoclinic space group Pbca with eight formula units per unit cell. The method of data collection, structure solution and refinement, the tables containing atomic coordinates, bond lengths and angles, isotropic and anisotropic displacement coefficients are all collected in the Appendix. The numbering scheme and molecular structure is shown in Figure 3.3.

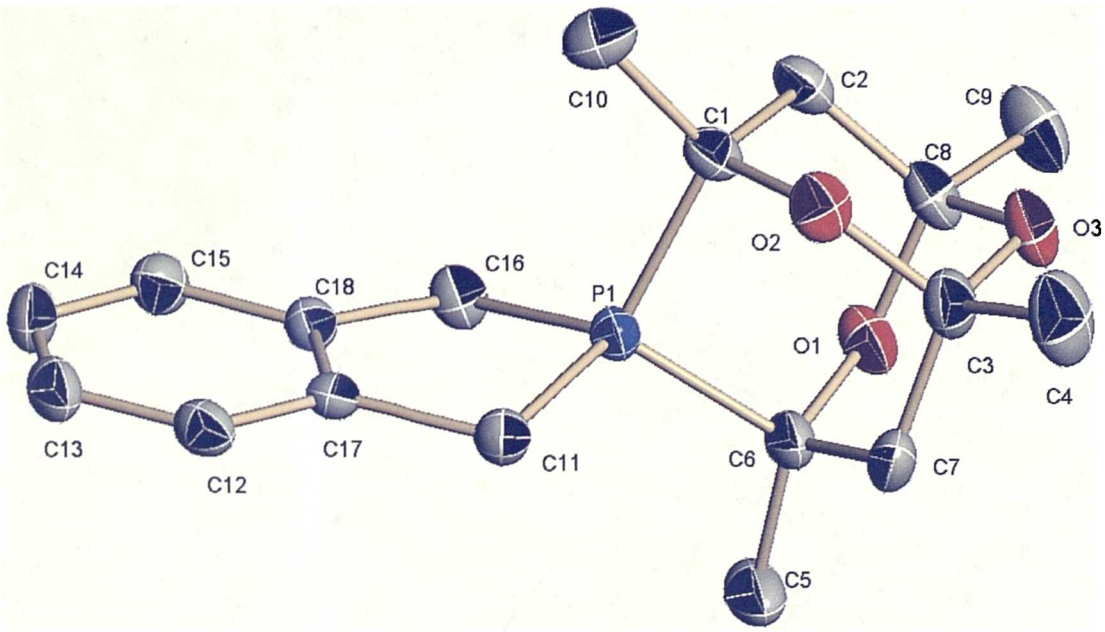

Figure 3.3 Molecular structure of the cyclic phospha-adamantane cation (**3.27**). All hydrogens and the $[BPh_4]^-$ counter ion are omitted for clarity

The formation of phosphonium (**3.27**) must proceed via nucleophilic attack of the phosphorus lone pair in intermediate (**A**) on the remaining benzylic bromo group (see Scheme 3.3).

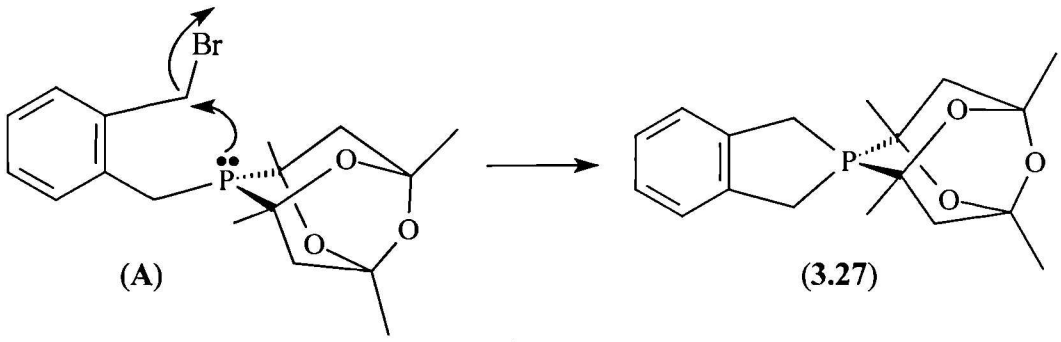

Scheme 3.3

We reasoned that by using the hydroxymethyl-phospha-adamantane (**3.28**) instead of adamphos in this reaction, the lone pair on phosphorus would be protected and thus unavailable for the ring-closing step. Synthesis of hydroxymethylphospha-adamantane

(**3.28**) was achieved following methods used for other phosphines,[384] by addition of formaldehyde to a methanolic solution of adamphos (Equation 3.3).

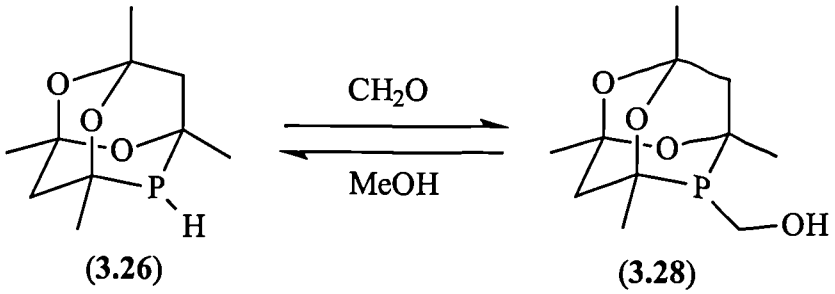

(**3.26**) (**3.28**)

Equation 3.3

Hydroxymethylphospha-adamantane (**3.28**) was characterised by $^{31}P\{^{1}H\}$ NMR spectroscopy and mass spectrometry (see Experimental). However, when it was reacted with α,α-dibromo-*o*-xylene (**3.24**) in acetonitrile, the cyclic phosphonium (**3.27**) was formed. The hydroxymethyl-phospha-adamantane (**3.28**) can dissociate into (**3.26**) and formaldehyde, and it is likely that this occurs here and the reaction is driven by the thermodynamic stability of (**3.27**).

3.2.2 Synthesis of bis(adamphosphino)-*o*-xylene from diphosphino-*o*-xylene

To our knowledge, diphosphino-*o*-xylene is not known. The reported reaction[385] of α,α-dibromo-*o*-xylene (**3.24**) with triethyl phosphite (Arbusov reaction) proceeds smoothly to the corresponding diphosphonate (**3.29**). Reduction of diphosphonate (**3.29**) with $LiAlH_4$ was unsuccessful, with the $^{31}P\{^{1}H\}$ NMR spectrum of the product exhibiting seven resonances. However modification of the reducing agent by using equimolar quantities of $LiAlH_4$ and Me_3SiCl[386] (generating AlH_3) was more successful, and the $^{31}P\{^{1}H\}$ NMR spectrum of the product exhibited a singlet at δ -127.5 p.p.m. (^{1}J(PH) 191 Hz), corresponding to the desired diprimary phosphine (**3.30**) (see Scheme 3.4).

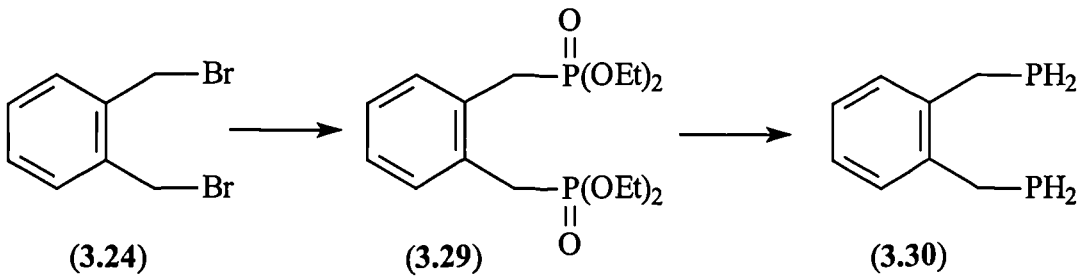

(**3.24**) (**3.29**) (**3.30**)

Scheme 3.4 Synthesis of diphosphino-*o*-xylene

However, upon workup a new resonance in the $^{31}P\{^{1}H\}$ NMR spectrum appeared at δ -106.0 p.p.m. The intensity of this peak grew steadily over time and despite repeated attempts, could not be avoided. The ^{1}H-coupled $^{31}P\{^{1}H\}$ NMR spectrum of the mixture transforms the signal at δ -106.0 p.p.m. to the second order pattern shown in Figure 3.4, consistent with the formation of a P-P bonded species (**3.31**) (see Equation 3.4) *via* spontaneous loss of hydrogen. This assignment was supported by mass spectrometry (m/z = 168 (M^{+})).

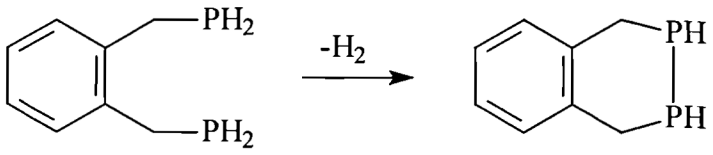

(**3.30**) (**3.31**)

Equation 3.4

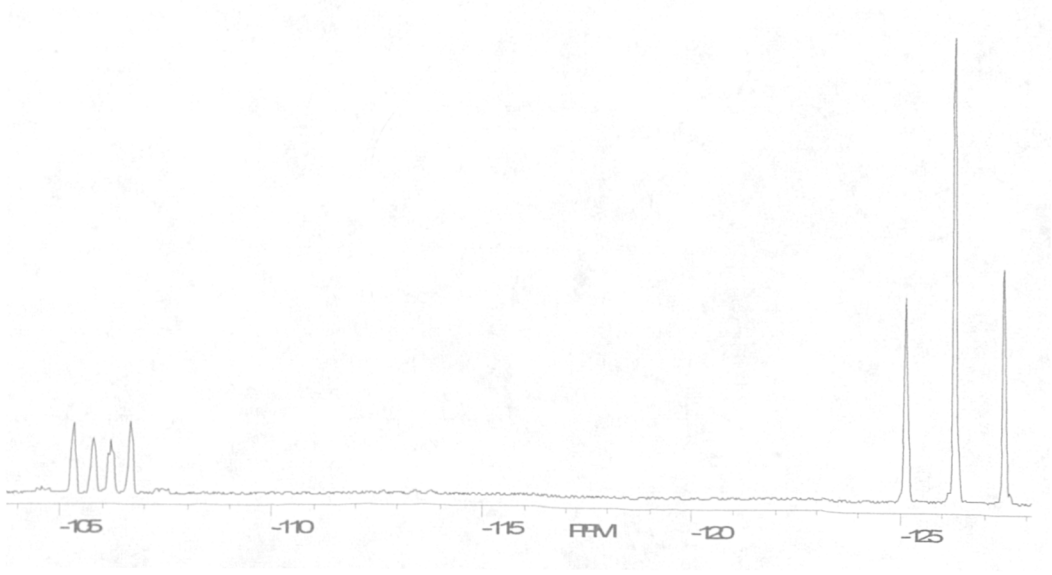

Figure 3.4 ^{1}H-coupled ^{31}P NMR spectrum of diprimary phosphine (**3.30**) and P-P bonded species (**3.31**).

We attempted to trap the diprimary phosphine (**3.30**) as its borane adduct (**3.32**) by adding BH_3.thf to a thf solution of crude (**3.30**) (see Equation 3.5). A white crystalline solid was isolated which gave a broad signal at δ -43.1 p.p.m. in the $^{31}P\{^{1}H\}$ NMR spectrum, consistent with the formation of the bis(borane) (**3.32**).

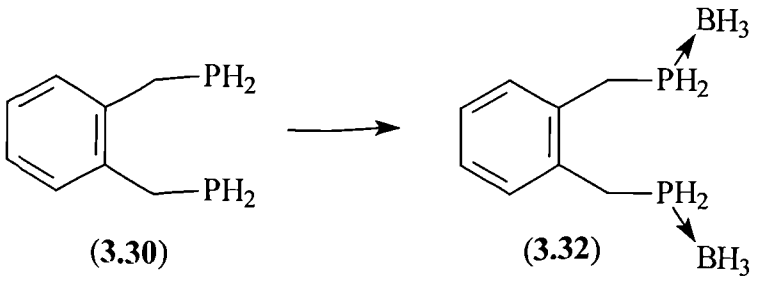

(3.30) (3.32)

Equation 3.5

Borane adduct (**3.32**) was also characterised by mass spectrometry (see Experimental), *X*-ray crystallography (see below) and ^{11}B NMR spectroscopy (see Figure 3.5) which shows a prominent broad quartet of doublets (^{1}J(BH) 97.6 Hz; ^{1}J(BP) 30.5 Hz).

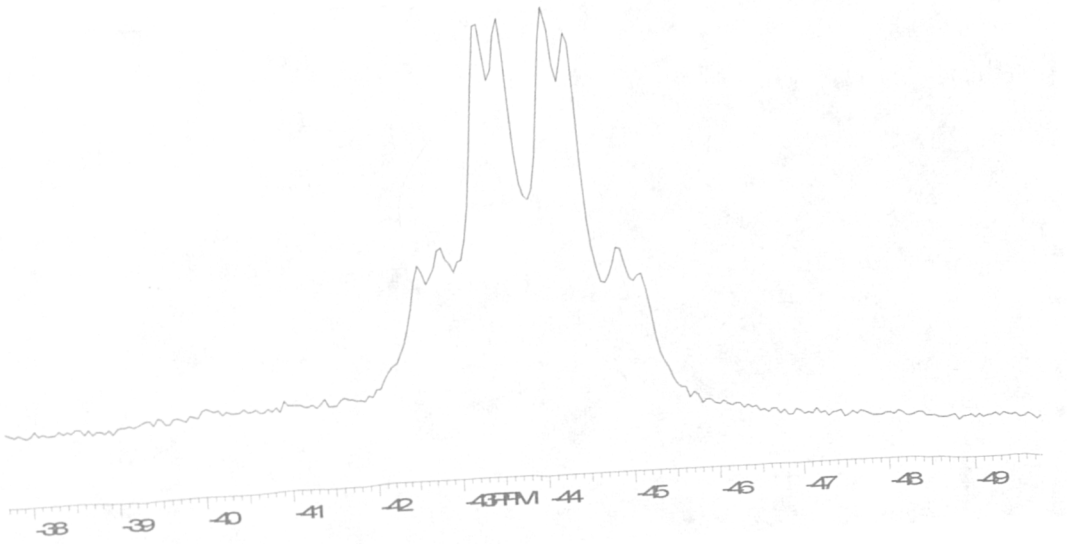

Figure 3.5 $^{11}B\{^{1}H\}$ NMR spectrum of bis(boranephosphino)-*o*-xylene (**3.32**).

Recrystallisation of (**3.32**) from diethyl ether/thf afforded single crystals of *X*-ray quality, and Miss H. Phetmung of this department carried out the structure determination. The structure was solved in the monoclinic space group Pbcn with four formula units per unit cell. The numbering scheme and molecular structure is shown in Figure 3.6. The method of data collection, structure solution and refinement, the tables containing atomic coordinates, bond lengths and angles, isotropic and anisotropic displacement coefficients are all collected in the Appendix.

Attempts to de-protect the borane adduct in order to form the desired bis(phosphaadamantane) analogue disappointingly led to spontaneous formation of the P-P species (**3.31**). However Gaumont *et al.*[387] have recently demonstrated that borane

adducts may be added directly to carbonyl derivatives without deprotection and this approach is therefore worthy of future investigation.

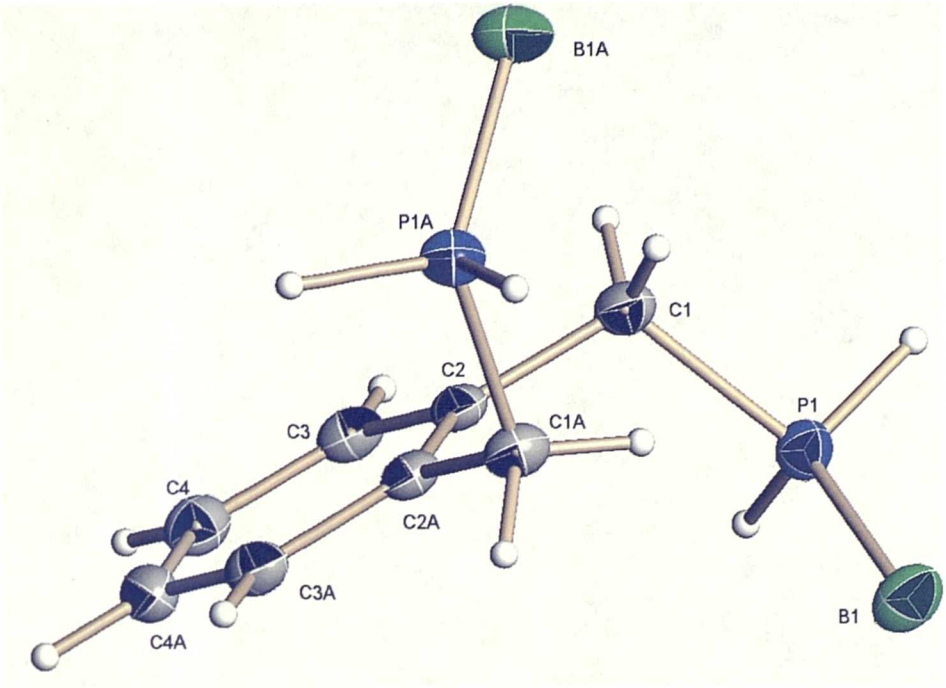

Figure 3.6 Molecular structure of bis(boranediphosphino)-*o*-xylene (**3.32**).

The synthesis of bis(phospha-adamantyl)-*o*-xylene was finally achieved by conventional hydrophosphination of crude bis(phosphino)-*o*-xylene (**3.30**) with pentane-2,4-dione. As discussed earlier (see Scheme 3.6), the time dependent decomposition of diprimary phosphine (**3.30**) to the P-P species (**3.31**) occurs by loss of hydrogen, and is hence a formal oxidation. To minimise this reaction, rigorous exclusion of oxygen was employed over and above the Schlenk-line techniques (see Experimental) generally used in the preparation of diprimary phosphines. After removal of solvent, crude (**3.30**) was added immediately to a solution of pentane-2,4-dione in 5 M HCl, affording bis(phospha-adamantane) diphosphine *meso/rac*-(**3.33**) as an off-white solid in very poor yield (6 %) (see Scheme 3.5).

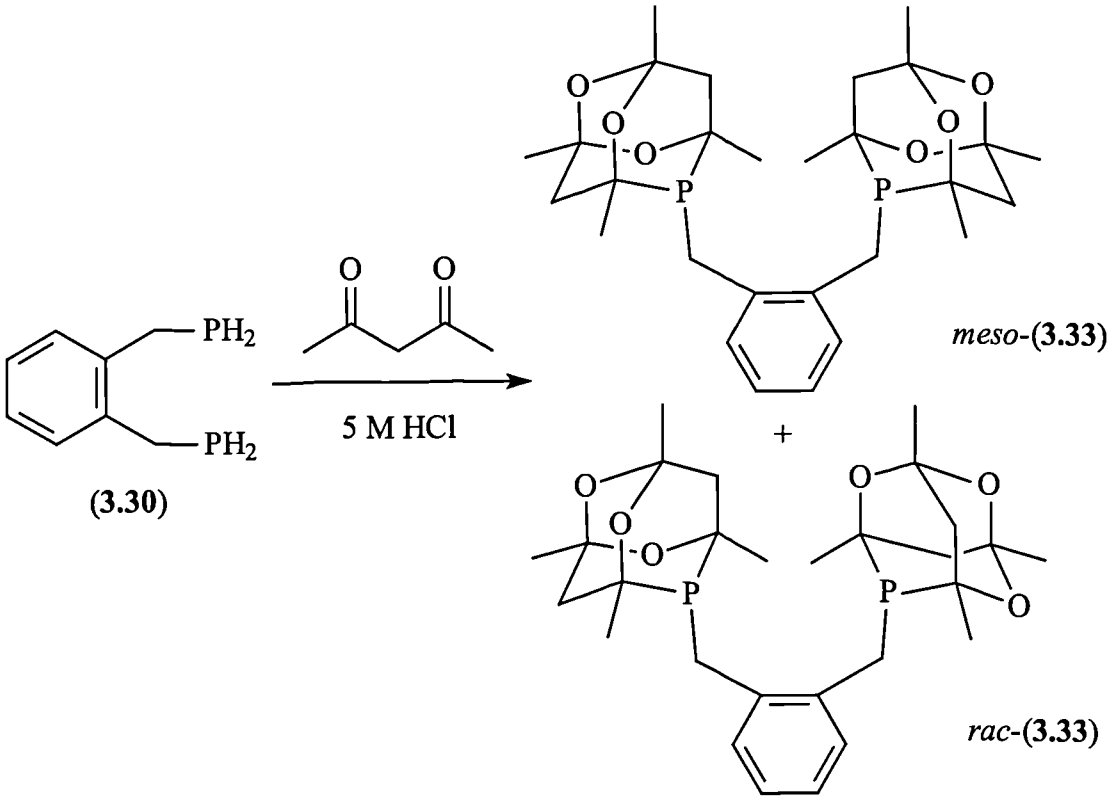

Scheme 3.5

The $^{31}P\{^{1}H\}$ NMR spectrum of bis(phospha-adamantane) *meso/rac*-(**3.33**) showed two singlets at δ -31.5 and -32.8 p.p.m. corresponding to the two diastereomers. Further characterisation was obtained by ^{1}H NMR, $^{13}C\{^{1}H\}$ NMR spectroscopy (see Table 3.4) and mass spectrometry (See Experimental). A minor product was isolated from this reaction, which will be discussed in Section 5.2.3.

Table 3.4 $^{13}C\{^1H\}$ NMR[a] and ^1H NMR[b] data for bis(phospha-adamantane)-*o*-xylene *meso/rac*-(**3.33**)

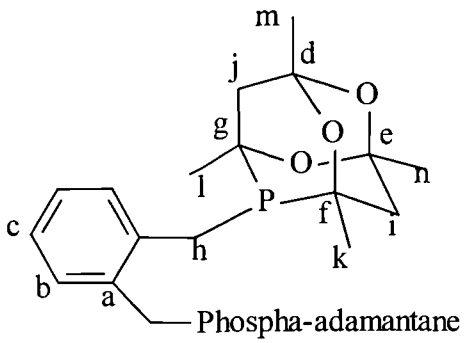

	$\delta(^{13}C)$[c]		$\delta(^1H)$[d]
a	136.2 (d, ^2J(PC) 4.4 Hz)	7.00-7.24	(m, 4H, C_6H_4)
b	131.0 (m)		
c	126.4 (s)		
d, e	96.6 (d, ^3J(PC) 2.5 Hz)	3.38	(ABX, 2H, benzyl CH_2;
	95.8 (s)	and	$^2J(H^AH^B)$ 14.4 Hz, $^2J(PH^A)$
		2.72	1.8 Hz, $^2J(PH^B)$ 2.3 Hz)
f, g	72.5 (m)	3.17[e]	(d, 1H, benzyl C*H*H;
	72.2 (d, ^1J(PC) 7.5 Hz)		^2J(*H*H) 14.2 Hz
i, j	44.8 (d, ^2J(PC) 15.5 Hz)	2.89[e]	(d, 1H, benzyl CH*H*;
	37.1 (d, ^2J(PC) 4.4 Hz)		^2J(H*H*) 14.2 Hz
h, k, l, m, n	26.7-28.2 (m)	0.98-1.97	(m, 40H, $4CH_2 + 8CH_3$)

[a] Spectra recorded at 100 MHz in $CDCl_3$ at 27 °C. Chemical shifts [$\delta(^{13}C)$] in p.p.m.(± 0.1) relative to $CDCl_3$ (77.0 p.p.m.). Coupling constants (*J*) in Hz (± 0.1).

[b] Spectra recorded at 300 MHz in $CDCl_3$ at 24 °C. Chemical shifts [$\delta(^1H)$] in p.p.m.(± 0.1) relative to tms (0.0 p.p.m.). Coupling constants (*J*) in Hz (± 0.1).

[c] Assigned in parallel with $^{13}C\{^1H\}$ NMR DEPT spectrum.

[d] Detailed assignments made on the basis of ^1H COSY NMR.

[e] [ABX] spin system; ^2J(HP) coupling constants could not be resolved.

An expansion of the benzylic region of the ^{1}H COSY NMR is shown in Figure 3.7.

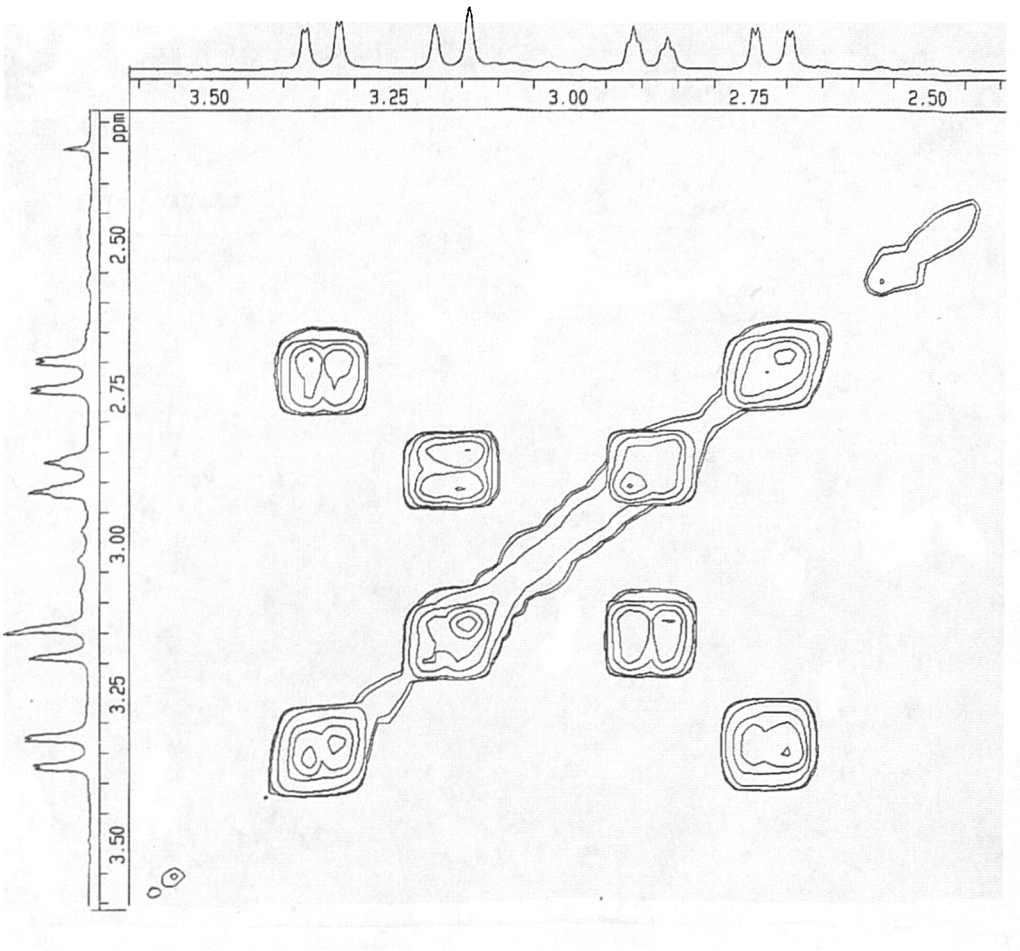

Figure 3.7 ^{1}H COSY NMR of benzyl protons in *meso/rac*-(**3.33**).

3.2.3 Attempted synthesis of 1,1'-bis(phospha-adamantyl)-ferrocene

3.2.3.1 Synthesis of 1,1'-diphosphinoferrocene

The preparation of this compound has been reported by Burk and Gross.[388] We have developed a new route (see Scheme 3.6) *via* reduction of 1,1`-bis(dichlorophosphino)ferrocene (**3.34**)[389,390] to (**3.35**), as an oily red/orange solid, characterised by ^{31}P NMR (δ -144.2 p.p.m., t; ^{1}J(PH) 203 Hz), ^{1}H NMR spectroscopy and mass spectrometry (see Experimental).

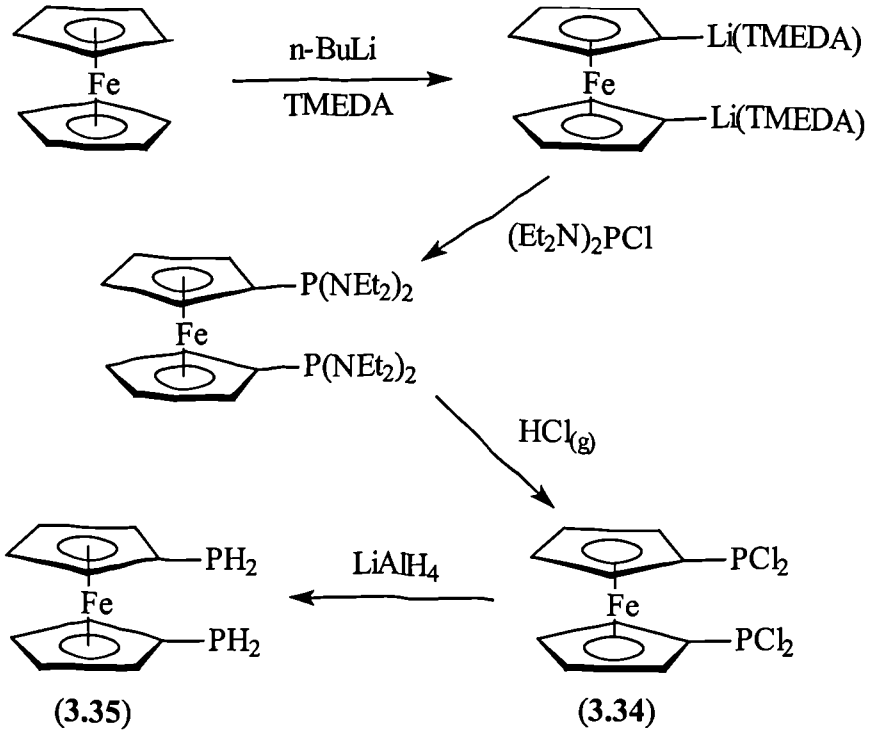

Scheme 3.6 Synthesis of 1,1'-diphosphinoferrocene

Reaction of diprimary phosphine (**3.35**) with pentane-2,4-dione in 5 M HCl yielded an orange solid. The $^{31}P\{^{1}H\}$ NMR spectrum of this product showed eight resonances, including two singlets at δ -32.6 and -32.8 p.p.m., tentatively assigned to 1,1-bis(phospha-adamantyl)ferrocene, on the basis of mass spectrometry (m/z 614 (M^+)). However we were unable to isolate this product in pure form; the problem may lie in the low solubility of (**3.35**) in the reaction medium, making for an inhomogenous reaction. Attempts to solubilise diprimary phosphine (**3.35**) with a co-solvent were successful but a different product was formed under these conditions (see Section 5.2.2)

We decided to attempt the preparation of 1,1-bis(phospha-adamantyl)ferrocene by conventional organophosphorus techniques, in this case by reaction of nucleophilic dilithioferrocene with halo-phosphine. Therefore the preparation of halo-phospha-adamantane was attempted.

3.2.3.2 Synthesis of chloro-phospha-adamantane

The use of C_2Cl_6 as a radical-source for the conversion of a P-H to a P-Cl containing compound is known.[391] Refluxing adamphos (**3.26**) with C_2Cl_6 in toluene (Equation 3.6) resulted in very slow conversion of the secondary phosphine to the desired species (**3.36**) having a resonance in the $^{31}P\{^{1}H\}$ NMR spectrum (δ 51.8 p.p.m.).

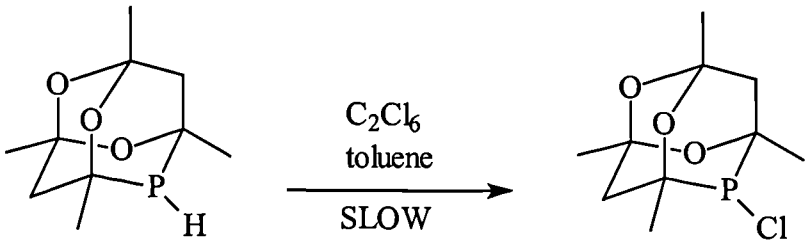

(3.26) **(3.36)**

Equation 3.6

However reaction times of up to two weeks resulted in incomplete conversion to the chloro-phospha-adamantane (**3.36**), and prolonged refluxing lead to decomposition. Addition of a radical initiator (V65, 5-10 mol%) [V65 = $CH_3(CH_3)CHCH_2(CN)(CH_3)CN{=}NC(CH_3)(CN)CH_2CH(CH_3)CH_3$] failed to promote the reaction.

N-chlorosuccinimide is known to be a source of Cl radicals, used in the conversion of some P(V)-H to P(V)-Cl species.[392] Reaction of adamphos with *N*-chlorosuccinimide in CCl_4 at *ca.* 0 °C affords the chloro-phospha-adamantane (**3.36**) as a yellow solid in essentially quantitative yield (Equation 3.6).

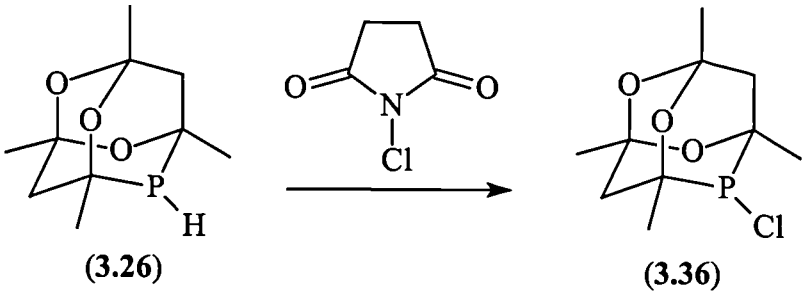

(3.26) **(3.36)**

Equation 3.6

Control of the reaction is quite difficult, as too high a temperature results in P(V) impurities and too low a temperature gives incomplete conversion. Synthon (**3.36**) was characterised by $^{31}P\{^1H\}$ and ^1H NMR spectroscopy (see Experimental). Single crystals of (**3.36**) were grown by slow evaporation of its CCl_4 solution, and Miss H. Phetmung of this department carried out the structure determination. The structure was solved in the monoclinic space group $P2_1/c$ with four formula units per unit cell. The numbering scheme and molecular structure is shown in Figure 3.8. The method of data collection, structure solution and refinement, the tables containing atomic coordinates, bond lengths and angles, isotropic and anisotropic displacement coefficients are all collected in the Appendix.

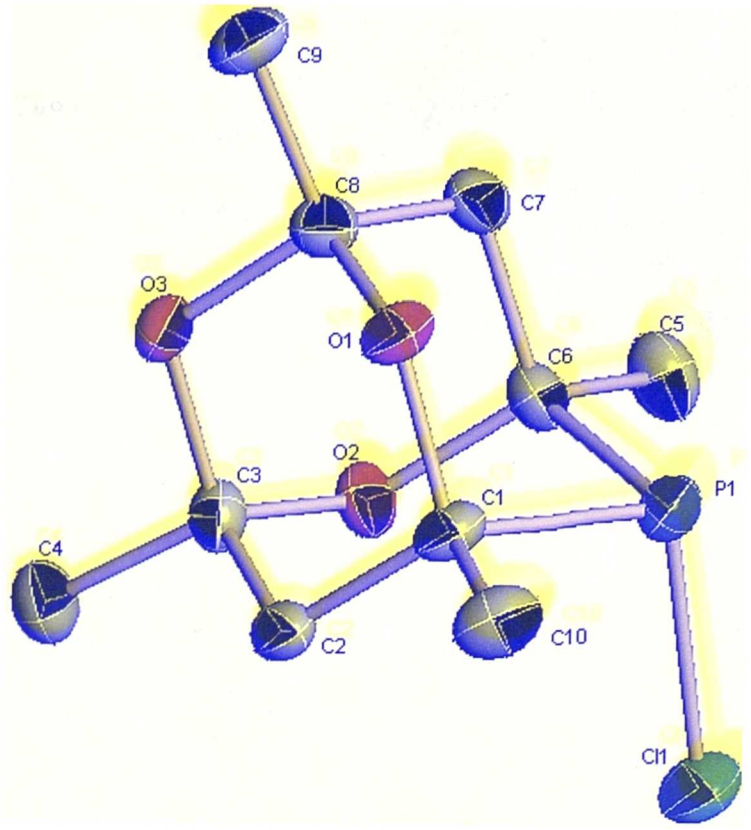

Figure 3.8 Molecular structure of chloro-phospha-adamantane α-(**3.36**). All hydrogens are ommited for clarity.

Preliminary attempts to prepare the bromo-phospha-adamantane (**3.37**) by reaction of *N*-bromosuccinimide and adamphos (Equation 3.7) showed that its synthesis is equally straightforward. The $^{31}P\{^{1}H\}$ NMR spectrum showed complete conversion of adamphos to a singlet at δ 52.6 p.p.m., assigned to bromo-phospha-adamantane (**3.37**).

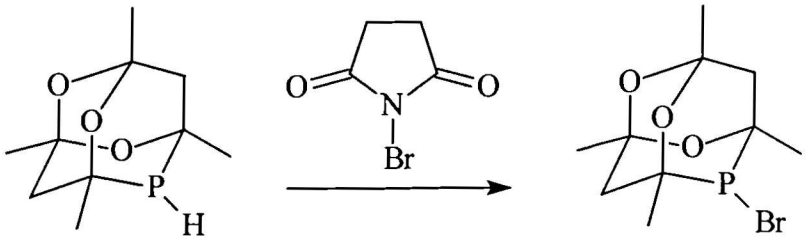

(**3.26**) (**3.37**)

Equation 3.7

3.2.3.3 *Synthesis of 1,1'-bis(phospha-adamantane)-ferrocene*

Reaction of dilithioferrocene with chloro-phospha-adamantane (**3.36**) in THF afforded 1,1'-bis(phospha-adamantyl)ferrocene, *meso/rac*-(**3.38**) (see Scheme 3.7) in moderate yield as an orange solid, characterised by $^{31}P\{^{1}H\}$ (see Figure 3.9), $^{13}C\{^{1}H\}$

and ^{1}H NMR spectroscopy (see Table 3.5), mass spectrometry (see Experimental), cyclic voltammetry and *X*-ray crystallography.

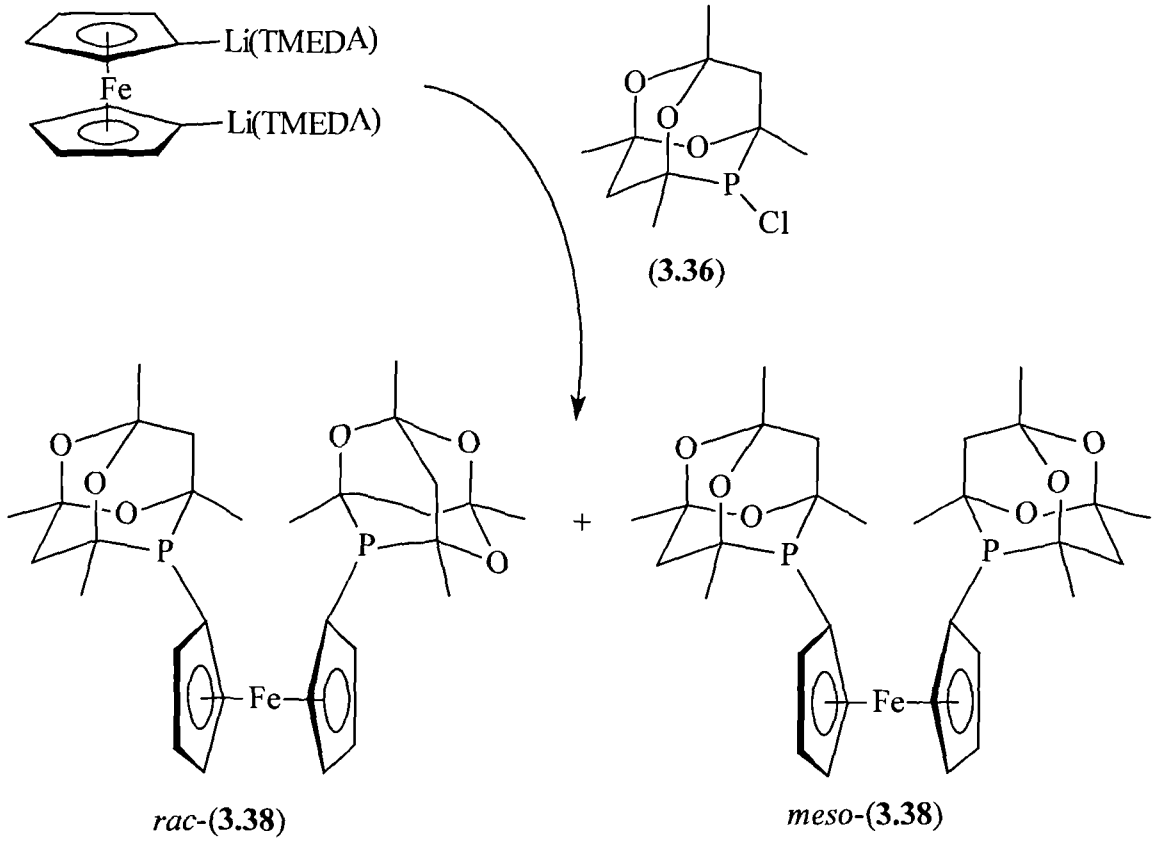

Scheme 3.7

The $^{31}P\{^{1}H\}$ NMR spectrum showed two singlets at δ -32.4 and -32.6 p.p.m. corresponding to the two diastereomers, and a minor (< 3 %) signal at δ -31.5, assigned to the monosubstituted 1-(phospha-adamantyl)ferrocene which was isolated (see Experimental for characterisation).

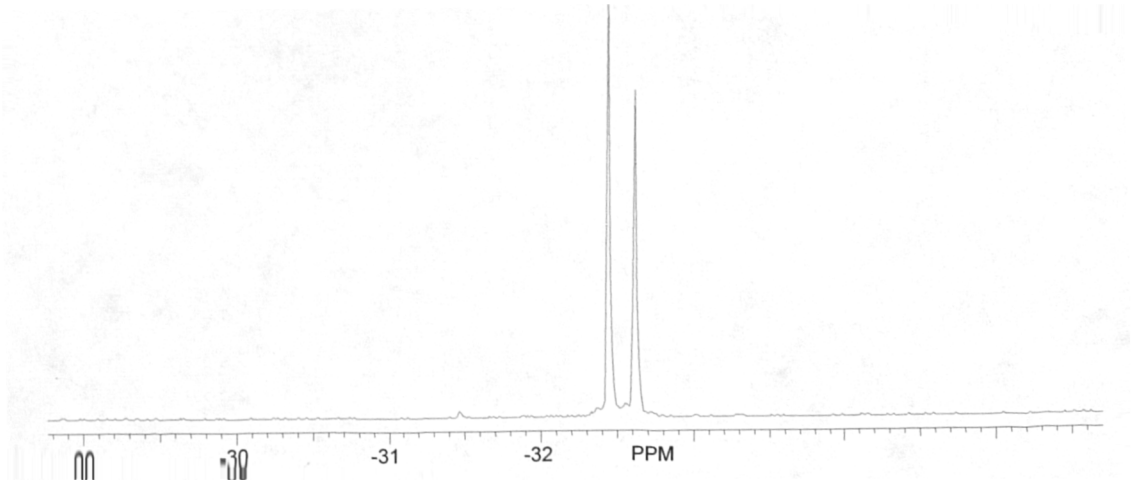

Figure 3.9 $^{31}P\{^{1}H\}$ NMR spectrum of 1,1'-bis(phospha-adamantyl)ferrocene *meso/rac*-(**3.38**).

Table 3.5 $^{13}C\{^1H\}$ NMR[a] and ^1H NMR[b] data for *meso/rac*-(**3.38**)

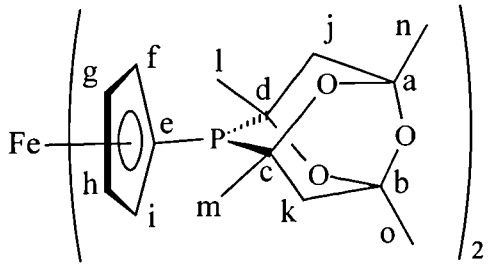

	$\delta(^{13}C)$[c]		$\delta(^1H)$[d]
a, b	96.5(s), 96.0(s)	4.23-4.63	(m, 8H, 8C*H*)
c, d, e, f, g h, i	71.3 – 75.5 (m)	2.00–2.09	(m, 2H, 2C*H*H)
		1.84–1.94	(m, 2H, 2CH*H*)
J, k	45.1 (d, ^2J(PC) 17.9) 36.9 (m)	1.49	(d of d, 2H, 2C*H*H; ^2J(HH) 1.2 Hz, ^2J(PH) 13.1 Hz)
		1.33	(d of d, 2H, 2CH*H*; ^2J(PH) 4.0 Hz, ^2J(HH) 1.2 Hz)
l, m, n, o	27.9 (s), 27.8 (s) 27.6 (s), 27.3 (s)	1.78	(d, 6H, 2CH_3; ^3J(PH) 11.9 Hz)
		1.21	(d, 6H, 2CH_3; ^3J(PH) 13.0 Hz)
		1.38	(s, 6H, 2CH_3)
		1.29	(s, 6H, 2CH_3)

[a] Spectra recorded at 100 MHz in $CDCl_3$ at 24 °C. Chemical shifts [$\delta(^{13}C)$] in p.p.m.(± 0.1) relative to $CDCl_3$ (77.0 p.p.m.). Coupling constants (*J*) in Hz (± 0.1).

[b] Spectra recorded at 300 MHz in $CDCl_3$ at 22 °C. Chemical shifts [$\delta(^1H)$] in p.p.m.(± 0.1) relative to residual solvent (7.27 p.p.m.). Coupling constants (*J*) in Hz (± 0.1).

[c] Assigned in parallel with $^{13}C\{^1H\}$ NMR DEPT spectrum.

[d] Detailed assignments made on the basis of ^1H COSY NMR.

A solution of *meso/rac*-(**3.38**) in dichloromethane showed a reversible oxidation wave (see Figure 3.10) at E° = 0.69 V. This value is 0.22 V higher than ferrocene, indicative of the π-acidic phospha-adamantane cage withdrawing electron density from ferrocene. The clean, smooth nature of the wave is unusual for phosphine ligands, and is probably a consequence of the steric protection of phosphorus by the phospha-adamantane moiety on this molecule.

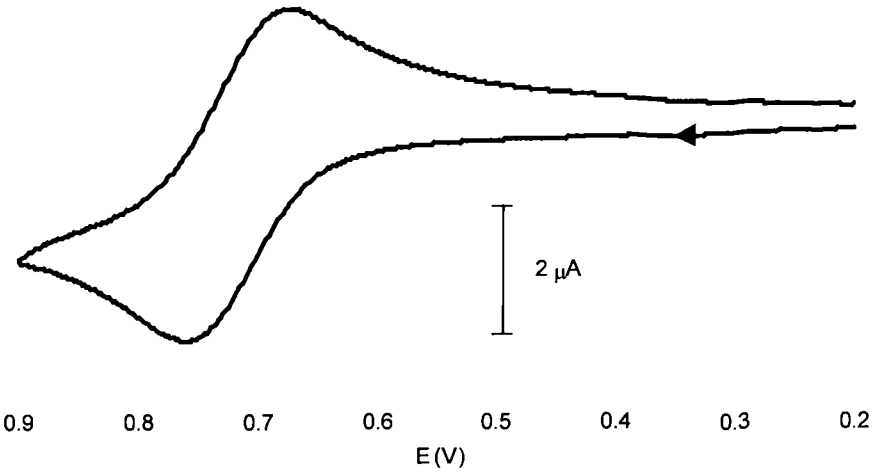

Figure 3.10 Cyclic voltammogram of *meso/rac*-(**3.38**) in dichloromethane.

Single crystals of *rac*-(**3.38**) were grown by slow evaporation of solvent from a thf solution, and Miss H. Phetmung of this department carried out the structure determination. The structure was solved in the monoclinic space group $P2_1/c$ with two formula units per unit cell. The numbering scheme and molecular structure is shown in Figure 3.11. The method of data collection, structure solution and refinement, the tables containing atomic coordinates, bond lengths and angles, isotropic and anisotropic displacement coefficients are all collected in the Appendix.

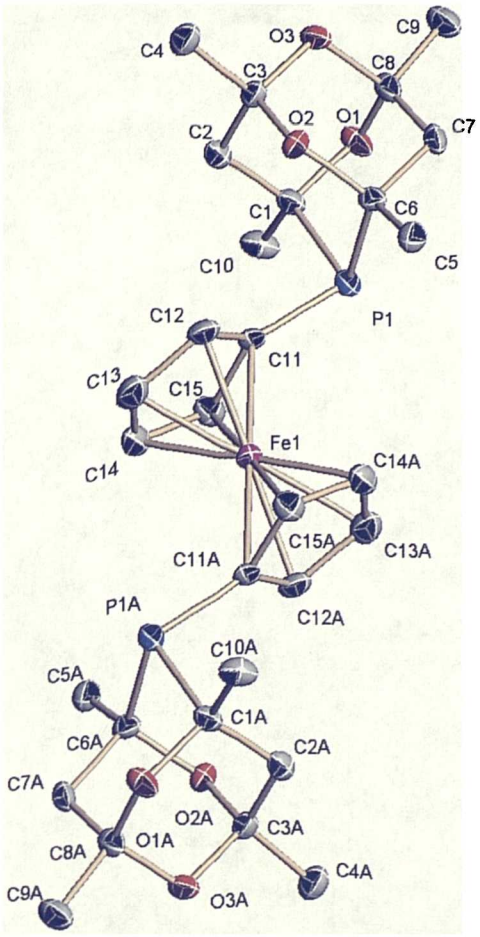

Figure 3.11 Molecular structure of 1,1'-bis(phospha-adamantyl)ferrocene *rac*-(**3.38**). All hydrogens are omitted for clarity

3.2.4 Separation of *meso* and *rac* diastereomers of 1,3-bis(phospha-adamantyl)propane (3.2)

As described earlier (see Section 3.1), diastereoselectivity was observed by Gee[375] in the reaction of 2.0 equiv. (**3.2**) with [Pt(norbornene)$_3$]. An analysis by $^{31}P\{^1H\}$ NMR spectroscopy suggested that *meso*-(**3.2**) had reacted with [Pt(norbornene)$_3$] leaving free *rac*-enriched (**3.2**). However in this very elegant work, the $^{31}P\{^1H\}$ NMR spectrum was slightly misinterpreted, and an impurity in the sample was mistaken for small amounts of *meso*-(**3.2**); in reality, all the *meso*-(**3.2**) had reacted with the Pt(0) leaving essentially 100 % *rac*-(**3.2**). This error led us to believe that the

more deshielded signal was due to *rac*-(**3.2**) rather than *meso*-(**3.2**). The results described below show that the opposite is the case.

Unpublished work[393] demonstrated that recrystallisation of crude *meso/rac*-(**3.2**) from dichloromethane/methanol afforded a sample enriched in the isomer with the less deshielded signal. Scale-up of this work yielded *meso/rac*-(**3.2**) in which the ratio of the diastereomers was 93:7 and 97:3 by $^{31}P\{^{1}H\}$ NMR spectroscopy (Figure 3.12) after one and two recrystallisations from dichloromethane/methanol[377] respectively (see Experimental).

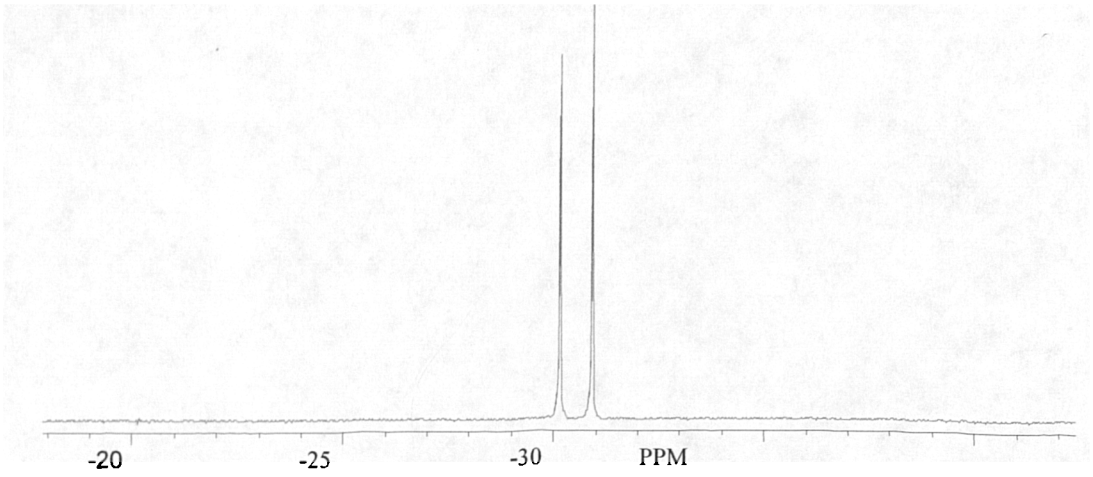

Figure 3.12a $^{31}P\{^{1}H\}$ NMR spectrum of crude *meso/rac*-(**3.2**).

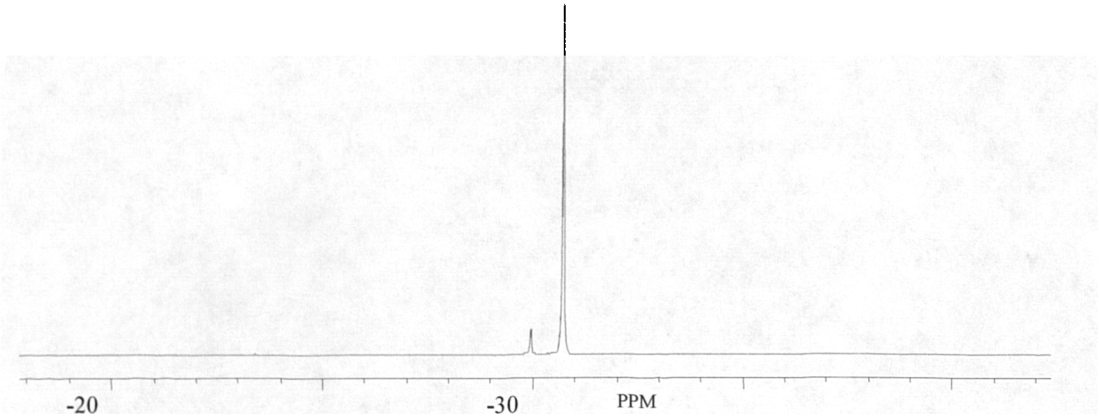

Figure 3.12b $^{31}P\{^{1}H\}$ NMR spectrum of *meso/rac*-(**3.2**) after one recrystallisation from dichloromethane/methanol

The ease of this separation is remarkable given the ostensibly similar structures of the two diastereomers. Crystals of *rac*-(**3.2**) were grown by slow evaporation of solvent from a dichloromethane solution of the doubly recrystallised *meso/rac*-(**3.2**) in order to determine which diastereomer corresponded to the lower frequency ^{31}P resonance. Miss H. Phetmung of this department carried out the structure determination, which was

solved in the monoclinic space group C2/c with four formula units per unit cell. The numbering scheme and molecular structure is shown in Figure 3.13. The method of data collection, structure solution and refinement, the tables containing atomic coordinates, bond lengths and angles, isotropic and anisotropic displacement coefficients are all collected in the Appendix.

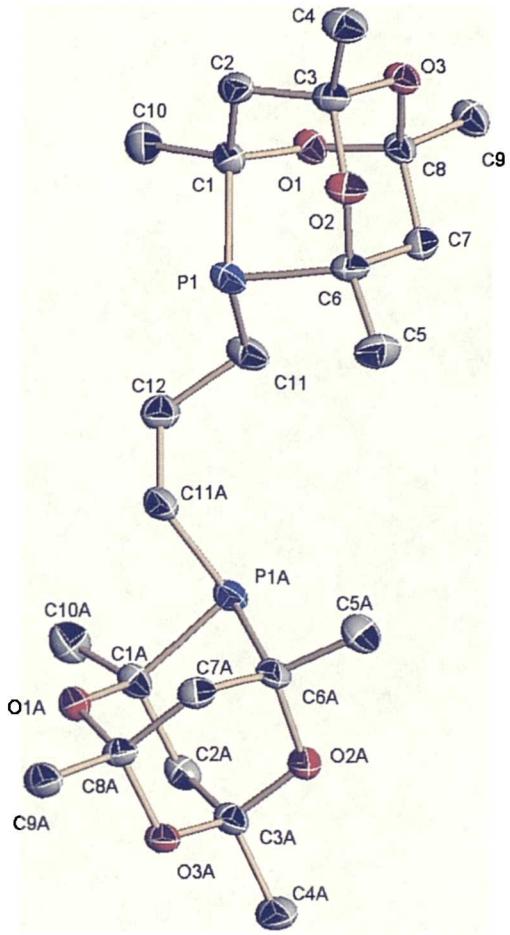

Figure 3.13 Molecular structure of *rac*-(**3.2**). All hydrogens are omitted for clarity.

The crystal structure determination showed unambiguously that the diastereomer was *rac*-(**3.2**), and this was confirmed by addition of [Pt(norbornene)$_3$] to an NMR sample of the crystals used. The $^{31}P\{^1H\}$ NMR spectrum showed an AB pattern with platinum satellites observed by Gee,[375] consistent with the formation of [Pt{*rac*-(**3.2**)}(norbornene)] (**3.14**). A change in the diastereomeric ratios for bis(phospha-adamantanes) (**3.1**), (**3.3**), (**3.4**)[375] and (**3.38**) was also observed upon recrystallisation. Further work should be carried out in order to determine whether the diastereomers can be separated in these ligands. Preliminary attempts were also made to resolve the

enantiomers of *rac*-(**3.2**) *via* the chiral solving agents (CSAs)[394] reported by Otsuka *et al.*[395] and Wild *et al.*[396] shown below.

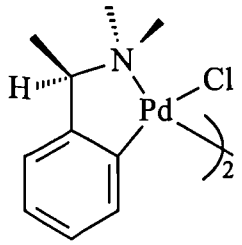

(*R*)-(**3.39**)

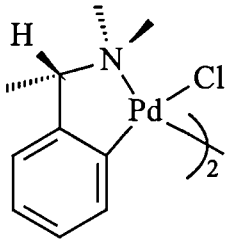

(*S*)-(**3.39**)

The reaction between 2.0 equiv. of *rac*-(**3.2**) and (*R*)-(**3.39**) (Equation 3.8) was monitored by $^{31}P\{^{1}H\}$ NMR spectroscopy. Two broad singlets were observed due to the two inequivalent phosphorus atoms in each of the diastereomeric palladium chelates (*R*)-(αα)-(**3.40**) and (*R*)-(ββ)-(**3.40**). Unfortunately, the diastereoisomerism was not manifested in either the $^{31}P\{^{1}H\}$ or ^{1}H NMR spectra, which would have been invaluable in monitoring attempts to separate these diastereomers.

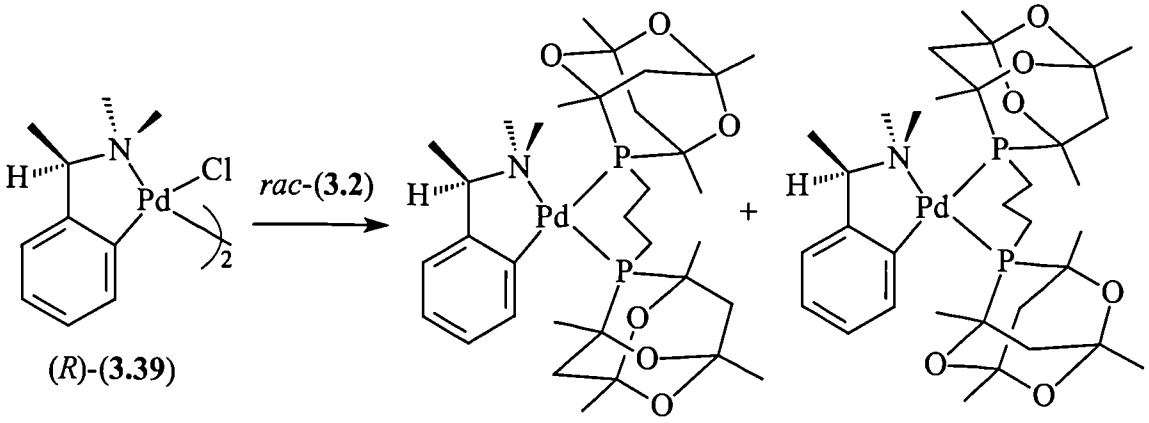

(*R*)-(**3.39**)

(*R*)-(αα)-(**3.40**)

(*R*)-(ββ)-(**3.40**)

Equation 3.8

Preliminary attempts to separate these diastercomers by chromatography were moderately successful. Two spots were observed on a silica T.L.C. plate (r.f. = 0.4 and 0.5) with diethyl ether as eluent. This is encouraging, and worthy of further work.

3.3 Coordination chemistry of bis(phospha-adamantyl) diphosphines

3.3.1 Coordination chemistry of bis(phospha-adamantyl)-*o*-xylene *meso/rac*-(3.33)

The reaction between 1.0 equiv. *meso/rac*-(**3.33**) and $[PdCl_2(NCPh)_2]$ in dichloromethane was monitored by $^{31}P\{^1H\}$ NMR spectroscopy. The spectrum exhibited two major species (see Figure 3.14), two singlets at δ -0.07 and -1.68 p.p.m., assigned to the diastereomeric chelates *meso/rac*-(**3.41**) and a dominant broad signal at δ 8.5 p.p.m., tentatively assigned to oligomeric species such as (**3.42**).

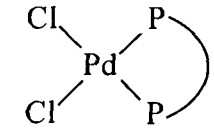

meso/rac-(**3.41**)

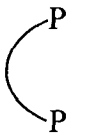

= *meso/rac*-(**3.33**)

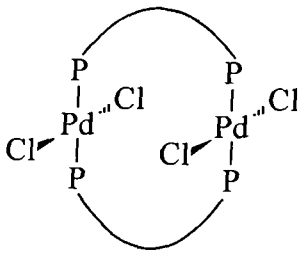

(**3.42**)

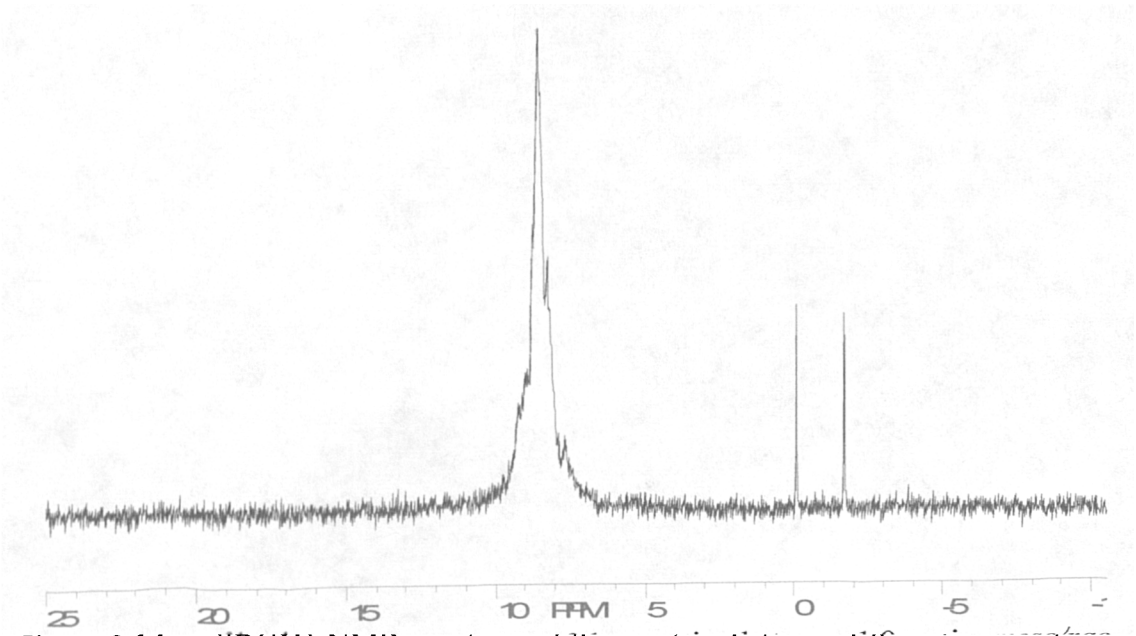

Figure 3.14 $^{31}P\{^1H\}$ NMR spectrum of the reaction between 1.0 equiv. *meso/rac*-(**3.33**) and $[PdCl_2(NCPh)_2]$.

Addition of 1.0 equiv. of *meso/rac*-(**3.33**) to $[PtCl_2(cod)]$ in dichloromethane afforded the complex *meso/rac*-(**3.43**) as a yellow solid. The $^{31}P\{^1H\}$NMR spectrum (see Figure 3.15) shows two singlets at δ -19.5 and –19.7 p.p.m. with platinum satellites (^1J(PtP) 3498 and 3482 Hz respectively). The ^{195}Pt NMR spectrum exhibited two triplets at δ 260.6 and 207.1 p.p.m.

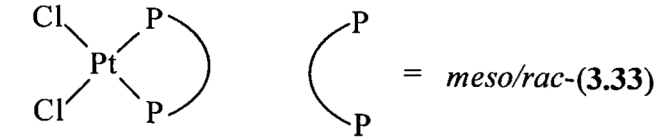

meso/rac-(**3.43**) = *meso/rac*-(**3.33**)

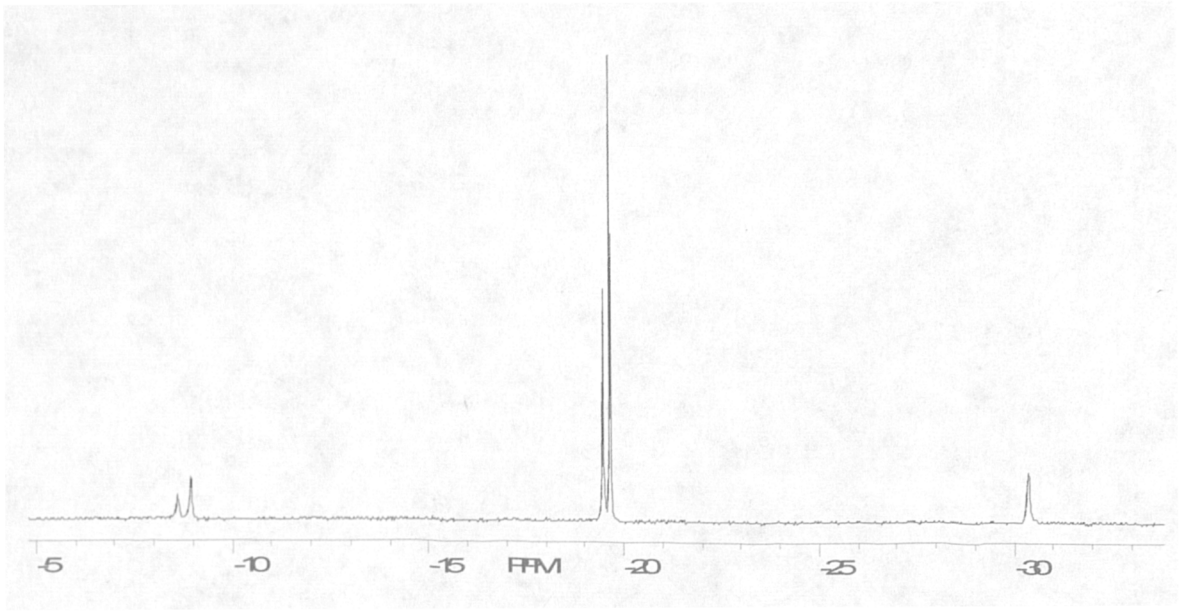

Figure 3.15 $^{31}P\{^{1}H\}$ NMR spectrum of product of the reaction between 1.0 equiv. *meso/rac*-(**3.33**) and $[PtCl_2(cod)]$.

Chelates *meso/rac*-(**3.43**) were also characterised by ^{1}H and $^{13}C\{^{1}H\}$ NMR spectroscopy, mass spectrometry (see Experimental) and *X*-ray crystallography.

Single crystals of *meso*-(**3.43**) suitable for *X*-ray diffraction were grown by slow diffusion of hexane into its dichloromethane solution. Dr. J. Charmant of this department carried out the structure determination, which was solved in the monoclinic space group Pbcn with eight formula units per unit cell. The numbering scheme and molecular structure is shown in Figure 3.16. The method of data collection, structure solution and refinement, the tables containing atomic coordinates, bond lengths and angles, isotropic and anisotropic displacement coefficients are all collected in the Appendix.

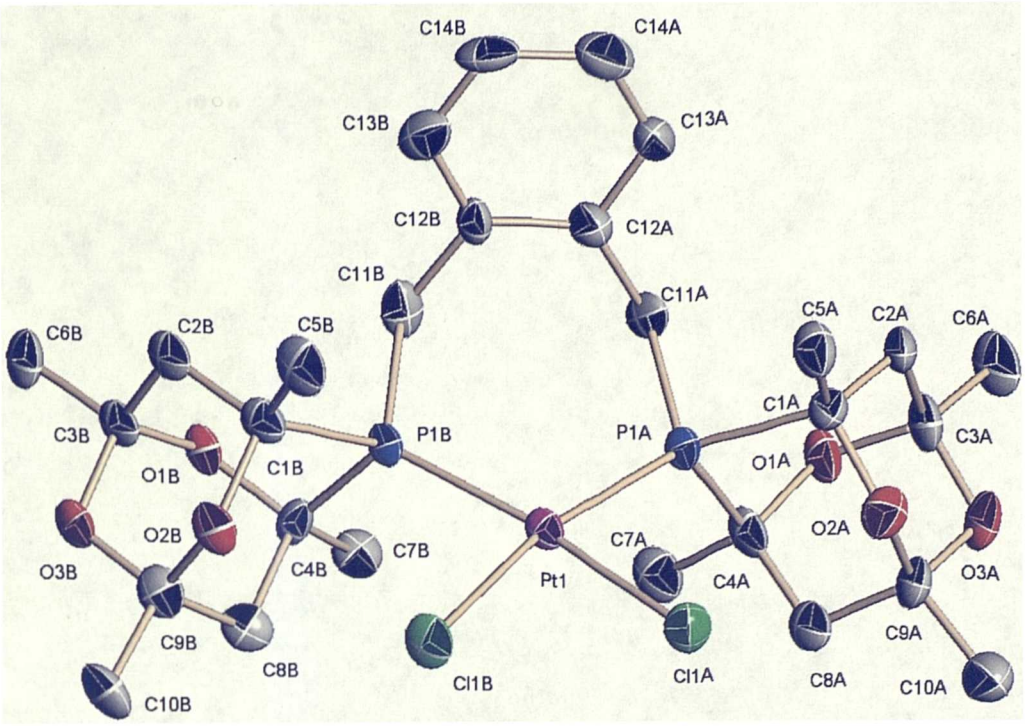

Figure 3.16 Molecular structure of *meso*-(**3.43**). All hydrogens are omitted for clarity.

To our knowledge, this is the only crystal structure reported[375,377] of a diastereomeric phospha-adamantane diphosphine or related transition metal complex that has crystallised as the *meso* diastereomer.

3.3.2 Coordination chemistry of 1,1'-bis(phospha-adamantyl)-ferrocene (3.38)

The reaction between 1.0 equiv. *meso/rac*-(**3.38**) and [$PtCl_2$(cod)] in dichloromethane was monitored by $^{31}P\{^1H\}$ NMR spectroscopy, which showed a mixture had formed (Figure 3.17): two singlets at δ -4.9 and -7.7 p.p.m. corresponding to *meso/rac*-(**3.44**) (^1J(PtP) 3703 and 3699 Hz respectively) and unreacted free ligand. Refluxing the mixture in toluene drove the reaction to completion with precipitation of a yellow solid. The $^{31}P\{^1H\}$ NMR spectrum of this product showed that, remarkably, it was solely one of the diastereomers of *meso/rac*-(**3.44**), leaving the other in solution. ^1H NMR spectroscopy and mass spectrometry data were obtained (see Experimental), but unfortunately attempts to grow crystals of the diastereomerically pure (**3.44**) proved unsuccessful.

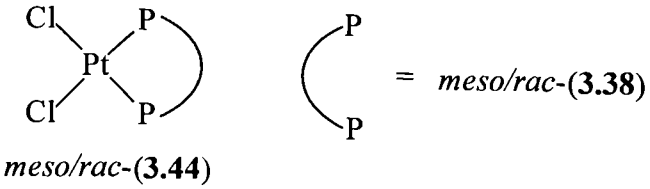

meso/rac-(**3.44**)

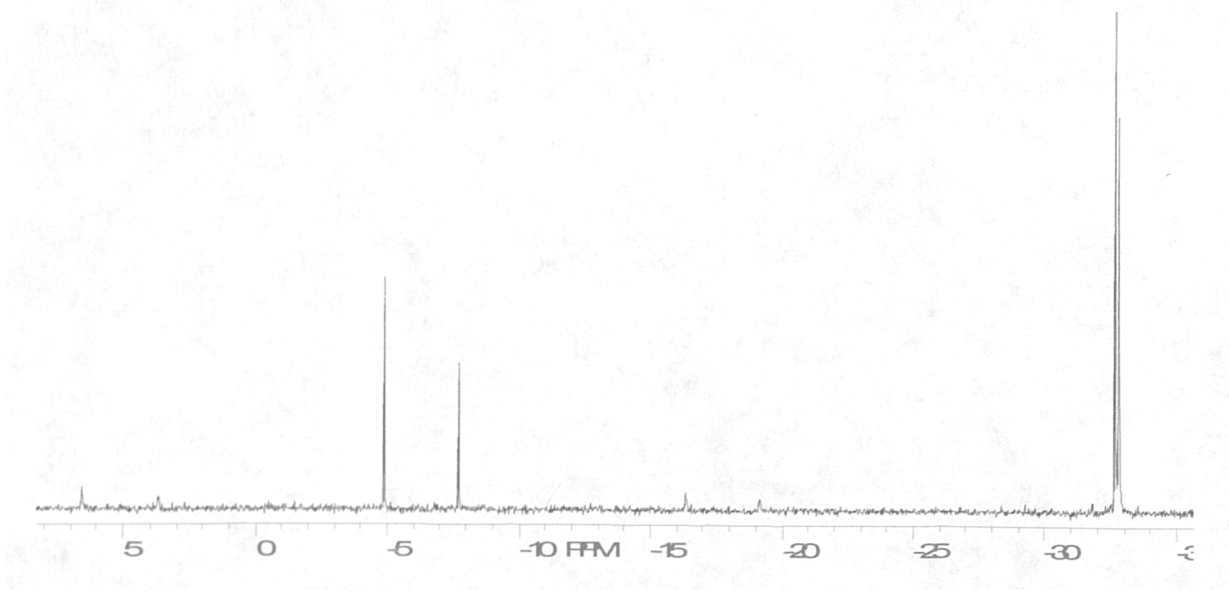

Figure 3.17 $^{31}P\{^{1}H\}$ NMR spectrum of the reaction between *meso/rac*-(**3.38**) and $[PtCl_2(cod)]$ in dichloromethane.

The reaction of 1.0 equiv. *meso/rac*-(**3.38**) with $[PdCl_2(NCPh)_2]$ in dichloromethane was monitored by $^{31}P\{^{1}H\}$ NMR spectroscopy. The spectrum exhibited two major species, a singlet at δ 15.2 p.p.m. and a dominant broad signal at δ -0.1 p.p.m. Attempts to characterise the products further from this reaction proved unsuccessful due to their very sparing solubility, perhaps indicating formation of oligomeric materials.

It seems the relatively flexible backbones in bis(phospha-adamantyl)diphosphines *meso/rac*-(**3.33**) and (**3.38**) inhibit them from forming chelates with Pd(II), in contrast to the C_2 and C_3 phospha-adamantanes *meso/rac*-(**3.1**) and (**3.2**). This feature is returned to in the discussion of the Pd(II) catalysed carbonylation results in Chapter 4. Similar behaviour is exhibited by the ligands 1,3-bis(di-*tert*-butylphosphino)propane and bis(di-*tert*-butylphosphino)-*o*-xylene.

Chapter 4

Homogeneous carbonylation catalysis with Pd(II) and Pt(II) complexes of C_2, C_3 and ferrocene bridged phospha-adamantanes.

4.1 Introduction

As discussed in Section 3.1, the C_2 and C_3 (phospha-adamantyl)alkanes (**3.1**) and (**3.2**) have been made previously in our group;[375,377] the synthesis of the 1,1'-bis(phospha-adamantyl)-ferrocene (**3.38**) and the separation of *meso*- and *rac*-(**3.2**) are described in Section 3.2. A comparison of the catalytic activity of the three ligands (**3.1**), (**3.2**) and (**3.38**) in complexes of the type $[M(diphosphine)(solv)_2]X_2$ (M = Pd, Pt) will be discussed in this chapter.

The carbonylation catalysts tested were formed by the combination of bidentate bis(phospha-adamantyl)diphosphines with a palladium(II) or platinum(II) species, *e.g.* $Pd(OAc)_2$, and an acid containing the weakly or non-coordinating anions (generally methanesulphonic acid), *via* the ligand complexation-anion displacement reaction, Equation 4.1.[397-399]

$$L_2 + Pd(OAc)_2 + 2HX \longrightarrow PdL_2X_2 + 2HOAc$$

Equation 4.1

The catalysts are conveniently generated (see section E.4) *in situ* by applying an excess of ligand and acid over the stoichiometric quantities required by Equation. 4.1. The beauty of this catalyst is that by variation of ligand, anion and/or solvent, the reaction can be directed towards the desired product.[400] Scheme 4.1 illustrates the proposed mechanisms that lead to the observed products.

The alkoxycarbonylation of olefins is of growing importance, and Equation 4.2 shows the range of products accessible. When n > 500, high molecular weight 'polyketones' are formed which have useful properties as engineering thermoplastics.[401] This CO/olefin polymerisation catalysed by the palladium system described in Equation 4.1 has recently been reviewed.[402] Alternatively, if n = 1, methyl propionate (MEP) is formed, a precursor for the manufacture of methyl methacrylate.

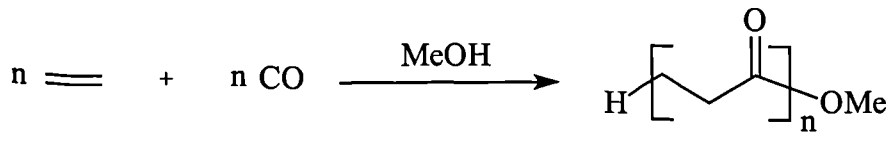

Equation 4.2

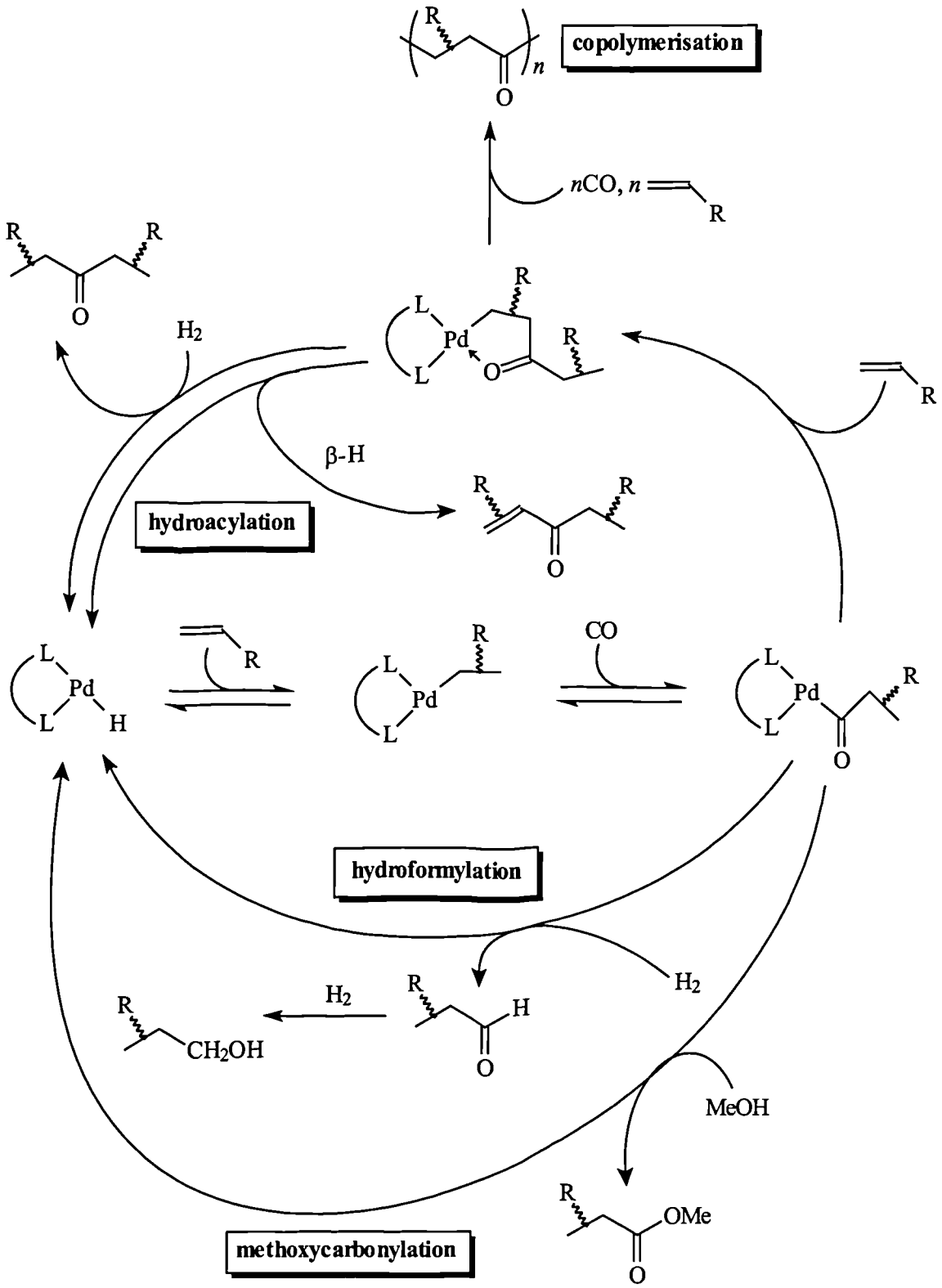

Scheme 1 proposed mechanisms of Pd-catalysed carbonylation reactions

Methyl methacrylate is also available *via* the palladium-catalysed carbonylation of propyne,[403] illustrated in Equation 4.3. In this very elegant carbonylation catalysis, the structure of the phosphine ligand is crucial, not only for an active catalyst, but also for selective formation of the branched methyl methacrylate over the linear methyl crotonate.

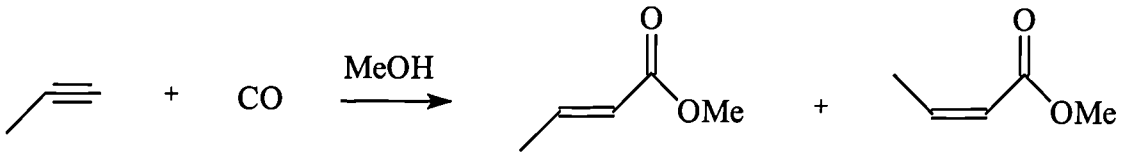

methyl crotonate methyl methacrylate

Equation 4.3

The palladium carbonylation catalysts for the copolymerisation of CO and ethene (Equation 4.2) also show marked selectivity dependence on the nature of the phosphine ligand, with monodentate phosphines generally giving MEP and bidentate phosphines yielding high molecular weight co-polymers.

4.1.1 Bulky phosphine ligands in carbonylation catalysis

Examples of bidentate phosphines that contradict this paradigm are rare, and demonstrate the use of sterically demanding phosphine ligands in catalysis. Both employ the *t*-butyl substituent on phosphorus in the ligands bis(di-tert-butylphosphino)propane[38] (**4.1**) and bis(di-tert-butylphosphino)-*o*-xylene[37] (**4.2**). These afford highly active palladium catalysts for the methoxycarbonylation of ethene to form MEP selectively.

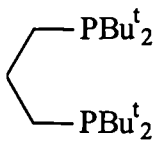

(4.1)

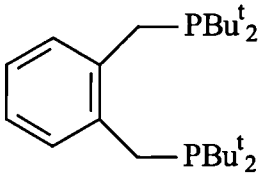

(4.2)

The remarkable activity and selectivity exhibited by these catalysts has been explored by Tooze *et al.*[36,404] Electronic effects on activity were investigated by functionalisation of the aryl bridge in ligand (**4.2**) with classical electron-releasing and -withdrawing groups (MeO and NO_2), but no significant effect on catalyst performance was observed. In contrast, the steric modification of substituents on phosphorus gave dramatic results; the cyclohexyl analogue of ligand (**4.2**) formed a catalyst that was 60 times less active for MEP formation than the system with ligand (**4.2**). Similar trends

are reported[38] for the propane-bridged diphosphine (**4.1**), which forms a catalyst far more active than its *s*-butyl analogue for MEP formation.

The selectivity of the reaction also changes markedly with ligand structure, less sterically demanding ligands generally give rise to products that are a mixture of polyketone oligomers and polymers.

The crystal structures of the zerovalent $[PdL_2(dba)]$ (dba = *trans,trans*-dibenzylideneacetone) complexes (L_2 = (**4.2**) and Cy, Pr^i, Ph analogues) suggest that although the P-Pd-P bite angle is approximately the same in these complexes, parallel pocket angles[405] do vary with the phosphorus substituent.

Coordination chemistry studies of more relevance to the catalysis with active ligands (**4.1**) and (**4.2**) and $Pd(OAc)_2$ were carried out; two structures determined demonstrate the sterically encumbering nature of the two ligands (Scheme 4.2).

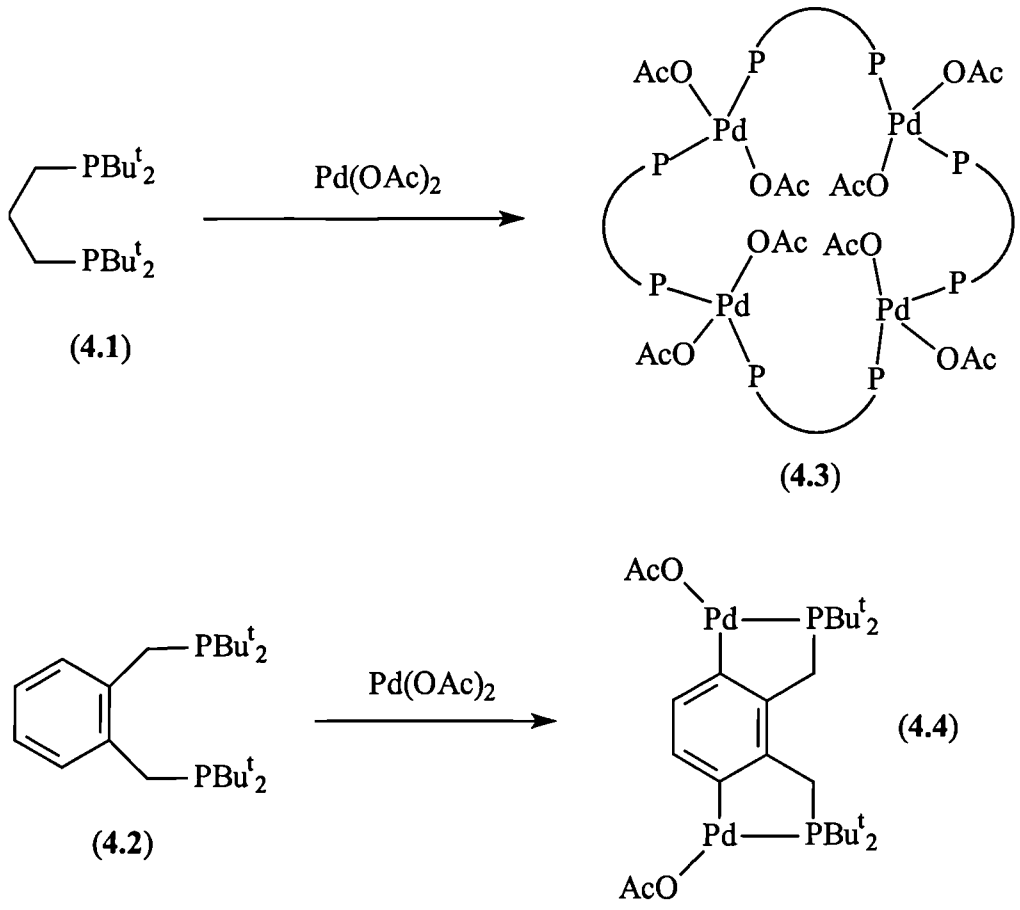

(**4.1**)

(**4.3**)

(**4.2**)

(**4.4**)

Scheme 4.2

Diphosphine (**4.1**) forms an unusual tetrameric complex (**4.3**) where the palladium atom has achieved *trans* disposition of the two phosphines. Reaction of ligand (**4.2**) with $Pd(OAc)_2$ affords the doubly orthometallated structure (**4.4**).

The tendancy to avoid the classical *cis* chelation (*cf.* dppp, the archetypal ligand for CO/ethene copolymerisation) is associated with the thermodynamic driving force to place the bulky phosphine ligands *trans* to each other (*e.g.* structure (**4.3**)). The methoxycarbonylation of ethene to MEP using PPh_3 as the ligand[406] is thought to proceed *via cis-trans* isomerisation of the ligand, thus isolating the growing chain from the vacant site and producing low weight molecular materials. The authors suggest that, in this way, the coordination behaviour exhibited by the ligands (**4.1**) and (**4.2**) is linked to the very selective formation of monomeric MEP in this catalysis, but they do not propose the structures (**4.3**) and (**4.4**) as catalytic intermediates.

Previous work in our group[375,377] has shown that the phospha-adamantane moiety has similar, if not more bulk than PBu^t_2 group (see Section 3.1). It was reasoned that this may translate into similar catalytic activity, and the resulting patents[382,383] describe this catalysis (see section 4.2.3 for further discussion).

In this chapter the bis(phospha-adamantane) diphosphines (**3.1**), (**3.2**) and (**3.38**) are compared in the palladium and platinum catalysed carbonylation of olefins and the platinum catalysed carbonylation of acetylene. The catalytic results are discussed in terms of (i) ligand backbone, (ii) the *meso* and *rac* diastereomers of the propane-bridged ligand (**3.2**) and (iii) the stereoelectronics of the phospha-adamantane cage.

4.2 Palladium catalysed hydroformylation and methoxycarbonylation of alkenes

4.2.1 Methoxycarbonylation of ethene

This reaction is illustrated in Equation 4.2 (n = 1) and the relevant data are shown in entries 1 and 2 of Table 4.1. The high selectivity for methyl propionate (MEP) observed for both ligands is consistent with the large steric bulk of these cage ligands rendering alternating CO/olefin polymerisation to form high molecular weight copolymers impossible. The analogous reaction with bis(di-*t*-butylphosphino)propane as ligand shows almost identical selectivity to MEP, with a slightly higher activity (~10000 turnovers per hour). The rate with the ferrocene ligand *meso/rac*-(**3.38**) was lower but plating of palladium was observed (see section 4.2.4). No comparable reaction with the C_2-cage ligand was carried out.

Table 4.1 Comparing palladium catalysed hydrocarbonylation of ethene, propene and C_{11}/C_{12}-olefins in methanol[a] with (**3.1**), (**3.2**) and (**3.38**).

Entry	Ligand	Olefin[b]	P_{CO} /bar	P_{H_2} /bar	T /°C	Rate[c]	Esters /%[d]	Ald/Alc /%[d]	Comments
1	*meso/rac* fc cage[e]	ethene	30	–	110	1670	96.8	–	Plating + oligomers (3.2%)
2	*meso/rac* C_3 cage	"	"	–	90	6000	> 95	–	<5% oligomers mainly dimer
3	*meso/rac* C_2 cage	propene	20	20	115	1040	42.4 (66.6)	19.5 (52.9)	38.1% oligomers + oligomeric ppt.
4	*meso/rac* fc cage[f]	"	"	"	"	1490	98.5 (85.2)	1.5 (58.5)	–
5	*rac*(80%) C_3 cage	"	"	"	65	10420	98.2 (78.6)	1.8 (54.0)	–
6	*meso*(70%) C_3 cage	"	"	"	"	37500	98.6 (76.0)	1.4 (57.8)	–
7	*meso/rac* C_2 cage[g]	SHOP C_{11}/C_{12}	20	40	130	310	79.4 (70.1)	20.6	30.1% conversion
8	*meso/rac* fc cage	"	"	20	125	100	99.1 (88.0)	0.9	8.3% conversion + plating
9	*meso/rac* C_3 cage[g]	"	"	40	130	420	98.9 (79.5)	1.1	97.9% conversion
10	*meso rac* C_3 cage	"	15	–	115	390	> 99 (80.3)	–	97.4% conversion
11	*rac*(99%) C_3 cage	"	"	–	"	190	> 99 (82.5)	–	94.3% conversion
12	*meso*(70%) C_3 cage	"	"	–	"	160	> 99 (79.3)	–	45.4% conversion + plating

a Batch experiments, 250 ml Hastelloy C autoclave. Solvent = methanol (50 cm^3), metal = $Pd(OAc)_2$ (0.1 mmol), acid = methanesulphonic acid (0.25 mmol), 0.15 mmol ligand unless otherwise stated.

b 20 bar ethene (at room temperature), 10 cm^3 propene and 20 cm^3 C_{11}/C_{12}- olefin unless otherwise stated.

c Turnover number/hour.

d Linearity in parentheses.

e 0.12 mmol ligand and 16 bar ethene.

f 0.07 mmol $Pd(acac)_2$.

g $Pd(OAc)_2$ (0.25 mmol), ligand (0.3 mmol) and methanesulphonic acid (0.5 mmol).

4.2.2 Methoxycarbonylation and hydroformylation of propene

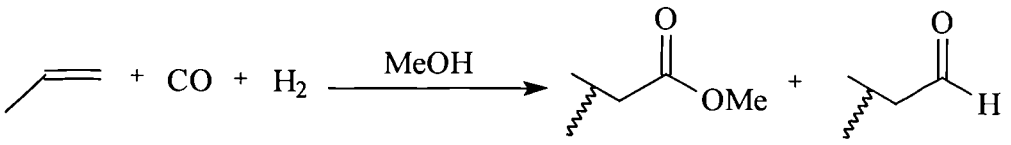

Equation 4.4

Entries 3-6 of Table 4.1 show the results for the reaction shown in eqn. 4.4. It is clear that the C_3 ligand is considerably more active (entries 5, 6) in these systems than

the C_2 and ferrocene analogues. The fc ligand shows a turnover number similar to the C_2 ligand, about an order of magnitude less (at a much higher reaction temperature) than that for C_3, and this was the only Pd/fc-ligand experiment performed that showed no plating (even with only 0.07 mmol [$Pd(acac)_2$]). Remarkably, a significant difference in activity was also observed between the two C_3 diastereomers, the *meso*-enriched diastereomer converting propene to the methoxycarbonylated species at over three times the rate of the *rac*-enriched diastereomer. This was surprising since we considered the *rac* and *meso* to have very similar structures. Molecular modelling of the diastereomeric diphosphine chelated to palladium was carried out and the hypothetical PdL_2 fragments (L_2 = *meso* or *rac* C_3 bis(phospha-adamantane)diphosphine) are illustrated in Figure 4.2.

For propene hydrocarbonylation, the C_3 and fc ligands show comparable high (98%) chemoselectivity to esters. In contrast the C_2-cage ligand, gives only 40% esters with 20% hydroformylation products and *ca.* 40% oligomeric products in solution along with a Carilite™-like precipitate; these polymeric products presumably arise from the decreased steric crowding around palladium.

The fc ligand produced the most linear esters, followed by the C_3 and C_2 ligands. It is also interesting to note that for all three ligands, the linearity of hydroformylation products differs significantly from the esters. Clearly the reaction between H_2 and the Pd-acyl (Scheme 4.1, section 4.1) to produce aldehydes is less regioselective than the corresponding reaction with methanol to form esters. This is possibly a result of H_2 being smaller than MeOH, reacting faster (with the Pd-acyl) and altering the equilibria between the starting Pd-hydride and the Pd-acyl, resulting in less linear products.

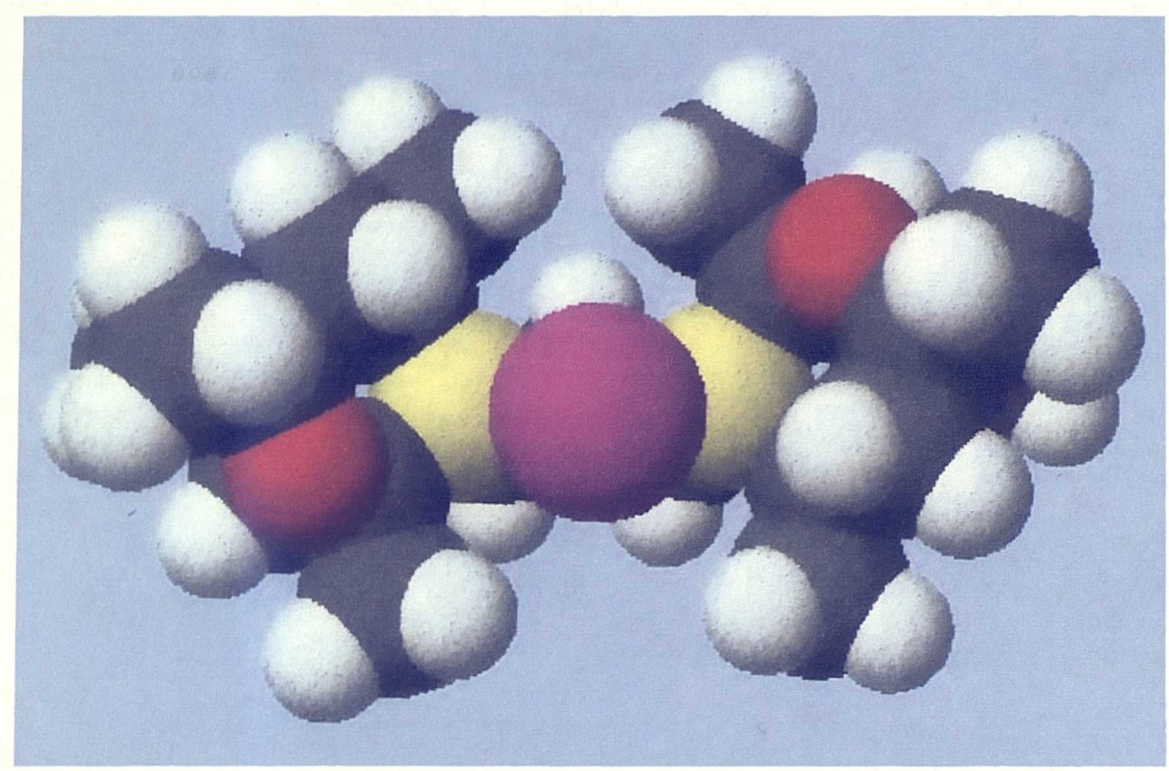

Figure 4.2a Model of *rac*-PdL_2

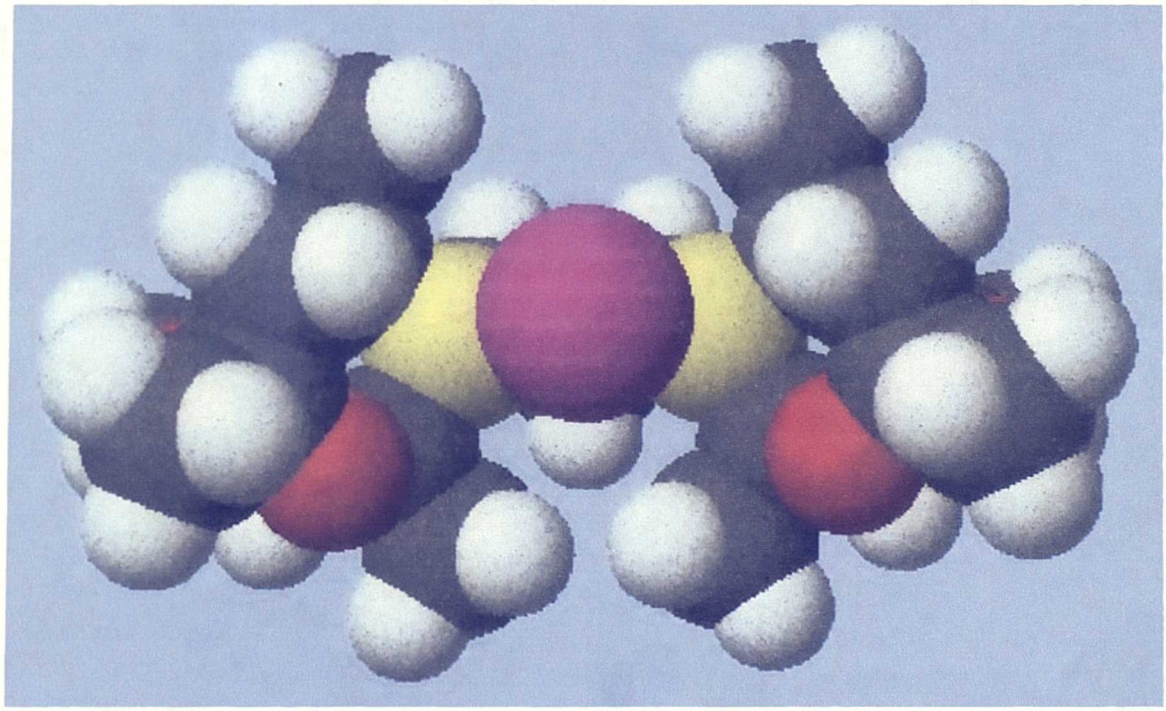

Figure 4.2b Model of *meso*-PdL_2

4.2.3 Methoxycarbonylation of internal C_{11}/C_{12}-olefins to linear esters

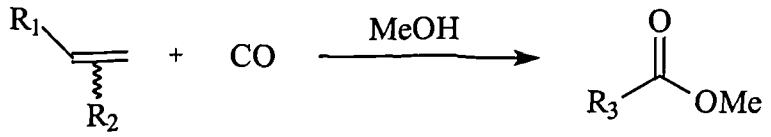

Equation 4.5

This work (illustrated in Equation 4.5) is very similar to that described in two recent patents.[382,383] The experiments shown in entries 7-12 of Table 4.1 compare the C_2, C_3 and ferrocene ligands in this reaction using C_{11}/C_{12}-olefins as substrate. The reactions described in entries 7-9 have 20 bar H_2 co-reactant, but as with the propene experiments, only the C_2 ligand shows any significant hydroformylation. The rates are, as expected, generally quite slow compared to the propene experiments, and activity should perhaps be considered in terms of % conversion (over *ca.* 6 hr.) as well as turnovers per hour. For the reactions with H_2 present the activity is in the order $C_3 > C_2 >$ fc, but again the reliability of the fc result is dubious due to precipitation of $Pd^0_{(s)}$ over the course of the reaction (see section 4.2.4). The ferrocene and C_3-cage ligands as in the propene experiments, show almost identical, very high selectivity (99%) towards ester formation and the fc-cage ligand again gives rise to the most linear products.

A comparison between *meso*- and *rac*-C_3 ligands for this process is shown in entries 10-12 of Table 4.1, in this case in the absence of H_2. The linearity of the quantitatively formed esters are similar in each case. The *rac*-C_3 experiment was performed before the *meso*-C_3, showing an activity about half that of the *meso/rac* mixture. Unfortunately, the analogous *meso*-enriched experiment did not give the expected complementary doubled activity enhancement and plating was observed. It is possible the ligand was contaminated with phosphine oxide, giving rise to reduced activity.

The patents[382,383] that describe the unique isomerisation/methoxycarbonylation of internal olefins by this catalyst system also give examples of analogous experiments using bis(di-*t*-butylphosphino)propane as ligand, for which very low rates and conversions to the linear esters were observed. The stereoelectronic difference between the cage diphosphines and *t*-butyl analogues will now be discussed to rationalise the catalysis.

The cone angle[25] for the C_3 ligand measured from the crystal structure of the metal complex [{*rac*-bis(phospha-adamantyl)propane}$PdCl_2$][375] is 173° which is even larger than for the analogous *t*-butyl platinum complex ([$PtCl_2${$Bu^t_2P(CH_2)_3PBu^t_2$}] =

155°).[381] The rigidity of the phospha-adamantane cage means that the cone angle measured is more reliable than the conformationally flexible PBu^t_2 ligands. It could be the rigidity of the bulky cage phosphine which leads to the observed unique isomerisation/methoxycarbonylation.

We have also probed the electronic effects of bis(phospha-admantyl)diphosphines e palladium centre and compared it with its bulky alkyl phosphine analogues. An extensive library of phosphine ligand basicity has been compiled at Shell Research and Technology, Amsterdam[407] by measuring the CO stretching frequency for the readily prepared metal complexes $[Ni(CO)_2(diphosphine)]$, and similar measurements were made with ligands (**3.1**), (**3.2**) and (**3.38**). These results (green diamonds) are shown below (Figure 4.3) alongside some CO stretching frequencies with analogous ligands.

The ν_{CO} values for the cage diphosphines are much higher than expected for alkyl phosphines, and are indeed to high frequency of most aryl diphosphines. This shows that the cage ligands are surprisingly less basic than their alkyl diphosphine analogues. All the crystal structures of these cage ligands, both free and coordinated reveal a significant decrease in the C-P-C angle from 109° to *ca.* 90° which is associated[79] with a corresponding increase in the π-acidity of the ligand (see Section 1.4.2), in agreement with the results shown in figure 4.3.

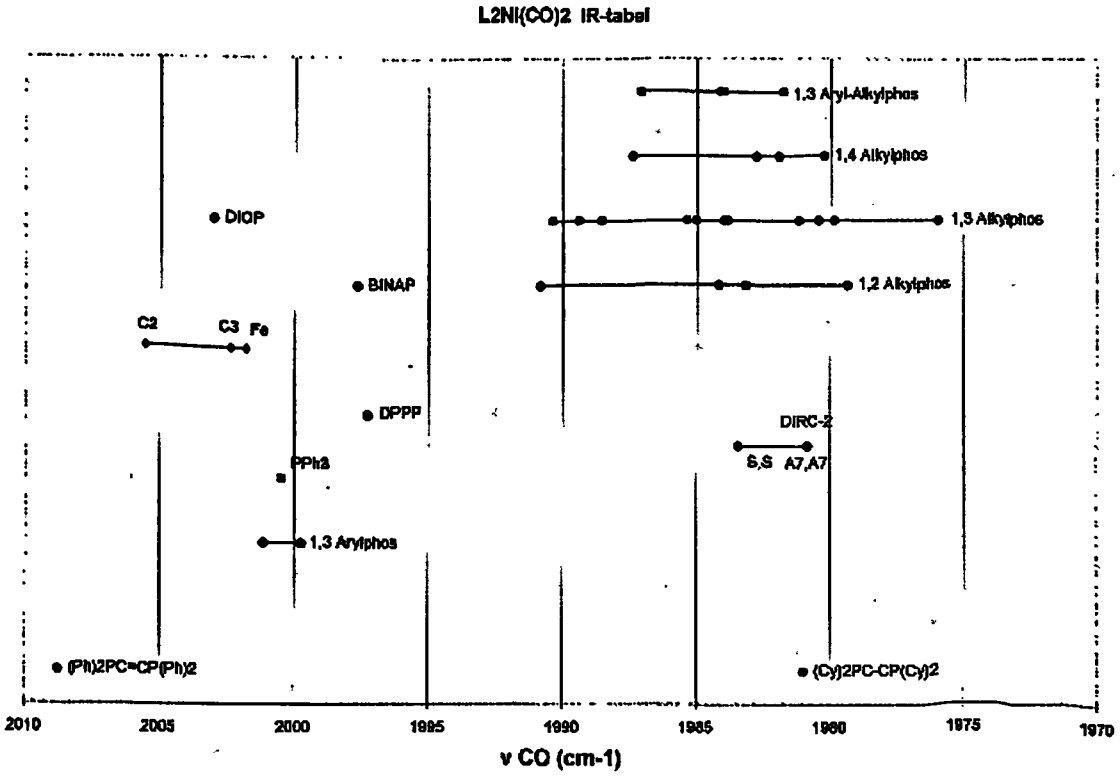

Figure 4.3: ν_{CO} values for cage and other diphosphines in their $Ni(CO)_2(diphos)$ complexes.

It is likely, therefore, that the difference in basicity between the C_3 ligand (**3.2**) and its *t*-butyl analogue contributes to their observed difference in activity in methoxycarbonylation of internal olefins to linear esters.

As mentioned earlier, the C_3 cage diphosphine shows similar activity to its *t*-butyl analogue in the methoxycarbonylation of ethene. This suggests that the assumed rate-determining step of this reaction (the methanolysis of the Pd-acyl to form MEP) is also similar with these two ligands. It is logical to deduce, therefore, that the rate-determining step in the methoxycarbonylation of internal olefins to linear esters is the isomerisation of internal olefins to α-olefins (involving sequential olefin insertion into a Pd-hydride and β-H elimination), which the C_3 Bu^t-diphosphine cannot perform. Confirmation of this hypothesis is shown by the similar rates of methoxycarbonylation of α-C_{11}/C_{12}-olefins with the bis(phospha-adamantyl)- and Bu^t C_3-diphosphines.[382]

4.2.4 Problems associated with ferrocene ligand (3.38) catalysis

In all but one of the catalytic runs with $Pd(OAc)_2$/(**3.38**), precipitation of palladium (plating) was observed. Numerous attempts were made to overcome this problem, including pre-forming the catalyst under N_2 in a variety of solvents (methanol, methanol/toluene, THF, diglyme and dichloromethane), none of which were successful. Experiments were attempted using $Pd(acac)_2$ as the catalyst precursor because the acac ligand is less labile than acetate and any process leading to plating might be arrested (see entry 4, Table 4.1). Although these reactions resulted in reduced plating, they did not show significantly increased activity.

A ^{31}P NMR study of the Pd/fc ligand system was carried out. Addition of 1 equivalent of diphosphine to $Pd(OAc)_2$ in CD_2Cl_2 gave a red solution and two major resonances corresponding to two diastereomeric chelates. After *ca.* 8 h, palladium metal was observed to precipitate, and the ^{31}P NMR spectrum showed a corresponding phosphine oxide resonance. It is difficult to translate this into catalytic reaction conditions, but it is clear that whilst the fc-cage diphosphine does readily complex with $Pd(OAc)_2$, the chelate appears to be unstable.

4.3 Platinum catalysed hydroformylation and methoxycarbonylation of alkenes

This work was prompted, in part, by the inability of the fc-cage ligand to form a stable and active catalyst with palladium(II). It was hoped that the relative kinetic

stability of platinum(II) would yield a more reliable comparison between the three cage ligands. All reactions were carried out in methanol, and the data are shown in Table 4.2.

Table 4.2 Comparing platinum catalysed hydrocarbonylation of ethene and propene in methanol[a] with C_2, C_3 and 1,1'-bis(phospha-adamantyl)ferrocene diphosphine ligands.

Entry	Ligand	Olefin[b]	Rate[c]	Products[d] Esters/%	Ald/%	Other/%
1	*meso/rac* fc cage[e]	ethene	1040	67.2	32.3	0.5 diethyl ketone
2	*meso/rac* C_3 cage[f]	"	590	64.6	34.6	0.8 diethyl ketone
3	*rac*(99%) C_3 cage	"	830	38.2	60.6	1.2 diethyl ketone
4	*meso/rac* C_2 cage	propene	100	_	96.6	3.4(60.8) alcohols
5	*meso/rac* fc cage	"	170	40.5 (89.0)	59.5 (77.3)	_
6	*meso/rac* C_3 cage	"	90	58.0 (79.8)	42.0 (75.2)	_
7	*rac*(80%) C_3 cage[g]	"	100	54.1 (80.9)	45.9 (74.1)	_
8	*meso*(70%) C_3-cage	"	90	66.6 (78.7)	33.4 (76.6)	_

[a] Batch experiments, 250 cm^3 Hastelloy C autoclave. Solvent = methanol (50 cm^3), metal = $Pt(OAc)_2$ (0.075 mmol), acid = methanesulphonic acid (0.25 mmol), 0.15 mmol ligand, 20 bar CO and 20 bar H_2 (at room temperature) unless otherwise stated.

[b] 20 bar ethene (at room temperature) and 10 ml propene.

[c] Turnover number/hour.

[d] linearity in parentheses.

[e] metal = $Pt(acac)_2$ (0.08 mmol).

[f] acid = trifluoromethanesulphonic acid.

[g] metal = $Pt(acac)_2$ (0.1 mmol).

4.3.1 Hydroformylation and methoxycarbonylation of ethene

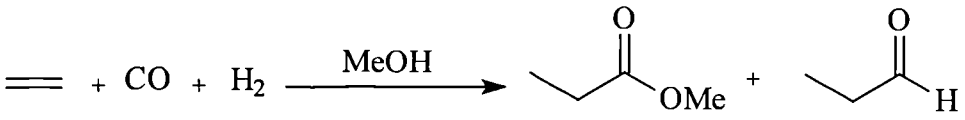

The reactions with ethene (Equation 4.6, entries 1-3 of Table 4.2) differ from those described in Table 4.1 with palladium, as H_2 (20 bar) is used as co-reactant, leading to significant amounts of hydroformylation products. No reaction has been performed with the C_2 ligand. The *meso/rac*-C_3 reaction shown uses

trifluoromethanesulphonic acid and therefore cannot be reliably compared to the other reactions, which employ methanesulphonic acid. Furthermore, no experiment was performed with the *meso*-C_3 ligand to compare with the *rac*-C_3 experiment shown. Nonetheless, it can be seen from the rates of the three reactions shown that the fc-cage ligand is comparable with, if not faster than the C_3-cage in this system. The selectivity towards esters is very similar with the fc and *meso/rac*-C_3 experiments shown, but it is fascinating to note that the *rac*-C_3 experiment shows essentially reversed selectivity compared to the *meso/rac* analogue between esters and aldehydes (implying that the *meso* isomer would give very high ester selectivity). The results are incomplete however, and more accurate conclusions can be drawn from the propene experiments.

4.3.2 Hydroformylation and methoxycarbonylation of propene

The rates of these experiments (entries 4-8), as expected, are much slower than their palladium-catalysed analogues (Table 4.1). The rates for the three ligands are all similar (the fc-cage ligand giving the highest activity) in contrast to the Pd analogues, where the C_3-cage ligand results in catalyst systems with activities at least an order of magnitude faster than the C_2 and ferrocene systems.

The chemoselectivity shows a shift towards hydroformylation compared to the palladium-catalysed process, indicating that the Pt-acyl shows a higher reactivity towards hydrogen relative to methanol compared to the Pd-acyl. Indeed, the C_2 experiment gives quantitative formation of aldehydes/alcohols (*cf.* 20% in the analogous Pd reaction). This can be rationalised in terms of the higher thermodynamic stability of the Pt-hydride compared to the Pd-hydride relative to the Pt and Pd-acyls. The fc ligand shows slightly reduced selectivity towards esters compared to the three C_3-cage reactions and the *meso*-C_3 ligand shows an increased selectivity for esters over the analogous *rac*-C_3 reaction.

The ferrocene ligand, as in the palladium reactions, forms catalysts that give the most linear products. Also, as observed in the Pd experiments, the linearities differ in the methoxycarbonylation and hydroformylation processes, indicating a subtle balance between the equilibria of the two processes.

4.4 Platinum catalysed methoxycarbonylation of acetylene and derivatives

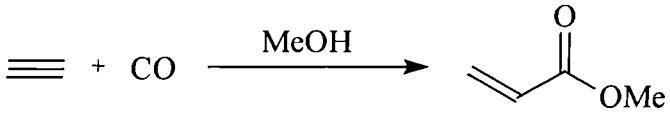

Equation 4.7

These reactions (Equation 4.7) are an extension of the methoxycarbonylation of ethene, and the results are shown in Table 4.3.

Table 4.3 Comparing platinum catalysed carbonylation of acetylene[a] with C_2, C_3 and ferrocene bis(phospha-adamantyl)diphosphine ligands.

Entry	Ligand	Solvent	Rate[b]	Products[c]
1	*meso/rac* C_2 cage[d]	methanol	290	methyl acrylate (76.4%)
2	*meso/rac* fc cage[e]	"	690	methyl acrylate (68.8%)
3	*meso/rac* C_3 cage	"	2080	methyl acrylate (76.7%)
4	*meso rac* C_3 cage	diglyme (30 ml)/ propan-1-ol (30 ml)	1390	propyl acrylate (89.4%)

[a] Batch experiments, 250 ml Hastelloy C autoclave. Solvent = methanol (50 cm^3), metal = $Pt(acac)_2$ (0.1 mmol), acid – methanesulphonic acid (0.25 mmol), T = 115 °C, 0.15 mmol ligand, 40 bar CO and 1.4 bar acetylene (at room temperature) unless otherwise stated.

[b] Turnover number/hour.

[c] minor products shown in Figure 4.4.

[d] 0.75 mmol $Pt(acac)_2$ and 0.12 mmol ligand.

[e] 0.12 mmol ligand.

Minor products from C_2 cage reaction

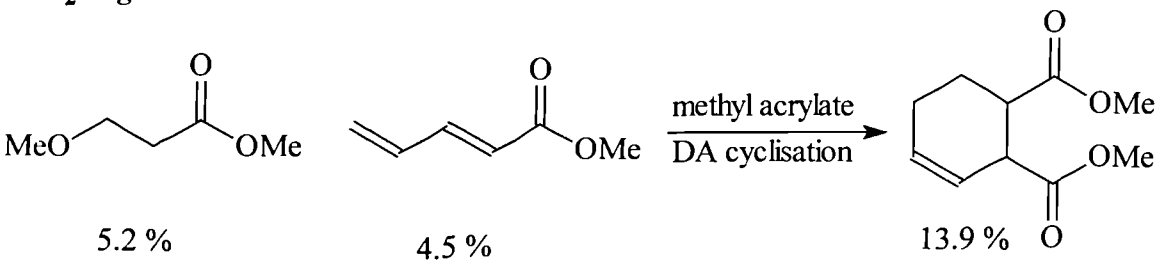

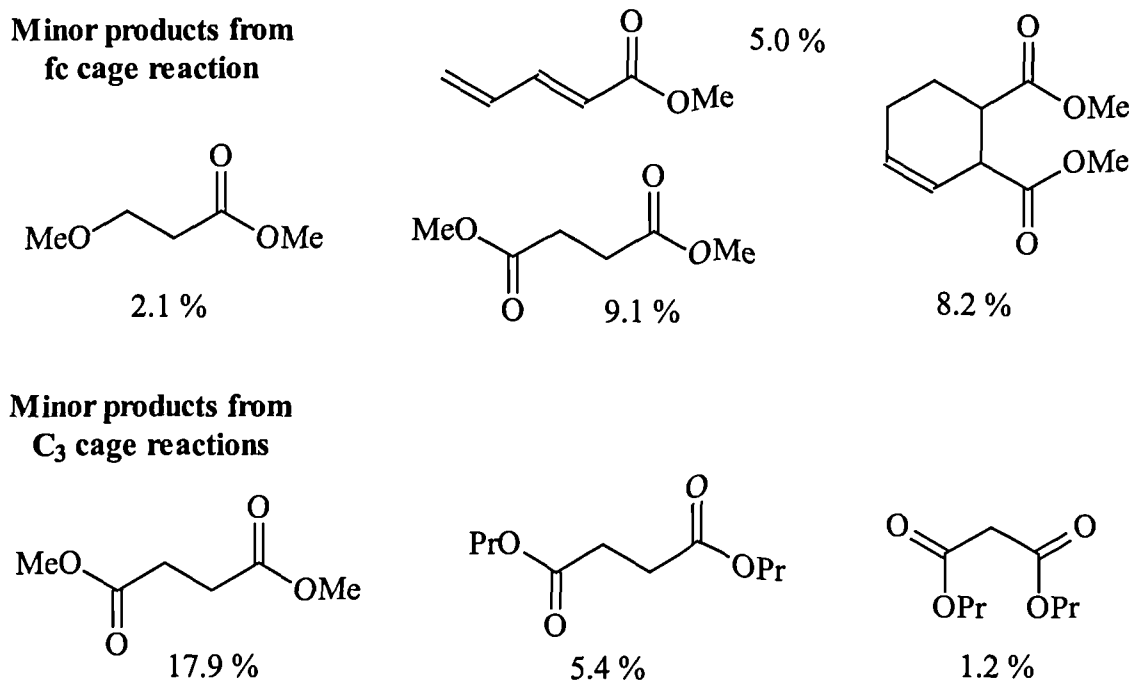

Figure 4.4

The first reaction performed was with the C_2 ligand (entry 1). Many variations were made to this system (*e.g.* the acid, using chloride additives) but the best results were obtained with the conditions shown. The rate of methyl acrylate formation can be seen to increase in the order $C_2 < fc < C_3$. This rate was difficult to measure as acetylene is not very soluble in methanol (leading to very fast complete consumption of acetylene), so the last reaction employs a diglyme/propanol solvent mixture to extend the reaction time. The rate of methyl acrylate formation using the C_3 ligand is comparable to the best activity known for platinum catalysed methoxycarbonylation of acetylene, and this work is being patented as a result.[408] These systems gave up to 90% methyl acrylate, and the by-products are shown in Figure 4.4 (all reactions also produced a small amount of polyacetylene). It should be noted that more selective methoxycarbonylation of acetylenes with these systems could be achieved by stopping the reaction immediately after consumption of acetylene; the reactions shown in Table 3 were all carried out over at least 5 hours, and many of the by products result from subsequent reactions between primary products.

This chemistry has also been extended to methyl acetylene and phenyl acetylene, using the most active C_3 ligand/Pt system. Whilst the conversion of methyl acetylene to methyl methacrylate (branched) and methyl crotonate (linear) was slow, the rate of methoxycarbonylation of phenyl acetylene was of the order of 1000 turnovers/hour at

115 °C, forming the linear methyl cinnamate and the branched methyl atropate in 48% and 52% yields respectively.

4.5 Conclusions

A graphical summary of the results described in this chapter are illustrated below. Only the reactions with propene, C_{11}/C_{12} internal olefins and acetylene are shown, as these reliably compare the three ligands (**3.1**), (**3.2**) and (**3.38**) in catalyst performance. Linearity's of products and selectivities for the acetylene reactions are left out for clarity (see section 4.4).

4.5.1 Pd-catalysed methoxycarbonylation and hydroformylation of propene

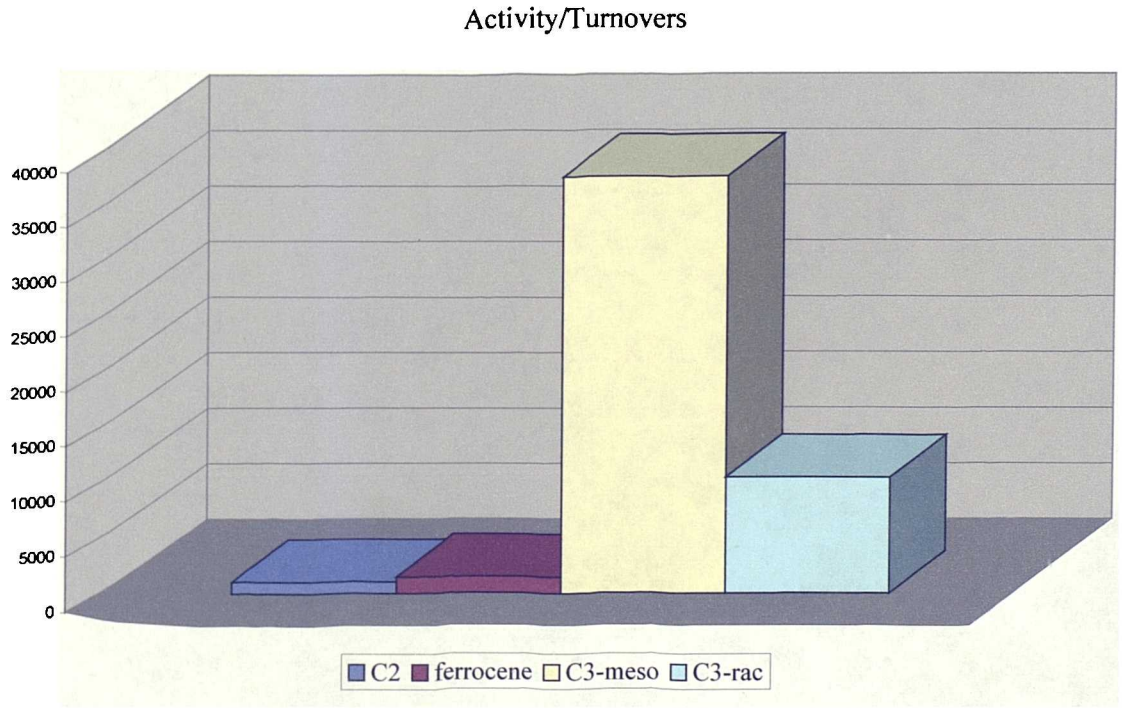

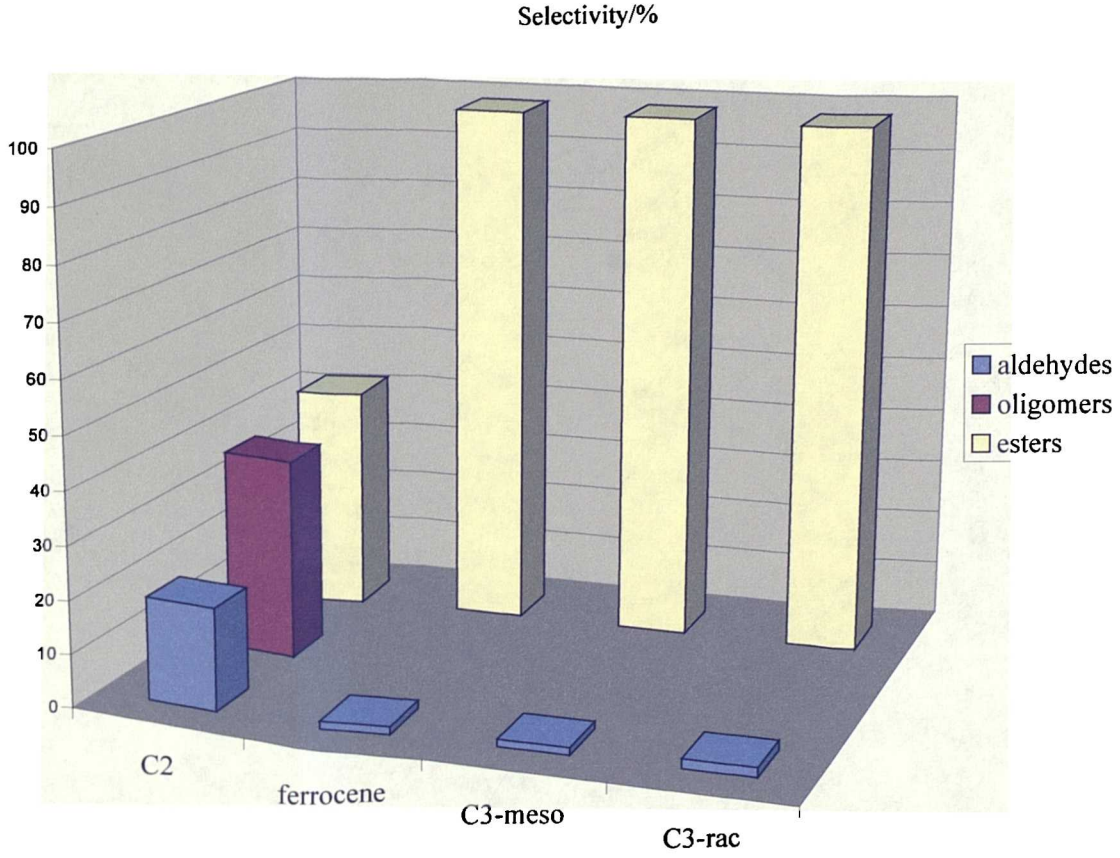

4.5.2 Pd-catalysed methoxycarbonylation and hydroformylation of C_{11}/C_{12} internal olefins

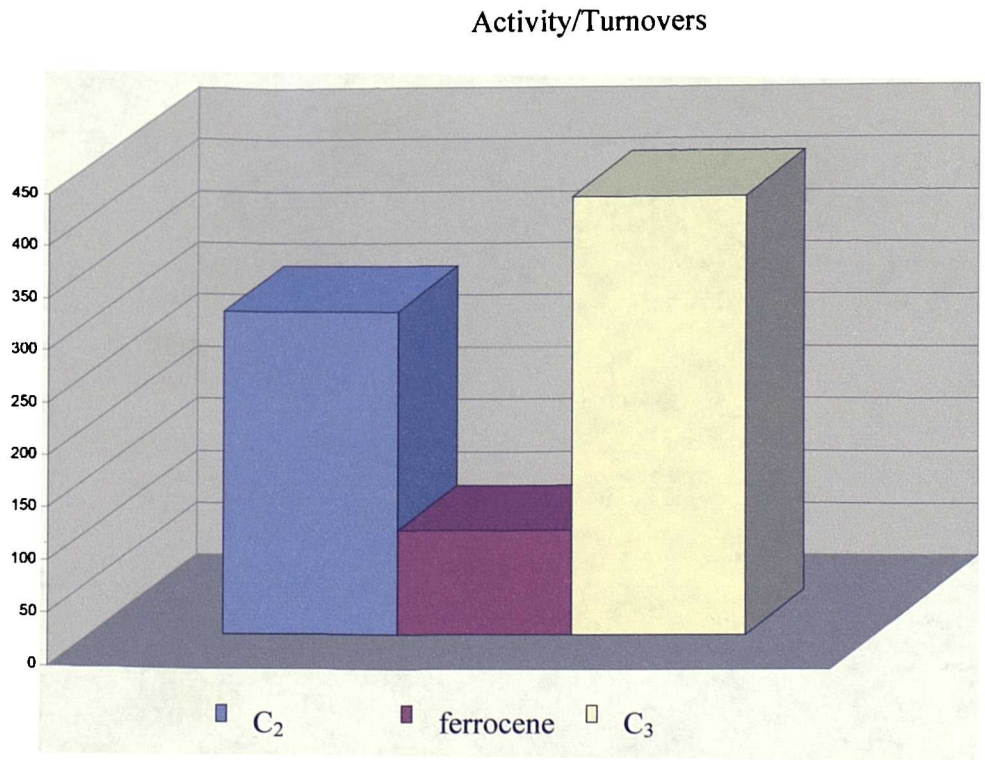

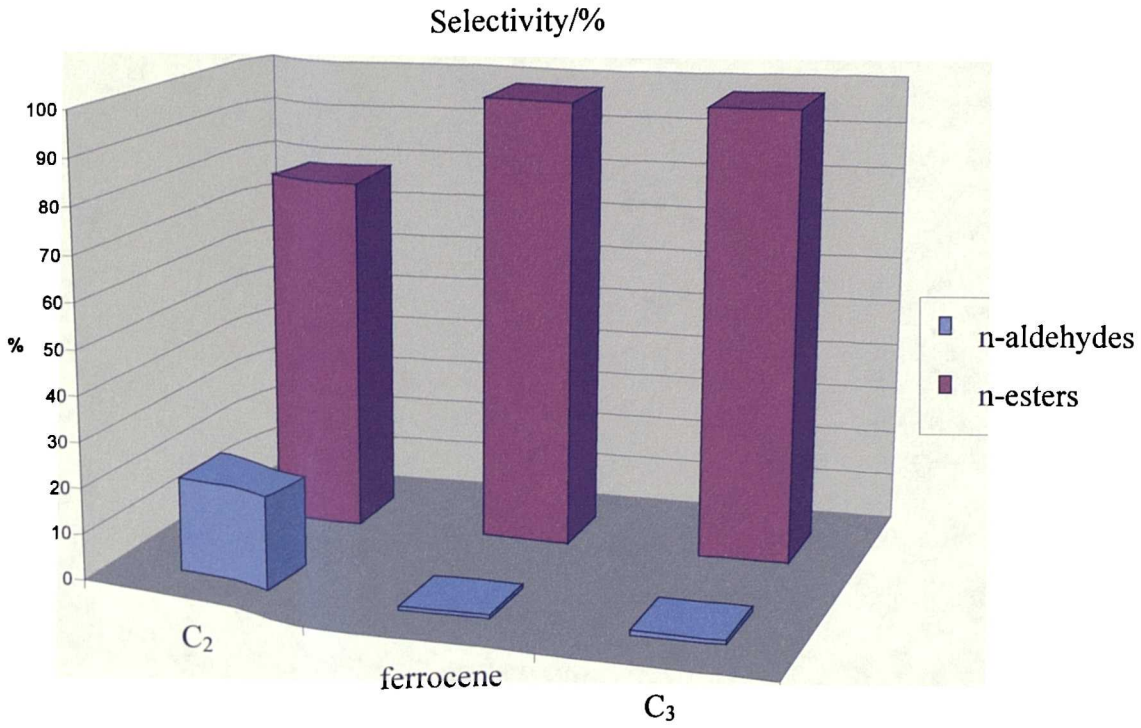

4.5.3 Pt-catalysed methoxycarbonylation and hydroformylation of propene

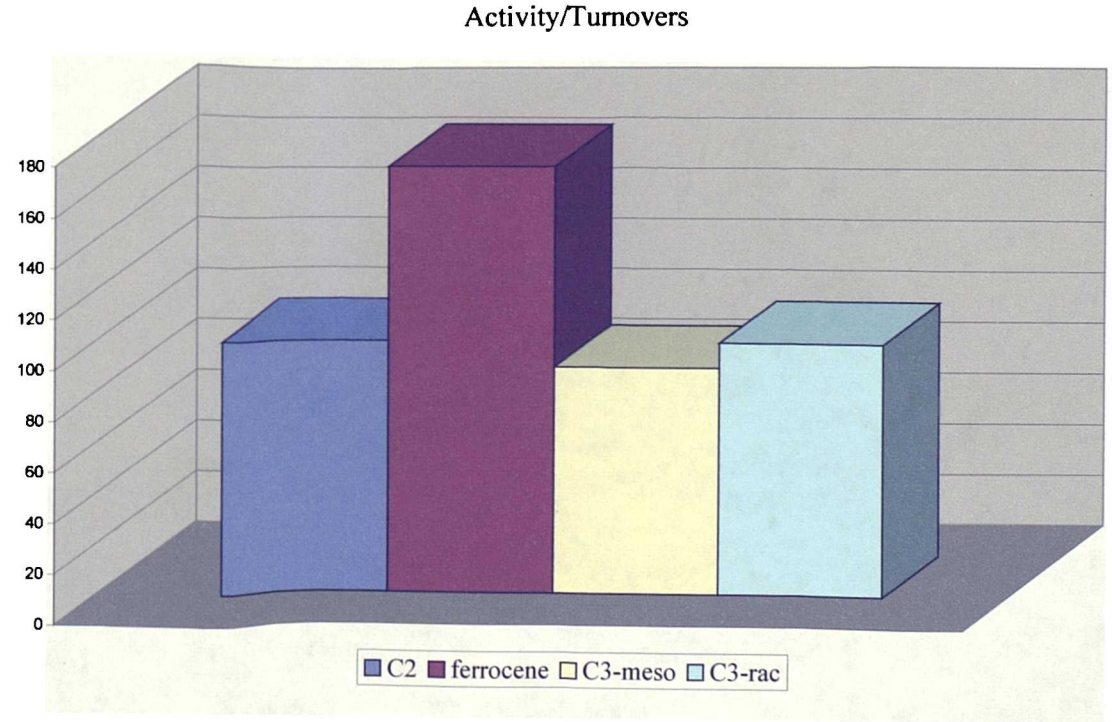

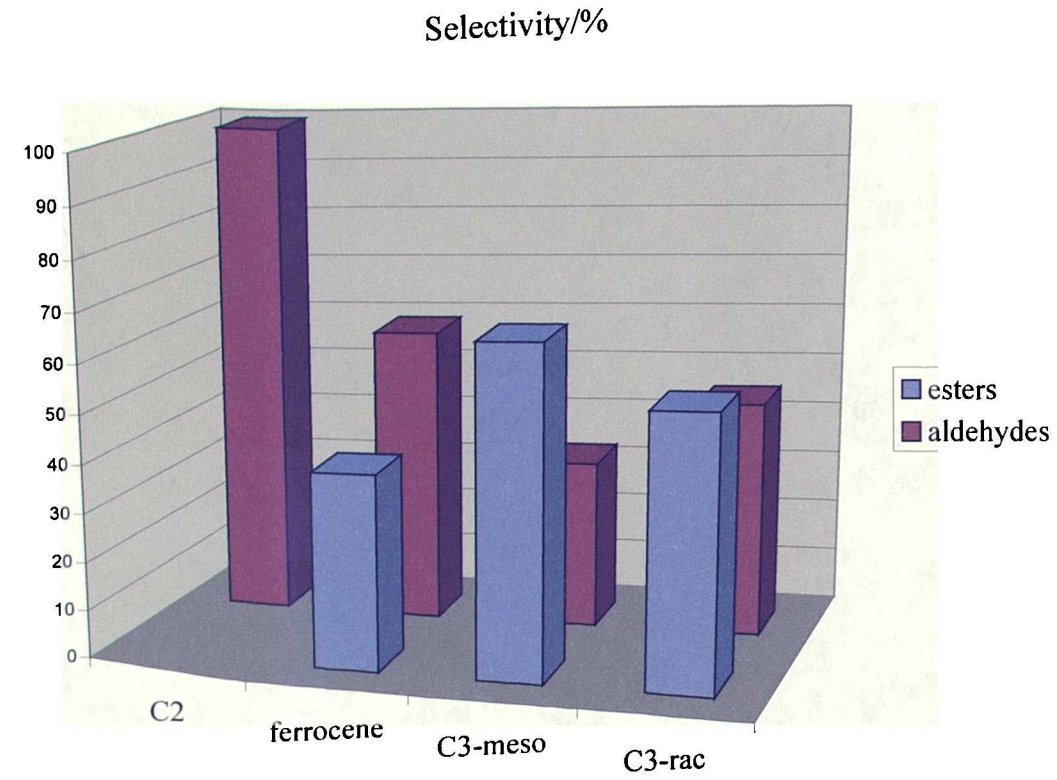

4.5.4 Pt-catalysed methoxycarbonylation of acetylene

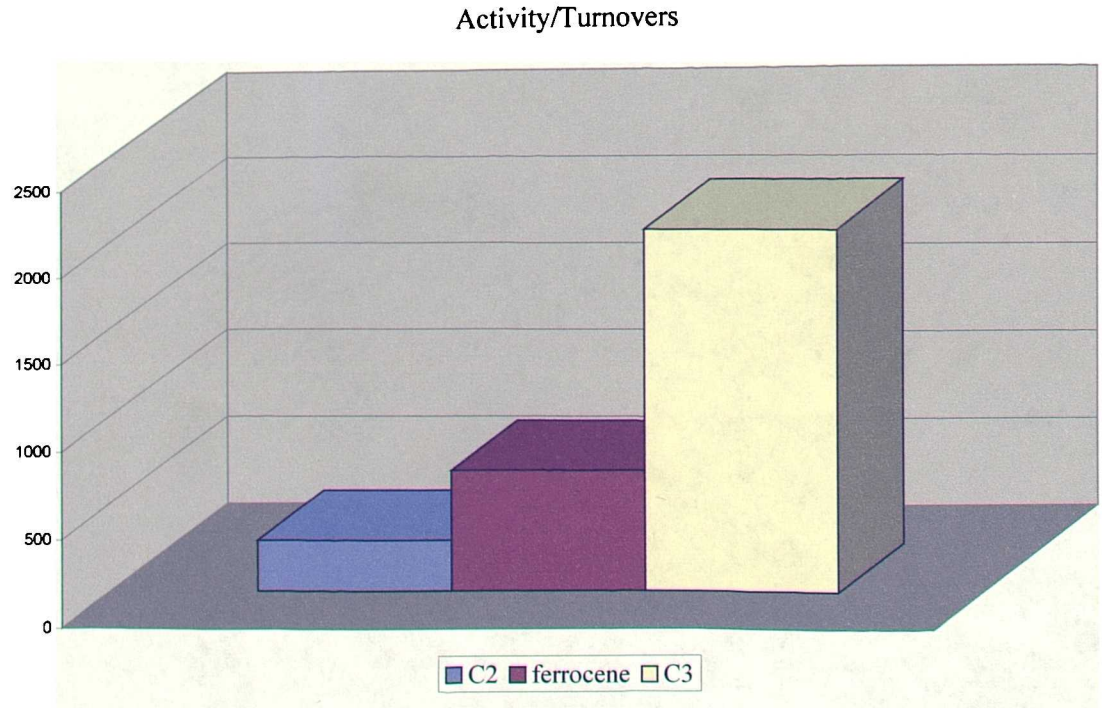

Chapter 5

Tetramethyl-dioxa-diphospha-adamantanes

5.1 Introduction

In their paper on the synthesis of mono-phospha-adamantanes, Epstein and Buckler[373,374] also reported that under certain conditions, adamantane-based cages containing more than one phosphorus atom could be prepared. For instance, reaction of equimolar amounts of 2-cyanoethylphosphine with 2,4-pentanedione in benzene with a methanesulphonic acid catalyst afforded the 1,3,5,7-tetramethyl-4,8-dioxa-2,6-diphospha-adamantane (**5.1**). Similarly, reaction of 1.5 equiv. phenylphosphine with 2,4-pentanedione in concentrated HCl and ethanol co-solvent yields the tetramethyl-oxa-triphospha-adamantane (**5.3**).

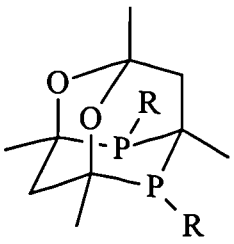

R = cyanoethyl (**5.1**)
R = cyclohexyl (**5.2**)

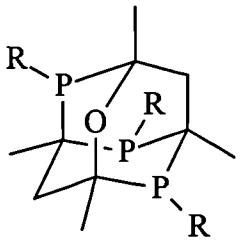

R = Ph (**5.3**)

The crude yield reported for diphospha-adamantane (**5.1**) was 7 %, and no yields were given for compounds (**5.2**) and (**5.3**). Elemental analyses were obtained for compounds (**5.1**)-(**5.3**), but the positions of the phosphorus atoms in cages (**5.1**) and (**5.2**) are not clear. The structures illustrated above show the two phosphorus atoms of diphospha-adamantanes (**5.1**) and (**5.2**) in the same six-membered ring, but it is perhaps more likely that they are positioned as far apart as possible (in separate six-membered rings) for steric reasons.

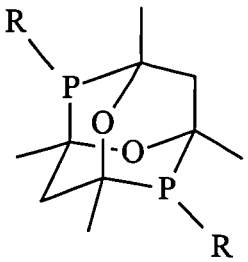

R = cyanoethyl (**5.1a**)
R = cyclohexyl (**5.2a**)

More recently, Gee[375] isolated the minor product from the reaction of 1,2-diphosphinoethane with 2,4-pentanedione, and assigned it to the diphospha-adamantane

(**5.4**). In this compound, the two phosphorus atoms are in the same six-membered ring by virtue of the C_2-unit linking them.

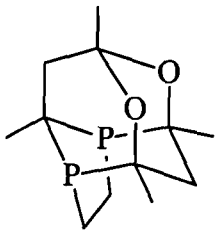

(**5.4**)

In this chapter, the synthesis and characterisation of new diphospha-adamantanes are described. Preliminary coordination chemistry studies of these compounds are presented, and postulated mechanisms for the formation of these phosphorus-containing cages are discussed.

5.2 Synthesis and characterisation of diphospha-adamantanes

5.2.1 Reaction of 1,2-diphosphinobenzene with 1,3-diketones

The synthesis of 1,2-diphosphinobenzene (**5.5**) (see Equation 5.1) has been reported.[386]

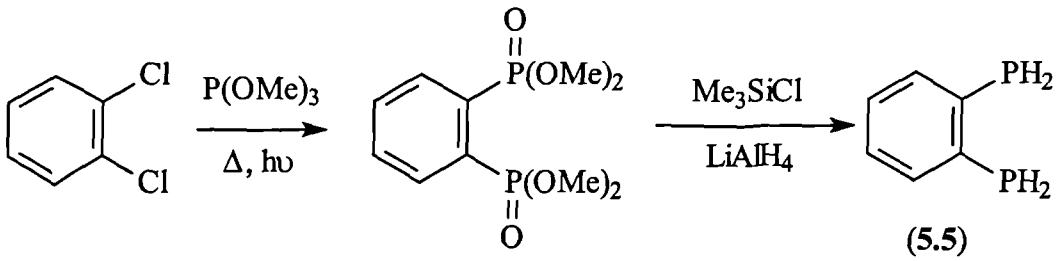

(**5.5**)

Equation 5.1

The reaction between 1,2-diphosphinobenzene and 2,4-pentanedione in 5 M HCl afforded diphospha-adamantane (**5.6**) (see Equation 5.2) in 25 % yield as an off-white solid. The $^{31}P\{^1H\}$ NMR spectrum of (**5.6**) showed a singlet at δ 6.2 p.p.m., and the structure was elucidated from the symmetry of its ^1H and $^{13}C\{^1H\}$ NMR spectra (see Table 5.1) and confirmed by *X*-ray crystallography, mass spectrometry and elemental analysis (see Experimental).

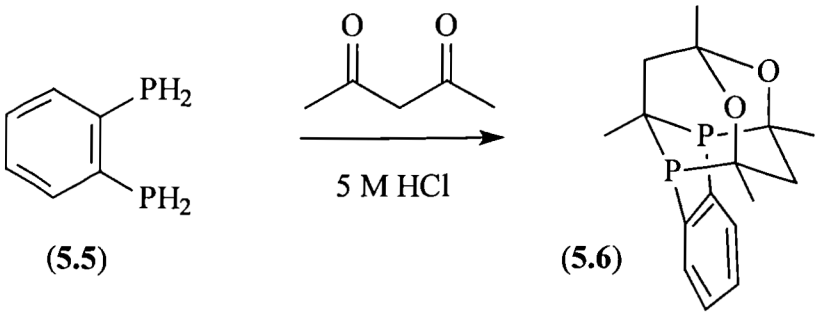

(5.5) (5.6)

Equation 5.2

Table 5.1 $^{13}C\{^1H\}$ NMR[a] and ^1H NMR[b] data for diphospha-adamantane (**5.6**)

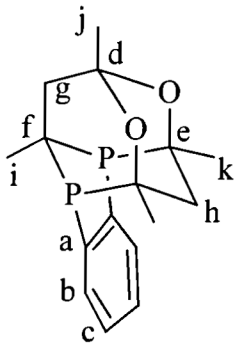

	$\delta(^{13}C)$		$\delta(^1H)$
a	148.6 (t, ^1J(PC) 9.6 Hz)	7.72	(m, 2H, *o*-$C_6H_2H_2$)
b	132.4 (m)	7.35	(m, 2H, *m*-$C_6H_2H_2$)
c	130.0 (t, ^3J(PC) 4.0 Hz)		
d	97.0 (s)	1.97-2.05	(m, 2H, CH_2)
e	70.5 (t, ^1J(PC) 6.4 Hz)	1.43	(s, 3H, CH_3)
f	31.9 (t, ^1J(PC) 11.8 Hz)		
g and h	41.7 (t, ^2J(PC) 6.4 Hz)	1.12-1.28	(br m, 10H, $3CH_3$ + C*H*H)
	40.4 (t, ^2J(PC) 3.1 Hz)		
i	26.7 (t, ^2J(PC) 19.0 Hz)	0.93	(d, 1H, CH*H*, ^1J(H*H*) 13.8
j	28.9 (s)		Hz)
k	28.5 (m)		

[a] Spectra recorded at 100 MHz in $CDCl_3$ at 26 °C. Chemical shifts [$\delta(^{13}C)$] in p.p.m.(± 0.1) relative to $CDCl_3$ (77.0 p.p.m.). Coupling constants (*J*) in Hz (± 0.1).

[b] Spectra recorded at 300 MHz in $CDCl_3$ at 24 °C. Chemical shifts [$\delta(^1H)$] in p.p.m.(± 0.1) relative to residual solvent (7.26 p.p.m.). Coupling constants (*J*) in Hz (± 0.1).

Single crystals of diphospha-adamantane (**5.6**) suitable for *X*-ray diffraction were grown by slow evaporation of solvent from a dichloromethane solution. Miss H. Phetmung of this department carried out the structure determination, which was solved in the orthorhombic space group Pnma with four formula units per unit cell. The numbering scheme and molecular structure is shown in Figure 5.1. The method of data collection, structure solution and refinement, the tables containing atomic coordinates, bond lengths and angles, isotropic and anisotropic displacement coefficients are all collected in the Appendix.

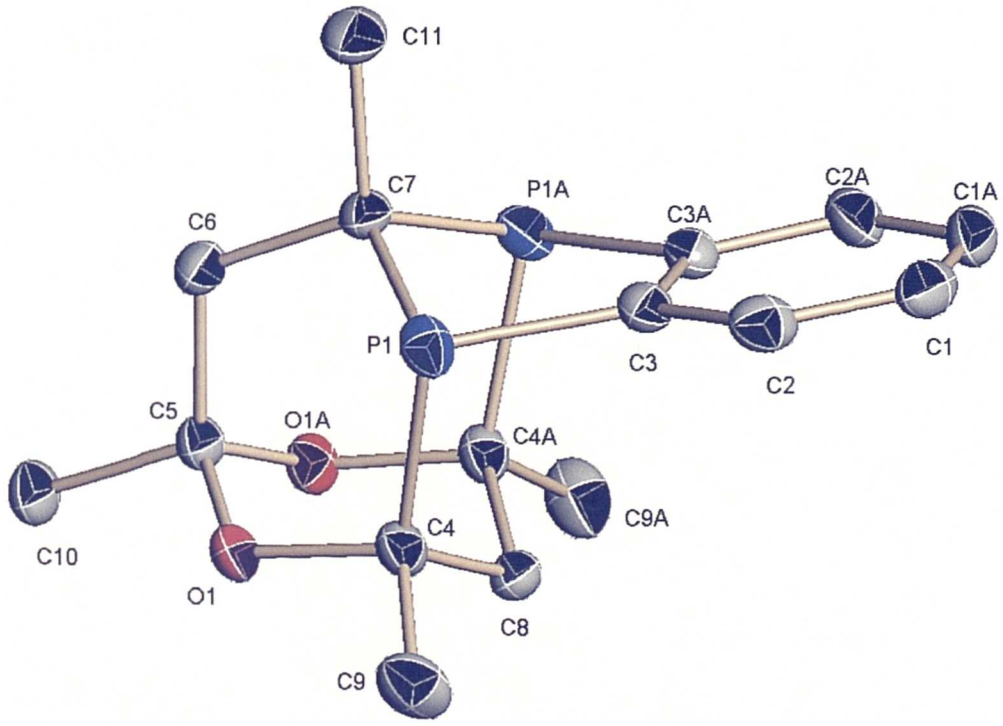

Figure 5.1 Molecular structure of diphospha-adamantane (**5.6**). All hydrogens are omitted for clarity.

From the crystal structure it is evident that the lone pairs on phosphorus are situated equatorially as a consequence of the pseudo-axial position of the *o*-phenylene moiety. This orientation of the lone pairs precludes chelation by this diphosphine (see Section 5.4).

The reaction between diprimary phosphine (**5.5**) and 1,1,1-trifluoro-2,4-pentanedione in 5 M HCl afforded an off-white solid, which showed more than ten signals in the $^{31}P\{^{1}H\}$ NMR spectrum (see Figure 5.2a). Recrystallisation from thf/hexane yielded the bicyclic diphosphine (**5.7**) as a yellow solid (see Scheme 5.1) whose $^{31}P\{^{1}H\}$ NMR spectrum exhibited a dominant broad quartet at δ -20.0 p.p.m.

(*J*(PF) 12.9 Hz) (see Figure 5.2b). The structure of the unusual diphosphine (**5.7**) was supported by mass spectrometry (see Experimental) and *X*-ray crystallography.

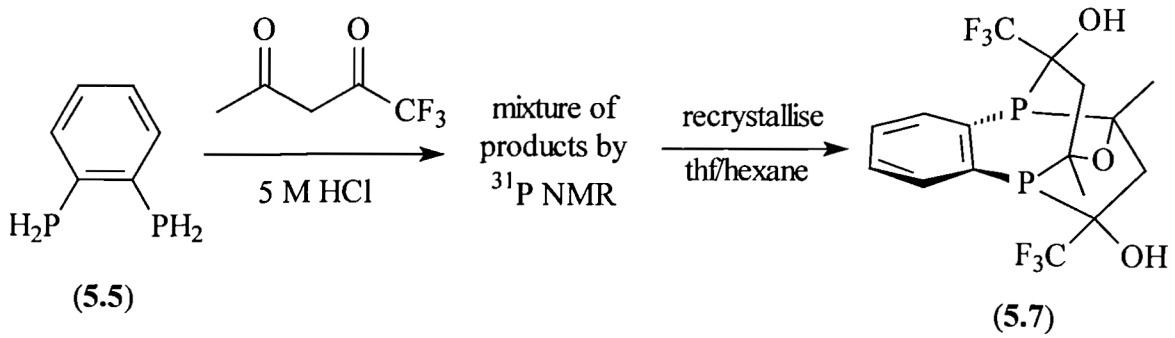

(**5.5**) (**5.7**)

Scheme 5.1

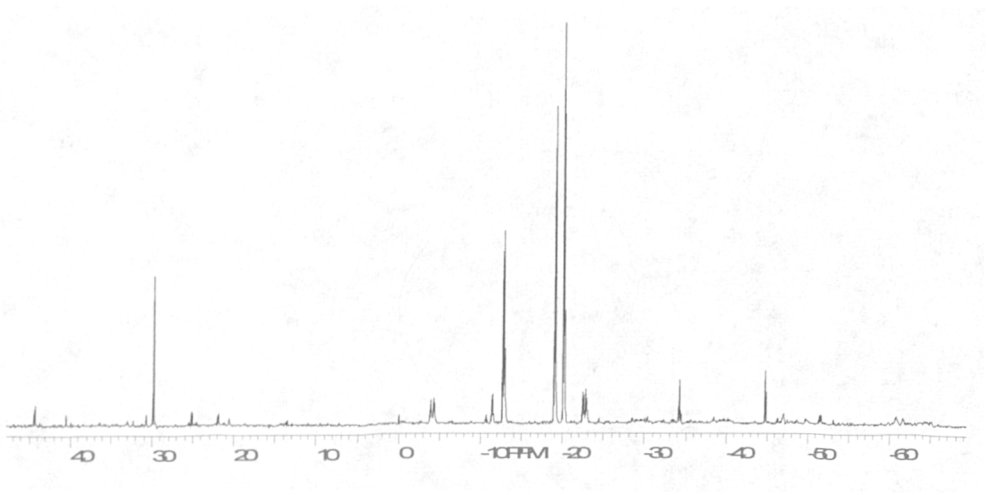

Figure 5.2a $^{31}P\{^{1}H\}$ NMR spectrum of crude product from reaction of 1,2-diphosphinobenzene and 1,1,1-trifluoro-2,4-pentanedione in 5 M HCl.

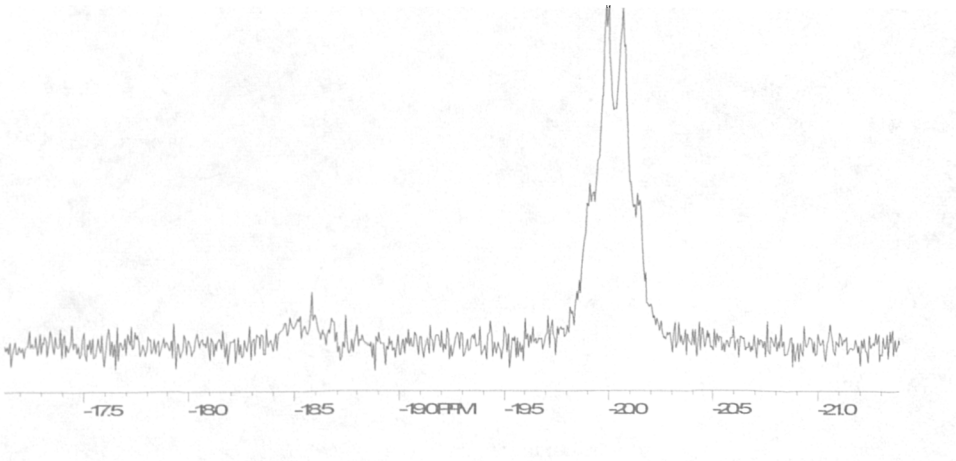

Figure 5.2b $^{31}P\{^{1}H\}$ NMR spectrum after recrystallisation from thf/hexane, showing broad quartet assigned to bicyclic diphosphine (**5.7**)

Single crystals suitable for *X*-ray diffraction were grown by slow evaporation of solvent from a thf solution of bicyclic diphosphine (**5.7**). Miss H. Phetmung of this

department carried out the structure determination, which was solved in the monoclinic space group C2/c with four formula units per unit cell. The numbering scheme and molecular structure is shown in Figure 5.3. The method of data collection, structure solution and refinement, the tables containing atomic coordinates, bond lengths and angles, isotropic and anisotropic displacement coefficients are all collected in the Appendix.

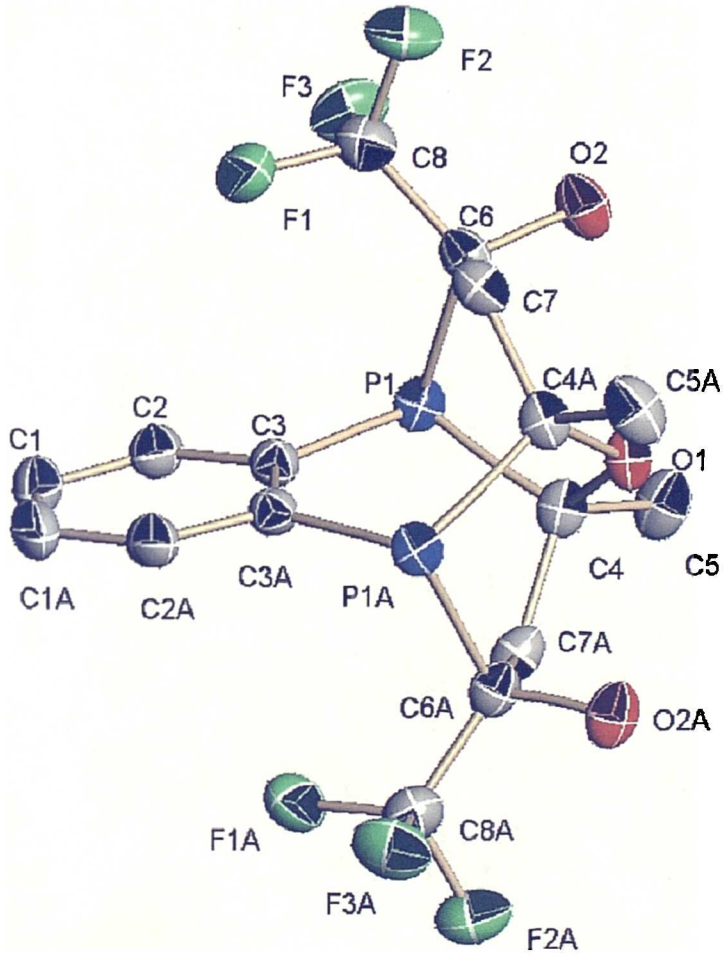

Figure 5.3 Molecular structure of bicyclic diphosphine (**5.7**). All hydrogens are omitted for clarity.

5.2.2 Reaction of 1,1'-diphosphinoferrocene with 2,4-pentanedione

As described earlier (see Section 3.2.3.1), reaction of 1,1'-diphosphinoferrocene with 2,4-pentanedione in 5 M HCl afforded a mixture of products, attributed to the sparing solubility of the diprimary phosphine in aqueous acid. Epstein and Buckler employed co-solvents in the preparation of some phospha-adamantanes,[373,374] and we reasoned that the use of a methanol co-solvent would solubilise the diprimary phosphine, leading to a cleaner reaction.

This proved to be the case, but the diphospha-adamantane (**5.8**) was isolated as a yellow/orange solid in moderate yield, and not the expected 1,1'-bis(phosha-adamantyl)ferrocene *meso/rac*-(**3.38**) (see Scheme 5.2).

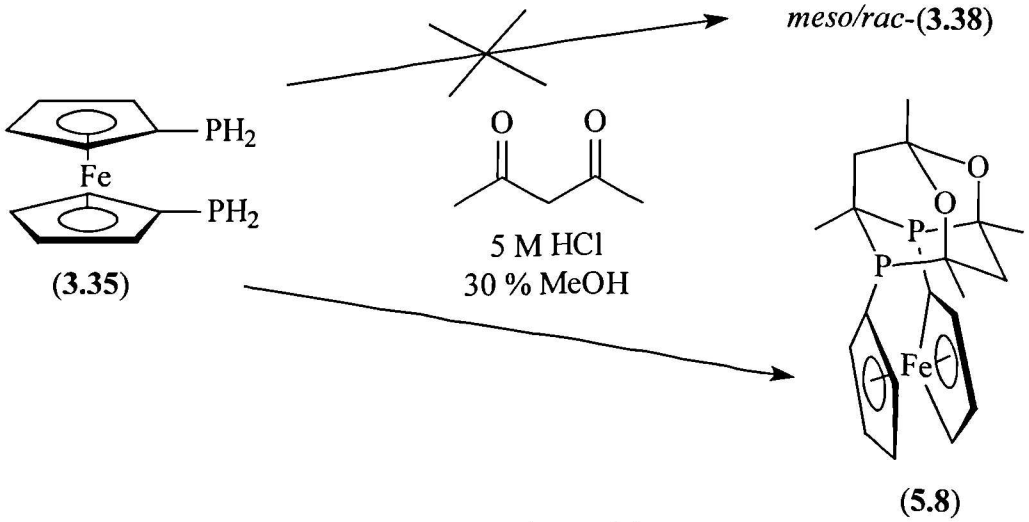

Scheme 5.2

The $^{31}P\{^{1}H\}$ NMR spectrum of the crude product showed a dominant singlet at δ -66.1 p.p.m. corresponding to diphospha-adamantane (**5.8**) and two minor singlets (*ca.* 5 %) at δ -32.5 and -32.7 p.p.m. assigned to diphosphine *meso/rac*-(**3.38**). Diphospha-adamantane (**5.8**) was further characterised by ^{1}H NMR spectroscopy (see Table 5.2), mass spectrometry (see Experimental) and *X*-ray crystallography.

Table 5.2 ^{1}H NMR[a] data for diphospha-adamantane (**5.8**)

δ(^{1}H)[b]	
3.42-4.16	m, 8H, 8C*H*
2.45	m, 2H, CH_2
1.84	m, 1H, C1*H*
1.48	s, 3H, CH_3
1.38	d, 6H, 2CH_3 (^{3}J(PH) 13.3 Hz)
1.22	m, 1H, C*H*H
1.07	t, 3H, CH_3 (^{3}J(PH) 15.0 Hz)

a Spectra recorded at 300 MHz in C_6D_6 at 45 °C. Chemical shifts [δ(^{1}H)] in p.p.m.(± 0.1) relative to residual solvent (7.15 p.p.m.). Coupling constants (*J*) in Hz (± 0.1).

b Detailed assignations made on the basis of ^{1}H COSY NMR.

Single crystals suitable for *X*-ray diffraction were grown by slow evaporation of solvent from a deutero-benzene solution of diphospha-adamantane (**5.8**). Miss H. Phetmung of this department carried out the structure determination, which was solved in the orthorhombic space group Fdd2 with sixteen formula units per unit cell. The numbering scheme and molecular structure is shown in Figure 5.4. The method of data collection, structure solution and refinement, the tables containing atomic coordinates, bond lengths and angles, isotropic and anisotropic displacement coefficients are all collected in the Appendix.

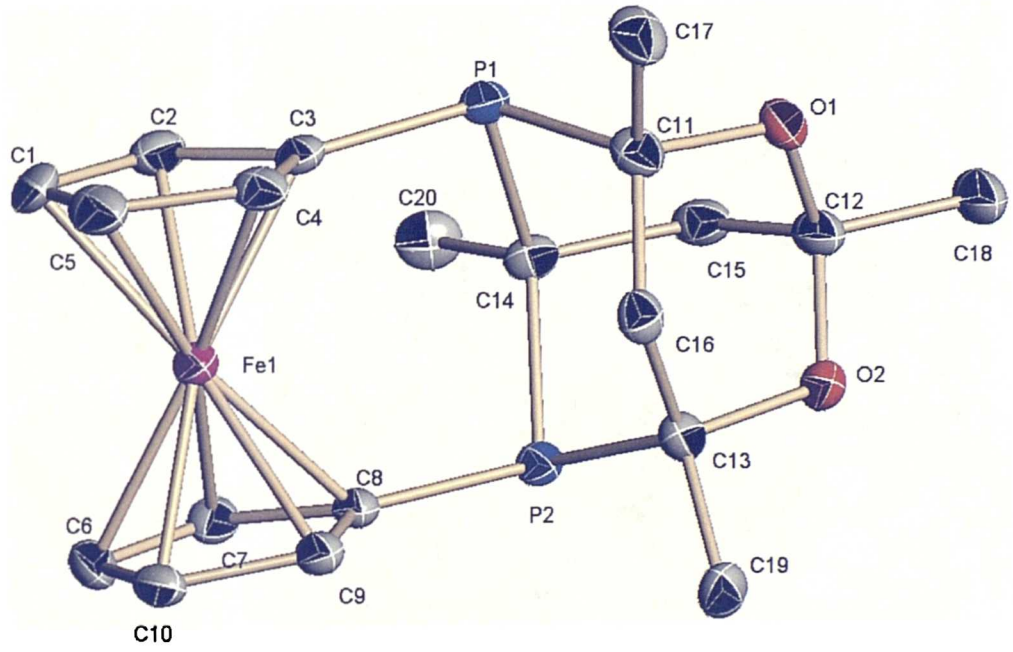

Figure 5.4 Molecular structure of diphospha-adamantane (**5.8**). All hydrogens are omitted for clarity.

The crystal structure of diphospha-adamantane (**5.8**) shows the axial orientation of the ferrocene backbone, placing the lone pairs on each phosphorus away from each other in a pseudo-equatorial fashion in an analogous manner to diphospha-adamantane (**5.6**).

5.2.3 A diphospha-adamantane from diphosphino-*o*-xylene

The troublesome preparation of bis(phospha-adamantyl)-*o*-xylene (**3.33**) was achieved by acid-catalysed reaction of crude diphosphino-*o*-xylene (**3.30**) with 2,4-pentanedione (see Section 3.2.2). A second product was isolated from this reaction whose $^{31}P\{^{1}H\}$ NMR spectrum showed a singlet at δ -26 p.p.m. We suspected from previous work that this might be the corresponding diphospha-adamantane (**5.9**) and this was confirmed by mass spectrometry (see Experimental) and *X*-ray crystallography.

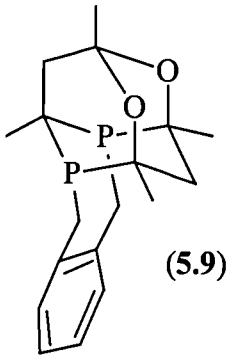

(5.9)

Single crystals suitable for *X*-ray diffraction were grown by slow evaporation of solvent from a dichloromethane solution of diphospha-adamantane (**5.9**). Dr. J. Charmant of this department carried out the structure determination, which was solved in the triclinic space group P-1 with two formula units per unit cell. The numbering scheme and molecular structure is shown in Figure 5.5. The method of data collection, structure solution and refinement, the tables containing atomic coordinates, bond lengths and angles, isotropic and anisotropic displacement coefficients are all collected in the Appendix.

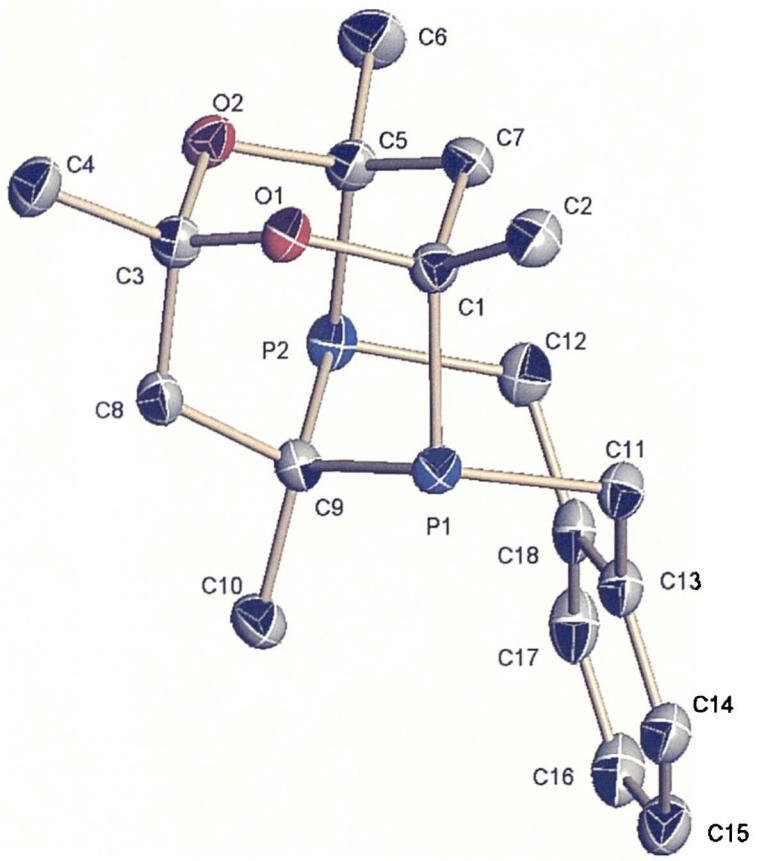

Figure 5.5 Molecular structure of diphospha-adamantane (**5.9**). All hydrogens are omitted for clarity.

5.2.4 A diphospha-adamantane from 1,8-bis(diphosphinomethyl)-naphthalene

A sample of the naphthyl dibromide 1,8-bis(bromomethyl)naphthalene (**5.10**), synthesised following literature procedures,[409,410] was kindly donated by Miss V. Rylott of this department. Arbusov reaction of dibromide (**5.10**) with triethyl phosphite afforded the diphosphonate (**5.11**) (Equation 5.3) as a colourless oil, characterised by $^{31}P\{^{1}H\}$ and ^{1}H NMR spectroscopy and mass spectrometry (see Experimental).

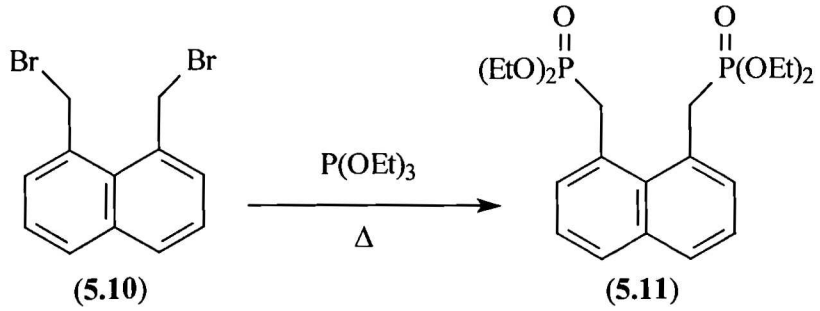

(5.10) **(5.11)**

Equation 5.3

Reduction with $LiAlH_4/Me_3SiCl$ to the corresponding diprimary phosphine (**5.12**) afforded a pink oily solid (see Equation 5.4). The ^{1}H-coupled $^{31}P\{^1H\}$ NMR spectrum (see Figure 5.6) of the crude product showed a triplet at δ -122.6 p.p.m (^1J(PH) 192.5 Hz) and another triplet of lower intensity (*ca.* 20 %) at δ -127.3 p.p.m. (^1J(PH) 194.5 Hz) tentatively assigned to the monoprimary phosphine.

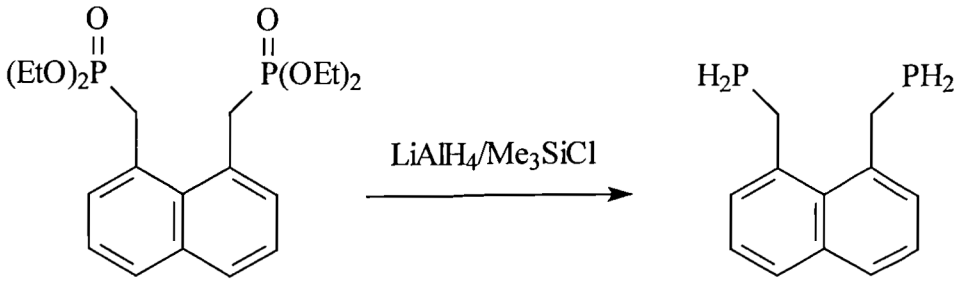

(**5.11**) (**5.12**)

Equation 5.4

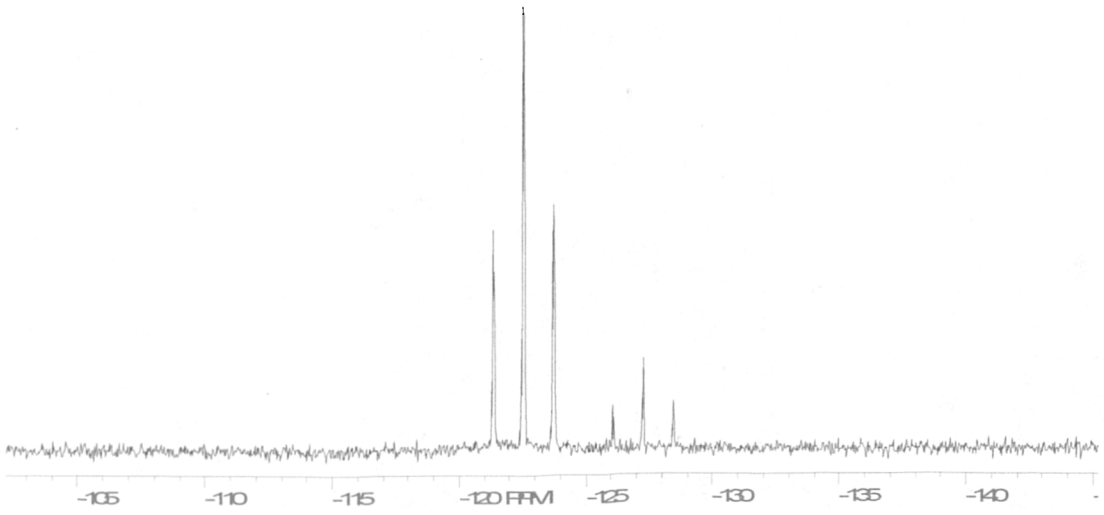

Figure 5.6 ^{1}H-coupled $^{31}P\{^1H\}$ NMR spectrum of crude diprimary phosphine (**5.12**)

The crude diprimary phosphine (**5.12**) was immediately reacted with 2,4-pentanedione to afford a white solid. The $^{31}P\{^1H\}$ NMR spectrum of this product showed a dominant broad singlet at δ -1.1 p.p.m tentatively assigned to the diphospha-adamantane (**5.13**) (see Equation 5.5) on the basis of mass spectrometry evidence (see Experimental).

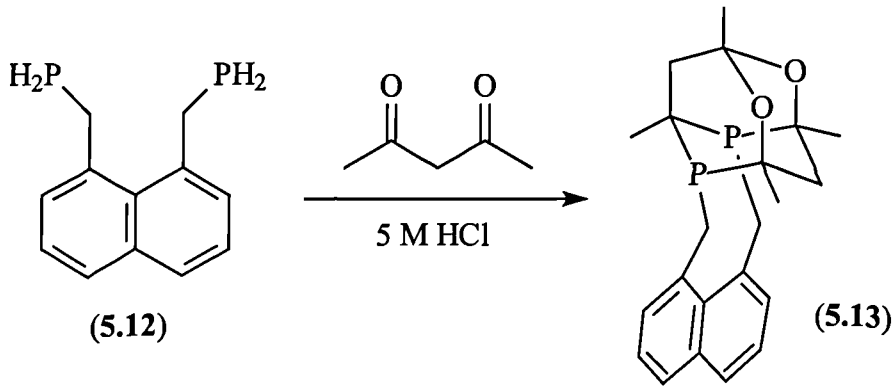

(5.12) (5.13)

Equation 5.5

5.3 Discussion of diphospha-adamantane formation

5.3.1 Reactions of 1,2-diphosphinobenzene with 1,3-diketones

5.3.1.1 Reaction of 1,2-diphosphinobenzene with 2,4-pentanedione

We recently reported the preparation of diphospha-adamantane (**5.6**),[377] including a postulated mechanism for its formation (see Scheme 5.3). The salient feature of this mechanism, compared to that discussed earlier for mono-phospha-adamantane formation (see Section 2.1.2), is the cyclisation step (i). The rigidity of the *o*-phenylene backbone promotes formation of diphospha-adamantane (**5.6**) because the pendant PH_2 group in **A** is held in close proximity to the electrophilic carbon, thus facilitating ring closure. It also seems likely that the constraints of the *o*-phenylene backbone inhibit mono-phospha-adamantane formation around each of the two phosphorus atoms on steric grounds. In contrast, free rotation in the C_2 and C_3 backbones facilitates the formation of bis(phospha-adamantyl)alkanes (**3.1**) and (**3.2**) discussed in Chapter 3. It is interesting to note that in the case of the C_2 backbone, trace amounts of diphospha-adamantane (**5.4**) were observed.

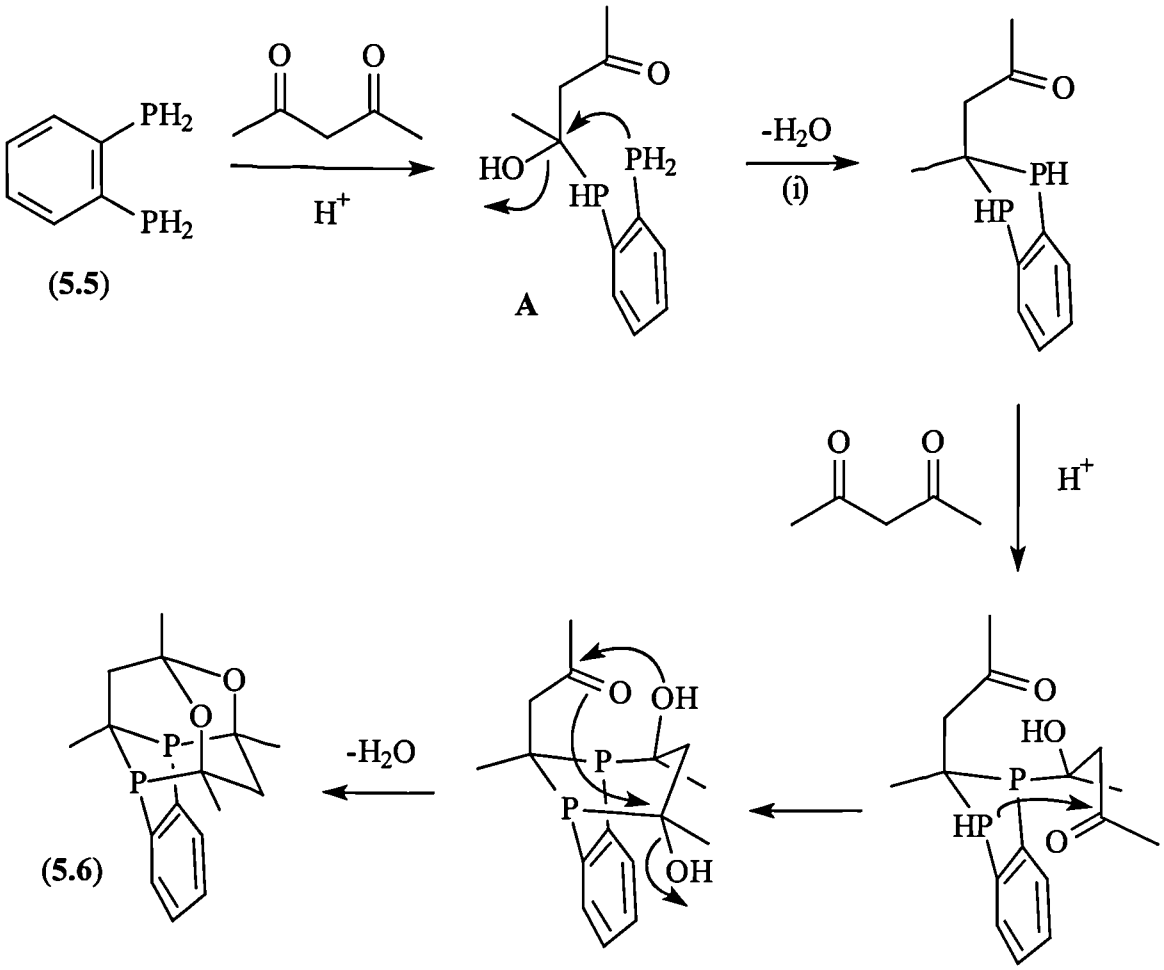

Scheme 5.3

5.3.1.2 Reaction of 1,2-diphosphinobenzene with 1,1,1-trifluoro-2,4-pentanedione

A mechanism for the formation of diphosphine (**5.7**) is suggested below (Scheme 5.4). In this instance, a five-membered diphosphacycle does not form (see Scheme 5.4), and instead each P-H functionality in intermediate **B** attacks a carbonyl moiety. This may be attributed to steric reasons, as the electron-withdrawing CF_3 groups would activate the electrophilic carbon for five-membered ring formation. Dehydration then occurs to form diphosphine (**5.7**), and further loss of water is prevented by the positions of the two pendant OH groups.

Bicyclic diphosphine (**5.7**) is one of many signals observed in the $^{31}P\{^{1}H\}$ NMR spectrum of the product, confirming our hypothesis that there are many species in equilibria in these reactions (see Section 2.1.2), and in this instance the stereoelectronics of the reagents and solubility of the products cause several species to precipitate from solution (see Section 5.2.1).

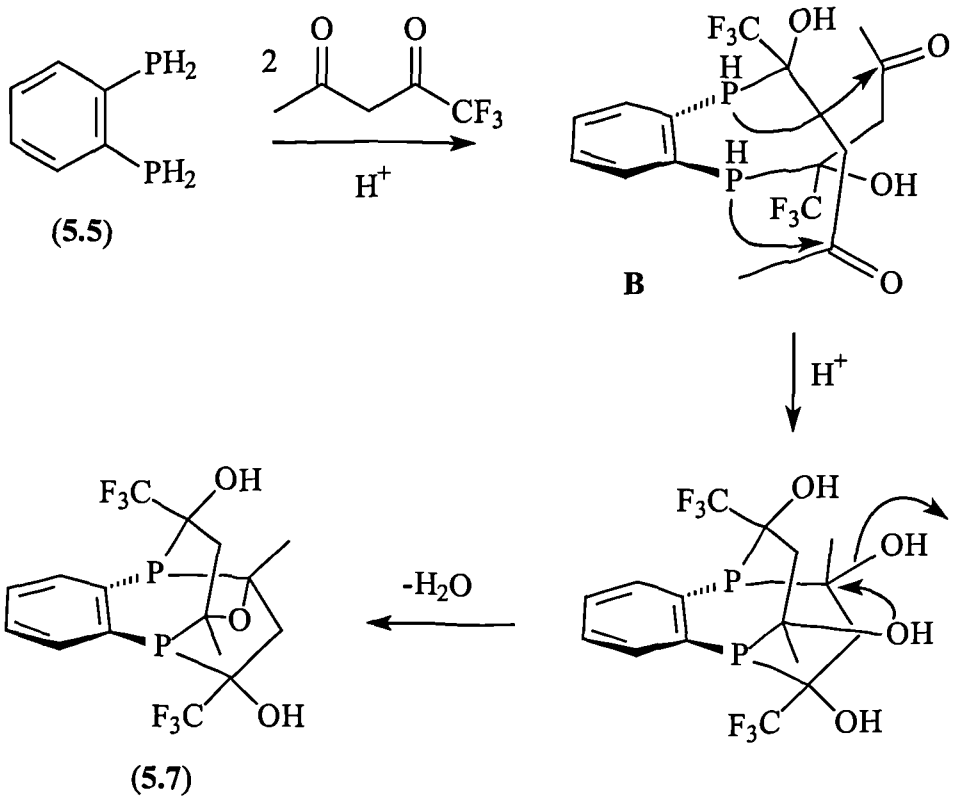

Scheme 5.4

It is revealing to compare the reaction in Scheme 5.4 with the analogous reactions of the C_2 and C_3 diprimary phosphines with 1,1,1-trifluoro-2,4-pentanedione performed by Gee,[375,377] which afford the bis(phospha-hexafluoro-adamantyl)alkanes (**3.3**) and (3.4) (see Section 3.1). The constrained *o*-phenylene backbone is presumably the principal reason for the very different precipitated reaction products observed, compared to products with the flexible C_2 and C_3 alkane backbones employed by Gee. Some similarity is also evident in this comparison, because the crude product of the reaction between 1,2-diphosphinoethane and 1,1,1-trifluoro-2,4-pentanedione showed a number of products in the $^{31}P\{^1H\}$ NMR spectrum, some of which were likely to be analogues of (**5.7**) and related species; trituration with methanol then removed the hydrophilic intermediates to yield pure bis(phospha-hexafluoro-adamantyl)ethane (**3.3**).

5.3.2 Reaction of other constrained diphosphines with 2,4-pentanedione

The effect of methanol co-solvent on the course of the reaction between 1,1'-diphosphinoferrocene (**3.35**) and 2,4-pentanedione is remarkable (< 5 % diphospha-adamantane without methanol; 95 % diphospha-adamantane with methanol according to $^{31}P\{^1H\}$ NMR spectroscopy). The methanol was employed to solubilise the oily solid diprimary phosphine (**3.35**), and whilst the resulting reaction medium was a suspension,

it was substantially more homogenous than the corresponding reaction in the absence of methanol. It is reasonable to assume that the diprimary phosphine (**3.35**) exists in a staggered conformation in the solid state, and that the eclipsed conformation (necessary for diphospha-adamantane formation) only exists in solution.

In conclusion, diphospha-adamantanes are formed when the two PH_2 moieties are either held in close proximity (e.g. 1,8-(dimethyl)naphthalene diphospha-adamantane (**5.13**)) or when such a conformation is accessible (i.e *in situ*, e.g. *o*-xylene diphospha-adamantane (**5.9**)).

5.4 Coordination chemistry of diphospha-adamantanes

The reaction between 2.0 equiv. diphospha-adamantane (**5.6**) and $[PdCl_2(NCPh)_2]$ in dichloromethane was monitored by $^{31}P\{^1H\}$ NMR spectroscopy, and five main signals were observed: a small amount of free ligand (δ 6.2 p.p.m.), and the remaining four signals were tentatively assigned to two species. The first was the mononuclear palladium complex *trans*-$[PdCl_2(\mathbf{5.6})_2]$ (**5.14**) that showed two virtual triplets at δ 5.2 and 29.1 p.p.m. corresponding to the pendant phosphorus and coordinated phosphorus respectively. The second species was assigned to the oligomeric palladium complex (**5.15**) (see Scheme 5.5) which exhibited a broad signal at δ 31.2 p.p.m (coordinated phosphorus) and a small virtual triplet at δ 5.0 p.p.m. (pendant phosphorus of terminal diphospha-adamantane (**5.6**)). The formation of this species also accounts for the significant amount of free ligand left in solution.

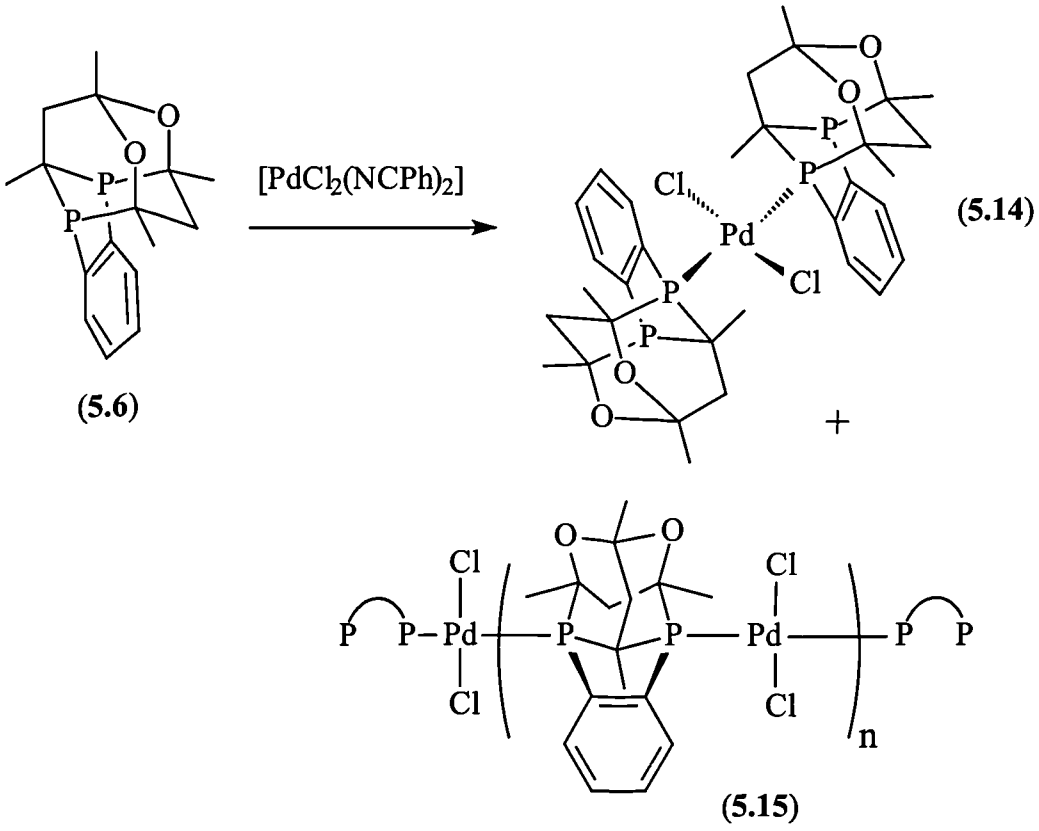

Scheme 5.5

The reaction between 2.1 equiv. diphospha-adamantane (**5.6**) and [$PtCl_2$(cod)] in dichloromethane was monitored by $^{31}P\{^1H\}$ NMR spectroscopy, and unlike the reaction with Pd(II) only the mononuclear complex *trans*-[$PtCl_2$(**5.6**)$_2$] (**5.16**) was formed (see Equation 5.6). The $^{31}P\{^1H\}$ NMR spectrum (see Figure 5.7) showed a broad singlet at δ 24.5 p.p.m with platinum satellites (^1J(PtP) 2685 Hz) and a virtual triplet at δ 2.1 p.p.m. corresponding to the coordinated and pendant phosphorus nuclei respectively. A small amount of free ligand was also observed.

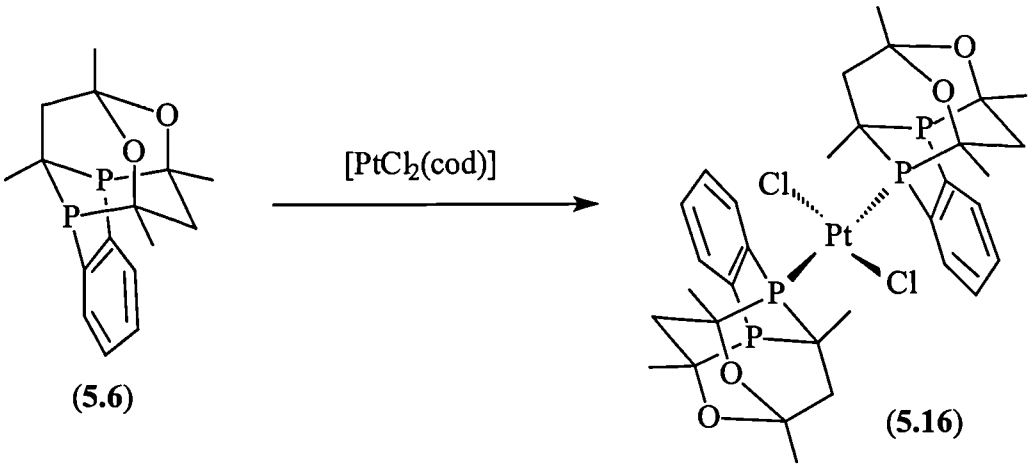

Equation 5.6

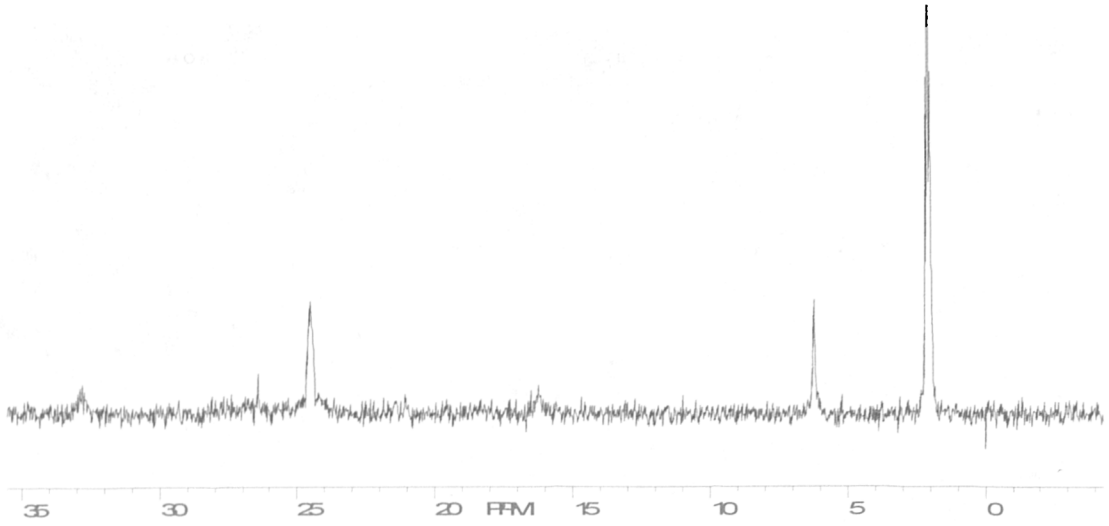

Figure 5.7 $^{31}P\{^{1}H\}$ NMR spectrum of reaction between 2.1 equiv. diphospha-adamantane (**5.6**) and $[PtCl_2(cod)]$.

The reactions of diphospha-adamantane (**5.6**) with Pd(II) and Pt(II) confirmed our suspicions that its lone pairs were not oriented for chelation. We reasoned that synthesis of a discreet binuclear species should be possible. Reaction of 0.5 equiv. (**5.6**) with [AuCl(tht)] in dichloromethane yielded the sparingly soluble binuclear complex (**5.17**) (see Equation 5.7) as an off-white solid, characterised by its ^{1}H, $^{13}C\{^{1}H\}$ (see Table 5.3), $^{31}P\{^{1}H\}$ NMR spectroscopy (singlet at δ 44.0 p.p.m.), mass spectrometry (see Experimental) and *X*-ray crystallography.

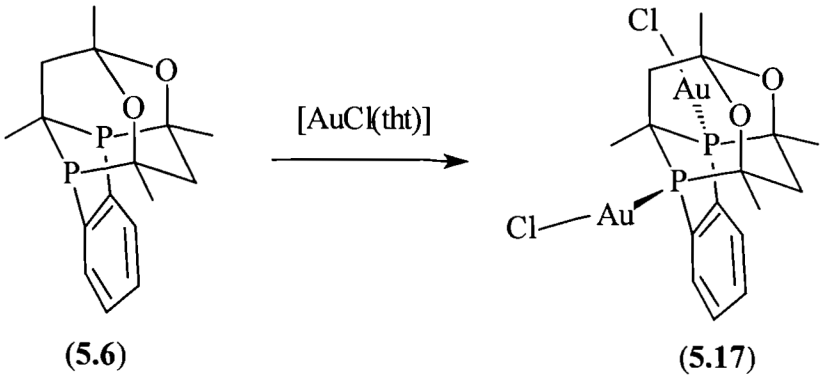

(5.6) **(5.17)**

Equation 5.7

Table 5.1 $^{13}C\{^{1}H\}$ NMR[a] and ^{1}H NMR[b] data for binuclear gold complex (**5.17**)

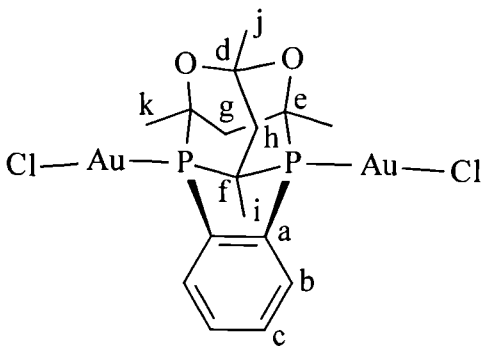

	$\delta(^{13}C)$		$\delta(^{1}H)$[c]
a, b, c	134.2-135.2 (m)	7.99	(m, 2H, *o*-$C_6H_2H_2$)
		7.81	(m, 2H, *m*-$C_6H_2H_2$)
d	97.9 (m)	2.28	(m, 2H, CH_2; AA'XX')
e	72.0 (s)	2.00	(ABX, 1H, C*H*H; ^{2}J(HH) 14.7 Hz, ^{3}J(PH) 21.4 Hz)
f, g, h	41.2 (m), 39.5 (s), 36.6 (m)	1.37	(ABX, 1H, CH*H*; ^{2}J(HH) 14.7 Hz, ^{3}J(PH) 1.2 Hz)
i	28.4 (t, ^{2}J(PC) 14.3 Hz)	1.55	(s, 3H, $^{j}CH_3$)
j	28.1 (s)	1.47	(d, 6H, $2^{k}CH_3$; ^{3}J(PH) 18.1 Hz)
k	28.5 (m)	1.46	(t, 3H, $^{i}CH_3$; ^{3}J(PH) 17.9 Hz)

[a] Spectra recorded at 100 MHz in CD_2Cl_2 at 24 °C. Chemical shifts [$\delta(^{13}C)$] in p.p.m.(± 0.1) relative to CD_2Cl_2 (53.8 p.p.m.). Coupling constants (*J*) in Hz (± 0.1).

[b] Spectra recorded at 300 MHz in CD_2Cl_2 at 22 °C. Chemical shifts [$\delta(^{1}H)$] in p.p.m.(± 0.1) relative to residual solvent (5.32 p.p.m.). Coupling constants (*J*) in Hz (± 0.1).

[c] Detailed assignations made on the basis of ^{1}H COSY NMR.

The beautiful ^{1}H NMR spectrum (see Figure 5.8) is rich in detailed structural information about binuclear complex (**5.17**), which is not reported in our recent publication.[377]

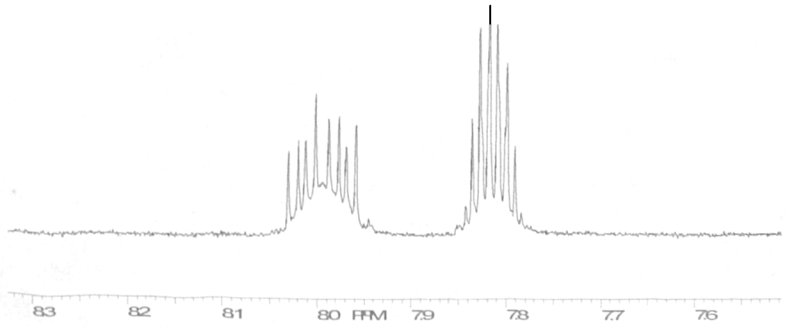

Figure 5.8a ^{1}H NMR spectrum (aromatic region) of binuclear complex (**5.17**)

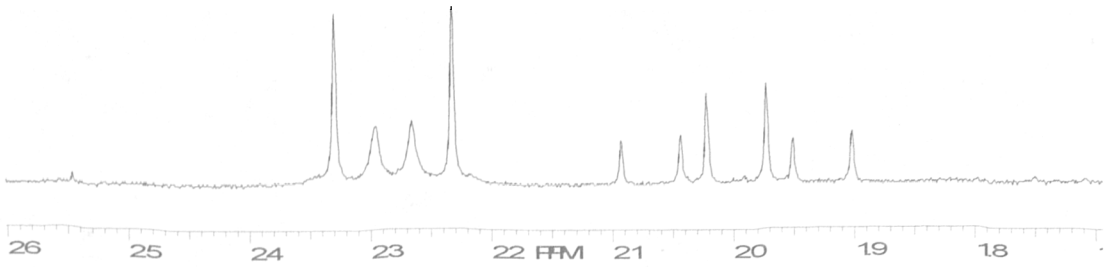

Figure 5.8b ^{1}H NMR spectrum (CH_2 and CHH) of binuclear complex (**5.17**)

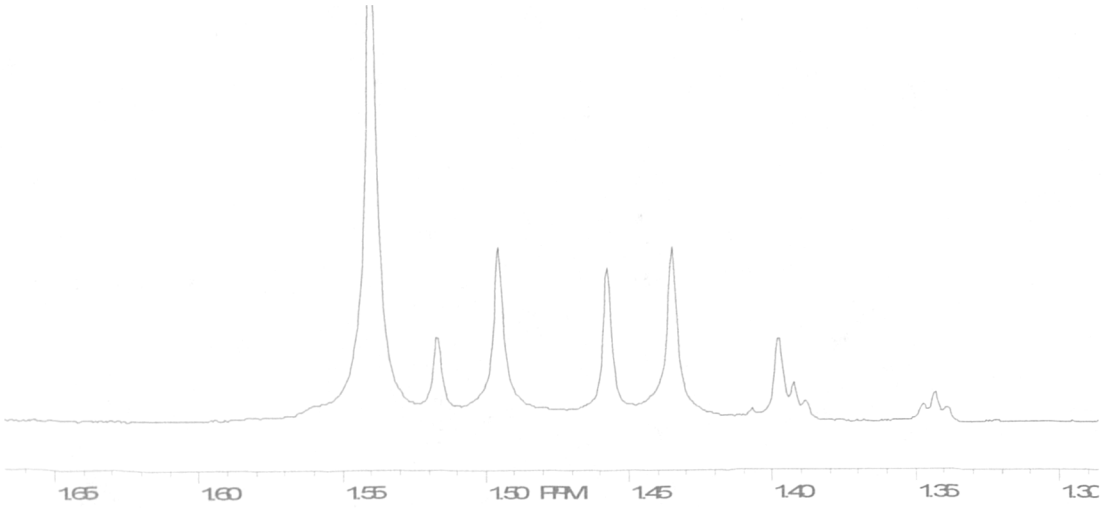

Figure 5.8c ^{1}H NMR spectrum (4CH_3 and CHH) of binuclear complex (**5.17**)

Single crystals of binuclear complex (**5.17**) suitable for *X*-ray diffraction were grown from a dichloromethane solution layered with diethyl ether (5:1) in a Schlenk tube. Miss H. Phetmung of this department carried out the structure determination, which was solved in the triclinic space group P $\bar{1}$ with two formula units per unit cell. The numbering scheme and molecular structure is shown in Figure 5.9. The method of data collection, structure solution and refinement, the tables containing atomic coordinates, bond lengths and angles, isotropic and anisotropic displacement coefficients are all collected in the Appendix.

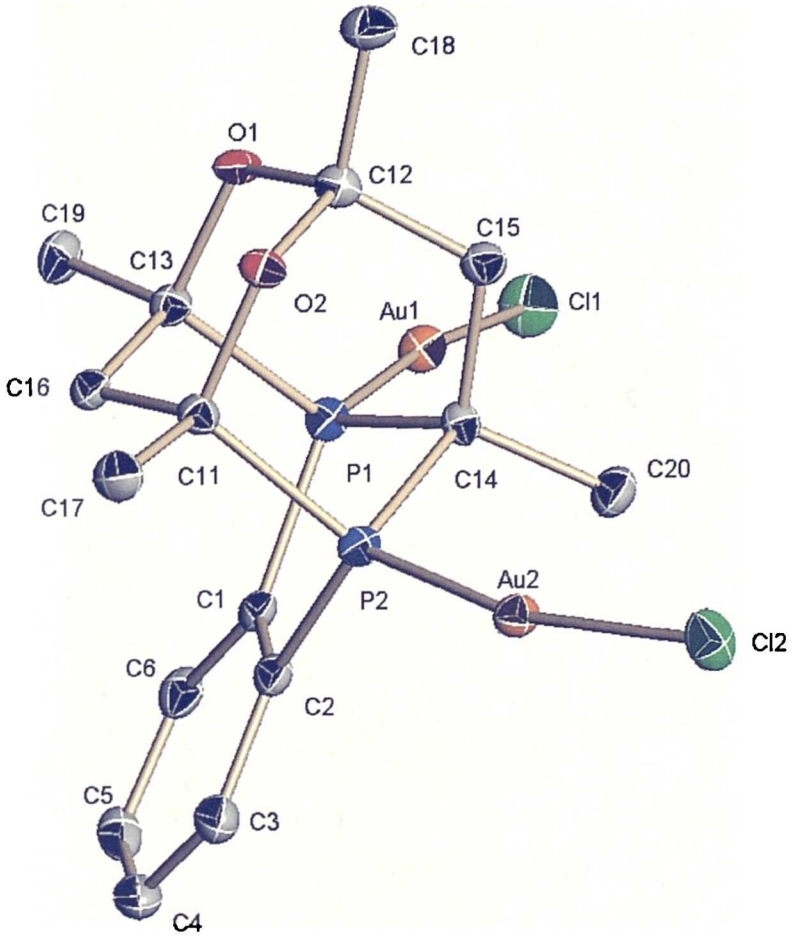

Figure 5.9 Molecular structure of binuclear complex (**5.17**). All hydrogens are omitted for clarity.

5.5 A chelate complex formed by a diphospha-adamantane

The coordination chemistry of cyclohexyl-phospha-adamantane α/β-(**2.15**) was discussed in Section 2.3.3. The $^{31}P\{^{1}H\}$ NMR spectrum of the sample of ligand provided (by Dr. Charles Carraz, University of Windsor) showed two singlets at δ -12.7 and 0.8 p.p.m. (*ca.* 85:15) corresponding to the mono-phospha-adamantane α/β-(**2.15**) and an unidentified impurity. The reaction of 2.0 equiv. of this mixture with $[PtCl_2(cod)]$ in dichloromethane afforded a yellow solid. The $^{31}P\{^{1}H\}$ NMR spectrum of this product showed a signal corresponding to the diastereomeric mixture *meso/rac*-(**2.20**) (see Section 2.3.3). A smaller singlet was also observed at δ -33.9 p.p.m. with platinum satellites (^{1}J(PtP) 3018 Hz), exhibiting a coordination chemical shift and coupling constant indicative of chelating diphosphine with a C_1 backbone. This was

tentatively assigned to the extraordinary complex (**5.18**), and confirmed by mass spectrometry (m/z 626, (M^+-Cl)) and *X*-ray crystallography.

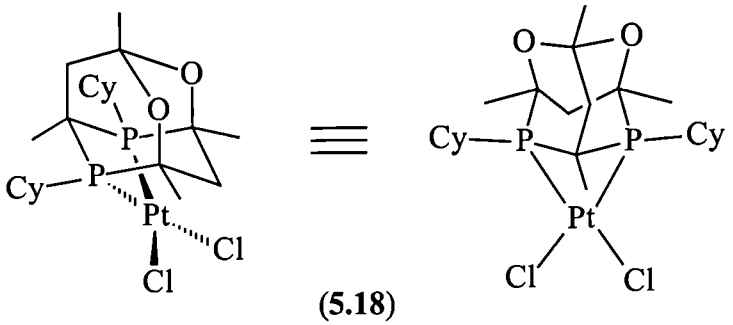

(**5.18**)

Crystals were grown by slow diffusion of hexane into a dichloromethane solution of the mixture *meso/rac*-(**2.20**) and (**5.18**). Two different crystalline morphologies were present in this sample, and crystal structures were solved for both products. Miss H. Phetmung of this department carried out the structure determination for complex (**5.18**), which was solved in the triclinic space group P $\bar{1}$ with two formula units per unit cell. The numbering scheme and molecular structure is shown in Figure 5.10. The method of data collection, structure solution and refinement, the tables containing atomic coordinates, bond lengths and angles, isotropic and anisotropic displacement coefficients are all collected in the Appendix.

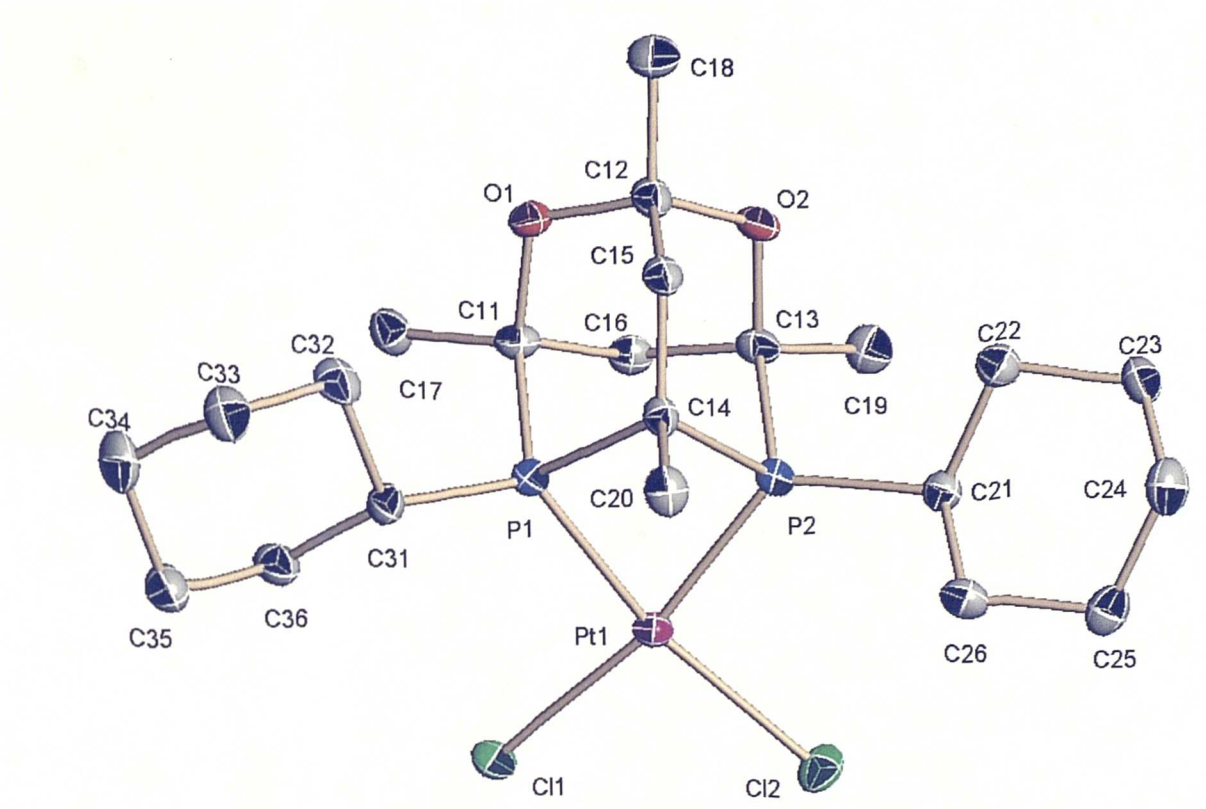

Figure 5.10 Molecular structure of chelating diphospha-adamantane Pt(II) complex (**5.18**). All hydrogens are omitted for clarity.

5.6 Conclusions

The novel diphospha-adamantanes (**5.6**)-(**5.8**), (**5.10**), (**5.13**) described in this chapter all possess a backbone that positions the phosphorus substituents axially, rendering lone-pair orientations equatorial. This precludes chelation to metal centres and thus bridged binuclear complexes (**5.17**) or mononuclear complexes with pendant phosphorus atoms (**5.15**) and (**5.16**) are formed. Further coordination chemistry of these non-chelating diphospha-adamantanes should be explored. The remarkable structure of chelating diphospha-adamantane complex (**5.18**) demonstrates that diphospha-adamantanes derived from monoprimary phosphines exist with phosphorus atoms in the same six-membered ring (see Section 5.1). The substituents on these two phosphorus atoms favour equatorial orientation on steric grounds, leaving lone pairs in an axial position. Thus, whilst the synthesis of diphospha-adamantane (**5.2**) has been reported,[373,374] we have shown that this compound represents a new class of chelating diphosphine ligand.

Chapter 6

Experimental

E.1 General experimental details

Unless otherwise stated, all reactions were carried out under a dry nitrogen atmosphere using standard Schlenk line techniques. Solvents were dried and deoxygenated by refluxing under a nitrogen atmosphere over appropriate drying agents: calcium hydride (for dichloromethane and acetonitrile), sodium/benzophenone (for diethyl ether and thf), sodium (for pentane, toluene and hexane) and magnesium methoxide (for methanol). Commercial reagents were used as supplied unless otherwise stated. $P(OEt)_3$, NEt_3 and $(Me_2N)CH_2CH_2(NMe_2)$ (TMEDA) were distilled prior to use. V65 $[CH_3(CH_3)CHCH_2(CN)(CH_3)CN{=}NC(CH_3)(CN)CH_2CH(CH_3)CH_3]$, the primary phosphine *i*-$PrPH_2$ and PH_3 were a kind donation from Albright and Wilson Ltd.

Starting materials prepared by literature methods were $(EtO)_2(O)P(CH_2)_3P(O)(OEt)_2$,[411] $H_2P(CH_2)_3PH_2$,[412] diphosphonato-*o*-xylene,[385] 1,1'-bis(dichlorophosphino)ferrocene,[389] $[PtCl_2(cod)]$,[413] $[PtCl_2(SMe_2)_2]$,[414] $[Pt(norbornene)_3]$,[415] $[PdCl_2(NCPh)_2]$,[416] $[RhCl(CO)_2]_2$[417] and [AuCl(tht)].[418]

Elemental analyses were carried out by the Microanalytical Laboratory of the School of Chemistry, University of Bristol. Electron Impact and Fast Atom Bombardment mass spectra were recorded on a MD800 and an Autospec by the Mass Spectrometry Service, University of Bristol.

$^{31}P\{^1H\}$, $^{13}C\{^1H\}$, $^{195}Pt\{^1H\}$, $^{19}F\{^1H\}$, $^{11}B\{^1H\}$ and ^1H NMR spectra were recorded either by the author or Ms. R. Sylvester or Ms. L. Harding at the ambient temperature of the probe unless otherwise stated, using deuterated solvents to provide the field/frequency lock. The following NMR spectrometers were used:

^1H NMR spectra;	Jeol Λ300 (300 MHz) or Jeol GX400 (400 MHz) with chemical shifts relative to residual solvent.
$^{13}C\{^1H\}$ NMR spectra;	Jeol Λ300 (75 MHz) or Jeol GX400 (100 MHz) with chemical shifts relative to the solvents used or to high frequency of tetramethylsilane.
$^{31}P\{^1H\}$ NMR spectra;	Jeol EX90 (36.2 MHz), Jeol Λ300 (121.55 MHz) or GX400 (162 MHz) with chemical shifts to high frequency of 85 % H_3PO_4.
$^{195}Pt\{^1H\}$ NMR spectra;	Jeol Λ300 (64.2 MHz) or Jeol GX400 (85.6 MHz) with chemical shifts to high frequency of Ξ (^{195}Pt) 21.4 MHz.

$^{19}F\{^1H\}$ NMR spectra; Jeol Λ300 (282.65 MHz) with chemical shifts to high frequency of $CFCl_3$.

$^{11}B\{^1H\}$ NMR spectra; Jeol GX400 (128.26 MHz) with chemical shifts to high frequency of $BF_3.OEt_2$.

The electrochemical study of *meso/rac*-(**3.38**) was carried out using an EG&G model 273 or 273A potentiostat in conjunction with a three-electrode cell. The auxiliary electrode was a platinum wire and the working electrode a platinum disc (1.6 mm diameter). The reference was an aqueous saturated calomel electrode separated from the test solution by a fine porosity frit and an agar bridge saturated with KCl. The solution was 5 x 10^{-4} mol dm^{-3} in the test compound and 0.1 mol dm^{-3} in $[NBu^n_4][PF_6]$ as the supporting electrolyte. Under these conditions, $E^{0'}$ for the redox couple $[FeCp^*_2]^{0/+1}$ added to the test solution as an internal calibrant, was –0.08 V in CH_2Cl_2.

E.2 Chapter 2: Monodentate phospha-adamantanes

E.2.1 Ligand syntheses

E.2.1.1 Synthesis of 1,3-bis(trifluoromethyl)-5,7-dimethyl-2-phenyl-4,6,8-trioxa-2-phospha-adamantane (2.13)

To a suspension of $PhPH_2$ (0.5 g, 4.54 mmol) in aqueous HCl (5 cm^3, 5 M, 25 mmol) was added 1,1,1-trifluoro-2,4-pentanedione (3.3 cm^3, 27.25 mmol). The solution was stirred at room temperature for 4 d, after which time further aqueous HCl (3 cm^3, 10 M, 30 mmol) was added. The $^{31}P\{^1H\}$ NMR spectrum was recorded which showed a singlet at δ -39.2 p.p.m, and the reaction mixture was then left to stand at room temperature for a further 5 d. After this time, crystals had formed which were filtered off, washed with water (2 x 10 cm^3) and dried *in vacuo* to yield hexafluoro-phospha-adamantane (**2.13**) as a white, crystalline solid (1.7 g, 94 %). EI mass spectrum: m/z 400 (M^+), 381 (M^+ - F).

E.2.1.2 Synthesis of 1,3,5,7-tetramethyl-2-isopropyl-4,6,8-trioxa-2-phospha-adamantane (2.14)

To a suspension of isopropyl phosphine (1 cm^3, 11.5 mmol) in aqueous HCl (10 cm^3, 10 M, 100 mmol) was added 2,4-pentanedione (7.1 cm^3, 69.1 mmol). The solution was stirred for 6 d at room temperature, after which time a white precipitate had formed. After stirring for a further 5 d, the precipitate was filtered off, and water (3 x 20 cm^3) was added to the filtrate, producing more precipitate which was filtered off and washed

with water (2 x 20 cm^3) to afford phospha-admanatane (**2.14**) as a white solid (1.19 g, 41 %).

E.2.2 Complexes of 1,3-bis(trifluoromethyl)-5,7-dimethyl-2-phenyl-4,6,8-trioxa-2-phospha-adamantane (2.13)

*Preparation of trans-[$PdCl_2$(**2.13**)$_2$] meso/rac-(**2.16**)*

To a solution of [$PdCl_2(NCPh)_2$] (30 mg, 0.0783 mmol) in dichloromethane (2 cm^3) was added (**2.13**) (69 mg, 0.172 mmol) in dichloromethane (2 cm^3). The orange solution was stirred for 18 h at room temperature, after which time a yellow precipitate had formed. This was filtered off to afford *trans*-[$PdCl_2$(**2.13**)$_2$] *meso/rac*-(**2.16**) as a very sparingly soluble, yellow solid (40 mg, 52 %). FAB mass spectrum: m/z 906 (M^+ - 2Cl).

*Preparation of trans-[RhCl(CO)(**2.13**)$_2$] meso/rac-(**2.17**)*

To a solution of $[RhCl(CO)_2]_2$ (20 mg, 0.045 mmol) in dichloromethane (2 cm^3) was added (**2.13**) (76 mg, 0.189 mmol) in dichloromethane (2 cm^3). The yellow/brown solution was stirred for 18 h at room temperature, after which time the reaction solution was concentrated under reduced pressure and pentane (10 cm^3) was added. The resulting yellow precipitate was filtered and washed with pentane (2 x 3 cm^3) to afford *trans*-[RhCl(CO)(**2.13**)$_2$] *meso/rac*-(**2.17**) as a sparingly soluble, yellow solid (50 mg, 58 %). FAB mass spectrum: m/z 938 (M^+ - CO), 903 (M^+ - CO - ^{35}Cl).

E.2.3 Complexes of 1,3,5,7-tetramethyl-2-isopropyl-4,6,8-trioxa-2-phospha-adamantane (2.14)

*Preparation of trans-[$PtCl_2$(**2.14**)$_2$] meso/rac-(**2.18**)*

To a solution of [$PtCl_2$(cod)] (30 mg, 0.0802 mmol) in dichloromethane (1 cm^3) was added (**2.14**) (44 mg, 0.17 mmol) in dichloromethane (2 cm^3). After stirring the pale yellow solution for 2 h at room temperature, all volatiles were removed under reduced pressure. The residue was recrystallised from diethyl ether/pentane to afford *trans*-[$PtCl_2$(**2.14**)$_2$] *meso/rac*-(**2.18**) as an off-white solid (32 mg, 51 %). FAB mass spectrum: m/z 783 (M^+), 748 (M^+ - ^{35}Cl), 711 (M^+ - 2 Cl).

*Preparation of [$PdCl_2${α/β-(**2.14**)}$_2$] meso/rac-(**2.19**)*

To a solution of [$PdCl_2(NCPh)_2$] (30 mg, 0.0783 mmol) in dichloromethane (1 cm^3) was added (**2.14**) (42.5 mg, 0.165 mmol) in dichloromethane (2 cm^3). The yellow

solution was stirred for 30 min at room temperature, after which time a yellow precipitate had formed. This was filtered off and washed with dichloromethane (2 cm^3) to afford a very sparingly soluble yellow solid (33 mg, 62 %) tentatively assigned to the complex *trans*-[$PdCl_2$(**2.13**)$_2$] *meso/rac*-(**2.16**) by $^{31}P\{^1H\}$ NMR . FAB mass spectrum: m/z 658, (M^+ - ^{35}Cl), 622 (M^+ - 2Cl).

E.2.4 Complexes of 1,3,5,7-tetramethyl-2-cyclohexyl-4,6,8-trioxa-2-phospha-adamantane (2.15)

N. B. The sample of (**2.15**) provided (by Dr. C. A. Carraz, University of Windsor) contained *ca.* 15 % 1,3,5,7-tetramethyl-2,4-dicyclohexyl-6,8-trioxa-2,4-diphospha-adamantane (see Section 5.3) and therefore errors are inevitable in the calculations of the molar equivalents of (**2.15**) in the coordination chemistry reactions. Satisfactory elemental analyses were also not obtained for this reason.

*Preparation of [$PtCl_2$(**2.15**)$_2$] meso/rac-(2.20)*

To a solution of [$PtCl_2$(cod)] (50 mg, 0.134 mmol) in dichloromethane (2 cm^3) was added dropwise (**2.15**) (80 mg, 0.268 mmol) in dichloromethane (2 cm^3). The pale yellow solution was stirred for 18 h and then concentrated under reduced pressure. Addition of hexane (5 cm^3) precipitated a yellow solid (78 mg, 68 %) which was *ca.* 85 % pure *meso/rac*-(**2.20**) by $^{31}P\{^1H\}$ NMR. FAB mass spectrum: m/z = 862 (M^+), 827 (M^+ - ^{35}Cl), 791 (M^+ - 2Cl). The remaining 15 % was assigned to diphospha-adamantane bis chelate complex (**5.18**). FAB mass spectrum: m/z 626 (M^+ - ^{35}Cl).

*Preparation of [$PdCl_2$(**2.15**)$_2$] meso/rac-(2.21)*

To a solution of [$PdCl_2$(NCPh)$_2$] (50 mg, 0.131 mmol) in dichloromethane (1 cm^3) was added dropwise (**2.15**) (78 mg, 0.262 mmol) in dichloromethane (2 cm^3). The orange solution was stirred for 18 h and the resulting suspension was filtered and washed with hexane (5 cm^3) to yield an orange solid (73 mg, 72 %). FAB mass spectrum: m/z = 739 (M^+ - ^{35}Cl), 703 (M^+ - 2Cl).

Table E.2.1 Elemental analyses[a] for Chapter 2

Compound	C	H
(**2.13**)	48.0 (48.0)	3.8 (3.8)
(**2.14**).CH_2Cl_2.H_2O	59.4 (60.5)	9.2 (9.0)
(**2.16**)	39.6 (39.3)	3.1 (3.1)
(**2.17**)	41.7 (41.0)	3.5 (3.1)
(**2.18**).$2CH_2Cl_2$	34.0 (35.3)	5.0 (5.3)
(**2.19**)	44.8 (45.0)	6.8 (6.7)

[a] Analyses in %. Calculated values in parentheses.

E.3 Chapter 3: Bidentate phospha-adamantanes

E.3.1 Synthesis of cyclic phosphonium [(1,3,5,7-tetramethyl-4,6,8-trioxa-2-phospha-adamantyl)-*o*-xylene][BPh_4] (3.27)

Preparation of 1,3,5,7-tetramethyl-4,6,8-trioxa-2-phospha-adamantane (adamphos) (3.26)

This procedure is an adaptation of the literature methods.[373,374,376] Nitrogen was bubbled through a solution of 2,4-pentanedione (150 ml, 1.46 mol) in aqueous HCl (300 cm^3, 5 M, 1.5 mol) for 18 h. Gaseous PH_3 was then bubbled through the reaction mixture for 7 h at 0 °C. The resulting white precipitate was filtered off in air, washed with water (3 x 200 cm^3) and dried *in vacuo* to give adamphos (**2.1**) (78.5 g, 50 %).

Preparation of cyclic phosphonium salt (3.27)

To a solution of dibromo-*o*-xylene (122 mg, 0.463 mmol) in acetonitrile (30 cm^3) was added adamphos (**3.26**) (200 mg, 0.926 mmol). The resulting solution was heated and stirred under reflux for 18 h and after cooling to ambient temperature, the solvents were removed under reduced pressure. To a solution of the crude product in methanol (10 cm^3) was added $NaBPh_4$ (171 mg, 0.5 mmol) and the resulting precipitate was filtered to afford cyclic phosphonium salt (**3.27**) as a white crystalline solid (255 mg, 86 %). FAB mass spectrum: m/z 319 (M^+ - BPh_4).

Preparation of hydroxymethyl-phospha-adamantane (3.28)

To a solution of adamphos (**3.26**) (1.7 g, 7.871 mmol) in methanol (50 cm^3) was added formaldehyde (2 cm^3, 72.2 mmol, 35 % in H_2O). The temperature was raised to

reflux and the reaction left stirring for 24 h. After this time the volatiles were removed *in vacuo* to afford a white solid. This product was washed with thf to afford a white solid (1.66 g, 86 %) which was 90 % pure (**3.28**) by $^{31}P\{^{1}H\}$ NMR, showing a singlet at δ -31.2 p.p.m. EI mass spectrum: m/z 246 (M^+).

E.3.2 Ligand syntheses

E.3.2.1 Synthesis of bis(1,3,5,7-tetramethyl-4,6,8-trioxa-2-phospha-adamantyl)-*o*-xylene *meso/rac*-(3.33)

Preparation of bis(diethylphosphonato)-o-xylene (3.29)

Following the literature method,[385] dibromo-*o*-xylene (68.3 g, 0.259 mol) and triethyl phosphite (100 cm^3, 0.621 mol) were stirred and heated to 160-170 °C at atmospheric pressure for 5 h. The apparatus allowed continuous distillation of bromoethane (*ca.* 40 cm^3) from the reaction mixture. The reaction was then allowed to cool and volatiles were removed under reduced pressure. The residue was distilled under vacuum (0.05 Torr, 180-186 °C) to give a colourless oil (78.9 g, 81 %), which was 97 % pure (**3.29**) by $^{31}P\{^{1}H\}$ NMR which showed a singlet at δ 26.7 p.p.m.

Preparation of bis(phosphino)-o-xylene (3.30)

To a slurry of $LiAlH_4$ (4.826 g, 127 mmol) in diethyl ether (100 cm^3) was added Me_3SiCl (16.2 cm^3, 127 mmol) dropwise at –78 °C over 10 min. The reaction was left to warm to room temperature and stirred for 2 h. After this time, diphosphonate (**3.29**) (16.0 g, 42.3 mmol) in thf (50 cm^3) was then added dropwise at –78 °C over 20 min. The reaction mixture was then allowed to warm to room temperature and stirred for 18 h. Excess $LiAlH_4$ was then quenched by addition of degassed aqueous HCl (52 cm^3, 5 M, 260 mmol) dropwise at –20 °C over 30 min. The organic layer was then decanted off, and the aqueous layer extracted with degassed diethyl ether (2 x 100 cm^3). These organic portions were combined and dried over $MgSO_4$, and the solvent was removed under reduced pressure to afford a pink/peach liquid (6.1 g, 85 %) which was *ca.* 90 % pure diprimary phosphine (**3.30**) by $^{31}P\{^{1}H\}$ NMR (see Section 3.2.2).

Preparation of bis(boranephosphino)-o-xylene (3.32)

To a solution of crude diprimary phosphine (**3.30**) (1.38 g, 8.1 mmol) in diethyl ether (10 cm^3) was added BH_3.thf (30 cm^3, 1 M, 30 mmol) at 0 °C in portions (3 x 10 cm^3) over 30 min. The reaction solution was allowed to warm to room temperature and

stirred for 1 d. After this time, the reaction was evaporated to dryness under reduced pressure and recrystallised from thf to afford borane adduct (**3.32**) as a white crystalline solid (0.78 g, 49 %). EI mass spectrum: m/z 198 (M^+).

Preparation of bis(1,3,5,7-tetramethyl-4,6,8-trioxa-2-phospha-adamantyl)-o-xylene meso/rac-(3.33)

To a solution of 2,4-pentanedione (18 cm^3, 0.175 mol) in aqueous HCl (50 cm^3, 5 M, 0.25 mol) was added crude bis(phosphino)-*o*-xylene (**3.30**) (6 g, 35.3 mmol) dropwise over 10 min. After the mixture was stirred for *ca.* 2 h, a white solid began to precipitate. The reaction mixture was stirred for a further 96 h, after which the white solid product was filtered off in air, washed with water (2 x 20 cm^3) and dried *in vacuo*, affording *meso/rac*-(**3.33**) as an off-white solid (0.78 g, 6 %). EI mass spectrum: m/z 534 (M^+). A second product was also isolated from this reaction (see Sections 5.2.3 and E.5.1.5).

E.3.2.2 Synthesis of 1,1'-bis(1,3,5,7-tetramethyl-4,6,8-trioxa-2-phospha-adamantyl)ferrocene *meso/rac*-(3.38)

Preparation of $PCl(NEt_2)_2$

To PCl_3 (25 cm^3, 0.286 mol) was added Et_2NH (118 cm^3, 1.145 mol) at 0 °C dropwise over 30 min. The resulting solid was extracted with diethyl ether (3 x 50 cm^3) and the solution decanted. Solvent was then removed under reduced pressure before distillation (0.6 Torr, 75-80 °C) and redistillation (0.5 Torr, 80-82 °C) to give a colourless liquid (13.54 g, 23 %). The $^{31}P\{^1H\}$ NMR spectrum showed a singlet at δ 159.2 p.p.m.

Preparation of 1,1'-dilithioferrocene

Following the literature procedure,[390] *n*-BuLi (59 cm^3, 94.5 mmol, 1.6 M) was added dropwise over 30 min to a solution of TMEDA (14.2 cm^3, 94.5 mmol) in hexane (40 cm^3). The reaction mixture was stirred at room temperature for 3 h before ferrocene (7.75 g, 41.6 mmol) was added. The reaction mixture was stirred for a further 18 h and the resulting orange precipitate was filtered off, washed with pentane (2 x 40 ml) and dried *in vacuo* to yield a highly air sensitive orange solid (11.01 g, 62 %).

*Preparation of 1,1'-bis{bis(diethylamino)phosphino}ferrocene (**3.34**)*

To a solution of (TMEDA)-dilithio-1,1'-ferrocene (9 g, 20.8 mmol) in toluene (100 cm^3) was added $PCl(NEt_2)_2$ (9.7 g, 45.9 mmol) dropwise at room temperature over 15 min. The reaction temperature was stirred at room temperature for 24 h and the $^{31}P\{^1H\}$ NMR spectrum of the resulting solution showed a singlet at 89.4 p.p.m. consistent with the formation of 1,1'-bis{bis(diethylamino)phosphino}ferrocene. Gaseous HCl was then bubbled through the reaction mixture, until the rate of bubbling was equal in the inlet and exit bubblers. The resulting precipitate of $[NEt_2H_2]Cl$ was filtered off, washed with diethyl ether (2 x 50 cm^3) and the solvent was removed from the filtrate under reduced pressure to yield a yellow oil. Recystallisation from hexane (120 cm^3) afforded (**3.34**) as a yellow solid (9.39 g, 58 % from ferrocene). The $^{31}P\{^1H\}$ NMR spectrum showed a singlet at 162.0 p.p.m.

*Preparation of 1,1'-diphosphinoferrocene (**3.35**)*

To a slurry of $LiAlH_4$ (2.5 g, 65.4 mmol) in diethyl ether (60 cm^3) was added bis(dichlorophosphino)-1,1'-ferrocene (8.53 g, 22.0 mmol) in diethyl ether (60 cm^3) dropwise at -78 °C over 20 min whilst stirring with an overhead mechanical stirrer. The reaction was allowed to warm to room temperature and stirred for 18 h. The excess $LiAlH_4$ was neutralised with H_2O (2.5 cm^3), 15 % NaOH (2.5 cm^3) followed by H_2O (7.5 cm^3) at 0 °C. The off-white precipitate formed was filtered off and washed with diethyl ether (3 x 20 cm^3). The solvent was then removed from the filtrate under reduced pressure to afford diprimary phosphine (**3.35**) as a red/orange oily solid (5 g, 91 %).

*Preparation of 1,3,5,7-tetramethyl-4,6,8-trioxa-2-chloro-2-phospha-adamantane (**3.36**)*

To a solution of adamphos (**3.26**) (4.32 g, 20.0 mmol) in CCl_4 (50 cm^3) was added *N*-chlorosuccinimde (4.42 g, 33.0 mmol) in portions (*ca.* 0.5 g) at –5 to 10 °C over 15 min. The reaction was then cooled to –10 °C and the white precipitate was filtered off and washed with CCl_4 (2 x 20 cm^3). The solvent was then removed from the filtrate under reduced pressure to afford chloro-phospha-adamantane (**3.36**) as a yellow solid (4.96 g, 99 %). The $^{31}P\{^1H\}$ NMR spectrum showed a singlet at 53.6 p.p.m. ^1H NMR (300 MHz, C_6D_6): δ 1.26 (s, 3H, C*H*$_3$), 1.28 (d, 3H, C*H*$_3$, ^3J(PH) 7.1 Hz), 1.31 (d, 3H, C*H*$_3$, *J*(PH) 7.7 Hz), 1.39 (m, 1H, C*H*H), 1.74 (m, 3H, C*H*$_2$ + CH*H*).

Preparation of the analogous bromo-phospha-adamantane (**3.37**) is achieved in a similar manner, employing *N*-bromosuccinimide as reagent.

Preparation of 1,1'-bis(1,3,5,7-tetramethyl-4,6,8-trioxa-2-phospha-adamantyl)ferrocene meso/rac-(3.38)

To a solution of 1,1'-dilithioferrocene (4.2 g, 9.77 mmol) in thf (50 cm^3) was added a solution of chloro-phospha-adamantane (**3.36**) in thf (50 cm^3) at –50 °C dropwise over 20 min. The deep red solution was allowed to warm to room temperature and stirred for 18 h. The $^{31}P\{^1H\}$ NMR spectrum of this solution showed three signals, the two major species (in a ratio of *ca.* 1:1) being assigned to the diastereomers *meso*-(**3.38**) and *rac*-(**3.38**), and the minor product (*ca.* 20 %) assigned to the mono-substituted 1-(phospha-adamantyl)ferrocene. The solvent was removed under reduced pressure, and the crude product doubly recrystallised from methanol to afford pure *meso/rac*-(**3.38**) as an orange solid (2.16 g, 36 %). EI mass spectrum: m/z 614 (M^+).

The mono-substituted 1-(phospha-adamantyl)ferrocene is isolable from the filtrate of the first recrystallisation (91 % pure by $^{31}P\{^1H\}$ NMR spectroscopy) as an orange solid (0.8 g, 13 %). EI mass spectrum: m/z 400 (M^+). ^1H NMR (400 MHz, $CDCl_3$): δ 4.28-4.59 (m, 4H, 4C*H*), 4.22 (s, 5H, 5C*H*), 2.07 (d of d, 2H, 2C*H*H, ^2J(HH) 13.2 Hz, ^3J(PH) 7.1 Hz), 1.89 (d of d, 2H, 2CH*H*, ^2J(HH) 13.2 Hz, ^3J(PH) 24.7 Hz), 1.81 (d, 6H, 2CH_3, ^3J(PH) 12.0 Hz), 1.57 (m, 2H, 2C*H*H), 1.41 (s, 6H, 2CH_3) 1.31-1.35 (m, 2H, 2CH*H*), 1.33 (s, 6H, 2CH_3), 1.24 (d, 6H, 2CH_3, ^3J(PH) 12.7 Hz).

E.3.3 Coordination chemistry of bis(phospha-adamantyl)-diphosphines

E.3.3.1 Coordination chemistry of bis(1,3,5,7-tetramethyl-4,6,8-trioxa-2-phospha-adamantyl)-*o*-xylene *meso/rac*-(3.33)

Reaction of $[PdCl_2(NCPh)_2]$ with 1.0 equiv. of meso/rac-(3.33)

To a solution of $[PdCl_2(NCPh)_2]$ (20 mg, 0.052 mmol) in dichloromethane (2 cm^3) was added *meso/rac*-(**3.33**) (28 mg, 0.052 mmol) in dichloromethane (2 cm^3). The solution was stirred for 18 h and the $^{31}P\{^1H\}$ NMR spectrum was recorded. This showed that two products had been formed, these being tentatively assigned to the bis-chelate complex $[PdCl_2$(**3.33**)] (**3.41**) and the bridged dimer (**3.42**).

Preparation of $[PtCl_2$(3.33)] meso/rac-(3.43)

To a solution of $[PtCl_2(cod)]$ (20 mg, 0.054 mmol) in dichloromethane (2 cm^3) was added *meso/rac*-(**3.33**) (29 mg, 0.054 mmol) in dichloromethane (2 cm^3). After stirring for 18 h, solvent was removed under reduced pressure and the crude product

was recrystallised from dichloromethane/hexane to afford bis chelate (**3.43**) as a yellow solid (35 mg, 76 %). FAB mass spectrum: m/z 765 (M^+ - ^{35}Cl), 729 (M^+ - 2Cl).

E.3.3.2 Coordination chemistry of 1,1'-bis(1,3,5,7-tetramethyl-4,6,8-trioxa-2-phospha-adamantyl)ferrocene *meso/rac*-(3.38)

Reaction of [$PtCl_2$(cod)] with 1.0 equiv. of meso/rac-(3.38)

To a solution of [$PtCl_2$(cod)] (40 mg, 0.107 mmol) in toluene (5 cm^3) was added *meso/rac*-(**3.38**) (66 mg, 0.107 mmol) in toluene (4 cm^3). The reaction mixture was stirred and heated to 120-130 °C at atmospheric pressure for 2 d. After this time, a yellow precipitate was observed which was filtered off, and the $^{31}P\{^1H\}$ NMR spectra of this solid and the filtrate were recorded. They showed that the diastereomerically pure bis chelate complex *meso*- or *rac*-(**3.44**) had precipitated, leaving the corresponding diastereomer in solution. FAB mass spectrum: m/z 845 (M^+ - ^{35}Cl), 809 (M^+ - 2Cl). ^1H NMR (300 MHz, CD_2Cl_2): 5.07 (br s, 2H, 2C*H*), 4.69 (br s, 2H, 2C*H*), 4.44 (br s, 2H, 2C*H*), 4.39 (br s, 2H, 2C*H*), 1.17-2.06 (m, 32H, 8CH_3 + 4CH_2).

Reaction of [$PdCl_2$(NCPh)$_2$] with 1.0 equiv. of meso/rac-(3.38)

To a solution of [$PdCl_2$(NCPh)$_2$] (40 mg, 0.104 mmol) in dichloromethane (4 cm^3) was added *meso/rac*-(**3.38**) (64 mg, 0.104 mmol) in dichloromethane (2 cm^3). The solution was stirred for 18 h and the $^{31}P\{^1H\}$ NMR spectrum was recorded. This was inconclusive, and the products are tentatively assigned to oligomeric materials on account of their sparing solubility.

Table E.3.2 Elemental analyses[a] for Chapter 3

Compound	C	H
(**3.26**)	78.7 (78.0)	6.5 (6.9)
(**3.33**)	58.4 (58.6)	7.0 (6.6)

[a] Analyses in %. Calculated values in parentheses.

E.4 Chapter 4: Homogeneous carbonylation catalysis with Pd and Pt complexes of C_2-, C_3- and ferrocene- bridged cage diphosphines.

The carbonylation experiments were carried out at *Shell Research and Technology, Amsterdam*, under the supervision of Prof. E. Drent.

Product analysis of the autoclave reaction mixtures was routinely performed by gas-liquid chromatographic (GLC) analysis on a Perkin-Elmer 8500 equipped with two capillary columns, Chrompack 50 m and 50 m FFAP. Structural analysis was performed with GLC- mass spectroscopic (GC/MS) analysis on a Finnigan-9610 gas chromatograph fitted with the CP-sil 5 column and coupled to a Finnigan-4000 triple-stage mass spectrometer using electron impact ionisation. ^{1}H and $^{31}P\{^{1}H\}$ NMR spectra were recorded on a Brucker WM 250 spectrometer to confirm the chemical structure and purity of applied phosphine ligands.

All experiments were carried out in 250 cm^3 magnetically stirred Hastelloy™ C autoclaves, heated electrically. A typical experimental procedure was as follows:

0.1 mmol (22.5 mg) $Pd(OAc)_2$, 0.15 mmol (71 mg) *meso/rac*-(**3.2**) and 0.25 mmol (17.2 μL) methanesulphonic acid were dissolved in 50 ml methanol in the autoclave.

The closed autoclave was flushed three times with 40 bar N_2 and liquid propene (10 ml) was pumped into the autoclave from a high pressure ISCO pump. Subsequently, the autoclave was first pressurised with 20 bar of CO and secondly with 20 bar H_2. In about 10 minutes the autoclave was heated to reaction temperature, and kept at this temperature by a Thermo-Electric 100 temperature control unit. The pressure was continuously recorded by using a Transamerica Instruments pressure transducer, series 2000. Activity data during the experiment were calculated from the pressure decrease in time and from the GLC analysis of the reaction product at the end of the reaction period.

E.5 Chapter 5: Diphospha-adamantanes

E.5.1 Synthesis of 1,3,5,7-tetramethyl-6,8-dioxa-2,4-diphospha-adamantanes

E.5.1.1 Synthesis of diphosphino-*o*-benzene (5.5)

The synthesis of diprimary phosphine (**5.5**) was carried out by Mr. Adrian Stevenson and Mr. Tony Rogers following literature procedures.[386]

Preparation of 1,2-bis(diethylphosphonato)benzene

A solution of 1,2-dichlorobenzene (590 cm^3, 5.25 mol) in trimethyl phosphite (2l, 16.95 mol) was photolysed at *ca.* 60 °C for 134 h using a 500 watt ultra-violet lamp housed in a quartz tube. Excess trimethyl phosphite and other volatiles were then removed under reduced pressure and the residue was cooled to *ca.* 20 °C for 18 h. The resulting solid was filtered off as the crude product. Further impurities were extracted with acetone to yield a pale yellow crystalline solid (482.5 g, 31 %).

Preparation of 1,2-diphosphinobenzene (5.5)

To a slurry of $LiAlH_4$ (30 g, 0.78 mol) in thf (400 cm^3) was added Me_3SiCl (100 cm^3, 0.78 mol) dropwise at –78 °C over 1h. The mixture was allowed to warm to room temperature and stirred for 2h using an overhead mechanical stirrer. 1,2-bis(diethylphosphonato)benzene (40 g, 0.14 mol) in thf (400 cm^3) was then added dropwise at –30 °C over 1 h and the mixture was allowed to warm to room temperature before stirring for 36 h. The excess $LiAlH_4$ was quenched by dropwise addition at 0 °C of H_2O (*ca.* 200 cm^3) followed by aqueous NaOH (100 cm^3, 1 M, 100 mmol) over 2 h. The aqueous layer was extracted with diethyl ether (3 x 150 cm^3) and the combined organic extract dried over $MgSO_4$. The crude product was distilled (0.1 Torr, 68 °C) to afford a colourless liquid (12.5 g, 63 %) which was 99 % pure diprimary phosphine (**5.5**) by $^{31}P\{^1H\}$ NMR.

E.5.1.2 Preparation of 1,2-(1,3,5,7-tetramethyl-6,8-dioxa-2,4-diphospha-adamantyl)benzene (5.6)

To a solution of 2,4-pentanedione (7.4 cm^3, 72 mmol) in aqueous HCl (18 cm^3, 5 M, 90 mmol) was added diprimary phosphine (**5.5**) (1.28 g, 9.014 mmol). The reaction mixture was left stirring for 6 d, by which time a white precipitate had formed. This was filtered, washed with water (3 x 10 cm^3) and dried over $CaCl_2$ to yield a white solid (700 mg, 25 %). EI mass spectrum: m/z 306 (M^+). The $^{31}P\{^1H\}$ NMR spectrum of the crude product showed a small impurity at δ -40.3 p.p.m. (*ca.* 3 %) assigned to 1,2-bis(phospha-adamantyl)benzene. EI mass spectrum: m/z 506 (M^+).

E.5.1.3 Preparation of bicyclic diphosphine (5.7)

To a solution of 1,1,1-trifluoro-2,4-pentanedione (5.34 cm^3, 44.03 mmol) in aqueous HCl (15 cm^3, 5 M, 75 mmol) was added diprimary phosphine (**5.5**) (0.782 g, 5.507 mmol). After stirring for *ca.* 1 h, a white precipitate was observed. The reaction was left stirring for a further 5 d after which the precipitate was filtered to give an off-white solid. Recrystallisation from thf/pentane a white crystalline solid (143 mg, 6 %) which was *ca.* 90 % pure bicyclic diphosphine (**5.7**) by $^{31}P\{^1H\}$ NMR. EI mass spectrum: m/z 432 (M^+).

E.5.1.4 Preparation of 1,1'-(1,3,5,7-tetramethyl-6,8-dioxa-2,4-diphospha-adamantyl)ferrocene (5.8)

To a solution of 2,4-pentanedione (8.2 cm^3, 80 mmol) in aqueous HCl (13.3 cm^3, 5 M, 66.5 mmol) and methanol (4 cm^3) was added 1,1-diphosphinoferrocene (**3.35**) (*ca.* 2.5 g, 10 mmol). After stirring the suspension for 1 d, a bright orange precipitate was observed. The reaction was left stirring for a further 5 d, after which time the precipitate was filtered, washed with water (3 x 10 cm^3) and dried *in vacuo* to yield an orange solid (1.32 g, 32 %) which was 95 % pure diphospha-adamantane (**5.8**) by $^{31}P\{^1H\}$ NMR. EI mass spectrum: m/z 414 (M^+). The remaining 5 % was assigned to 1,1-bis(phospha-adamantyl)ferrocene *meso/rac*-(**3.38**); EI mass spectrum: m/z 614 (M^+).

E.5.1.5 Preparation of 1,3,5,7-tetramethyl-6,8-dioxa-2,4-diphospha-adamantyl-*o*-xylene (5.10)

To a solution of 2,4-pentanedione (18 cm^3, 0.175 mol) in aqueous HCl (50 cm^3, 5 M, 0.25 mol) was added crude bis(phosphino)-*o*-xylene (**3.30**) (6 g, 35.3 mmol) dropwise over 10 min. After the mixture was stirred for *ca.* 2 h, a white solid began to precipitate. The reaction mixture was stirred for a further 96 h, after which the white solid product was filtered off and washed with water (2 x 20 cm^3). This water caused precipitation of a second solid in the filtrate that was filtered off and washed with water (2 x 20 cm^3). Precipitation of a third off-white solid in the resulting filtrate was caused by this water. The second and third products were combined and dried *in vacuo* to afford an off-white solid (1.64 g, 13 %) which was 90 % pure diphospha-adamantane (**5.10**) by $^{31}P\{^1H\}$ NMR. EI mass spectrum: m/z 334 (M^+).

E.5.1.6 Synthesis of 1,8-(1,3,5,7-tetramethyl-6,8-dioxa-2,4-diphospha-adamantyl)dimethylnaphthalene (5.13)

Preparation of 1,8-bis(diethylphosphonatomethyl)naphthalene (5.11)

1,8-bis(dibromomethyl)napthalene (1.5 g, 4.78 mmol) and triethyl phosphite (2.46 cm^3, 14.3 mmol) were stirred and heated to 160-170 °C at atmospheric pressure for 12 h. The apparatus allowed continuous distillation of bromoethane (*ca.* 40 cm^3) from the reaction mixture. The reaction was then allowed to cool and volatiles were removed *in vacuo* (10^{-3} – 10^{-5} Torr) to give a colourless oil (1.88 g, 92 %), which was 98 % pure (**5.11**) by $^{31}P\{^1H\}$ NMR which showed a singlet at δ 26.2 p.p.m. EI mass spectrum: m/z 428 (M^+), 292 (M^+ - $P(O)(OEt_2)_2$). ^1H NMR (300 MHz, $CDCl_3$):7.68 (m, 2H, 2C*H*),

7.22-7.42 (m, 4H, 4C*H*), 3.75-4.06 (m, 12H, 2CH_2 (benzyl) + 4CH_2 (ethoxy)), 1.09 (t, 12H, 4CH_3, ^3J(HH) 7.1 Hz).

*Preparation of 1,8-bis(phosphinomethyl)napthalene (**5.12**)*

To a slurry of $LiAlH_4$ (0.48 g, 12.6 mmol) in thf (50 cm^3) was added Me_3SiCl (1.6 cm^3, 12.6 mmol) at –78 °C dropwise over 5 min. The reaction mixture was left to warm to room temperature and stirred for 2 h. The reaction mixture was then cooled to –78 °C and diphosphonate (**5.11**) (1.8 g, 4.2 mmol) in thf (35 cm^3) was then added dropwise over 5 min. The reaction was then left to warm to room temperature and stirred for 18 h. After this time, excess $LiAlH_4$ by adding aqueous HCl (5 cm^3, 5 M, 25 mmol) at –50 °C dropwise over 10 min. After warming to room temperature, the solid which had formed was filtered off and the filtrate was dried over $MgSO_4$. The solvent was removed under reduced pressure to afford a pink oily solid (0.9 g, 97 %) which was *ca.* 85 % pure diprimary phosphine (**5.12**) by $^{31}P\{^1H\}$ NMR (see Section 5.2.4)

*Preparation of 1,8-(1,3,5,7-tetramethyl-6,8-dioxa-2,4-diphospha-adamantyl)dimethylnapthalene (**5.13**)*

To a solution of crude diprimary phosphine (**5.12**) (0.9 g, 4.09 mmol) in aqueous HCl (20 cm^3, 5 M, 100 mmol) and methanol (2 cm^3) was added 2,4-pentanedione (4 cm^3, 39 mmol). The reaction mixture was left stirring at room temperature for 5 d, after which time precipitation of a solid had occurred. This was filtered, washed with water (2 x 20 cm^3) and dried over $CaCl_2$ to afford an off-white solid (320 mg, 21 %) which was tentatively assigned to *ca.* 90 % pure diphospha-adamantane (**5.13**) by $^{31}P\{^1H\}$ NMR (see Section 5.2.4). EI mass spectrum: m/z 384 (M^+).

E.5.2 Coordination chemistry of 1,2-(1,3,5,7-tetramethyl-6,8-dioxa-2,4-diphospha-adamantyl)benzene (5.6)

*Reaction of $[PdCl_2(NCPh)_2]$ with 2.0 equiv. of (**5.6**)*

To a solution of $[PdCl_2(NCPh)_2]$ (40 mg, 0.104 mmol) in dichloromethane (2 cm^3) was added dropwise (**5.6**) (64 mg, 0.209 mmol) in dichloromethane (2 cm^3). The orange solution was stirred for 18 h and the $^{31}P\{^1H\}$ NMR spectrum recorded. This showed that two species had been formed, tentatively assigned to the mononuclear complex *trans*-$[PdCl_2(\mathbf{5.6})_2]$ (**5.14**) and an oligomeric species (**5.15**).

*Reaction of $[PtCl_2(cod)]$ with 2.0 equiv. of (**5.6**)*

To a solution of $[PtCl_2(cod)]$ (40 mg, 0.107 mmol) in dichloromethane (2 cm^3) was added dropwise (**5.6**) (66 mg, 0.215 mmol) in dichloromethane (2 cm^3). The solution was stirred for 18 h and the $^{31}P\{^1H\}$ NMR spectrum recorded. This was consistent with the formation of the mononuclear complex *trans*-$[PtCl_2(\mathbf{5.6})_2]$ (**5.16**).

*Preparation of binuclear gold complex [(AuCl)$_2$(μ-**5.6**)] (**5.17**)*

To a solution of [AuCl(tht)] (124 mg, 0.392 mmol) in dichloromethane (2 cm^3) was added a solution of (**5.6**) (60 mg, 0.196 mmol) in dichloromethane (2 cm^3). After stirring the reaction mixture for 18 h a precipitate had formed which was filtered and washed with dichloromethane (2 x 3 cm^3) to yield complex (**5.17**) (90 mg, 60 %) as a white solid. FAB mass spectrum: m/z 771 (M^+).

Table E.5.2 Elemental analysis[a] for Chapter 5

Compound	C	H
(**5.6**)	62.1 (62.8)	6.8 (6.6)

[a] Analyses in %. Calculated values in parentheses.

Appendices

A.1 Crystal data and structure refinement for α/β-(2.13)

This crystal structure determination was carried out by Miss D. Ellis and Miss H. Phetmung under the supervision of Prof. A. G. Orpen

Identification code	taya/rip25/rip25d	
Empirical formula	$C_{16}H_{15}F_6O_3P$	
Formula weight	400.25	
Temperature	173(2) K	
Wavelength	0.71073 Å	
Crystal system	Monoclinic	
Space group	$P2_1/c$	
Unit cell dimensions	a = 15.812(4) Å	α = 90.00°
	b = 7.698(3) Å	β = 97.92(2)°
	c = 13.874(5) Å	γ = 90.00°
Volume	1672.6(9) $Å^{-3}$	
Z	4	
Density (calculated)	1.589 Mgm^{-3}	
Absorption coefficient	0.242 mm^{-1}	
F(000)	816	
Crystal size	0.1 x 0.3 x 0.45 mm	
θ range for data collection	2.60 - 27.47°	
Index ranges	-19<=h<=20, -6<=k<=9, -18<=l<=17	
Reflections collected	10116	
Independent reflections	3799 [R(int) = 0.0340]	
Refinement method	Full-matrix least-squares on F^2	
Data/restraints/parameters	3795/0/236	
Goodness-of-fit on F^2 (S)*	1.070	
Final R indices [$I>2\sigma(I)$]*	R_1 = 0.0343, wR_2 = 0.0830 [3259 data]	
R indices (all data)*	R_1 = 0.0425, wR_2 = 0.0903 [3799 data]	
Weighting scheme	calc $w = 1/[\sigma^2(F_o^2) + (0.0350P)^2 + 0.8736P]$	
	where $P = \max(F_o^2 + 2F_c^2)/3$	
Extinction coefficient	0.0022(4)	
Largest diff. peak and hole	0.393 and -0.236 $e.Å^{-3}$	

*$wR_2 = [\Sigma w\Delta^2/\Sigma wF_o^4]^{0.5}$; $S = [\Sigma w\Delta^2/(N.O. - N.V.)]^{0.5}$; $\Delta = F_o^2 - F_c^2$;
$R_1 = \Sigma |F_o - F_c|/\Sigma |F_o|$; N.O. = data + restraints; N.V. = parameters

Table A.1.1 Atomic coordinates (x 10^4) and equivalent isotropic displacement parameters ($Å^2$ x 10^2) for α/β-(**2.13**). U(eq) is defined as one third of the trace of the orthogonalized U_{ij} tensor.

Atom	x	y	z	U(eq)
P(1)	7494(1)	-21(1)	4136(1)	22(1)
C(11)	8096(1)	-991(2)	3233(1)	25(1)
C(12)	8728(1)	-2162(2)	3627(1)	29(1)
C(13)	9258(1)	-2971(2)	3040(1)	35(1)
C(14)	9144(1)	-2656(3)	2048(1)	40(1)
C(15)	8512(1)	-1516(2)	1645(1)	37(1)
C(16)	7994(1)	-679(2)	2227(1)	30(1)
O(1)	6595(1)	1983(1)	2621(1)	24(1)
O(2)	7461(1)	3250(1)	4878(1)	24(1)
O(3)	6674(1)	4586(1)	3516(1)	25(1)
C(1)	6480(1)	949(2)	3451(1)	23(1)
C(10)	5847(1)	-463(2)	3049(1)	31(1)
F(1)	5128(1)	216(2)	2582(1)	43(1)
F(2)	5629(1)	-1436(2)	3776(1)	45(1)
F(3)	6156(1)	-1528(1)	2426(1)	41(1)
C(2)	6083(1)	2071(2)	4186(1)	26(1)
C(3)	6621(1)	3704(2)	4403(1)	25(1)
C(4)	6256(1)	4961(2)	5070(1)	32(1)
C(5)	8844(1)	2238(2)	4892(1)	28(1)
F(4)	9398(1)	1308(1)	4457(1)	37(1)
F(5)	8832(1)	1560(2)	5774(1)	42(1)
F(6)	9178(1)	3838(1)	5023(1)	37(1)
C(6)	7963(1)	2267(2)	4286(1)	22(1)
C(7)	7985(1)	3180(2)	3316(1)	23(1)
C(8)	7071(1)	3562(2)	2849(1)	23(1)
C(9)	7019(1)	4562(2)	1911(1)	29(1)

Table A.1.2 Bond lengths (Å) for α/β-(**2.13**).

Atoms	length(Å)	Atoms	length(Å)
P(1)-C(11)	1.834(2)	C(1)-C(10)	1.530(2)
P(1)-C(1)	1.900(2)	C(1)-C(2)	1.535(2)
P(1)-C(6)	1.911(2)	C(10)-F(3)	1.332(2)
C(11)-C(12)	1.400(2)	C(10)-F(1)	1.335(2)
C(11)-C(16)	1.403(2)	C(10)-F(2)	1.340(2)
C(12)-C(13)	1.392(2)	C(2)-C(3)	1.524(2)
C(13)-C(14)	1.384(3)	C(3)-C(4)	1.507(2)
C(14)-C(15)	1.388(3)	C(5)-F(5)	1.333(2)
C(15)-C(16)	1.387(2)	C(5)-F(4)	1.339(2)
O(1)-C(1)	1.432(2)	C(5)-F(6)	1.342(2)
O(1)-C(8)	1.441(2)	C(5)-C(6)	1.524(2)
O(2)-C(6)	1.435(2)	C(6)-C(7)	1.524(2)
O(2)-C(3)	1.442(2)	C(7)-C(8)	1.529(2)
O(3)-C(3)	1.418(2)	C(8)-C(9)	1.503(2)
O(3)-C(8)	1.425(2)		

Table A.1.3 Bond angles(°) for α/β-(**2.13**).

Atoms	angle(°)	Atoms	angle(°)
C(11)-P(1)-C(1)	107.41(7)	C(3)-C(2)-C(1)	109.13(12)
C(11)-P(1)-C(6)	102.67(7)	O(3)-C(3)-O(2)	110.59(11)
C(1)-P(1)-C(6)	88.87(7)	O(3)-C(3)-C(4)	107.39(13)
C(12)-C(11)-C(16)	118.5(2)	O(2)-C(3)-C(4)	106.31(12)
C(12)-C(11)-P(1)	113.89(12)	O(3)-C(3)-C(2)	108.75(12)
C(16)-C(11)-P(1)	127.60(13)	O(2)-C(3)-C(2)	110.12(13)
C(13)-C(12)-C(11)	120.9(2)	C(4)-C(3)-C(2)	113.63(13)
C(14)-C(13)-C(12)	119.8(2)	F(5)-C(5)-F(4)	107.29(13)
C(13)-C(14)-C(15)	119.9(2)	F(5)-C(5)-F(6)	106.84(13)
C(16)-C(15)-C(14)	120.6(2)	F(4)-C(5)-F(6)	106.40(12)
C(15)-C(16)-C(11)	120.2(2)	F(5)-C(5)-C(6)	112.60(12)
C(1)-O(1)-C(8)	114.38(11)	F(4)-C(5)-C(6)	111.40(13)
C(6)-O(2)-C(3)	114.43(11)	F(6)-C(5)-C(6)	111.95(13)
C(3)-O(3)-C(8)	112.52(11)	O(2)-C(6)-C(7)	110.16(12)
O(1)-C(1)-C(10)	104.54(12)	O(2)-C(6)-C(5)	103.18(11)
O(1)-C(1)-C(2)	109.25(12)	C(7)-C(6)-C(5)	111.29(12)
C(10)-C(1)-C(2)	109.58(12)	O(2)-C(6)-P(1)	108.15(9)
O(1)-C(1)-P(1)	115.43(10)	C(7)-C(6)-P(1)	112.61(10)
C(10)-C(1)-P(1)	111.57(11)	C(5)-C(6)-P(1)	110.98(11)
C(2)-C(1)-P(1)	106.41(10)	C(6)-C(7)-C(8)	109.14(12)
F(3)-C(10)-F(1)	106.83(13)	O(3)-C(8)-O(1)	110.21(11)
F(3)-C(10)-F(2)	107.47(14)	O(3)-C(8)-C(9)	107.62(12)
F(1)-C(10)-F(2)	107.09(13)	O(1)-C(8)-C(9)	106.11(12)
F(3)-C(10)-C(1)	113.20(13)	O(3)-C(8)-C(7)	107.82(11)
F(1)-C(10)-C(1)	111.67(14)	O(1)-C(8)-C(7)	111.42(12)
F(2)-C(10)-C(1)	110.28(13)	C(9)-C(8)-C(7)	113.60(13)

Table A.1.4 Anisotropic displacement parameters ($Å^2$ x 10^3) for α/β-(**2.13**). The anisotropic displacement factor exponent takes the form:

$-2\Pi^2[h^2a^{*2}U_{11} + ... + 2hka^*b^*U_{12}]$

Atom	U_{11}	U_{22}	U_{33}	U_{23}	U_{13}	U_{12}
P(1)	23(1)	24(1)	20(1)	3(1)	2(1)	0(1)
C(11)	26(1)	22(1)	26(1)	-1(1)	4(1)	-3(1)
C(12)	29(1)	27(1)	31(1)	0(1)	1(1)	-2(1)
C(13)	26(1)	29(1)	48(1)	-6(1)	5(1)	1(1)
C(14)	39(1)	37(1)	48(1)	-10(1)	21(1)	-5(1)
C(15)	49(1)	35(1)	29(1)	-4(1)	15(1)	-4(1)
C(16)	38(1)	27(1)	26(1)	0(1)	5(1)	0(1)
O(1)	28(1)	24(1)	19(1)	2(1)	-1(1)	-2(1)
O(2)	23(1)	30(1)	19(1)	-2(1)	1(1)	3(1)
O(3)	28(1)	25(1)	21(1)	1(1)	4(1)	4(1)
C(1)	23(1)	24(1)	22(1)	3(1)	1(1)	-2(1)
C(10)	28(1)	32(1)	32(1)	3(1)	-1(1)	-6(1)
F(1)	29(1)	43(1)	54(1)	1(1)	-13(1)	-5(1)
F(2)	46(1)	44(1)	45(1)	10(1)	4(1)	-20(1)
F(3)	42(1)	35(1)	45(1)	-11(1)	1(1)	-8(1)

Atom	U_{11}	U_{22}	U_{33}	U_{23}	U_{13}	U_{12}
C(2)	22(1)	34(1)	23(1)	4(1)	3(1)	1(1)
C(3)	23(1)	31(1)	20(1)	1(1)	2(1)	4(1)
C(4)	32(1)	39(1)	27(1)	-3(1)	7(1)	8(1)
C(5)	23(1)	32(1)	28(1)	0(1)	1(1)	-1(1)
F(4)	22(1)	42(1)	48(1)	-7(1)	3(1)	4(1)
F(5)	31(1)	62(1)	29(1)	12(1)	-7(1)	-2(1)
F(6)	31(1)	34(1)	44(1)	-6(1)	-7(1)	-6(1)
C(6)	19(1)	25(1)	21(1)	0(1)	2(1)	1(1)
C(7)	24(1)	23(1)	22(1)	0(1)	5(1)	-1(1)
C(8)	26(1)	23(1)	19(1)	-1(1)	3(1)	0(1)
C(9)	37(1)	27(1)	23(1)	5(1)	5(1)	2(1)

Table A.1.5 Hydrogen coordinates (x 10^4) and isotropic displacement parameters ($Å^2$ x 10^3) for α/β-(**2.13**).

Atom	x	y	z	U(eq)
H(12)	8797(1)	-2408(2)	4304(1)	35
H(13)	9695(1)	-3736(2)	3319(1)	41
H(14)	9499(1)	-3218(3)	1644(1)	48
H(15)	8434(1)	-1308(2)	964(1)	44
H(16)	7568(1)	109(2)	1945(1)	36
H(2A)	5492(1)	2395(2)	3915(1)	31
H(2B)	6063(1)	1408(2)	4794(1)	31
H(4A)	6211(1)	4390(2)	5692(1)	48
H(4B)	5689(1)	5337(2)	4769(1)	48
H(4C)	6633(1)	5974(2)	5182(1)	48
H(7A)	8272(1)	2430(2)	2880(1)	28
H(7B)	8311(1)	4278(2)	3420(1)	28
H(9A)	7288(1)	3887(2)	1437(1)	43
H(9B)	7317(1)	5673(2)	2031(1)	43
H(9C)	6419(1)	4776(2)	1656(1)	43

A.2 Crystal data and structure refinement for *rac*-(2.16)

This crystal structure determination was carried out by Miss D. Ellis and Miss H. Phetmung under the supervision of Prof. A. G. Orpen

Identification code	taya/rip35/rip35s	
Empirical formula	$C_{34}H_{34}Cl_6F_{12}O_6P_2Pd$	
Formula weight	1147.65	
Temperature	173(2) K	
Wavelength	0.71073 Å	
Crystal system	Monoclinic	
Space group	C2/c	
Unit cell dimensions	a = 19.147(6) Å	α = 90.00°
	b = 14.425(4) Å	β = 101.21(3)°
	c = 15.953(3) Å	γ = 90.00°
Volume	4322(2) Å^3	
Z	4	
Density (calculated)	1.764 Mgm^{-3}	
Absorption coefficient	0.969 mm^{-1}	
F(000)	2288	
Crystal size	0.2 x 0.2 x 0.2 mm	
Theta range for data collection	1.78° - 27.58°	
Index ranges	-23<=h<=24, -9<=k<=18, -20<=l<=20	
Reflections collected	13544	
Independent reflections	4956 [R(int) = 0.0394]	
Absorption correction	SADABS	
Refinement method	Full-matrix least-squares on F^2	
Data/restraints/parameters	4956/0/286	
Goodness-of-fit on F^2	0.993	
Final R indices [$I > 2\sigma(I)$]*	R_1 = 0.0360, wR_2 = 0.0833 [3680 data]	
R indices (all data)*	R_1 = 0.0585, wR_2 = 0.0900 [4956 data]	
Weighting scheme	calc $w = 1/[\sigma^2(F_o^2) + (0.0442P)^2 + 0.0000P]$	
	where $P = \max(F_o^2 + 2F_c^2)/3$	
Largest diff. peak and hole	0.639 and -0.850 e.Å^{-3}	

*$wR_2 = [\Sigma w\Delta^2/\Sigma wF_o^4]^{0.5}$; $S = [\Sigma w\Delta^2/(N.O. - N.V.)]^{0.5}$; $\Delta = F_o^2 - F_c^2$;
$R_1 = \Sigma |F_o - F_c|/\Sigma |F_o|$; N.O. = data + restraints; N.V. = parameters

Table A.2.1 Atomic coordinates (x 10^4) and equivalent isotropic displacement parameters ($Å^2$ x 10^2) for *rac*-**(2.16)**. U(eq) is defined as one third of the trace of the orthogonalized U_{ij} tensor.

Atoms	x	y	z	U(eq)
Pd(1)	0	8089(1)	2500	20(1)
Cl(1)	-450(1)	8293(1)	1063(1)	27(1)
P(1)	-1176(1)	7911(1)	2688(1)	19(1)
C(11)	-1706(2)	7261(2)	1815(2)	29(1)
C(12)	-1342(3)	6531(3)	1511(2)	41(1)
C(13)	-1701(4)	5979(3)	850(3)	61(2)
C(14)	-2404(4)	6144(4)	508(3)	70(2)
C(15)	-2763(3)	6856(4)	791(3)	60(2)
C(16)	-2417(2)	7424(3)	1461(2)	38(1)
O(1)	-2368(1)	8841(2)	2986(1)	24(1)
O(2)	-2101(1)	8679(2)	4484(1)	24(1)
O(3)	-1061(1)	7834(2)	4436(1)	21(1)
C(1)	-1642(2)	9000(2)	2933(2)	20(1)
C(10)	-1666(2)	9753(2)	2257(2)	26(1)
F(1)	-2002(1)	10510(2)	2457(1)	38(1)
F(2)	-2003(1)	9483(2)	1487(1)	40(1)
F(3)	-1008(1)	10010(1)	2196(1)	32(1)
C(2)	-1225(2)	9370(2)	3787(2)	20(1)
C(3)	-1356(2)	8743(2)	4509(2)	21(1)
C(4)	-1003(2)	9101(2)	5373(2)	29(1)
C(5)	-1069(2)	6352(2)	3832(2)	27(1)
F(4)	-1411(1)	5771(1)	3237(1)	39(1)
F(5)	-382(1)	6314(2)	3803(2)	41(1)
F(6)	-1142(1)	6016(2)	4586(1)	42(1)
C(6)	-1386(2)	7331(2)	3690(2)	21(1)
C(7)	-2190(2)	7302(2)	3631(2)	24(1)
C(8)	-2470(2)	8278(2)	3705(2)	23(1)
C(9)	-3255(2)	8319(3)	3700(2)	32(1)
C(20)	-278(3)	2859(4)	4013(4)	76(2)
Cl(2)	-615(1)	1953(1)	3320(1)	75(1)
Cl(3)	-227(5)	3951(4)	3526(5)	125(4)
C(21)	-278(3)	2859(4)	4013(4)	76(2)
Cl(4)	-615(1)	1953(1)	3320(1)	75(1)
Cl(5)	-750(3)	3829(2)	3777(2)	82(2)

Table A.2.2 Bond lengths (Å) for *rac*-(**2.16**).

Atoms	length(Å)	Atoms	length(Å)
Pd(1)-Cl(1)	2.3063(10)	C(1)-C(10)	1.525(4)
Pd(1)-P(1)	2.3429(11)	C(1)-C(2)	1.534(4)
P(1)-C(11)	1.817(3)	C(10)-F(2)	1.331(4)
P(1)-C(1)	1.885(3)	C(10)-F(3)	1.334(4)
P(1)-C(6)	1.916(3)	C(10)-F(1)	1.338(4)
C(11)-C(16)	1.388(6)	C(2)-C(3)	1.523(4)
C(11)-C(12)	1.401(6)	C(3)-C(4)	1.504(4)
C(12)-C(13)	1.391(6)	C(5)-F(5)	1.325(4)
C(13)-C(14)	1.371(9)	C(5)-F(6)	1.330(4)
C(14)-C(15)	1.361(9)	C(5)-F(4)	1.337(4)
C(15)-C(16)	1.405(6)	C(5)-C(6)	1.537(5)
O(1)-C(1)	1.427(4)	C(6)-C(7)	1.526(5)
O(1)-C(8)	1.448(4)	C(7)-C(8)	1.519(5)
O(2)-C(3)	1.423(4)	C(8)-C(9)	1.504(5)
O(2)-C(8)	1.427(4)	C(20)-Cl(2)	1.751(6)
O(3)-C(6)	1.429(4)	C(20)-Cl(3)	1.768(8)
O(3)-C(3)	1.441(4)	C(21)-Cl(5)	1.669(6)
		C(21)-Cl(4)	1.751(6)

Table A.2.3 Bond angles(°) for *rac*-(**2.16**)

Atoms	angle(°)	Atoms	angle(°)
Cl(1)#1-Pd(1)-Cl(1)	165.34(5)	F(2)-C(10)-C(1)	112.8(3)
Cl(1)-Pd(1)-P(1)#1	93.99(4)	F(3)-C(10)-C(1)	110.6(3)
Cl(1)-Pd(1)-P(1)	87.61(4)	F(1)-C(10)-C(1)	111.2(3)
P(1)#1-Pd(1)-P(1)	167.42(4)	C(3)-C(2)-C(1)	109.4(3)
C(11)-P(1)-C(1)	111.9(2)	O(2)-C(3)-O(3)	110.2(2)
C(11)-P(1)-C(6)	103.76(14)	O(2)-C(3)-C(4)	108.5(3)
C(1)-P(1)-C(6)	90.37(14)	O(3)-C(3)-C(4)	105.9(3)
C(11)-P(1)-Pd(1)	111.49(12)	O(2)-C(3)-C(2)	109.2(3)
C(1)-P(1)-Pd(1)	116.16(10)	O(3)-C(3)-C(2)	110.7(2)
C(6)-P(1)-Pd(1)	121.15(11)	C(4)-C(3)-C(2)	112.3(3)
C(16)-C(11)-C(12)	120.1(3)	F(5)-C(5)-F(6)	107.3(3)
C(16)-C(11)-P(1)	125.6(3)	F(5)-C(5)-F(4)	107.6(3)
C(12)-C(11)-P(1)	114.3(3)	F(6)-C(5)-F(4)	106.9(3)
C(13)-C(12)-C(11)	119.1(5)	F(5)-C(5)-C(6)	113.5(3)
C(14)-C(13)-C(12)	120.3(5)	F(6)-C(5)-C(6)	111.1(3)
C(15)-C(14)-C(13)	121.2(4)	F(4)-C(5)-C(6)	110.2(3)
C(14)-C(15)-C(16)	119.9(5)	O(3)-C(6)-C(7)	109.7(2)
C(11)-C(16)-C(15)	119.4(5)	O(3)-C(6)-C(5)	104.4(2)
C(1)-O(1)-C(8)	114.8(2)	C(7)-C(6)-C(5)	110.4(3)
C(3)-O(2)-C(8)	112.0(2)	O(3)-C(6)-P(1)	110.2(2)
C(6)-O(3)-C(3)	114.5(2)	C(7)-C(6)-P(1)	109.5(2)
O(1)-C(1)-C(10)	105.2(3)	C(5)-C(6)-P(1)	112.5(2)
O(1)-C(1)-C(2)	110.3(2)	C(8)-C(7)-C(6)	109.6(3)
C(10)-C(1)-C(2)	108.6(3)	O(2)-C(8)-O(1)	110.1(2)
O(1)-C(1)-P(1)	112.6(2)	O(2)-C(8)-C(9)	108.2(3)
C(10)-C(1)-P(1)	113.4(2)	O(1)-C(8)-C(9)	105.2(3)
C(2)-C(1)-P(1)	106.7(2)	O(2)-C(8)-C(7)	108.7(3)

Atoms	angle(°)	Atoms	angle(°)
F(2)-C(10)-F(3)	108.1(3)	O(1)-C(8)-C(7)	110.8(2)
F(2)-C(10)-F(1)	106.8(3)	C(9)-C(8)-C(7)	113.7(3)
F(3)-C(10)-F(1)	107.2(3)	Cl(2)-C(20)-Cl(3)	115.6(4)
Cl(5)-C(21)-Cl(4)	111.5(3)		

Symmetry transformations used to generate equivalent atoms: #1 -x, y, -z + 1/2

Table A.2.4 Anisotropic displacement parameters ($Å^2$ x 10^3) for *rac*-(**2.16**). The anisotropic displacement factor exponent takes the form:

$-2\Pi^2[h^2a^{*2}U_{11} + ... + 2hka^*b^*U_{12}]$

Atom	U_{11}	U_{22}	U_{33}	U_{23}	U_{13}	U_{12}
Pd(1)	24(1)	20(1)	17(1)	0	8(1)	0
Cl(1)	28(1)	34(1)	19(1)	2(1)	7(1)	0(1)
P(1)	24(1)	19(1)	16(1)	-2(1)	7(1)	-3(1)
C(11)	43(2)	29(2)	17(2)	-3(1)	8(2)	-16(2)
C(12)	69(3)	29(2)	30(2)	-8(2)	24(2)	-18(2)
C(13)	120(5)	37(2)	36(2)	-18(2)	37(3)	-40(3)
C(14)	117(5)	72(4)	22(2)	-13(2)	15(3)	-67(4)
C(15)	78(3)	75(4)	24(2)	4(2)	-2(2)	-50(3)
C(16)	44(2)	49(2)	21(2)	1(2)	4(2)	-24(2)
O(1)	22(1)	29(1)	21(1)	4(1)	5(1)	1(1)
O(2)	25(1)	29(1)	19(1)	-4(1)	8(1)	0(1)
O(3)	27(1)	19(1)	17(1)	-3(1)	6(1)	-1(1)
C(1)	22(2)	21(2)	19(1)	-1(1)	6(1)	-3(1)
C(10)	30(2)	26(2)	21(2)	3(1)	3(1)	-1(1)
F(1)	47(1)	29(1)	41(1)	11(1)	11(1)	14(1)
F(2)	50(1)	46(1)	21(1)	7(1)	-2(1)	-10(1)
F(3)	37(1)	29(1)	31(1)	8(1)	13(1)	-5(1)
C(2)	23(2)	19(2)	20(2)	-2(1)	6(1)	-1(1)
C(3)	26(2)	20(2)	19(2)	-2(1)	6(1)	1(1)
C(4)	38(2)	28(2)	19(2)	-4(1)	5(1)	-1(2)
C(5)	35(2)	22(2)	26(2)	1(1)	13(2)	-1(1)
F(4)	54(1)	22(1)	42(1)	-8(1)	7(1)	-4(1)
F(5)	35(1)	26(1)	63(2)	7(1)	16(1)	6(1)
F(6)	72(2)	26(1)	33(1)	9(1)	22(1)	6(1)
C(6)	29(2)	18(2)	17(1)	-1(1)	7(1)	-4(1)
C(7)	27(2)	27(2)	19(2)	-3(1)	8(1)	-9(1)
C(8)	23(2)	28(2)	18(1)	-3(1)	7(1)	-3(1)
C(9)	27(2)	43(2)	28(2)	1(2)	8(2)	-1(2)
C(20)	76(4)	59(3)	79(4)	8(3)	-21(3)	-8(3)
Cl(2)	69(1)	65(1)	77(1)	-1(1)	-18(1)	4(1)
Cl(3)	107(7)	68(3)	178(6)	34(3)	-26(5)	3(3)
C(21)	76(4)	59(3)	79(4)	8(3)	-21(3)	-8(3)
Cl(4)	69(1)	65(1)	77(1)	-1(1)	-18(1)	4(1)
Cl(5)	87(3)	43(1)	102(2)	-6(1)	-16(2)	21(2)

Table A.2.5 Hydrogen coordinates (x 10^4) and isotropic displacement parameters ($Å^2$ x 10^3) for *rac*-(**2.16**).

Atom	x	y	z	U(eq)
H(12)	-857(3)	6413(3)	1753(2)	49
H(13)	-1459(4)	5485(3)	635(3)	74
H(14)	-2645(4)	5755(4)	64(3)	84
H(15)	-3246(3)	6970(4)	537(3)	72
H(16)	-2668(2)	7914(3)	1670(2)	46
H(2A)	-710(2)	9385(2)	3775(2)	24
H(2B)	-1381(2)	10009(2)	3881(2)	24
H(4A)	-489(2)	9150(2)	5401(2)	43
H(4B)	-1095(2)	8674(2)	5817(2)	43
H(4C)	-1196(2)	9714(2)	5466(2)	43
H(7A)	-2422(2)	7026(2)	3079(2)	28
H(7B)	-2305(2)	6911(2)	4097(2)	28
H(9A)	-3518(2)	8047(3)	3169(2)	48
H(9B)	-3401(2)	8967(3)	3740(2)	48
H(9C)	-3359(2)	7971(3)	4189(2)	48
H(20A)	205(3)	2685(4)	4318(4)	91
H(20B)	-581(3)	2922(4)	4447(4)	91
H(21A)	-288(3)	2674(2)	4608(2)	91
H(21B)	224(3)	2977(2)	3974(2)	91

A.3 Crystal data and structure refinement for *rac*-(2.17)

This crystal structure determination was carried out by Miss D. Ellis and Miss H. Phetmung under the supervision of Prof. A. G. Orpen.

Identification code	taya/rip36	
Empirical formula	$C_{33.50}H_{30.50}Cl_{2.50}F_{12}O_7P_2Rh$	
Formula weight	1026.55	
Temperature	173(2) K	
Wavelength	0.71073 Å	
Crystal system	Monoclinic	
Space group	P2(1)/c	
Unit cell dimensions	a = 17.804(2) Å	α = 90.000°
	b = 15.315(2) Å	β = 112.722(5)°
	c = 15.6450(13) Å	γ = 90.000°
Volume	3934.9(7) $Å^3$	
Z	4	
Density (calculated)	*1.733 Mgm*$^{-3}$	
Absorption coefficient	0.788 mm^{-1}	
F(000)	2052	
Crystal size	0.4 x 0.4 x 0.3 mm	
θ range for data collection	1.82° - 27.49°	
Index ranges	-23<=h<=22, -13<=k<=19, -16<=l<=20	
Reflections collected	24491	
Independent reflections	8977 [R(int) = 0.0357]	
Absorption correction	None	
Refinement method	Full-matrix least-squares on F^2	
Data/restraints/parameters	8968/0/544	
Goodness-of-fit on F^2 *	1.106	
Final R indices [$I > 2\sigma(I)$]*	R_1 = 0.0298, wR_2 = 0.0703 [8968 data]	
R indices (all data)*	R_1 = 0.0379, wR_2 = 0.0777 [8977 data]	
Weighting scheme	calc $w = 1/[\sigma^2(F_o^2) + (0.0263P)^2 + 4.3814P]$	
	where $P = Max(F_o^2 + 2F_c^2)/3$	
Largest diff. peak and hole	1.225 and -0.507 e.$Å^{-3}$	

*$wR_2 = [\Sigma w\Delta^2/\Sigma wF_o^4]^{0.5}$; $S = [\Sigma w\Delta^2/(N.O. - N.V.)]^{0.5}$; $\Delta = F_o^2 - F_c^2$;
$R_1 = \Sigma |F_o - F_c|/\Sigma |F_o|$; N.O. = data + restraints; N.V. = parameters

Table A.3.1 Atomic coordinates (x 10^4) and equivalent isotropic displacement parameters ($Å^2$ x 10^2) for *rac*-(**2.17**). U(eq) is defined as one third of the trace of the orthogonalized U_{ij} tensor.

Atom	x	y	z	U(eq)
Rh	7444(1)	9689(1)	3845(1)	18(1)
Cl	6799(1)	8831(1)	4608(1)	26(1)
P(1')	6973(1)	8688(1)	2628(1)	17(1)
P(1)	7704(1)	10698(1)	5032(1)	20(1)
F(1')	5416(1)	9668(1)	2797(1)	32(1)
F(1)	9515(1)	9573(1)	7225(1)	44(1)
F(2')	5190(1)	8293(1)	2495(1)	35(1)
F(2)	8220(1)	9526(1)	6868(1)	41(1)
F(3')	4547(1)	9256(1)	1479(1)	39(1)
F(3)	8734(1)	8987(1)	5941(1)	34(1)
F(6')	8604(1)	8546(1)	1390(1)	46(1)
F(4')	8394(1)	7609(1)	2290(1)	41(1)
F(5')	8770(1)	8915(1)	2771(1)	41(1)
F(6)	7639(1)	13137(1)	3943(1)	45(1)
F(5)	7143(1)	11929(1)	3263(1)	47(1)
F(4)	6690(1)	12496(1)	4233(1)	42(1)
O(1')	5625(1)	8515(1)	948(1)	21(1)
O(1)	8867(1)	11157(1)	6762(1)	26(1)
O(2')	7385(1)	9602(1)	1403(1)	24(1)
O(2)	8700(1)	11837(1)	4638(1)	26(1)
O(3')	6167(1)	9411(1)	99(1)	24(1)
O(3)	9611(1)	12082(1)	6172(1)	29(1)
O(4)	8394(1)	10713(1)	2992(1)	43(1)
C(1')	5942(1)	9057(1)	1753(1)	20(1)
C(1)	8718(1)	10532(2)	6038(2)	23(1)
C(2')	6067(1)	9987(1)	1466(2)	23(1)
C(2)	9374(1)	10607(2)	5633(2)	24(1)
C(3')	6583(1)	9946(2)	885(2)	23(1)
C(3)	9443(1)	11556(2)	5371(2)	27(1)
C(4')	6720(2)	10832(2)	546(2)	34(1)
C(4)	10103(2)	11710(2)	5012(2)	33(1)
C(5')	8301(1)	8445(2)	2040(2)	27(1)
C(5)	7364(2)	12355(2)	4070(2)	32(1)
C(6')	7404(1)	8712(1)	1686(1)	21(1)
C(6)	8007(1)	11864(2)	4882(2)	24(1)
C(7')	6916(1)	8139(2)	857(1)	22(1)
C(7)	8203(1)	12393(2)	5777(2)	27(1)
C(8')	6078(1)	8535(1)	355(1)	21(1)
C(8)	8982(1)	12041(2)	6522(2)	28(1)
C(9')	5575(1)	8055(2)	-516(2)	27(1)
C(9)	9265(2)	12550(2)	7418(2)	38(1)
C(10')	5272(1)	9061(2)	2139(2)	26(1)
C(10)	8789(2)	9647(2)	6521(2)	29(1)
C(11')	6944(1)	7534(1)	2891(2)	22(1)
C(11)	6893(1)	10847(2)	5459(2)	24(1)
C(12')	6363(2)	6935(2)	2344(2)	29(1)
C(12)	6107(1)	10829(2)	4772(2)	28(1)
C(13')	6431(2)	6061(2)	2594(2)	39(1)

Atom	x	y	z	U(eq)
C(13)	5437(2)	10960(2)	5001(2)	31(1)
C(14')	7073(2)	5772(2)	3369(2)	44(1)
C(14)	5549(2)	11097(2)	5921(2)	33(1)
C(15')	7650(2)	6360(2)	3922(2)	39(1)
C(15)	6323(2)	11120(2)	6601(2)	32(1)
C(16')	7582(2)	7238(2)	3690(2)	28(1)
C(16)	7000(2)	10998(2)	6380(2)	28(1)
C(17)	8012(2)	10326(2)	3302(2)	27(1)
C(30)	9998(8)	14528(7)	5447(7)	103(4)
Cl(31)	9073(2)	14709(1)	5667(2)	78(1)
Cl(32)	10281(5)	15750(3)	5724(4)	145(3)
Cl(33)	9406(4)	14484(4)	4291(5)	136(2)

Table A.3.2 Bond lengths (Å) for *rac*-(**2.17**).

Atoms	length(Å)	Atoms	length(Å)
Rh-C(17)	1.834(2)	C(1')-C(2')	1.534(3)
Rh-P(1)	2.3202(6)	C(1)-C(2)	1.533(3)
Rh-P(1')	2.3342(6)	C(1)-C(10)	1.535(3)
Rh-Cl	2.3507(6)	C(2')-C(3)	1.523(3)
P(1')-C(11')	1.819(2)	C(2)-C(3)	1.528(3)
P(1')-C(1')	1.903(2)	C(3')-C(4')	1.510(3)
P(1')-C(6')	1.906(2)	C(3)-C(4)	1.504(3)
P(1)-C(11)	1.824(2)	C(5')-C(6')	1.530(3)
P(1)-C(1)	1.899(2)	C(5)-C(6)	1.539(3)
P(1)-C(6)	1.907(2)	C(6')-C(7')	1.530(3)
F(1')-C(10')	1.337(3)	C(6)-C(7)	1.536(3)
F(1)-C(10)	1.340(3)	C(7')-C(8')	1.519(3)
F(2')-C(10')	1.334(3)	C(7)-C(8)	1.524(3)
F(2)-C(10)	1.333(3)	C(8')-C(9')	1.503(3)
F(3')-C(10')	1.339(3)	C(8)-C(9)	1.510(3)
F(3)-C(10)	1.336(3)	C(11')-C(12')	1.401(3)
F(6')-C(5')	1.330(3)	C(11')-C(16')	1.401(3)
F(4')-C(5')	1.331(3)	C(11)-C(12)	1.396(3)
F(5')-C(5')	1.335(3)	C(11)-C(16)	1.398(3)
F(6)-C(5)	1.337(3)	C(12')-C(13')	1.387(3)
F(5)-C(5)	1.339(3)	C(12)-C(13)	1.386(3)
F(4)-C(5)	1.336(3)	C(13')-C(14')	1.379(4)
O(1')-C(1')	1.430(2)	C(13)-C(14)	1.391(4)
O(1')-C(8')	1.446(3)	C(14')-C(15')	1.389(4)
O(1)-C(1)	1.427(3)	C(14)-C(15)	1.378(4)
O(1)-C(8)	1.441(3)	C(15')-C(16')	1.385(4)
O(2')-C(6')	1.429(3)	C(15)-C(16)	1.390(3)
O(2')-C(3')	1.442(3)	C(30)-Cl(33)	1.707(13)
O(2)-C(6)	1.426(3)	C(30)-Cl(31)	1.829(12)
O(2)-C(3)	1.442(3)	C(30)-Cl(32)	1.945(13)
O(3')-C(3')	1.424(3)	Cl(32)-Cl(33)#1	0.671(9)
O(3')-C(8')	1.427(3)	Cl(32)-C(30)#1	1.756(11)
O(3)-C(3)	1.422(3)	Cl(33)-Cl(32)#1	0.671(9)
O(3)-C(8)	1.426(3)	Cl(33)-C(30)#1	1.803(14)
O(4)-C(17)	1.141(3)	C(1')-C(10)	1.531(3)

Table A.3.3 Bond angles(°) for *rac*-(**2.17**)

Atoms	angle(°)	Atoms	angle(°)
C(17)-Rh-P(1)	92.39(7)	O(2')-C(6')-C(7')	110.3(2)
C(17)-Rh-P(1')	93.41(7)	C(5')-C(6')-C(7')	109.0(2)
P(1)-Rh-P(1')	171.16(2)	O(2')-C(6')-P(1')	106.81(14)
C(17)-Rh-Cl	176.17(8)	C(5')-C(6')-P(1')	113.0(2)
P(1)-Rh-Cl	87.23(2)	C(7')-C(6')-P(1')	112.22(14)
P(1')-Rh-Cl	87.43(2)	O(2)-C(6)-C(7)	110.1(2)
C(11')-P(1')-C(1')	110.31(10)	O(2)-C(6)-C(5)	103.8(2)
C(11')-P(1')-C(6')	104.43(10)	C(7)-C(6)-C(5)	109.3(2)
C(1')-P(1')-C(6')	90.17(9)	O(2)-C(6)-P(1)	108.69(14)
C(11')-P(1')-Rh	119.07(7)	C(7)-C(6)-P(1)	111.0(2)
C(1')-P(1')-Rh	109.50(7)	C(5)-C(6)-P(1)	113.8(2)
C(6')-P(1')-Rh	119.55(7)	C(8')-C(7')-C(6')	109.4(2)
C(11)-P(1)-C(1)	110.34(10)	C(8)-C(7)-C(6)	109.3(2)
C(11)-P(1)-C(6)	103.23(10)	O(3')-C(8')-O(1')	110.5(2)
C(1)-P(1)-C(6)	90.19(10)	O(3')-C(8')-C(9')	107.3(2)
C(11)-P(1)-Rh	115.77(8)	O(1')-C(8')-C(9')	106.7(2)
C(1)-P(1)-Rh	113.97(7)	O(3')-C(8')-C(7')	109.1(2)
C(6)-P(1)-Rh	120.24(7)	O(1')-C(8')-C(7')	109.9(2)
C(1')-O(1')-C(8')	115.1(2)	C(9')-C(8')-C(7')	113.3(2)
C(1)-O(1)-C(8)	115.1(2)	O(3)-C(8)-O(1)	110.6(2)
C(6')-O(2')-C(3')	115.0(2)	O(3)-C(8)-C(9)	107.7(2)
C(6)-O(2)-C(3)	114.8(2)	O(1)-C(8)-C(9)	105.9(2)
C(3')-O(3')-C(8')	112.1(2)	O(3)-C(8)-C(7)	107.9(2)
C(3)-O(3)-C(8)	112.6(2)	O(1)-C(8)-C(7)	110.7(2)
O(1')-C(1')-C(10')	104.2(2)	C(9)-C(8)-C(7)	114.1(2)
O(1')-C(1')-C(2')	109.5(2)	F(2')-C(10')-F(1')	108.1(2)
C(10')-C(1')-C(2')	109.6(2)	F(2')-C(10')-F(3')	106.9(2)
O(1')-C(1')-P(1')	113.86(14)	F(1')-C(10')-F(3')	106.3(2)
C(10')-C(1')-P(1')	113.6(2)	F(2')-C(10')-C(1')	112.9(2)
C(2')-C(1')-P(1')	106.11(14)	F(1')-C(10')-C(1')	111.1(2)
O(1)-C(1)-C(2)	109.9(2)	F(3')-C(10')-C(1')	111.3(2)
O(1)-C(1)-C(10)	104.3(2)	F(2)-C(10)-F(3)	107.7(2)
C(2)-C(1)-C(10)	109.8(2)	F(2)-C(10)-F(1)	107.3(2)
O(1)-C(1)-P(1)	113.19(14)	F(3)-C(10)-F(1)	106.8(2)
C(2)-C(1)-P(1)	106.3(2)	F(2)-C(10)-C(1)	113.1(2)
C(10)-C(1)-P(1)	113.4(2)	F(3)-C(10)-C(1)	111.3(2)
C(3')-C(2')-C(1')	109.0(2)	F(1)-C(10)-C(1)	110.4(2)
C(3)-C(2)-C(1)	109.6(2)	C(12')-C(11')-C(16')	119.1(2)
O(3')-C(3')-O(2')	110.3(2)	C(12')-C(11')-P(1')	125.2(2)
O(3')-C(3')-C(4')	108.3(2)	C(16')-C(11')-P(1')	115.6(2)
O(2')-C(3')-C(4')	105.5(2)	C(12)-C(11)-C(16)	119.6(2)
O(3')-C(3')-C(2')	107.9(2)	C(12)-C(11)-P(1)	114.5(2)
O(2')-C(3')-C(2')	112.0(2)	C(16)-C(11)-P(1)	125.8(2)
C(4')-C(3')-C(2')	112.9(2)	C(13')-C(12')-C(11')	119.8(2)
O(3)-C(3)-O(2)	110.3(2)	C(13)-C(12)-C(11)	120.3(2)
O(3)-C(3)-C(4)	108.2(2)	C(14')-C(13')-C(12')	120.7(3)
O(2)-C(3)-C(4)	105.4(2)	C(12)-C(13)-C(14)	119.8(2)
O(3)-C(3)-C(2)	108.3(2)	C(13')-C(14')-C(15')	120.1(2)
O(2)-C(3)-C(2)	110.7(2)	C(15)-C(14)-C(13)	120.2(2)
C(4)-C(3)-C(2)	113.9(2)	C(16')-C(15')-C(14')	119.8(2)
F(4')-C(5')-F(6')	107.1(2)	C(14)-C(15)-C(16)	120.6(2)
F(4')-C(5')-F(5')	107.5(2)	C(15')-C(16')-C(11')	120.4(2)

Atoms	angle(°)	Atoms	angle(°)
F(6')-C(5')-F(5')	106.7(2)	C(15)-C(16)-C(11)	119.5(2)
F(4')-C(5')-C(6')	110.9(2)	O(4)-C(17)-Rh	177.3(2)
F(6')-C(5')-C(6')	111.5(2)	Cl(33)-C(30)-Cl(31)	88.4(6)
F(5')-C(5')-C(6')	112.7(2)	Cl(33)-C(30)-Cl(32)	105.9(6)
F(4)-C(5)-F(6)	107.0(2)	Cl(31)-C(30)-Cl(32)	89.2(5)
F(4)-C(5)-F(5)	107.5(2)	Cl(33)#1-Cl(32)-C(30)#1	74.8(10)
F(6)-C(5)-F(5)	106.7(2)	Cl(33)#1-Cl(32)-C(30)	67.9(10)
F(4)-C(5)-C(6)	111.0(2)	C(30)#1-Cl(32)-C(30)	65.7(6)
F(6)-C(5)-C(6)	111.2(2)	Cl(32)#1-Cl(33)-C(30)	82.9(12)
F(5)-C(5)-C(6)	113.2(2)	Cl(32)#1-Cl(33)-C(30)#1	91.9(12)
O(2')-C(6')-C(5')	105.3(2)	C(30)-Cl(33)-C(30)#1	70.0(6)

Symmetry transformations used to generate equivalent atoms: #1 -x+2,-y+3,-z+1

Table A.3.4 Anisotropic displacement parameters ($Å^2$ x 10^3) for *rac*-(**2.17**). The anisotropic displacement factor exponent takes the form:

$-2\Pi^2[h^2a^{*2}U_{11} + ... + 2hka^*b^*U_{12}]$

Atom	U_{11}	U_{22}	U_{33}	U_{23}	U_{13}	U_{12}
Rh	21(1)	18(1)	16(1)	-2(1)	7(1)	-2(1)
Cl	33(1)	24(1)	26(1)	-1(1)	16(1)	-4(1)
P(1')	20(1)	17(1)	15(1)	-1(1)	6(1)	-1(1)
P(1)	20(1)	20(1)	18(1)	-3(1)	6(1)	2(1)
F(1')	32(1)	38(1)	28(1)	-9(1)	14(1)	2(1)
F(1)	43(1)	42(1)	31(1)	6(1)	-1(1)	15(1)
F(2')	37(1)	35(1)	42(1)	1(1)	26(1)	-4(1)
F(2)	53(1)	38(1)	44(1)	13(1)	30(1)	14(1)
F(3')	22(1)	60(1)	30(1)	-3(1)	6(1)	6(1)
F(3)	44(1)	23(1)	34(1)	-2(1)	15(1)	6(1)
F(6')	29(1)	80(1)	35(1)	3(1)	20(1)	2(1)
F(4')	34(1)	37(1)	54(1)	5(1)	17(1)	12(1)
F(5')	22(1)	56(1)	37(1)	-16(1)	1(1)	0(1)
F(6)	48(1)	28(1)	52(1)	13(1)	11(1)	2(1)
F(5)	60(1)	38(1)	27(1)	0(1)	-2(1)	13(1)
F(4)	29(1)	38(1)	53(1)	8(1)	9(1)	13(1)
O(1')	23(1)	22(1)	17(1)	-5(1)	6(1)	-4(1)
O(1)	29(1)	28(1)	20(1)	-7(1)	6(1)	3(1)
O(2')	25(1)	24(1)	21(1)	1(1)	8(1)	-5(1)
O(2)	25(1)	24(1)	27(1)	-2(1)	9(1)	1(1)
O(3')	33(1)	21(1)	15(1)	0(1)	6(1)	-4(1)
O(3)	23(1)	29(1)	32(1)	-12(1)	7(1)	-3(1)
O(4)	60(1)	40(1)	38(1)	-14(1)	30(1)	-27(1)
C(1')	21(1)	21(1)	16(1)	-3(1)	4(1)	-1(1)
C(1)	23(1)	23(1)	20(1)	-4(1)	5(1)	4(1)
C(2')	28(1)	18(1)	21(1)	-1(1)	7(1)	2(1)
C(2)	22(1)	25(1)	23(1)	-5(1)	6(1)	4(1)
C(3')	30(1)	20(1)	17(1)	0(1)	6(1)	-5(1)
C(3)	24(1)	26(1)	28(1)	-7(1)	7(1)	1(1)
C(4')	46(2)	24(1)	26(1)	3(1)	9(1)	-10(1)
C(4)	29(1)	34(1)	39(1)	-7(1)	15(1)	-2(1)

Atom	U_{11}	U_{22}	U_{33}	U_{23}	U_{13}	U_{12}
C(5')	25(1)	35(1)	21(1)	-3(1)	10(1)	0(1)
C(5)	34(1)	22(1)	33(1)	2(1)	6(1)	4(1)
C(6')	22(1)	23(1)	17(1)	-2(1)	8(1)	-2(1)
C(6)	23(1)	22(1)	25(1)	-3(1)	6(1)	3(1)
C(7')	25(1)	24(1)	17(1)	-4(1)	9(1)	-2(1)
C(7)	27(1)	23(1)	30(1)	-8(1)	9(1)	3(1)
C(8')	25(1)	21(1)	17(1)	0(1)	9(1)	-1(1)
C(8)	26(1)	26(1)	28(1)	-10(1)	7(1)	1(1)
C(9')	30(1)	26(1)	20(1)	-5(1)	4(1)	0(1)
C(9)	37(1)	39(2)	35(1)	-20(1)	9(1)	-2(1)
C(10')	24(1)	29(1)	23(1)	-3(1)	7(1)	2(1)
C(10)	31(1)	31(1)	24(1)	0(1)	8(1)	8(1)
C(11')	28(1)	19(1)	21(1)	0(1)	11(1)	1(1)
C(11)	24(1)	21(1)	26(1)	-3(1)	11(1)	3(1)
C(12')	39(1)	22(1)	23(1)	0(1)	9(1)	-2(1)
C(12)	28(1)	27(1)	27(1)	-4(1)	9(1)	3(1)
C(13')	62(2)	21(1)	34(1)	-3(1)	16(1)	-9(1)
C(13)	26(1)	32(1)	36(1)	2(1)	12(1)	4(1)
C(14')	80(2)	19(1)	36(1)	4(1)	24(2)	6(1)
C(14)	36(1)	30(1)	42(1)	6(1)	23(1)	10(1)
C(15')	55(2)	33(1)	26(1)	9(1)	14(1)	16(1)
C(15)	42(1)	31(1)	30(1)	1(1)	20(1)	7(1)
C(16')	33(1)	28(1)	22(1)	1(1)	9(1)	5(1)
C(16)	30(1)	28(1)	25(1)	-2(1)	10(1)	4(1)
C(17)	34(1)	25(1)	21(1)	-9(1)	9(1)	-8(1)
C(30)	162(11)	95(8)	67(6)	9(5)	61(7)	16(7)
Cl(31)	99(2)	59(1)	66(1)	10(1)	21(1)	26(1)
Cl(32)	298(9)	76(2)	97(3)	-8(2)	116(4)	14(3)
Cl(33)	148(4)	138(5)	142(4)	-37(3)	77(3)	-31(3)

Table A.3.5 Hydrogen coordinates (x 10^4) and isotropic displacement parameters ($Å^2$ x 10^3) for *rac*-(**2.17**).

Atom	x	y	z	U(eq)
H(2'A)	5534(1)	10257(1)	1103(2)	28
H(2'B)	6344(1)	10348(1)	2025(2)	28
H(2A)	9904(1)	10407(2)	6096(2)	29
H(2B)	9230(1)	10231(2)	5078(2)	29
H(4'A)	7028(10)	11201(4)	1078(2)	50
H(4'B)	6193(2)	11105(6)	192(12)	50
H(4'C)	7027(10)	10765(2)	148(11)	50
H(4A)	9965(6)	11408(11)	4417(7)	50
H(4B)	10621(3)	11484(12)	5458(7)	50
H(4C)	10154(8)	12337(2)	4925(13)	50
H(7'A)	7204(1)	8096(2)	429(1)	26
H(7'B)	6862(1)	7543(2)	1072(1)	26
H(7A)	8275(1)	13016(2)	5659(2)	33
H(7B)	7748(1)	12346(2)	5988(2)	33
H(9'A)	5501(1)	7448(2)	-365(2)	40
H(9'B)	5853(1)	8066(2)	-948(2)	40
H(9'C)	5042(1)	8337(2)	-804(2)	40
H(9A)	8860(6)	12499(11)	7698(7)	58
H(9B)	9333(12)	13165(3)	7293(3)	58
H(9C)	9787(6)	12314(9)	7846(6)	58
H(12A)	5923(2)	7127(2)	1803(2)	35
H(12B)	6032(1)	10726(2)	4145(2)	33
H(13A)	6031(2)	5657(2)	2227(2)	47
H(13B)	4904(2)	10956(2)	4532(2)	38
H(14A)	7120(2)	5169(2)	3525(2)	53
H(14B)	5090(2)	11174(2)	6082(2)	40
H(15A)	8089(2)	6161(2)	4458(2)	46
H(15B)	6395(2)	11221(2)	7227(2)	39
H(16A)	7972(2)	7641(2)	4075(2)	34
H(16B)	7533(2)	11017(2)	6851(2)	34
H(30)	10390(8)	14050(7)	5764(7)	123

A.4 Crystal data and structure refinement for *rac*-(2.21)

This crystal structure determination was carried out by Miss H. Phetmung under the supervision of Prof. A. G. Orpen.

Identification code	rip191	
Empirical formula	$C_{32}H_{54}Cl_2O_6P_2Pt$	
Formula weight	862.68	
Temperature	293(2) K	
Wavelength	0.71073Å	
Crystal system	Triclinic	
Space group	P1	
Unit cell dimensions	a = 8.3776(13) Å	α = 87.53(2)°
	b = 9.9637(11) Å	β = 85.72(2)°
	c = 11.061(2) Å	γ = 84.220(10)°
Volume	915.5(2) Å^3	
Z	1	
Density (calculated)	1.565 Mgm^{-3}	
Absorption coefficient	4.104 mm^{-1}	
F(000)	436	
Crystal size	0.22 x 0.18 x 0.16 mm (yellow)	
θ range for data collection	1.85 - 25.00°	
Index ranges	-10<=h<=10, -12<=k<=12, -14<=l<=14	
Reflections collected	7976	
Independent reflections	3203 [R(int) = 0.0206]	
Refinement method	Full-matrix least-squares on F^2	
Data/restraints/parameters	3203/0/200	
Goodness-of-fit on F^2*	1.004	
Final R indices [$I > 2\sigma(I)$]*	R_1 = 0.0156, wR_2 = 0.0357 [3181 data]	
R indices (all data)*	R_1 = 0.0157, wR_2 = 0.0357 [3203 data]	
Weighting scheme	calc $w = 1/[\sigma^2(F_o^2) + (0.0183P)^2 + 0.0000P]$	
	where $P = Max(F_o^2 + 2F_c^2)/3$	
Largest diff. peak and hole	0.653 and -0.414 e.Å^{-3}	

*$wR_2 = [\Sigma w\Delta^2/\Sigma wF_o^4]^{0.5}$; $S = [\Sigma w\Delta^2/(N.O. - N.V.)]^{0.5}$; $\Delta = F_o^2 - F_c^2$;
$R_1 = \Sigma |F_o - F_c|/\Sigma |F_o|$; N.O. = data + restraints; N.V. = parameters

Table A.4.1 Atomic coordinates (x 10^4) and equivalent isotropic displacement parameters ($Å^2$ x 10^2) for *rac*-(**2.21**). U(eq) is defined as one third of the trace of the orthogonalized U_{ij} tensor.

Atom	x	y	z	U(eq)
Pt(1)	5000	5000	5000	18(1)
Cl(1)	2332(1)	5480(1)	5636(1)	28(1)
P(1)	4058(1)	4231(1)	3241(1)	17(1)
O(1)	4242(2)	1553(2)	3734(1)	24(1)
O(2)	4764(2)	869(2)	1720(1)	24(1)
O(3)	4655(2)	3134(2)	1010(1)	22(1)
C(11)	2811(3)	5566(2)	2412(2)	20(1)
C(12)	990(3)	5706(2)	2746(2)	24(1)
C(13)	130(3)	6799(2)	1957(2)	30(1)
C(14)	804(3)	8155(3)	2049(3)	38(1)
C(15)	2611(3)	8032(3)	1738(3)	35(1)
C(16)	3467(3)	6936(2)	2541(2)	26(1)
C(21)	5539(3)	3547(2)	1990(2)	20(1)
C(22)	6519(3)	2300(2)	2486(2)	22(1)
C(23)	5467(3)	1172(2)	2800(2)	24(1)
C(24)	3754(3)	1991(2)	1271(2)	23(1)
C(25)	2394(3)	2307(2)	2224(2)	20(1)
C(26)	3018(3)	2625(2)	3423(2)	19(1)
C(27)	6587(3)	4586(2)	1405(2)	26(1)
C(28)	6348(3)	-118(3)	3266(3)	36(1)
C(29)	3204(3)	1605(3)	77(2)	31(1)
C(30)	1732(3)	2599(2)	4459(2)	26(1)

Table A.4.2 Bond lengths (Å) for *rac*-(**2.21**).

Atoms	length(Å)	Atoms	length(Å)
Pt(1)-Cl(1)	2.3019(7)	C(11)-C(16)	1.538(3)
Pt(1)-Cl(1)#1	2.3019(7)	C(12)-C(13)	1.523(3)
Pt(1)-P(1)	2.3402(7)	C(13)-C(14)	1.526(4)
Pt(1)-P(1)#1	2.3402(7)	C(14)-C(15)	1.521(4)
P(1)-C(11)	1.860(2)	C(15)-C(16)	1.532(4)
P(1)-C(21)	1.891(2)	C(21)-C(27)	1.517(3)
P(1)-C(26)	1.894(2)	C(21)-C(22)	1.524(3)
O(1)-C(23)	1.437(3)	C(22)-C(23)	1.510(3)
O(1)-C(26)	1.453(3)	C(23)-C(28)	1.507(3)
O(2)-C(24)	1.427(3)	C(24)-C(29)	1.508(3)
O(2)-C(23)	1.428(3)	C(24)-C(25)	1.512(3)
O(3)-C(24)	1.436(3)	C(25)-C(26)	1.518(3)
O(3)-C(21)	1.454(3)	C(26)-C(30)	1.515(3)
C(11)-C(12)	1.537(3)		

Table A.4.3 Bond angles(°) for *rac*-(**2.21**).

Atoms	angle(°)	Atoms	angle(°)
Cl(1)-Pt(1)-Cl(1)#1	180.0	C(27)-C(21)-C(22)	112.6(2)
Cl(1)-Pt(1)-P(1)	85.92(2)	O(3)-C(21)-P(1)	108.9(2)
Cl(1)#1-Pt(1)-P(1)	94.08(2)	C(27)-C(21)-P(1)	113.8(2)
Cl(1)-Pt(1)-P(1)#1	94.08(2)	C(22)-C(21)-P(1)	108.6(2)
Cl(1)#1-Pt(1)-P(1)#1	85.92(2)	C(23)-C(22)-C(21)	110.9(2)
P(1)-Pt(1)-P(1)#1	180.0	O(2)-C(23)-O(1)	110.6(2)
C(11)-P(1)-C(21)	101.92(11)	O(2)-C(23)-C(28)	107.2(2)
C(11)-P(1)-C(26)	110.51(10)	O(1)-C(23)-C(28)	105.6(2)
C(21)-P(1)-C(26)	93.40(10)	O(2)-C(23)-C(22)	107.7(2)
C(11)-P(1)-Pt(1)	112.80(8)	O(1)-C(23)-C(22)	111.1(2)
C(21)-P(1)-Pt(1)	119.78(8)	C(28)-C(23)-C(22)	114.5(2)
C(26)-P(1)-Pt(1)	116.23(8)	O(2)-C(24)-O(3)	110.5(2)
C(23)-O(1)-C(26)	116.8(2)	O(2)-C(24)-C(29)	107.3(2)
C(24)-O(2)-C(23)	111.9(2)	O(3)-C(24)-C(29)	106.3(2)
C(24)-O(3)-C(21)	116.3(2)	O(2)-C(24)-C(25)	107.8(2)
C(12)-C(11)-C(16)	109.2(2)	O(3)-C(24)-C(25)	111.1(2)
C(12)-C(11)-P(1)	117.3(2)	C(29)-C(24)-C(25)	113.7(2)
C(16)-C(11)-P(1)	109.4(2)	C(24)-C(25)-C(26)	111.6(2)
C(13)-C(12)-C(11)	111.1(2)	O(1)-C(26)-C(30)	104.8(2)
C(12)-C(13)-C(14)	111.5(2)	O(1)-C(26)-C(25)	108.2(2)
C(15)-C(14)-C(13)	110.9(2)	C(30)-C(26)-C(25)	112.1(2)
C(14)-C(15)-C(16)	110.9(2)	O(1)-C(26)-P(1)	106.3(2)
C(15)-C(16)-C(11)	111.0(2)	C(30)-C(26)-P(1)	115.1(2)
O(3)-C(21)-C(27)	104.7(2)	C(25)-C(26)-P(1)	109.8(2)
O(3)-C(21)-C(22)	107.9(2)		

Symmetry transformations used to generate equivalent atoms: #1 -x+1,-y+1,-z+1

Table A.4.4 Anisotropic displacement parameters ($Å^2$ x 10^3) for *rac*-(**2.21**). The anisotropic displacement factor exponent takes the form:

$-2\Pi^2[h^2a^{*2}U_{11} + ... + 2hka^*b^*U_{12}]$

Atom	U_{11}	U_{22}	U_{33}	U_{23}	U_{13}	U_{12}
Pt(1)	14(1)	23(1)	16(1)	-5(1)	-1(1)	0(1)
Cl(1)	15(1)	44(1)	25(1)	-13(1)	0(1)	0(1)
P(1)	16(1)	18(1)	16(1)	-2(1)	-1(1)	-1(1)
O(1)	26(1)	23(1)	22(1)	3(1)	-1(1)	3(1)
O(2)	31(1)	19(1)	24(1)	-4(1)	-6(1)	2(1)
O(3)	27(1)	22(1)	18(1)	-3(1)	-3(1)	-3(1)
C(11)	20(1)	18(1)	21(1)	0(1)	-4(1)	0(1)
C(12)	20(1)	23(1)	28(1)	1(1)	-3(1)	0(1)
C(13)	23(1)	31(1)	36(2)	4(1)	-7(1)	2(1)
C(14)	34(2)	26(1)	52(2)	6(1)	-9(1)	4(1)
C(15)	35(2)	22(1)	49(2)	4(1)	-7(1)	-4(1)
C(16)	24(1)	21(1)	34(2)	-2(1)	-3(1)	-3(1)
C(21)	20(1)	24(1)	17(1)	-4(1)	-2(1)	-1(1)
C(22)	20(1)	26(1)	18(1)	-6(1)	-2(1)	4(1)

Atom	U_{11}	U_{22}	U_{33}	U_{23}	U_{13}	U_{12}
C(23)	27(1)	25(1)	20(1)	-3(1)	-3(1)	5(1)
C(24)	26(1)	18(1)	23(1)	-1(1)	-6(1)	-1(1)
C(25)	22(1)	14(1)	25(1)	1(1)	-3(1)	-4(1)
C(26)	19(1)	17(1)	22(1)	0(1)	-2(1)	0(1)
C(27)	25(1)	29(1)	24(1)	-4(1)	2(1)	-4(1)
C(28)	42(2)	28(1)	35(2)	-2(1)	-8(1)	10(1)
C(29)	40(2)	25(1)	28(1)	-7(1)	-10(1)	-4(1)
C(30)	26(1)	26(1)	26(1)	2(1)	2(1)	-2(1)

Table A.4.5 Hydrogen coordinates (x 10^4) and isotropic displacement parameters ($Å^2$ x 10^3) for *rac*-(**2.21**)

Atom	x	y	z	U(eq)
H(11A)	2961(3)	5360(2)	1551(2)	24
H(12A)	566(3)	4851(2)	2641(2)	28
H(12B)	788(3)	5929(2)	3592(2)	28
H(13A)	-1009(3)	6891(2)	2209(2)	36
H(13B)	249(3)	6533(2)	1119(2)	36
H(14A)	282(3)	8813(3)	1496(3)	45
H(14B)	575(3)	8472(3)	2866(3)	45
H(15A)	3022(3)	8890(3)	1852(3)	42
H(15B)	2833(3)	7811(3)	893(3)	42
H(16A)	3312(3)	7191(2)	3381(2)	31
H(16B)	4612(3)	6858(2)	2311(2)	31
H(22A)	7369(3)	2002(2)	1886(2)	26
H(22B)	7015(3)	2527(2)	3206(2)	26
H(25A)	1765(3)	1540(2)	2344(2)	24
H(25B)	1694(3)	3074(2)	1942(2)	24
H(27A)	7354(13)	4161(4)	817(11)	39
H(27B)	7145(15)	4963(12)	2016(3)	39
H(27C)	5925(4)	5291(9)	1012(12)	39
H(28A)	5606(5)	-789(6)	3423(16)	53
H(28B)	6823(19)	46(5)	4002(9)	53
H(28C)	7176(15)	-434(10)	2669(7)	53
H(29A)	4125(3)	1372(17)	-470(6)	46
H(29B)	2553(17)	2353(6)	-265(8)	46
H(29C)	2585(18)	845(11)	207(3)	46
H(30A)	1285(14)	1747(7)	4494(9)	39
H(30B)	897(10)	3314(10)	4331(8)	39
H(30C)	2198(5)	2721(16)	5209(3)	39

A.5 Crystal data and structure refinement for *rac*-(2.22)

This crystal structure determination was carried out by Miss H. Phetmung under the supervision of Prof. A. G. Orpen.

Identification code	rip190s	
Empirical formula	$C_{32}\ H_{54}\ Cl_2\ O_6\ P_2\ Pd$	
Formula weight	773.99	
Temperature	293(2) K	
Wavelength	0.71073 Å	
Crystal system	triclinic	
Space group	$P\bar{1}$	
Unit cell dimensions	a = 8.3750(6) Å	α = 87.1300(10)°
	b = 9.9901(7) Å	β = 85.5810(10)°
	c = 11.0436(8) Å	γ = 84.1210(10)°
Volume	915.56(11) $Å^3$	
Z	1	
Density (calculated)	1.404 Mg/m^3	
Absorption coefficient	0.779 mm^{-1}	
F(000)	404	
Crystal size	0.24 x 0.20 x 0.18 mm (yellow)	
θ range for data collection	1.85 - 25.00°	
Index ranges	-10<=h<=10, -12<=k<=12, -14<=l<=14	
Reflections collected	7939	
Independent reflections	3201 [R(int) = 0.0205]	
Refinement method	Full-matrix least-squares on F^2	
Data/restraints/parameters	3201/0/200	
Goodness-of-fit on F^2*	1.029	
Final R indices [$I > 2\sigma(I)$]*	R_1 = 0.0195, wR_2 = 0.0504[2864 data]	
R indices (all data)*	R_1 = 0.0220, wR_2 = 0.0507[3201 data]	
Weighting scheme	calc $w = 1/[[\sigma^2(F_o^2) + (0.0275P)^2 + 0.0000P]$	
	where $P= (Max\ F_o^2, 0 + 2F_c^2)/3$	
Largest diff. peak and hole	0.275 and -0.327 $e.Å^{-3}$	

*$wR_2 = [\Sigma w\Delta^2/\Sigma wF_o^4]^{0.5}$; $S = [\Sigma w\Delta^2/(N.O. - N.V.)]^{0.5}$; $\Delta = F_o^2 - F_c^2$;
$R_1 = \Sigma\ |F_o - F_c|/\Sigma\ |F_o|$; N.O. = data + restraints; N.V. = parameters

Table A.5.1 Atomic coordinates (x 10^4) and equivalent isotropic displacement parameters ($Å^2$ x 10^2) for *rac*-(**2.22**). U(eq) is defined as one third of the trace of the orthogonalized U_{ij} tensor.

Atom	x	y	z	U(eq)
Pd(1)	5000	5000	5000	17(1)
Cl(1)	7661(1)	4541(1)	4358(1)	25(1)
P(1)	5949(1)	5783(1)	6771(1)	16(1)
O(1)	5775(2)	8453(1)	6266(1)	21(1)
O(2)	5240(2)	9134(1)	8280(1)	23(1)
O(3)	5346(2)	6873(1)	9002(1)	20(1)
C(11)	7190(2)	4440(2)	7598(2)	18(1)
C(12)	6521(2)	3077(2)	7462(2)	24(1)
C(13)	7380(2)	1969(2)	8250(2)	31(1)
C(14)	9198(3)	1842(2)	7940(2)	35(1)
C(15)	9869(2)	3188(2)	8037(2)	28(1)
C(16)	9012(2)	4297(2)	7258(2)	22(1)
C(21)	6992(2)	7379(2)	6584(2)	19(1)
C(22)	4542(2)	8833(2)	7196(2)	23(1)
C(23)	6239(2)	8015(2)	8737(2)	21(1)
C(24)	4457(2)	6469(2)	8021(2)	19(1)
C(25)	3481(2)	7710(2)	7513(2)	21(1)
C(26)	7616(2)	7691(2)	7790(2)	20(1)
C(27)	8282(2)	7409(2)	5544(2)	25(1)
C(28)	3663(3)	10119(2)	6720(2)	31(1)
C(29)	6783(3)	8393(2)	9935(2)	28(1)
C(30)	3416(2)	5429(2)	8611(2)	23(1)

Table A.5.2 Bond lengths (Å) for *rac*-(**2.22**)

Atoms	length(Å)	Atoms	length(Å)
Pd(1)-Cl(1)#1	2.2934(5)	C(11)-C(12)	1.543(2)
Pd(1)-Cl(1)	2.2934(5)	C(12)-C(13)	1.529(3)
Pd(1)-P(1)	2.3641(4)	C(13)-C(14)	1.528(3)
Pd(1)-P(1)#1	2.3641(4)	C(14)-C(15)	1.521(3)
P(1)-C(11)	1.858(2)	C(15)-C(16)	1.523(3)
P(1)-C(21)	1.890(2)	C(21)-C(27)	1.517(2)
P(1)-C(24)	1.894(2)	C(21)-C(26)	1.526(2)
O(1)-C(22)	1.435(2)	C(22)-C(28)	1.506(3)
O(1)-C(21)	1.452(2)	C(22)-C(25)	1.513(3)
O(2)-C(23)	1.421(2)	C(23)-C(29)	1.510(2)
O(2)-C(22)	1.430(2)	C(23)-C(26)	1.517(3)
O(3)-C(23)	1.433(2)	C(24)-C(30)	1.514(3)
O(3)-C(24)	1.457(2)	C(24)-C(25)	1.521(2)
C(11)-C(16)	1.537(2)		

Table A.5.3 Bond angles (°) for *rac*-(**2.22**)

Atoms	angle(°)	Atoms	angle(°)
Cl(1)#1-Pd(1)-Cl(1)	179.999(2)	C(27)-C(21)-C(26)	112.1(2)
Cl(1)#1-Pd(1)-P(1)	94.11(2)	O(1)-C(21)-P(1)	106.45(11)
Cl(1)-Pd(1)-P(1)	85.89(2)	C(27)-C(21)-P(1)	115.20(13)
Cl(1)#1-Pd(1)-P(1)#1	85.89(2)	C(26)-C(21)-P(1)	109.78(12)
Cl(1)-Pd(1)-P(1)#1	94.11(2)	O(2)-C(22)-O(1)	110.5(2)
P(1)-Pd(1)-P(1)#1	179.999(1)	O(2)-C(22)-C(28)	107.3(2)
C(11)-P(1)-C(21)	110.66(8)	O(1)-C(22)-C(28)	105.7(2)
C(11)-P(1)-C(24)	102.30(8)	O(2)-C(22)-C(25)	107.7(2)
C(21)-P(1)-C(24)	93.38(8)	O(1)-C(22)-C(25)	111.24(14)
C(11)-P(1)-Pd(1)	112.12(6)	C(28)-C(22)-C(25)	114.2(2)
C(21)-P(1)-Pd(1)	116.66(6)	O(2)-C(23)-O(3)	111.01(14)
C(24)-P(1)-Pd(1)	119.65(6)	O(2)-C(23)-C(29)	107.48(14)
C(22)-O(1)-C(21)	116.88(13)	O(3)-C(23)-C(29)	106.15(14)
C(23)-O(2)-C(22)	111.85(13)	O(2)-C(23)-C(26)	108.03(14)
C(23)-O(3)-C(24)	116.11(13)	O(3)-C(23)-C(26)	110.72(14)
C(16)-C(11)-C(12)	109.27(14)	C(29)-C(23)-C(26)	113.4(2)
C(16)-C(11)-P(1)	117.17(12)	O(3)-C(24)-C(30)	104.60(14)
C(12)-C(11)-P(1)	109.06(12)	O(3)-C(24)-C(25)	108.39(14)
C(13)-C(12)-C(11)	110.9(2)	C(30)-C(24)-C(25)	112.9(2)
C(14)-C(13)-C(12)	111.4(2)	O(3)-C(24)-P(1)	108.68(11)
C(15)-C(14)-C(13)	110.8(2)	C(30)-C(24)-P(1)	113.52(12)
C(14)-C(15)-C(16)	111.9(2)	C(25)-C(24)-P(1)	108.48(12)
C(15)-C(16)-C(11)	111.1(2)	C(22)-C(25)-C(24)	110.6(2)
O(1)-C(21)-C(27)	104.53(14)	C(23)-C(26)-C(21)	111.1(2)
O(1)-C(21)-C(26)	108.27(14)		

Symmetry transformations used to generate equivalent atoms: #1 -x+1,-y+1,-z+1

Table A.5.4 Anisotropic displacement parameters ($Å^2$ x 10^3) for *rac*-(**2.22**). The anisotropic displacement factor exponent takes the form:

$-2\Pi^2[h^2a^{*2}U_{11} + ... + 2hka^*b^*U_{12}]$

Atom	U_{11}	U_{22}	U_{33}	U_{23}	U_{13}	U_{12}
Pd(1)	14(1)	23(1)	14(1)	-3(1)	-1(1)	-1(1)
Cl(1)	15(1)	40(1)	21(1)	-9(1)	0(1)	-1(1)
P(1)	15(1)	18(1)	14(1)	-1(1)	-1(1)	-1(1)
O(1)	24(1)	20(1)	18(1)	4(1)	-1(1)	3(1)
O(2)	29(1)	18(1)	21(1)	-4(1)	-5(1)	1(1)
O(3)	26(1)	20(1)	14(1)	-2(1)	-4(1)	-3(1)
C(11)	19(1)	18(1)	17(1)	0(1)	-2(1)	-1(1)
C(12)	21(1)	21(1)	30(1)	-2(1)	-2(1)	-3(1)
C(13)	33(1)	19(1)	40(1)	5(1)	-4(1)	-3(1)
C(14)	33(1)	25(1)	44(1)	4(1)	-4(1)	4(1)
C(15)	21(1)	30(1)	31(1)	2(1)	-5(1)	2(1)
C(16)	21(1)	22(1)	22(1)	0(1)	-3(1)	0(1)
C(21)	18(1)	17(1)	22(1)	2(1)	-2(1)	0(1)
C(22)	26(1)	23(1)	19(1)	-2(1)	-2(1)	4(1)

Atom	U_{11}	U_{22}	U_{33}	U_{23}	U_{13}	U_{12}
C(23)	25(1)	17(1)	20(1)	-1(1)	-5(1)	-2(1)
C(24)	20(1)	22(1)	14(1)	-3(1)	-1(1)	-3(1)
C(25)	20(1)	25(1)	17(1)	-5(1)	-1(1)	2(1)
C(26)	21(1)	16(1)	23(1)	1(1)	-5(1)	-2(1)
C(27)	24(1)	24(1)	26(1)	2(1)	1(1)	-2(1)
C(28)	36(1)	25(1)	31(1)	1(1)	-5(1)	7(1)
C(29)	35(1)	27(1)	23(1)	-6(1)	-9(1)	-4(1)
C(30)	23(1)	26(1)	19(1)	-2(1)	1(1)	-4(1)

Table A.5.5 Hydrogen coordinates (x 10^4) and isotropic displacement parameters (Å^2 x 10^3) for *rac*-(**2.22**)

Atom	x	y	z	U(eq)
H(11A)	7041(2)	4636(2)	8463(2)	21
H(12A)	5377(2)	3156(2)	7701(2)	28
H(12B)	6665(2)	2838(2)	6617(2)	28
H(13A)	7158(2)	2171(2)	9100(2)	37
H(13B)	6968(2)	1117(2)	8127(2)	37
H(14A)	9716(3)	1179(2)	8493(2)	41
H(14B)	9431(3)	1534(2)	7120(2)	41
H(15A)	11008(2)	3097(2)	7781(2)	33
H(15B)	9754(2)	3439(2)	8878(2)	33
H(16A)	9209(2)	4090(2)	6407(2)	26
H(16B)	9441(2)	5144(2)	7370(2)	26
H(25A)	2992(2)	7484(2)	6792(2)	25
H(25B)	2626(2)	8010(2)	8110(2)	25
H(26A)	8307(2)	6921(2)	8080(2)	24
H(26B)	8253(2)	8451(2)	7669(2)	24
H(27A)	8707(11)	8268(5)	5492(7)	38
H(27B)	7824(4)	7265(13)	4796(2)	38
H(27C)	9132(7)	6711(8)	5685(6)	38
H(28A)	4404(4)	10791(4)	6565(12)	47
H(28B)	2825(11)	10431(7)	7312(5)	47
H(28C)	3199(14)	9956(4)	5979(7)	47
H(29A)	5859(3)	8631(13)	10479(5)	42
H(29B)	7409(14)	9147(9)	9804(2)	42
H(29C)	7426(14)	7642(5)	10283(6)	42
H(30A)	2633(10)	5853(3)	9188(8)	34
H(30B)	4079(3)	4735(7)	9020(9)	34
H(30C)	2876(11)	5041(9)	7999(2)	34

A.6 Crystal data and structure refinement for secondary phospha-adamantane β-(3.26)

This crystal structure determination was carried out by Miss H. Phetmung under the supervision of Prof. A. G. Orpen.

Identification code	rip126s	
Empirical formula	$C_{10}H_{17}O_3P$	
Formula weight	216.21	
Temperature	173(2) K	
Wavelength	0.71073 Å	
Crystal system	Monoclinic	
Space group	$P2_1/c$	
Unit cell dimensions	a = 8.176(2) Å	α = 90.00°
	b = 8.0969(13) Å	β = 94.144(13)°
	c = 16.669(3) Å	γ = 90 00°
Volume	1100.7(4) $Å^3$	
Z	4	
Density (calculated)	1.305 Mgm^{-3}	
Absorption coefficient	0.230 mm^{-1}	
F(000)	464	
Crystal size	0.28 x 0.24 x 0.20 mm	
θ range for data collection	2.45 - 23.99°	
Index ranges	-10<=h<=7, -9<=k<=10, -15<=l<=21	
Reflections collected	5082	
Independent reflections	1723 [R(int) = 0.0255]	
Refinement method	Full-matrix least-squares on F^2	
Data/restraints/parameters	1723/0/135	
Goodness-of-fit on F^2	1.027	
Final R indices [$I>2\sigma(I)$]*	$R_1 = 0.0331$, $wR_2 = 0.0858$	
R indices (all data)*	$R_1 = 0.0456$, $wR_2 = 0.0908$	
Weighting scheme	calc $w = 1/[\sigma^2(F_o^2) + (0.0547P)^2 + 0.0340P]$	
	where $P = (\text{Max } F_o^2 + 2F_c^2)/3$	
Largest diff. peak and hole	0.366 and -0.237 $e.Å^{-3}$	

*$wR_2 = [\Sigma w\Delta^2/\Sigma wF_o^4]^{0.5}$; $S = [\Sigma w\Delta^2/(N.O. - N.V.)]^{0.5}$; $\Delta = F_o^2 - F_c^2$;
$R_1 = \Sigma |F_o - F_c|/\Sigma |F_o|$; N.O. = data + restraints; N.V. = parameters

Table A.6.1 Atomic coordinates (x 10^4) and equivalent isotropic displacement parameters ($Å^2$ x 10^2) for β-(**3.26**). U(eq) is defined as one third of the trace of the orthogonalized U_{ij} tensor.

Atom	x	y	z	U(eq)
P(1)	2923(1)	1721(1)	1987(1)	31(1)
O(1)	1897(2)	4834(2)	1591(1)	24(1)
O(2)	3446(2)	1943(2)	384(1)	24(1)
O(3)	2492(2)	4674(2)	236(1)	23(1)
C(1)	1256(2)	3161(2)	1601(1)	24(1)
C(2)	685(2)	2679(2)	742(1)	24(1)
C(3)	2048(2)	2960(2)	184(1)	24(1)
C(4)	1537(3)	2615(3)	-689(1)	31(1)
C(5)	5799(2)	1188(3)	1210(1)	33(1)
C(6)	4281(2)	2259(2)	1174(1)	25(1)
C(7)	4659(2)	4103(2)	1230(1)	25(1)
C(8)	3122(2)	5116(2)	1031(1)	23(1)
C(9)	3428(3)	6946(2)	1031(1)	32(1)
C(10)	-129(3)	3217(3)	2155(1)	32(1)

Table A.6.2 Bond lengths (Å) for β-(**3.26**)

Atoms	length(Å)	Atoms	length(Å)
P(1)-C(6)	1.865(2)	C(3)-C(4)	1.512(3)
P(1)-C(1)	1.872(2)	C(4)-H(4A)	0.98
P(1)-H(1)	1.30(4)	C(4)-H(4B)	0.98
O(1)-C(8)	1.435(2)	C(4)-H(4C)	0.98
O(1)-C(1)	1.453(2)	C(5)-C(6)	1.512(3)
O(2)-C(3)	1.428(2)	C(5)-H(5A)	0.98
O(2)-C(6)	1.462(2)	C(5)-H(5B)	0.98
O(3)-C(8)	1.433(2)	C(5)-H(5C)	0.98
O(3)-C(3)	1.435(2)	C(6)-C(7)	1.527(3)
C(1)-C(10)	1.513(3)	C(7)-C(8)	1.518(3)
C(1)-C(2)	1.525(3)	C(7)-H(7A)	0.99
C(2)-C(3)	1.519(3)	C(7)-H(7B)	0.99
C(2)-H(2A)	0.99	C(8)-C(9)	1.502(3)
C(2)-H(2B)	0.99	C(9)-H(9A)	0.98
C(9)-H(9B)	0.98	C(10)-H(10B)	0.98
C(9)-H(9C)	0.98	C(10)-H(10C)	0.98
C(10)-H(10A)	0.98		

Table A.6.3 Bond angles(°) for β-(**3.26**)

Atoms	Angle(°)	Atoms	Angle(°)
C(6)-P(1)-C(1)	93.54(9)	C(6)-C(5)-H(5C)	109.47(11)
C(6)-P(1)-H(1)	95(2)	H(5A)-C(5)-H(5C)	109.5
C(1)-P(1)-H(1)	102(2)	H(5B)-C(5)-H(5C)	109.5
C(8)-O(1)-C(1)	115.19(13)	O(2)-C(6)-C(5)	105.4(2)
C(3)-O(2)-C(6)	115.01(14)	O(2)-C(6)-C(7)	107.80(14)
C(8)-O(3)-C(3)	111.66(13)	C(5)-C(6)-C(7)	113.4(2)
O(1)-C(1)-C(10)	105.5(2)	O(2)-C(6)-P(1)	110.49(13)
O(1)-C(1)-C(2)	108.31(14)	C(5)-C(6)-P(1)	111.53(14)
C(10)-C(1)-C(2)	112.9(2)	C(7)-C(6)-P(1)	108.21(14)
O(1)-C(1)-P(1)	109.28(12)	C(8)-C(7)-C(6)	110.8(2)
C(10)-C(1)-P(1)	111.52(13)	C(8)-C(7)-H(7A)	109.49(10)
C(2)-C(1)-P(1)	109.18(13)	C(6)-C(7)-H(7A)	109.49(10)
C(3)-C(2)-C(1)	110.4(2)	C(8)-C(7)-H(7B)	109.49(10)
C(3)-C(2)-H(2A)	109.58(10)	C(6)-C(7)-H(7B)	109.49(11)
C(1)-C(2)-H(2A)	109.58(10)	H(7A)-C(7)-H(7B)	108.1
C(3)-C(2)-H(2B)	109.58(10)	O(3)-C(8)-O(1)	109.93(14)
C(1)-C(2)-H(2B)	109.58(10)	O(3)-C(8)-C(9)	107.2(2)
H(2A)-C(2)-H(2B)	108.1	O(1)-C(8)-C(9)	106.4(2)
O(2)-C(3)-O(3)	110.44(14)	O(3)-C(8)-C(7)	107.6(2)
O(2)-C(3)-C(4)	106.2(2)	O(1)-C(8)-C(7)	112.2(2)
O(3)-C(3)-C(4)	106.7(2)	C(9)-C(8)-C(7)	113.4(2)
O(2)-C(3)-C(2)	112.4(2)	C(8)-C(9)-H(9A)	109.47(10)
O(3)-C(3)-C(2)	107.6(2)	C(8)-C(9)-H(9B)	109.47(11)
C(4)-C(3)-C(2)	113.4(2)	H(9A)-C(9)-H(9B)	109.5
C(3)-C(4)-H(4A)	109.47(11)	C(8)-C(9)-H(9C)	109.47(11)
C(3)-C(4)-H(4B)	109.47(11)	C(1)-C(10)-H(10C)	109.47(11)
H(4A)-C(4)-H(4B)	109.5	H(9A)-C(9)-H(9C)	109.5
C(3)-C(4)-H(4C)	109.47(11)	H(9B)-C(9)-H(9C)	109.5
H(4A)-C(4)-H(4C)	109.5	C(1)-C(10)-H(10A)	109.47(11)
H(4B)-C(4)-H(4C)	109.5	C(1)-C(10)-H(10B)	109.47(11)
C(6)-C(5)-H(5A)	109.47(11)	H(10A)-C(10)-H(10B)	109.5
C(6)-C(5)-H(5B)	109.47(11)	H(10A)-C(10)-H(10C)	109.5
H(5A)-C(5)-H(5B)	109.5	H(10B)-C(10)-H(10C)	109.5

Table A.6.4 Anisotropic displacement parameters ($Å^2$ x 10^3) for β-(**3.26**). The anisotropic displacement factor exponent takes the form: $-2\Pi^2[h^2a^{*2}U_{11} + ... + 2hka^*b^*U_{12}]$

Atom	U_{11}	U_{22}	U_{33}	U_{23}	U_{13}	U_{12}
P(1)	29(1)	33(1)	32(1)	11(1)	5(1)	5(1)
O(1)	26(1)	22(1)	25(1)	-3(1)	5(1)	-2(1)
O(2)	24(1)	25(1)	24(1)	-4(1)	-1(1)	1(1)
O(3)	25(1)	22(1)	23(1)	2(1)	0(1)	-4(1)
C(1)	23(1)	21(1)	27(1)	2(1)	4(1)	-2(1)
C(2)	22(1)	21(1)	29(1)	1(1)	1(1)	-1(1)
C(3)	22(1)	21(1)	26(1)	-2(1)	-1(1)	-1(1)
C(4)	32(1)	33(1)	28(1)	-3(1)	-1(1)	-1(1)
C(5)	26(1)	33(1)	40(1)	2(1)	2(1)	4(1)
C(6)	23(1)	25(1)	26(1)	1(1)	-2(1)	0(1)
C(7)	25(1)	26(1)	25(1)	-1(1)	2(1)	-4(1)
C(8)	25(1)	24(1)	21(1)	-1(1)	3(1)	-4(1)
C(9)	34(1)	24(1)	37(1)	-1(1)	1(1)	-4(1)
C(10)	31(1)	35(1)	32(1)	3(1)	10(1)	1(1)

Table A.6.5 Hydrogen coordinates (x 10^4) and isotropic displacement parameters ($Å^2$ x 10^3) for β-(**3.26**)

Atom	x	y	z	U(eq)
H(2A)	362(2)	1500(2)	726(1)	29
H(2B)	-285(2)	3346(2)	558(1)	29
H(4A)	1213(16)	1455(5)	-752(2)	47
H(4B)	2458(6)	2843(16)	-1018(2)	47
H(4C)	608(11)	3325(12)	-865(2)	47
H(5A)	5486(3)	42(4)	1090(8)	49
H(5B)	6355(9)	1249(13)	1751(3)	49
H(5C)	6541(7)	1580(10)	815(5)	49
H(7A)	5116(2)	4373(2)	1780(1)	30
H(7B)	5494(2)	4387(2)	850(1)	30
H(9A)	3849(15)	7297(4)	1570(2)	48
H(9B)	2400(4)	7527(3)	881(8)	48
H(9C)	4235(12)	7207(3)	643(6)	48
H(10A)	279(5)	3661(15)	2679(3)	49
H(10B)	-554(10)	2099(3)	2226(6)	49
H(10C)	-1008(7)	3927(13)	1921(4)	49
H(1)	2434(49)	332(53)	1667(22)	153(15)

A.7 Crystal data and structure refinement for phospha-adamantane phosphonium salt (3.27)

This crystal structure determination was carried out by Miss H. Phetmung under the supervision of Prof. A. G. Orpen.

Identification code	rip87s	
Empirical formula	$C_{42}H_{44}BO_3P$	
Formula weight	638.55	
Temperature	173(2) K	
Wavelength	0.71073 Å	
Crystal system	Orthorhombic	
Space group	Pbca	
Unit cell dimensions	a = 18.749(2) Å	α = 90.00°
	b = 18.588(2) Å	β = 90.00°
	c = 19.887(3) Å	γ = 90.00°
Volume	6930.7(14) $Å^{-3}$	
Z	8	
Density (calculated)	1.224 mgm^{-3}	
Absorption coefficient	0.118 mm^{-1}	
F(000)	2720	
Crystal size	0.50 x 0.30 x 0.20 mm	
q range for data collection	1.85 - 27.48°	
Index ranges	-24<=h<=18, -14<=k<=24, -25<=l<=19	
Reflections collected	23784	
Independent reflections	7827 [$R_{(int)}$ = 0.0608]	
Refinement method	Full-matrix least-squares on F^2	
Data/restraints/parameters	7827/0/428	
Goodness-of-fit on F^2 (S)*	1.029	
Final R indices [$I > 2\sigma(I)$]*	R_1 = 0.0499, wR_2 = 0.0949[4695 data]	
R indices (all data)*	R_1 = 0.1101, wR_2 = 0.1202[7827 data]	
Weighting scheme	calc $w = 1/[\sigma^2(F_o^2)+(0.0483P)^2+0.582P]$	
	where $P= Max(F_o^2,0 + 2F_c^2)/3$	
Largest diff. peak and hole	0.402 and -0.358 $e.Å^{-3}$	

*$wR_2 = [\Sigma w\Delta^2/\Sigma wF_o^4]^{0.5}$; $S = [\Sigma w\Delta^2/(N.O. - N.V.)]^{0.5}$; $\Delta = F_o^2 - F_c^2$;
$R_1 = \Sigma |F_o - F_c|/\Sigma |F_o|$; N.O. = data + restraints; N.V. = parameters

Table A.7.1 Atomic coordinates (x 10^4) and equivalent isotropic displacement parameters ($Å^2$ x 10^2) for salt (**3.27**). U(eq) is defined as one third of the trace of the orthogonalized U_{ij} tensor

Atom	x	y	z	U(eq)
P(1)	1877(1)	4165(1)	1397(1)	22(1)
O(1)	2498(1)	3569(1)	342(1)	33(1)
O(2)	971(1)	4531(1)	451(1)	32(1)
O(3)	1625(1)	3974(1)	-420(1)	36(1)
B(1)	803(1)	1165(1)	2155(1)	25(1)
C(1)	1077(1)	3934(1)	904(1)	26(1)
C(2)	1253(1)	3254(1)	507(1)	29(1)
C(3)	1515(1)	4625(1)	-59(1)	33(1)
C(4)	1221(2)	5175(1)	-545(1)	53(1)
C(5)	3273(1)	4369(2)	915(1)	45(1)
C(6)	2514(1)	4244(1)	698(1)	29(1)
C(7)	2219(1)	4842(1)	252(1)	32(1)
C(8)	1839(1)	3398(1)	4(1)	32(1)
C(9)	1999(1)	2764(1)	-439(1)	45(1)
C(10)	415(1)	3863(1)	1335(1)	37(1)
C(11)	1779(1)	4971(1)	1896(1)	25(1)
C(12)	1501(1)	5096(1)	3152(1)	28(1)
C(13)	1444(1)	4781(1)	3778(1)	33(1)
C(14)	1583(1)	4056(1)	3863(1)	35(1)
C(15)	1784(1)	3633(1)	3319(1)	30(1)
C(16)	2068(1)	3535(1)	2061(1)	28(1)
C(17)	1699(1)	4678(1)	2604(1)	22(1)
C(18)	1841(1)	3947(1)	2688(1)	23(1)
C(21)	302(1)	1399(1)	1510(1)	27(1)
C(22)	-252(1)	1900(1)	1555(1)	33(1)
C(23)	-694(1)	2073(1)	1014(1)	43(1)
C(24)	-601(1)	1745(1)	400(1)	45(1)
C(25)	-57(1)	1249(2)	326(1)	44(1)
C(26)	381(1)	1086(1)	868(1)	37(1)
C(31)	850(1)	282(1)	2210(1)	24(1)
C(32)	329(1)	-171(1)	1934(1)	30(1)
C(33)	309(1)	-908(1)	2040(1)	38(1)
C(34)	823(1)	-1232(1)	2435(1)	36(1)
C(35)	1345(1)	-808(1)	2725(1)	31(1)
C(36)	1358(1)	-71(1)	2610(1)	26(1)
C(41)	432(1)	1441(1)	2864(1)	23(1)
C(42)	36(1)	978(1)	3275(1)	30(1)
C(43)	-272(1)	1189(1)	3878(1)	35(1)
C(44)	-202(1)	1888(1)	4099(1)	33(1)
C(45)	176(1)	2367(1)	3706(1)	35(1)
C(46)	480(1)	2148(1)	3106(1)	31(1)
C(51)	1622(1)	1484(1)	2080(1)	24(1)
C(52)	2060(1)	1603(1)	2644(1)	28(1)
C(53)	2771(1)	1817(1)	2596(1)	33(1)
C(54)	3079(1)	1922(1)	1971(1)	36(1)
C(55)	2669(1)	1819(1)	1404(1)	35(1)
C(56)	1958(1)	1609(1)	1459(1)	28(1)

Table A.7.2 Bond lengths (Å) for salt (**3.27**)

Atom	length (Å)	Atom	length (Å)
P(1)-C(16)	1.802(2)	C(15)-C(18)	1.388(3)
P(1)-C(11)	1.806(2)	C(16)-C(18)	1.524(3)
P(1)-C(6)	1.839(2)	C(17)-C(18)	1.395(3)
P(1)-C(1)	1.842(2)	C(21)-C(22)	1.398(3)
O(1)-C(6)	1.441(3)	C(21)-C(26)	1.410(3)
O(1)-C(8)	1.443(3)	C(22)-C(23)	1.395(3)
O(2)-C(1)	1.443(2)	C(23)-C(24)	1.376(4)
O(2)-C(3)	1.450(3)	C(24)-C(25)	1.382(4)
O(3)-C(8)	1.420(3)	C(25)-C(26)	1.390(3)
O(3)-C(3)	1.422(3)	C(31)-C(32)	1.402(3)
B(1)-C(31)	1.648(3)	C(31)-C(36)	1.403(3)
B(1)-C(21)	1.649(3)	C(32)-C(33)	1.385(3)
B(1)-C(51)	1.653(3)	C(33)-C(34)	1.383(3)
B(1)-C(41)	1.655(3)	C(34)-C(35)	1.384(3)
C(1)-C(10)	1.514(3)	C(35)-C(36)	1.390(3)
C(1)-C(2)	1.527(3)	C(41)-C(42)	1.400(3)
C(2)-C(8)	1.510(3)	C(41)-C(46)	1.401(3)
C(3)-C(4)	1.510(3)	C(42)-C(43)	1.388(3)
C(3)-C(7)	1.512(3)	C(43)-C(44)	1.377(3)
C(5)-C(6)	1.504(3)	C(44)-C(45)	1.381(3)
C(6)-C(7)	1.526(3)	C(45)-C(46)	1.384(3)
C(8)-C(9)	1.502(3)	C(51)-C(56)	1.405(3)
C(11)-C(17)	1.517(3)	C(51)-C(52)	1.408(3)
C(12)-C(13)	1.381(3)	C(52)-C(53)	1.394(3)
C(12)-C(17)	1.388(3)	C(53)-C(54)	1.384(3)
C(13)-C(14)	1.383(3)	C(54)-C(55)	1.377(3)
C(14)-C(15)	1.389(3)	C(55)-C(56)	1.394(3)

Table A.7.3 Bond angles (°) for salt (**3.27**)

Atoms	angle (°)	Atoms	angle (°)
C(16)-P(1)-C(11)	99.04(9)	C(12)-C(13)-C(14)	120.5(2)
C(16)-P(1)-C(6)	118.51(10)	C(13)-C(14)-C(15)	120.6(2)
C(11)-P(1)-C(6)	114.56(10)	C(18)-C(15)-C(14)	119.1(2)
C(16)-P(1)-C(1)	113.56(10)	C(18)-C(16)-P(1)	102.52(14)
C(11)-P(1)-C(1)	113.75(10)	C(12)-C(17)-C(18)	120.1(2)
C(6)-P(1)-C(1)	98.31(10)	C(12)-C(17)-C(11)	123.6(2)
C(6)-O(1)-C(8)	116.0(2)	C(18)-C(17)-C(11)	116.3(2)
C(1)-O(2)-C(3)	115.7(2)	C(15)-C(18)-C(17)	120.3(2)
C(8)-O(3)-C(3)	112.6(2)	C(15)-C(18)-C(16)	123.3(2)
C(31)-B(1)-C(21)	110.2(2)	C(17)-C(18)-C(16)	116.5(2)
C(31)-B(1)-C(51)	108.3(2)	C(22)-C(21)-C(26)	114.3(2)
C(21)-B(1)-C(51)	111.5(2)	C(22)-C(21)-B(1)	123.3(2)
C(31)-B(1)-C(41)	105.9(2)	C(26)-C(21)-B(1)	122.4(2)
C(21)-B(1)-C(41)	110.0(2)	C(23)-C(22)-C(21)	123.0(2)
C(51)-B(1)-C(41)	110.9(2)	C(24)-C(23)-C(22)	120.4(2)
O(2)-C(1)-C(10)	107.9(2)	C(23)-C(24)-C(25)	119.0(2)
O(2)-C(1)-C(2)	110.1(2)	C(24)-C(25)-C(26)	119.9(3)

Atoms	Angle (°)	Atoms	Angle (°)
C(10)-C(1)-C(2)	113.4(2)	C(25)-C(26)-C(21)	123.4(2)
O(2)-C(1)-P(1)	105.42(13)	C(32)-C(31)-C(36)	114.5(2)
C(10)-C(1)-P(1)	112.8(2)	C(32)-C(31)-B(1)	122.3(2)
C(2)-C(1)-P(1)	107.01(14)	C(36)-C(31)-B(1)	122.6(2)
C(8)-C(2)-C(1)	110.7(2)	C(33)-C(32)-C(31)	123.6(2)
O(3)-C(3)-O(2)	110.6(2)	C(34)-C(33)-C(32)	119.9(2)
O(3)-C(3)-C(4)	107.9(2)	C(33)-C(34)-C(35)	118.8(2)
O(2)-C(3)-C(4)	105.8(2)	C(34)-C(35)-C(36)	120.4(2)
O(3)-C(3)-C(7)	107.8(2)	C(35)-C(36)-C(31)	122.8(2)
O(2)-C(3)-C(7)	111.0(2)	C(42)-C(41)-C(46)	114.2(2)
C(4)-C(3)-C(7)	113.6(2)	C(42)-C(41)-B(1)	122.0(2)
O(1)-C(6)-C(5)	107.2(2)	C(46)-C(41)-B(1)	123.8(2)
O(1)-C(6)-C(7)	109.9(2)	C(43)-C(42)-C(41)	123.5(2)
C(5)-C(6)-C(7)	113.4(2)	C(44)-C(43)-C(42)	120.2(2)
O(1)-C(6)-P(1)	106.81(14)	C(43)-C(44)-C(45)	118.4(2)
C(5)-C(6)-P(1)	114.2(2)	C(44)-C(45)-C(46)	120.6(2)
C(7)-C(6)-P(1)	105.2(2)	C(45)-C(46)-C(41)	123.1(2)
C(3)-C(7)-C(6)	111.1(2)	C(56)-C(51)-C(52)	114.4(2)
O(3)-C(8)-O(1)	110.7(2)	C(56)-C(51)-B(1)	123.7(2)
O(3)-C(8)-C(9)	107.5(2)	C(52)-C(51)-B(1)	121.8(2)
O(1)-C(8)-C(9)	105.9(2)	C(53)-C(52)-C(51)	123.2(2)
O(3)-C(8)-C(2)	108.7(2)	C(54)-C(53)-C(52)	120.1(2)
O(1)-C(8)-C(2)	110.7(2)	C(55)-C(54)-C(53)	118.9(2)
C(9)-C(8)-C(2)	113.3(2)	C(54)-C(55)-C(56)	120.5(2)
C(17)-C(11)-P(1)	102.81(13)	C(55)-C(56)-C(51)	122.9(2)
C(13)-C(12)-C(17)	119.5(2)		

Table A.7.4 Anisotropic displacement parameters ($Å^2$ x 10^3) for salt (**3.27**). The anisotropic displacement factor exponent takes the form:

$-2\Pi^2[h^2a^{*2}U_{11} + ... + 2hka^*b^*U_{12}]$

Atom	U_{11}	U_{22}	U_{33}	U_{23}	U_{13}	U_{12}
P(1)	25(1)	23(1)	19(1)	-1(1)	0(1)	0(1)
O(1)	32(1)	41(1)	26(1)	-10(1)	-3(1)	4(1)
O(2)	36(1)	29(1)	30(1)	5(1)	-5(1)	6(1)
O(3)	48(1)	38(1)	21(1)	-4(1)	-8(1)	3(1)
B(1)	24(1)	24(1)	26(1)	-1(1)	-1(1)	1(1)
C(1)	26(1)	24(1)	26(1)	0(1)	-6(1)	-2(1)
C(2)	34(1)	25(1)	28(1)	-4(1)	-8(1)	-2(1)
C(3)	46(2)	32(1)	22(1)	2(1)	-3(1)	-2(1)
C(4)	83(2)	44(2)	32(2)	9(1)	-12(1)	5(2)
C(5)	28(1)	78(2)	30(1)	-10(1)	2(1)	-11(1)
C(6)	28(1)	38(1)	20(1)	-5(1)	2(1)	-5(1)
C(7)	42(1)	35(1)	19(1)	0(1)	6(1)	-9(1)
C(8)	37(1)	33(1)	24(1)	-6(1)	-10(1)	4(1)
C(9)	54(2)	46(2)	34(2)	-19(1)	-7(1)	10(1)
C(10)	30(1)	38(1)	44(2)	2(1)	4(1)	-5(1)
C(11)	31(1)	20(1)	24(1)	-1(1)	1(1)	-2(1)
C(12)	27(1)	27(1)	29(1)	-6(1)	-1(1)	-1(1)
C(13)	31(1)	44(1)	24(1)	-7(1)	3(1)	-1(1)
C(14)	38(1)	47(2)	19(1)	4(1)	0(1)	-4(1)

Atom	U_{11}	U_{22}	U_{33}	U_{23}	U_{13}	U_{12}
C(15)	34(1)	29(1)	26(1)	5(1)	-5(1)	-3(1)
C(16)	34(1)	23(1)	26(1)	-1(1)	-3(1)	4(1)
C(17)	21(1)	23(1)	22(1)	-1(1)	-2(1)	-4(1)
C(18)	25(1)	24(1)	21(1)	0(1)	-1(1)	-1(1)
C(21)	25(1)	28(1)	29(1)	2(1)	-1(1)	-4(1)
C(22)	32(1)	31(1)	38(1)	4(1)	-1(1)	0(1)
C(23)	34(2)	42(2)	54(2)	14(1)	-10(1)	1(1)
C(24)	46(2)	48(2)	40(2)	18(1)	-17(1)	-11(1)
C(25)	50(2)	53(2)	30(2)	2(1)	-8(1)	-11(1)
C(26)	36(1)	44(2)	31(1)	-1(1)	-3(1)	-2(1)
C(31)	22(1)	27(1)	23(1)	-4(1)	7(1)	-2(1)
C(32)	27(1)	28(1)	34(1)	-6(1)	3(1)	0(1)
C(33)	33(1)	31(1)	50(2)	-11(1)	11(1)	-9(1)
C(34)	42(2)	23(1)	45(2)	-1(1)	21(1)	-1(1)
C(35)	34(1)	29(1)	30(1)	2(1)	12(1)	7(1)
C(36)	28(1)	27(1)	23(1)	-2(1)	5(1)	1(1)
C(41)	22(1)	22(1)	25(1)	1(1)	-4(1)	2(1)
C(42)	32(1)	25(1)	33(1)	-3(1)	3(1)	-3(1)
C(43)	37(1)	35(1)	33(1)	2(1)	7(1)	-2(1)
C(44)	38(1)	35(1)	27(1)	-5(1)	2(1)	7(1)
C(45)	46(2)	25(1)	34(1)	-5(1)	-3(1)	4(1)
C(46)	38(1)	23(1)	31(1)	1(1)	-2(1)	-2(1)
C(51)	25(1)	18(1)	30(1)	-1(1)	1(1)	3(1)
C(52)	28(1)	25(1)	31(1)	1(1)	0(1)	-1(1)
C(53)	29(1)	25(1)	46(2)	-5(1)	-8(1)	0(1)
C(54)	24(1)	26(1)	59(2)	-1(1)	3(1)	0(1)
C(55)	36(1)	26(1)	43(2)	3(1)	12(1)	0(1)
C(56)	32(1)	23(1)	31(1)	3(1)	1(1)	2(1)

Table A.7.5 Hydrogen coordinates (x 10^4) and isotropic displacement parameters ($Å^2$ x 10^3) for salt (**3.27**)

Atom	x	y	z	U(eq)
H(2A)	1406(1)	2870(1)	821(1)	34
H(2B)	821(1)	3085(1)	269(1)	34
H(4A)	775(5)	4996(4)	-740(7)	79
H(4B)	1568(4)	5261(7)	-904(5)	79
H(4C)	1128(9)	5626(3)	-305(2)	79
H(5A)	3577(2)	4417(9)	516(1)	68
H(5B)	3436(3)	3962(4)	1186(7)	68
H(5C)	3299(2)	4811(5)	1182(7)	68
H(7A)	2151(1)	5283(1)	524(1)	39
H(7B)	2566(1)	4952(1)	-109(1)	39
H(9A)	2392(6)	2885(3)	-744(6)	67
H(9B)	1574(3)	2641(6)	-702(6)	67
H(9C)	2136(9)	2352(3)	-160(1)	67
H(10A)	0(2)	3778(8)	1046(1)	56
H(10B)	343(5)	4307(3)	1592(6)	56
H(10C)	472(3)	3458(5)	1646(5)	56
H(11A)	2206(1)	5283(1)	1858(1)	30
H(11B)	1352(1)	5248(1)	1759(1)	30

Atom	x	y	z	U(eq)
H(12A)	1405(1)	5594(1)	3096(1)	33
H(13A)	1307(1)	5064(1)	4155(1)	39
H(14A)	1542(1)	3846(1)	4296(1)	41
H(15A)	1881(1)	3135(1)	3378(1)	36
H(16A)	1787(1)	3087(1)	2008(1)	33
H(16B)	2581(1)	3413(1)	2076(1)	33
H(22A)	-331(1)	2134(1)	1973(1)	40
H(23A)	-1061(1)	2419(1)	1070(1)	52
H(24A)	-905(1)	1857(1)	33(1)	54
H(25A)	17(1)	1020(2)	-96(1)	53
H(26A)	754(1)	747(1)	803(1)	44
H(32A)	-30(1)	38(1)	1660(1)	36
H(33A)	-58(1)	-1189(1)	1841(1)	45
H(34A)	817(1)	-1738(1)	2507(1)	44
H(35A)	1698(1)	-1022(1)	3004(1)	37
H(36A)	1727(1)	207(1)	2811(1)	31
H(42A)	-26(1)	494(1)	3133(1)	36
H(43A)	-531(1)	851(1)	4140(1)	42
H(44A)	-410(1)	2037(1)	4512(1)	40
H(45A)	228(1)	2852(1)	3849(1)	42
H(46A)	734(1)	2492(1)	2847(1)	37
H(52A)	1862(1)	1533(1)	3079(1)	34
H(53A)	3044(1)	1892(1)	2993(1)	40
H(54A)	3565(1)	2062(1)	1934(1)	43
H(55A)	2873(1)	1893(1)	973(1)	42
H(56A)	1689(1)	1547(1)	1059(1)	34

A.8 Crystal data and structure refinement for bis(borane) adduct (3.32)

This crystal structure determination was carried out by Miss H. Phetmung under the supervision of Prof. A. G. Orpen.

Identification code	rip57	
Empirical formula	$C_8H_{18}B_2P_2$	
Formula weight	197.78	
Temperature	173(2) K	
Wavelength	0.71073 Å	
Crystal system	Orthorhombic	
Space group	Pbcn	
Unit cell dimensions	a = 13.831(2) Å	$\alpha = 90.00°$
	b = 8.416(3) Å	$\beta = 90.00°$
	c = 10.006(3) Å	$\gamma = 90.00°$
Volume	1164.7(6) $Å^3$	
Z	4	
Density (calculated)	1.128 mgm^{-3}	
Absorption coefficient	0.322 mm^{-1}	
F(000)	424	
Crystal size	0.44 x 0.28 x 0.10 mm	
q range for data collection	2.83° - 27.48°	
Index ranges	-15<=h<=17, -8<=k<=10, -12<=l<=12	
Reflections collected	6802	
Independent reflections	1334 [R(int) = 0.0543]	
Refinement method	Full-matrix least-squares on F^2	
Data/restraints/parameters	1332/0/56	
Goodness-of-fit on F^2*	1.009	
Final R indices [$I > 2\sigma(I)$]*	$R_1 = 0.0474$, $wR_2 = 0.1281$ [1059 data]	
R indices (all data)*	$R_1 = 0.0666$, $wR_2 = 0.1468$ [1334 data]	
Weighting scheme	calc $w = 1/[\sigma^2(F_o^2) + (0.0782P)^2 + 1.6903P]$	
	where $P = (\text{Max } F_o^2, 0 + 2F_c^2)/3$	
Largest diff. peak and hole	0.367 and -0.530 $e.Å^{-3}$	

*$wR_2 = [\Sigma w\Delta^2/\Sigma wF_o^4]^{0.5}$; $S = [\Sigma w\Delta^2/(N.O. - N.V.)]^{0.5}$; $\Delta = F_o^2 - F_c^2$;
$R_1 = \Sigma |F_o - F_c|/\Sigma |F_o|$; N.O. = data + restraints; N.V. = parameters

Table A.8.1 Atomic coordinates (x 10^4) and equivalent isotropic displacement parameters ($Å^2$ x 10^2) for bis(borane) adduct (**3.32**). U(eq) is defined as one third of the trace of the orthogonalized U_{ij} tensor

Atom	x	y	z	U(eq)
P(1)	1846(1)	1831(1)	2937(1)	22(1)
B(1)	1834(2)	928(4)	1180(3)	31(1)
C(1)	703(2)	2466(3)	3678(2)	23(1)
C(2)	319(2)	3972(3)	3046(2)	19(1)
C(3)	619(2)	5429(3)	3573(2)	23(1)
C(4)	315(2)	6863(3)	3046(3)	26(1)

Table A.8.2 Bond lengths (Å) for bis(borane) adduct (**3.32**)

Atom	length(Å)	Atom	length(Å)
P(1)-C(1)	1.826(2)	C(1)-H(1A)	0.99
P(1)-B(1)	1.915(3)	C(1)-H(1B)	0.99
P(1)-P(1)#1	5.181(2)	C(2)-C(3)	1.398(3)
P(1)-H(1A)	0.99	C(2)-C(2)#1	1.403(5)
P(1)-H(1B)	0.99	C(3)-C(4)	1.382(4)
B(1)-H(1A)	0.98	C(3)-H(3A)	0.95
B(1)-H(1B)	0.98	C(4)-C(4)#1	1.397(5)
B(1)-H(1C)	0.98	C(4)-H(4A)	0.95
C(1)-C(2)	1.513(3)		

Table A.7.3 Bond angles (°) for bis(borane) adduct (**3.32**)

Atoms	angle(°)	Atoms	angle(°)
C(1)-P(1)-B(1)	118.78(13)	C(2)-C(1)-P(1)	112.3(2)
C(1)-P(1)-P(1)#1	38.30(8)	C(2)-C(1)-H(1A)	109.14(13)
B(1)-P(1)-P(1)#1	80.60(10)	P(1)-C(1)-H(1A)	109.14(9)
C(1)-P(1)-H(1A)	107.62(8)	C(2)-C(1)-H(1B)	109.14(13)
B(1)-P(1)-H(1A)	107.62(11)	P(1)-C(1)-H(1B)	109.14(8)
P(1)#1-P(1)-H(1A)	120.650(10)	H(1A)-C(1)-H(1B)	107.9
C(1)-P(1)-H(1B)	107.62(9)	C(3)-C(2)-C(2)#1	118.72(14)
B(1)-P(1)-H(1B)	107.62(11)	C(3)-C(2)-C(1)	118.2(2)
P(1)#1-P(1)-H(1B)	126.661(11)	C(2)#1-C(2)-C(1)	123.10(13)
H(1A)-P(1)-H(1B)	107.1	C(4)-C(3)-C(2)	122.1(2)
P(1)-B(1)-H(1A)	109.47(10)	C(4)-C(3)-H(3A)	119.0(2)
P(1)-B(1)-H(1B)	109.47(11)	C(2)-C(3)-H(3A)	118.96(14)
H(1A)-B(1)-H(1B)	109.5	C(3)-C(4)-C(4)#1	119.2(2)
P(1)-B(1)-H(1C)	109.47(11)	C(3)-C(4)-H(4A)	120.4(2)
H(1A)-B(1)-H(1C)	109.5	C(4)#1-C(4)-H(4A)	120.393(10)
H(1B)-B(1)-H(1C)	109.5		

Symmetry transformations used to generate equivalent atoms: #1 -x, y, -z +1/2

Table A.8.4 Anisotropic displacement parameters ($Å^2$ x 10^3) for bis(borane) adduct (**3.32**). The anisotropic displacement factor exponent takes the form: $-2\Pi^2[h^2a^{*2}U_{11} + ... + 2hka^*b^*U_{12}]$

Atom	U_{11}	U_{22}	U_{33}	U_{23}	U_{13}	U_{12}
P(1)	22(1)	24(1)	21(1)	0(1)	-1(1)	4(1)
B(1)	31(2)	39(2)	23(1)	-5(1)	2(1)	5(1)
C(1)	23(1)	28(1)	19(1)	2(1)	4(1)	2(1)
C(2)	17(1)	23(1)	18(1)	2(1)	4(1)	1(1)
C(3)	18(1)	32(1)	18(1)	-2(1)	1(1)	-2(1)
C(4)	24(1)	25(1)	27(1)	-4(1)	4(1)	-4(1)

Table A.8.5 Hydrogen coordinates (x 10^4) and isotropic displacement parameters ($Å^2$ x 10^3) for bis(borane) adduct (**3.32**)

Atom	x	y	z	U(eq)
H(1A)	2141(1)	1041(1)	3547(1)	27
H(1B)	2282(1)	2764(1)	2918(1)	27
H(1A)	2492(3)	614(23)	930(9)	46
H(1B)	1592(14)	1715(9)	541(4)	46
H(1C)	1413(12)	-8(15)	1170(6)	46
H(1A)	219(2)	1608(3)	3571(2)	28
H(1B)	798(2)	2646(3)	4647(2)	28
H(3A)	1046(2)	5434(3)	4317(2)	27
H(4A)	532(2)	7836(3)	3421(3)	31

A.9 Crystal data and structure refinement for chloro-phospha-adamantane (3.36)

This crystal structure determination was carried out by Miss H. Phetmung under the supervision of Prof. A. G. Orpen.

Identification code	rip146s	
Empirical formula	$C_{10}H_{16}ClO_3P$	
Formula weight	250.65	
Temperature	173(2) K	
Wavelength	0.71073 Å	
Crystal system	Monoclinic	
Space group	$P2_1/c$	
Unit cell dimensions	a = 9.656(3) Å	α = 90.00°.
	b = 8.314(2) Å	β = 100.463(12)°
	c = 15.116(2) Å	γ = 90.00°
Volume	1193.4(5) $Å^3$	
Z	4	
Density (calculated)	1.395 mg/m^3	
Absorption coefficient	0.439 mm^{-1}	
F(000)	528	
Crystal size	0.30 x 0.24 x 0.20 mm (colourless)	
q range for data collection	2.14 - 25.00°	
Index ranges	-12<=h<=12, -9<=k<=10, -19<=l<=16	
Reflections collected	6005	
Independent reflections	2090 [R(int) = 0.0510]	
Refinement method	Full-matrix least-squares on F^2	
Data/restraints/parameters	2088/0/141	
Goodness-of-fit on F^2*	1.009	
Final R indices [$I > 2\sigma(I)$]*	R_1 = 0.0418, wR_2 = 0.0844[1449 data]	
R indices (all data)*	R_1 = 0.0743, wR_2 = 0.0975 [2090 data]	
Weighting scheme	calc $w = 1/[[\sigma^2(F_o^2)+(0.0416P)^2+0.530P]$	
	where $P = (\text{Max } F_o^2\ 0 + 2F_c^2)/3$	
Extinction coefficient	0.0042(10)	
Largest diff. peak and hole	0.322 and -0.272 $e.Å^{-3}$	

*$wR_2 = [\Sigma w\Delta^2/\Sigma wF_o^4]^{0.5}$; $S = [\Sigma w\Delta^2/(N.O. - N.V.)]^{0.5}$; $\Delta = F_o^2 - F_c^2$;
$R_1 = \Sigma |F_o - F_c|/\Sigma |F_o|$; N.O. = data + restraints; N.V. = parameters

Table A.9.1 Atomic coordinates (x 10^4) and equivalent isotropic displacement parameters ($Å^2$ x 10^2) for chloro-phospha-adamantane (**3.36**). U(eq) is defined as one third of the trace of the orthogonalized U_{ij} tensor

Atom	x	y	z	U(eq)
Cl(1)	9455(1)	1635(1)	3773(1)	37(1)
P(1)	11147(1)	2436(1)	3221(1)	25(1)
O(1)	13806(2)	1563(2)	3444(1)	24(1)
O(2)	12208(2)	3409(2)	4984(1)	25(1)
O(3)	14519(2)	2572(3)	4913(1)	25(1)
C(1)	12512(3)	886(4)	3645(2)	23(1)
C(2)	12692(3)	613(4)	4654(2)	24(1)
C(3)	13209(3)	2127(4)	5170(2)	24(1)
C(4)	13491(3)	1894(4)	6173(2)	33(1)
C(5)	10997(3)	5440(4)	4043(2)	33(1)
C(6)	11940(3)	3981(4)	4063(2)	25(1)
C(7)	13346(3)	4370(4)	3785(2)	26(1)
C(8)	14345(3)	2943(4)	3972(2)	25(1)
C(9)	15782(3)	3258(4)	3762(2)	33(1)
C(10)	12244(3)	-650(4)	3105(2)	32(1)

Table A.9.2 Bond lengths (Å) for chloro-phospha-adamantane (**3.36**)

Atom	length(Å)	Atom	length(Å)
Cl(1)-P(1)	2.0754(11)	C(1)-C(10)	1.512(4)
P(1)-C(1)	1.871(3)	C(1)-C(2)	1.521(4)
P(1)-C(6)	1.871(3)	C(2)-C(3)	1.516(4)
O(1)-C(8)	1.439(3)	C(3)-C(4)	1.504(4)
O(1)-C(1)	1.452(3)	C(5)-C(6)	1.514(4)
O(2)-C(3)	1.432(3)	C(6)-C(7)	1.528(4)
O(2)-C(6)	1.449(3)	C(7)-C(8)	1.523(4)
O(3)-C(8)	1.435(3)	C(8)-C(9)	1.502(4)
O(3)-C(3)	1.438(3)		

Table A.9.3 Bond angles (°) for chloro-phospha-adamantane (**3.36**)

Atom	angle(°)	Atom	angle(°)
C(1)-P(1)-C(6)	93.69(13)	O(2)-C(3)-C(2)	111.7(2)
C(1)-P(1)-Cl(1)	101.42(9)	O(3)-C(3)-C(2)	107.4(2)
C(6)-P(1)-Cl(1)	101.61(10)	C(4)-C(3)-C(2)	113.2(2)
C(8)-O(1)-C(1)	115.6(2)	O(2)-C(6)-C(5)	106.5(2)
C(3)-O(2)-C(6)	115.4(2)	O(2)-C(6)-C(7)	108.7(2)
C(8)-O(3)-C(3)	111.8(2)	C(5)-C(6)-C(7)	112.7(2)
O(1)-C(1)-C(10)	106.5(2)	O(2)-C(6)-P(1)	114.1(2)
O(1)-C(1)-C(2)	108.7(2)	C(5)-C(6)-P(1)	111.5(2)
C(10)-C(1)-C(2)	113.1(3)	C(7)-C(6)-P(1)	103.5(2)
O(1)-C(1)-P(1)	103.9(2)	C(8)-C(7)-C(6)	110.4(2)
C(10)-C(1)-P(1)	110.8(2)	O(3)-C(8)-O(1)	110.1(2)

Atom	angle(°)	Atom	angle(°)
C(2)-C(1)-P(1)	113.0(2)	O(3)-C(8)-C(9)	107.5(2)
C(3)-C(2)-C(1)	111.0(2)	O(1)-C(8)-C(9)	106.1(2)
O(2)-C(3)-O(3)	110.5(2)	O(3)-C(8)-C(7)	107.9(2)
O(2)-C(3)-C(4)	106.6(2)	O(1)-C(8)-C(7)	111.4(2)
O(3)-C(3)-C(4)	107.4(2)	C(9)-C(8)-C(7)	113.8(3)

Table A.9.4 Anisotropic displacement parameters ($Å^2$ x 10^3) for chloro-phospha-adamantane (**3.36**). The anisotropic displacement factor exponent takes the form: $-2\Pi^2[h^2a^{*2}U_{11} + ... + 2hka^*b^*U_{12}]$

Atom	U_{11}	U_{22}	U_{33}	U_{23}	U_{13}	U_{12}
Cl(1)	20(1)	46(1)	46(1)	6(1)	9(1)	-2(1)
P(1)	19(1)	31(1)	25(1)	1(1)	2(1)	-2(1)
O(1)	18(1)	30(1)	26(1)	-5(1)	6(1)	-4(1)
O(2)	27(1)	29(1)	18(1)	2(1)	3(1)	4(1)
O(3)	17(1)	34(1)	22(1)	2(1)	0(1)	-2(1)
C(1)	16(2)	27(2)	27(2)	-4(1)	6(1)	-4(1)
C(2)	17(2)	26(2)	29(2)	5(1)	4(1)	0(1)
C(3)	21(2)	28(2)	21(2)	2(1)	1(1)	3(1)
C(4)	34(2)	40(2)	24(2)	5(2)	1(1)	1(2)
C(5)	38(2)	29(2)	31(2)	4(2)	4(2)	9(2)
C(6)	27(2)	25(2)	21(2)	5(1)	2(1)	1(1)
C(7)	29(2)	28(2)	20(2)	3(1)	2(1)	-5(1)
C(8)	24(2)	27(2)	22(2)	0(1)	5(1)	-4(1)
C(9)	21(2)	43(2)	36(2)	0(2)	6(1)	-8(2)
C(10)	28(2)	30(2)	41(2)	-7(2)	10(1)	-3(2)

Table A.9.5 Hydrogen coordinates (x 10^4) and isotropic displacement parameters ($Å^2$ x 10^3) for chloro-phospha-adamantane (**3.36**)

Atom	x	y	z	U(eq)
H(2A)	11779(3)	284(4)	4808(2)	28
H(2B)	13376(3)	-267(4)	4832(2)	28
H(4A)	13858(19)	2895(8)	6468(2)	50
H(4B)	14185(16)	1034(16)	6333(2)	50
H(4C)	12613(5)	1600(23)	6372(2)	50
H(5A)	11444(9)	6227(10)	4488(9)	50
H(5B)	10088(7)	5114(5)	4187(12)	50
H(5C)	10848(16)	5924(13)	3442(4)	50
H(7A)	13189(3)	4634(4)	3136(2)	31
H(7B)	13774(3)	5320(4)	4124(2)	31
H(9A)	16370(7)	2298(8)	3902(12)	50
H(9B)	16215(8)	4165(14)	4124(9)	50
H(9C)	15698(3)	3516(23)	3122(3)	50
H(10A)	13008(10)	-1414(9)	3307(8)	49
H(10B)	12202(18)	-411(5)	2466(2)	49
H(10C)	11347(9)	-1120(12)	3191(10)	49

A.10 Crystal data and structure refinement for 1,1'-bis(phospha-adamantyl)-ferrocene *rac*-(3.38)

This crystal structure determination was carried out by Miss H. Phetmung under the supervision of Prof. A. G. Orpen.

Identification code	rip144s	
Empirical formula	$C_{30}H_{40}FeO_6P_2$	
Formula weight	614.41	
Temperature	173(2) K	
Wavelength	0.71073 Å	
Crystal system	Monoclinic	
Space group	$P2_1/c$	
Unit cell dimensions	a = 15.455(4) Å	α = 90°
	b = 10.261(4) Å	β = 102.23(2)°
	c = 9.152(2) Å	γ = 90°
Volume	1418.3(8) $Å^3$	
Z	2	
Density (calculated)	1.439 Mg/m^3	
Absorption coefficient	0.687 mm^{-1}	
F(000)	648	
Crystal size	0.18x0.14x0.10 mm (dark yellow)	
θ range for data collection	2.40 - 25.00°	
Index ranges	-16<=h<=20, -12<=k<=13, -11<=l<=9	
Reflections collected	7203	
Independent reflections	2483 [R(int) = 0.0972]	
Refinement method	Full-matrix least-squares on F^2	
Data/restraints/parameters	2469/0/182	
Goodness-of-fit on F^2*	0.983	
Final R indices [$I > 2\sigma(I)$]*	R_1 = 0.0531, wR_2 = 0.0887[1524 data]	
R indices (all data)*	R_1 = 0.1129, wR_2 = 0.1082[2483 data]	
Weighting scheme	calc w = $1/[[\sigma^2(F_o^2) + (0.0330P)^2 + 0.0340P]$	
	where P= (Max F_o^2 0 + $2F_c^2$)/3	
Largest diff. peak and hole	0.378 and -0.366 e.$Å^{-3}$	

*$wR_2 = [\Sigma w\Delta^2/\Sigma wF_o^4]^{0.5}$; $S = [\Sigma w\Delta^2/(N.O. - N.V.)]^{0.5}$; $\Delta = F_o^2 - F_c^2$;
$R_1 = \Sigma |F_o - F_c|/\Sigma |F_o|$; N.O. = data + restraints; N.V. = parameters

Table A.10.1 Atomic coordinates (x 10^4) and equivalent isotropic displacement parameters ($Å^2$ x 10^2) for 1,1'-bis(phospha-adamantyl)-ferrocene *rac*-(**3.38**). U(eq) is defined as one third of the trace of the orthogonalized U_{ij} tensor

Atom	x	y	z	U(eq)
Fe(1)	0	0	0	19(1)
P(1)	-1848(1)	-891(1)	1414(1)	19(1)
O(1)	-3071(2)	-717(3)	3129(3)	23(1)
O(2)	-3066(2)	955(3)	-85(3)	20(1)
O(3)	-4004(2)	790(3)	1625(3)	22(1)
C(1)	-2267(2)	-46(5)	2969(4)	21(1)
C(2)	-2494(3)	1368(4)	2570(4)	22(1)
C(3)	-3273(3)	1485(4)	1244(5)	20(1)
C(4)	-3584(3)	2858(4)	906(5)	28(1)
C(5)	-2792(3)	-809(4)	-1592(5)	25(1)
C(6)	-2861(3)	-435(4)	-31(5)	19(1)
C(7)	-3624(3)	-1153(4)	463(5)	22(1)
C(8)	-3811(3)	-561(4)	1885(5)	22(1)
C(9)	-4592(3)	-1157(5)	2391(5)	31(1)
C(10)	-1634(3)	-205(5)	4467(4)	28(1)
C(11)	-992(3)	269(4)	1150(5)	18(1)
C(12)	-1001(3)	1291(4)	97(5)	24(1)
C(13)	-167(3)	1928(5)	446(5)	32(1)
C(14)	360(3)	1321(5)	1701(5)	29(1)
C(15)	-135(3)	283(5)	2148(5)	23(1)

Table A.10.2 Bond lengths (Å) for 1,1'-bis(phospha-adamantyl)-ferrocene *rac*-(**3.38**)

Atom	length(Å)	Atom	length(Å)
Fe(1)-C(15)	2.041(4)	O(2)-C(6)	1.460(5)
Fe(1)-C(15)#1	2.041(4)	O(3)-C(8)	1.427(5)
Fe(1)-C(13)#1	2.047(5)	O(3)-C(3)	1.440(5)
Fe(1)-C(13)	2.047(5)	C(1)-C(10)	1.515(5)
Fe(1)-C(14)	2.051(4)	C(1)-C(2)	1.519(6)
Fe(1)-C(14)#1	2.051(4)	C(2)-C(3)	1.523(5)
Fe(1)-C(12)#1	2.053(4)	C(3)-C(4)	1.500(6)
Fe(1)-C(12)	2.053(4)	C(5)-C(6)	1.505(5)
Fe(1)-C(11)#1	2.054(4)	C(6)-C(7)	1.537(6)
Fe(1)-C(11)	2.054(4)	C(7)-C(8)	1.519(6)
P(1)-C(11)	1.834(4)	C(8)-C(9)	1.510(6)
P(1)-C(6)	1.882(4)	C(11)-C(12)	1.422(6)
P(1)-C(1)	1.895(4)	C(11)-C(15)	1.441(5)
O(1)-C(8)	1.442(5)	C(12)-C(13)	1.420(6)
O(1)-C(1)	1.455(4)	C(13)-C(14)	1.405(6)
O(2)-C(3)	1.430(5)	C(14)-C(15)	1.422(6)

Table A.10.3 Bond angles (°) for 1,1'-bis(phospha-adamantyl)-ferrocene *rac*-(**3.38**)

Atom	angle(°)	Atom	angle(°)
C(15)-Fe(1)-C(15)#1	180.0	C(8)-O(1)-C(1)	114.8(3)
C(15)-Fe(1)-C(13)#1	111.9(2)	C(3)-O(2)-C(6)	115.4(3)
C(15)#1-Fe(1)-C(13)#1	68.1(2)	C(8)-O(3)-C(3)	112.1(3)
C(15)-Fe(1)-C(13)	68.1(2)	O(1)-C(1)-C(10)	105.1(3)
C(15)#1-Fe(1)-C(13)	111.9(2)	O(1)-C(1)-C(2)	108.6(3)
C(13)#1-Fe(1)-C(13)	180.0	C(10)-C(1)-C(2)	113.1(4)
C(15)-Fe(1)-C(14)	40.7(2)	O(1)-C(1)-P(1)	107.1(3)
C(15)#1-Fe(1)-C(14)	139.3(2)	C(10)-C(1)-P(1)	111.8(3)
C(13)#1-Fe(1)-C(14)	139.9(2)	C(2)-C(1)-P(1)	110.8(3)
C(13)-Fe(1)-C(14)	40.1(2)	C(1)-C(2)-C(3)	111.7(3)
C(15)-Fe(1)-C(14)#1	139.3(2)	O(2)-C(3)-O(3)	110.3(3)
C(15)#1-Fe(1)-C(14)#1	40.7(2)	O(2)-C(3)-C(4)	107.5(3)
C(13)#1-Fe(1)-C(14)#1	40.1(2)	O(3)-C(3)-C(4)	106.4(3)
C(13)-Fe(1)-C(14)#1	139.9(2)	O(2)-C(3)-C(2)	111.5(3)
C(14)-Fe(1)-C(14)#1	180.0	O(3)-C(3)-C(2)	107.3(3)
C(15)-Fe(1)-C(12)#1	111.4(2)	C(4)-C(3)-C(2)	113.8(4)
C(15)#1-Fe(1)-C(12)#1	68.6(2)	O(2)-C(6)-C(5)	106.0(3)
C(13)#1-Fe(1)-C(12)#1	40.5(2)	O(2)-C(6)-C(7)	107.7(3)
C(13)-Fe(1)-C(12)#1	139.5(2)	C(5)-C(6)-C(7)	111.7(4)
C(14)-Fe(1)-C(12)#1	111.9(2)	O(2)-C(6)-P(1)	114.2(3)
C(14)#1-Fe(1)-C(12)#1	68.1(2)	C(5)-C(6)-P(1)	112.8(3)
C(15)-Fe(1)-C(12)	68.6(2)	C(7)-C(6)-P(1)	104.5(3)
C(15)#1-Fe(1)-C(12)	111.4(2)	C(8)-C(7)-C(6)	111.0(4)
C(13)#1-Fe(1)-C(12)	139.5(2)	O(3)-C(8)-O(1)	110.0(3)
C(13)-Fe(1)-C(12)	40.5(2)	O(3)-C(8)-C(9)	107.0(4)
C(14)-Fe(1)-C(12)	68.1(2)	O(1)-C(8)-C(9)	105.4(3)
C(14)#1-Fe(1)-C(12)	111.9(2)	O(3)-C(8)-C(7)	108.4(3)
C(12)#1-Fe(1)-C(12)	180.0	O(1)-C(8)-C(7)	111.6(3)
C(15)-Fe(1)-C(11)#1	138.8(2)	C(9)-C(8)-C(7)	114.2(4)
C(15)#1-Fe(1)-C(11)#1	41.2(2)	C(12)-C(11)-C(15)	107.4(4)
C(13)#1-Fe(1)-C(11)#1	68.2(2)	C(12)-C(11)-P(1)	131.7(3)
C(13)-Fe(1)-C(11)#1	111.8(2)	C(15)-C(11)-P(1)	121.0(3)
C(14)-Fe(1)-C(11)#1	111.5(2)	C(12)-C(11)-Fe(1)	69.7(2)
C(14)#1-Fe(1)-C(11)#1	68.5(2)	C(15)-C(11)-Fe(1)	68.9(2)
C(12)#1-Fe(1)-C(11)#1	40.5(2)	P(1)-C(11)-Fe(1)	128.2(2)
C(12)-Fe(1)-C(11)#1	139.5(2)	C(13)-C(12)-C(11)	108.0(4)
C(15)-Fe(1)-C(11)	41.2(2)	C(13)-C(12)-Fe(1)	69.5(3)
C(15)#1-Fe(1)-C(11)	138.8(2)	C(11)-C(12)-Fe(1)	69.8(2)
C(13)#1-Fe(1)-C(11)	111.8(2)	C(14)-C(13)-C(12)	108.7(4)
C(13)-Fe(1)-C(11)	68.2(2)	C(14)-C(13)-Fe(1)	70.1(3)
C(14)-Fe(1)-C(11)	68.5(2)	C(12)-C(13)-Fe(1)	69.9(3)
C(14)#1-Fe(1)-C(11)	111.5(2)	C(13)-C(14)-C(15)	108.3(4)
C(12)#1-Fe(1)-C(11)	139.5(2)	C(13)-C(14)-Fe(1)	69.8(3)
C(12)-Fe(1)-C(11)	40.5(2)	C(15)-C(14)-Fe(1)	69.3(3)
C(11)#1-Fe(1)-C(11)	180.0	C(14)-C(15)-C(11)	107.6(4)
C(11)-P(1)-C(6)	105.2(2)	C(14)-C(15)-Fe(1)	70.0(3)
C(11)-P(1)-C(1)	99.9(2)	C(11)-C(15)-Fe(1)	69.9(2)
C(6)-P(1)-C(1)	92.7(2)		

Symmetry transformations used to generate equivalent atoms: #1 -x, -y, -z

Table A.10.4 Anisotropic displacement parameters ($Å^2$ x 10^3) for 1,1'-bis(phospha-adamantyl)-ferrocene *rac*-(**3.38**). The anisotropic displacement factor exponent takes the form: $-2\Pi^2[h^2a^{*2}U_{11} + ... + 2hka^*b^*U_{12}]$

Atom	U_{11}	U_{22}	U_{33}	U_{23}	U_{13}	U_{12}
Fe(1)	17(1)	17(1)	23(1)	-2(1)	7(1)	0(1)
P(1)	18(1)	17(1)	22(1)	1(1)	3(1)	0(1)
O(1)	18(2)	26(2)	25(2)	6(1)	4(1)	-3(1)
O(2)	23(2)	15(2)	21(2)	-2(1)	5(1)	2(1)
O(3)	16(2)	20(2)	31(2)	6(1)	9(1)	2(1)
C(1)	15(2)	26(3)	22(2)	-4(2)	6(2)	-2(2)
C(2)	20(2)	26(3)	20(3)	-8(2)	7(2)	-4(2)
C(3)	22(2)	15(3)	24(3)	-1(2)	9(2)	0(2)
C(4)	32(3)	19(3)	33(3)	0(2)	12(2)	1(2)
C(5)	25(2)	22(3)	28(3)	-4(2)	3(2)	0(2)
C(6)	17(2)	17(3)	22(2)	2(2)	5(2)	4(2)
C(7)	20(2)	15(3)	28(3)	2(2)	1(2)	-4(2)
C(8)	18(2)	16(3)	30(3)	8(2)	3(2)	-2(2)
C(9)	21(2)	30(3)	41(3)	8(2)	7(2)	-4(2)
C(10)	20(2)	39(3)	24(2)	2(2)	6(2)	3(2)
C(11)	16(2)	20(3)	20(2)	-5(2)	9(2)	2(2)
C(12)	23(2)	21(3)	32(3)	0(2)	13(2)	6(2)
C(13)	35(3)	23(3)	43(3)	-4(2)	22(3)	0(2)
C(14)	25(3)	29(3)	34(3)	-16(2)	10(2)	-3(2)
C(15)	23(2)	29(3)	19(2)	-3(2)	7(2)	-1(2)

Table A.10.5 Hydrogen coordinates (x 10^4) and isotropic displacement parameters ($Å^2$ x 10^3) for 1,1'-bis(phospha-adamantyl)-ferrocene *rac*-(**3.38**)

Atom	x	y	z	U(eq)
H(2A)	-1971(3)	1806(4)	2326(4)	26
H(2B)	-2640(3)	1817(4)	3445(4)	26
H(4A)	-4090(10)	2861(5)	56(18)	41
H(4B)	-3102(6)	3378(7)	658(26)	41
H(4C)	-3761(15)	3234(9)	1782(11)	41
H(5A)	-3359(6)	-646(24)	-2280(6)	38
H(5B)	-2643(16)	-1736(7)	-1617(8)	38
H(5C)	-2328(12)	-288(17)	-1896(12)	38
H(7A)	-4163(3)	-1101(4)	-342(5)	26
H(7B)	-3467(3)	-2084(4)	637(5)	26
H(9A)	-4656(11)	-754(19)	3333(17)	46
H(9B)	-4496(9)	-2096(6)	2540(30)	46
H(9C)	-5132(4)	-1009(24)	1627(15)	46
H(10A)	-1896(8)	177(23)	5254(6)	41
H(10B)	-1075(7)	238(21)	4444(10)	41
H(10C)	-1520(13)	-1134(5)	4673(14)	41
H(12A)	-1505(3)	1518(4)	-745(5)	29
H(13A)	17(3)	2680(5)	-113(5)	38
H(14A)	981(3)	1569(5)	2187(5)	35
H(15A)	71(3)	-321(5)	3009(5)	28

A.11 Crystal data and structure refinement for 1,3-bis(phospha-adamantyl)propane *rac*-(3.2)

This crystal structure determination was carried out by Miss H. Phetmung under the supervision of Prof. A. G. Orpen.

Identification code	rip188s	
Empirical formula	$C_{23}H_{38}O_6P_2$	
Formula weight	472.47	
Temperature	173(2) K	
Wavelength	0.71073 Å	
Crystal system	Monoclinic	
Space group	C2/c	
Unit cell dimensions	a = 8.267(2) Å	α = 90.00°
	b = 14.934(3) Å	β = 94.32(2)°
	c = 19.685(5) Å	γ = 90.00°
Volume	2423.4(9) $Å^3$	
Z	4	
Density (calculated)	1.295 Mg/m^3	
Absorption coefficient	0.215 mm^{-1}	
F(000)	1016	
Crystal size	0.24 x 0.20 x 0.14 mm	
θ range for data collection	2.07 - 25.00°	
Index ranges	-4<=h<=10, -19<=k<=18, -25<=l<=25	
Reflections collected	6244	
Independent reflections	2133 [R(int) = 0.0366]	
Refinement method	Full-matrix least-squares on F^2	
Data/restraints/parameters	2128/0/146	
Goodness-of-fit on F^2	1.030	
Final R indices [I>2s(I)]	R_1 = 0.0371, wR_2 = 0.0830[1589 data]	
R indices (all data)*	R_1 = 0.0583, wR_2 = 0.0914[2133 data]	
Weighting scheme	calc w = $1/[[\sigma^2(F_o^2) + (0.0543P)^2 + 0.4713P]$	
	where P = (Max F_o^2 0 + $2F_c^2$)/3	
Extinction coefficient	0.0009(4)	
Largest diff. peak and hole	0.318 and -0.186 $e.Å^{-3}$	

*$wR_2 = [\Sigma w\Delta^2/\Sigma wF_o^4]^{0.5}$; $S = [\Sigma w\Delta^2/(N.O. - N.V.)]^{0.5}$; $\Delta = F_o^2 - F_c^2$;
$R_1 = \Sigma |F_o - F_c|/\Sigma |F_o|$; N.O. = data + restraints; N.V. = parameters

Table A.11.1 Atomic coordinates (x 10^4) and equivalent isotropic displacement parameters ($Å^2$ x 10^2) for 1,3-bis(phospha-adamantyl)propane *rac*-(**3.2**). U(eq) is defined as one third of the trace of the orthogonalized U_{ij} tensor.

Atom	x	y	z	U(eq)
P(1)	2570(1)	4362(1)	1967(1)	26(1)
O(1)	2304(2)	4858(1)	600(1)	25(1)
O(2)	4246(2)	3086(1)	1351(1)	28(1)
O(3)	3884(2)	3665(1)	240(1)	25(1)
C(1)	3321(2)	4995(1)	1230(1)	26(1)
C(2)	4999(2)	4634(1)	1120(1)	27(1)
C(3)	4894(2)	3677(1)	865(1)	26(1)
C(4)	6508(2)	3288(2)	712(1)	35(1)
C(5)	2123(3)	2500(2)	1952(1)	37(1)
C(6)	2576(2)	3267(1)	1499(1)	26(1)
C(7)	1547(2)	3306(1)	826(1)	26(1)
C(8)	2266(2)	3959(1)	340(1)	23(1)
C(9)	1352(3)	3999(2)	-348(1)	31(1)
C(10)	3329(3)	5995(1)	1355(1)	37(1)
C(11)	401(3)	4698(2)	1895(1)	30(1)
C(12)	0	5278(2)	2500	31(1)

Table A.11.2 Bond lengths (Å) for 1,3-bis(phospha-adamantyl)propane *rac*-(**3.2**)

Atom	length(Å)	Atom	length(Å)
P(1)-C(11)	1.857(2)	C(1)-C(2)	1.518(3)
P(1)-C(1)	1.875(2)	C(2)-C(3)	1.515(3)
P(1)-C(6)	1.877(2)	C(3)-C(4)	1.507(3)
O(1)-C(8)	1.436(2)	C(5)-C(6)	1.516(3)
O(1)-C(1)	1.459(2)	C(6)-C(7)	1.520(3)
O(2)-C(3)	1.435(2)	C(7)-C(8)	1.519(3)
O(2)-C(6)	1.458(2)	C(8)-C(9)	1.502(3)
O(3)-C(3)	1.433(2)	C(11)-C(12)	1.530(3)
O(3)-C(8)	1.435(2)	C(12)-C(11)#1	1.530(3)
C(1)-C(10)	1.513(3)		

Table A.11.3 Bond angles (°) for 1,3-bis(phospha-adamantyl)propane *rac*-(**3.2**)

Atom	angle(°)	Atom	angle(°)
C(11)-P(1)-C(1)	100.32(9)	O(2)-C(3)-C(2)	112.0(2)
C(11)-P(1)-C(6)	103.67(10)	C(4)-C(3)-C(2)	113.6(2)
C(1)-P(1)-C(6)	92.66(9)	O(2)-C(6)-C(5)	104.9(2)
C(8)-O(1)-C(1)	115.46(14)	O(2)-C(6)-C(7)	108.1(2)
C(3)-O(2)-C(6)	115.18(14)	C(5)-C(6)-C(7)	113.2(2)
C(3)-O(3)-C(8)	111.55(14)	O(2)-C(6)-P(1)	107.28(13)
O(1)-C(1)-C(10)	105.7(2)	C(5)-C(6)-P(1)	111.1(2)
O(1)-C(1)-C(2)	107.7(2)	C(7)-C(6)-P(1)	111.79(14)
C(10)-C(1)-C(2)	112.3(2)	C(8)-C(7)-C(6)	110.7(2)
O(1)-C(1)-P(1)	112.54(13)	O(3)-C(8)-O(1)	109.8(2)
C(10)-C(1)-P(1)	111.68(14)	O(3)-C(8)-C(9)	107.5(2)
C(2)-C(1)-P(1)	106.91(13)	O(1)-C(8)-C(9)	106.3(2)
C(3)-C(2)-C(1)	110.6(2)	O(3)-C(8)-C(7)	107.7(2)
O(3)-C(3)-O(2)	110.0(2)	O(1)-C(8)-C(7)	112.0(2)
O(3)-C(3)-C(4)	106.9(2)	C(9)-C(8)-C(7)	113.6(2)
O(2)-C(3)-C(4)	106.1(2)	C(12)-C(11)-P(1)	111.00(12)
O(3)-C(3)-C(2)	108.1(2)	C(11)#1-C(12)-C(11)	111.0(3)

Symmetry transformations used to generate equivalent atoms: #1 -x,y,-z+1/2

Table A.11.4 Anisotropic displacement parameters ($Å^2$ x 10^3) for 1,3-bis(phospha-adamantyl)propane *rac*-(**3.2**). The anisotropic displacement factor exponent takes the form: $-2\Pi^2[h^2a^{*2}U_{11} + ... + 2hka^*b^*U_{12}]$

Atom	U_{11}	U_{22}	U_{33}	U_{23}	U_{13}	U_{12}
P(1)	26(1)	35(1)	19(1)	1(1)	3(1)	2(1)
O(1)	25(1)	29(1)	19(1)	0(1)	-1(1)	2(1)
O(2)	24(1)	34(1)	27(1)	6(1)	5(1)	4(1)
O(3)	20(1)	35(1)	20(1)	-1(1)	2(1)	2(1)
C(1)	26(1)	30(1)	20(1)	0(1)	0(1)	-4(1)
C(2)	22(1)	38(1)	22(1)	2(1)	0(1)	-6(1)
C(3)	21(1)	36(1)	22(1)	3(1)	3(1)	-2(1)
C(4)	22(1)	51(2)	34(1)	2(1)	5(1)	6(1)
C(5)	39(1)	36(1)	38(1)	9(1)	12(1)	-3(1)
C(6)	21(1)	33(1)	25(1)	4(1)	7(1)	0(1)
C(7)	21(1)	29(1)	28(1)	-3(1)	4(1)	-1(1)
C(8)	19(1)	29(1)	22(1)	-3(1)	3(1)	2(1)
C(9)	27(1)	41(1)	24(1)	-3(1)	0(1)	4(1)
C(10)	44(2)	34(1)	33(1)	-3(1)	2(1)	-6(1)
C(11)	26(1)	43(1)	21(1)	5(1)	2(1)	4(1)
C(12)	31(2)	27(2)	37(2)	0	9(1)	0

Table A.11.5 Hydrogen coordinates (x 10^4) and isotropic displacement parameters (Å^2 x 10^3) for 1,3-bis(phospha-adamantyl)propane *rac*-(**3.2**)

Atom	x	y	z	E(eq)
H(2A)	5512(2)	5013(1)	784(1)	33
H(2B)	5685(2)	4658(1)	1554(1)	33
H(4A)	6346(3)	2686(4)	520(6)	53
H(4B)	7217(6)	3252(8)	1133(2)	53
H(4C)	7012(8)	3671(5)	383(5)	53
H(5A)	2190(17)	1933(2)	1703(3)	56
H(5B)	1014(7)	2586(5)	2083(6)	56
H(5C)	2874(11)	2484(6)	2361(4)	56
H(7A)	1484(2)	2703(1)	618(1)	31
H(7B)	432(2)	3497(1)	910(1)	31
H(9A)	1917(9)	4400(7)	-646(2)	46
H(9B)	254(6)	4227(8)	-300(1)	46
H(9C)	1287(14)	3398(2)	-548(3)	46
H(10A)	3806(15)	6300(2)	977(4)	55
H(10B)	3972(14)	6127(2)	1781(4)	55
H(10D)	2214(3)	6205(2)	1386(7)	55
H(11A)	162(3)	5037(2)	1467(1)	36
H(11B)	-290(3)	4156(2)	1877(1)	36
H(12A)	938	5668(2)	2636	37
H(12B)	-938	5668(2)	2364	37

A.12 Crystal data and structure refinement for *cis*-[$PtCl_2$(3.33)] *meso/rac*-(3.43)

This crystal structure determination was carried out by Dr. J. Charmant.

Identification code	haymarket
Empirical formula	$C_{29.50}H_{43}Cl_5O_6P_2Pt$
Formula weight	927.92
Temperature	163(2) K
Wavelength	0.71073 Å
Crystal system	Orthorhombic
Space group	Pbcn
Unit cell dimensions	a = 16.446(2) Å $\alpha = 90°$
	b = 16.120(2) Å $\beta = 90°$
	c = 26.317(4) Å $\gamma = 90°$
Volume	6976.5(17) $Å^3$
Z	8
Density (calculated)	1.767 Mg/m^3
Absorption coefficient	4.538 mm^{-1}
F(000)	3688
Crystal size	0.4 x 0.2 x 0.2 mm
θ range for data collection	1.55 to 27.49°
Index ranges	-21<=h<=21, -20<=k<=20, -34<=l<=34
Reflections collected	70672
Independent reflections	8004 [R_{int} = 0.1438]
Completeness to θ = 27.49°	99.9 %
Absorption correction	Semi-empirical from equivalents
Max. and min. transmission	0.526 and 0.268
Refinement method	Full-matrix least-squares on F^2
Data/restraints/parameters	8004/0/401
Goodness-of-fit on F^2	S = 1.039
R indices [for 4805 reflections with $I > 2\sigma(I)$]	$R_1 = 0.0745$, $wR_2 = 0.1934$
R indices (for all 8004 data)	$R_1 = 0.1288$, $wR_2 = 0.2319$
Weighting scheme	$w^{-1} = \sigma^2(F_o^2) + (aP)^2 + (bP)$, where $P = [\max(F_o^2, 0) + 2F_c^2]/3$
Largest diff. peak and hole	4.554 and -4.292 $eÅ^{-3}$

Table A.12.1 Atomic coordinates (x 10^4) and equivalent isotropic displacement parameters ($Å^2$ x 10^2) for *meso/rac*-(**3.43**). U(eq) is defined as one third of the trace of the orthogonalized U_{ij} tensor.

Atom	x	y	z	U(eq)
Pt(1)	6929(1)	8342(1)	5081(1)	24(1)
P(1A)	6848(2)	8722(2)	5916(1)	26(1)
P(1B)	7686(2)	9410(2)	4754(1)	24(1)
Cl(1A)	6101(2)	7203(2)	5275(1)	39(1)
Cl(1B)	6954(2)	7705(2)	4284(1)	41(1)
C(1A)	5889(7)	8475(7)	6307(4)	29(3)
C(2A)	5982(8)	8793(8)	6826(4)	35(3)
C(3A)	6687(8)	8384(8)	7115(5)	37(3)
C(4A)	7525(7)	8130(8)	6371(4)	32(3)
C(5A)	5129(7)	8749(9)	6027(5)	40(3)
C(6A)	6811(8)	8728(10)	7641(5)	46(3)
C(7A)	8420(8)	8200(9)	6217(5)	42(3)
C(8A)	7238(8)	7246(8)	6383(4)	36(3)
C(9A)	6425(8)	7176(7)	6643(4)	35(3)
C(10A)	6152(9)	6298(8)	6723(5)	47(3)
C(11A)	7078(8)	9811(7)	6086(4)	34(3)
C(12A)	6623(8)	10449(7)	5774(4)	33(3)
C(13A)	5919(8)	10811(7)	5963(5)	36(3)
C(14A)	5502(9)	11385(9)	5687(6)	47(3)
C(1B)	7442(7)	9731(7)	4073(4)	32(3)
C(2B)	7942(7)	10477(8)	3933(4)	33(3)
C(3B)	8861(7)	10270(7)	3935(4)	31(3)
C(4B)	8789(7)	9253(7)	4615(4)	29(3)
C(5B)	6564(8)	9858(9)	3995(4)	44(3)
C(6B)	9390(8)	11013(8)	3803(4)	37(3)
C(7B)	9290(7)	9039(8)	5089(4)	35(3)
C(8B)	8873(7)	8577(8)	4205(4)	33(3)
C(9B)	8560(8)	8907(8)	3699(4)	34(3)
C(10B)	8659(8)	8285(8)	3272(5)	42(3)
C(11B)	7732(8)	10392(8)	5120(4)	36(3)
C(12B)	6927(7)	10720(7)	5313(4)	28(2)
C(13B)	6516(10)	11337(8)	5049(5)	42(3)
C(14B)	5808(9)	11656(7)	5221(6)	45(3)
O(1A)	7445(5)	8513(5)	6856(3)	35(2)
O(2A)	5804(5)	7590(5)	6359(3)	37(2)
O(3A)	6502(6)	7528(5)	7140(3)	43(2)
O(1B)	9119(4)	10022(5)	4430(2)	27(2)
O(2B)	7702(5)	9085(5)	3729(3)	32(2)
O(3B)	8994(5)	9634(5)	3574(3)	33(2)
C(15)	10000	9783(13)	7500	49(5)
C(16)	6446(11)	1934(15)	7835(11)	133(12)
Cl(2)	9153(3)	9188(3)	7330(1)	65(1)
Cl(3)	6631(4)	1046(5)	7468(2)	118(2)
Cl(4)	5435(5)	1851(5)	8111(3)	138(3)

Table A.12.2 Bond lengths (Å) for *meso/rac*-(**3.43**)

Atoms	length(Å)	Atoms	length(Å)
Pt(1)-P(1A)	2.283(3)	C(12A)-C(12B)	1.382(16)
Pt(1)-P(1B)	2.293(3)	C(12A)-C(13A)	1.390(17)
Pt(1)-Cl(1B)	2.337(3)	C(13A)-C(14A)	1.361(18)
Pt(1)-Cl(1A)	2.341(3)	C(14A)-C(14B)	1.39(2)
P(1A)-C(11A)	1.851(12)	C(1B)-O(2B)	1.444(13)
P(1A)-C(4A)	1.894(12)	C(1B)-C(5B)	1.471(17)
P(1A)-C(1A)	1.926(12)	C(1B)-C(2B)	1.503(17)
P(1B)-C(11B)	1.853(12)	C(2B)-C(3B)	1.548(15)
P(1B)-C(4B)	1.869(13)	C(3B)-O(3B)	1.415(12)
P(1B)-C(1B)	1.909(11)	C(3B)-O(1B)	1.427(12)
C(1A)-O(2A)	1.440(13)	C(3B)-C(6B)	1.520(16)
C(1A)-C(2A)	1.466(16)	C(4B)-O(1B)	1.438(13)
C(1A)-C(5A)	1.516(16)	C(4B)-C(7B)	1.534(15)
C(2A)-C(3A)	1.535(17)	C(4B)-C(8B)	1.539(15)
C(3A)-O(3A)	1.414(14)	C(8B)-C(9B)	1.524(16)
C(3A)-O(1A)	1.435(14)	C(9B)-O(3B)	1.411(14)
C(3A)-C(6A)	1.507(17)	C(9B)-O(2B)	1.442(14)
C(4A)-O(1A)	1.424(13)	C(9B)-C(10B)	1.514(16)
C(4A)-C(8A)	1.501(17)	C(11B)-C(12B)	1.513(17)
C(4A)-C(7A)	1.532(18)	C(12B)-C(13B)	1.388(17)
C(8A)-C(9A)	1.507(17)	C(13B)-C(14B)	1.35(2)
C(9A)-O(2A)	1.431(14)	C(15)-Cl(2)	1.749(12)
C(9A)-O(3A)	1.433(14)	C(15)-Cl(2)#1	1.749(12)
C(9A)-C(10A)	1.498(18)	C(16)-Cl(3)	1.75(2)
C(11A)-C(12A)	1.514(16)	C(16)-Cl(4)	1.82(2)

Table A.12.3 Bond angles (°) for *meso/rac*-(**3.43**)

Atoms	angle(°)	Atoms	angle(°)
P(1A)-Pt(1)-P(1B)	100.98(10)	C(12B)-C(12A)-C(13A)	118.9(11)
P(1A)-Pt(1)-Cl(1B)	169.33(11)	C(12B)-C(12A)-C(11A)	120.8(11)
P(1B)-Pt(1)-Cl(1B)	89.02(10)	C(13A)-C(12A)-C(11A)	120.1(11)
P(1A)-Pt(1)-Cl(1A)	88.14(11)	C(14A)-C(13A)-C(12A)	120.9(12)
P(1B)-Pt(1)-Cl(1A)	170.52(10)	C(13A)-C(14A)-C(14B)	120.0(13)
Cl(1B)-Pt(1)-Cl(1A)	82.07(11)	O(2B)-C(1B)-C(5B)	107.7(9)
C(11A)-P(1A)-C(4A)	101.8(5)	O(2B)-C(1B)-C(2B)	105.1(9)
C(11A)-P(1A)-C(1A)	103.5(5)	C(5B)-C(1B)-C(2B)	113.1(11)
C(4A)-P(1A)-C(1A)	92.2(5)	O(2B)-C(1B)-P(1B)	109.3(7)
C(11A)-P(1A)-Pt(1)	118.5(4)	C(5B)-C(1B)-P(1B)	112.0(8)
C(4A)-P(1A)-Pt(1)	116.1(4)	C(2B)-C(1B)-P(1B)	109.4(8)
C(1A)-P(1A)-Pt(1)	120.4(4)	C(1B)-C(2B)-C(3B)	111.2(10)
C(11B)-P(1B)-C(4B)	100.3(5)	O(3B)-C(3B)-O(1B)	111.4(9)
C(11B)-P(1B)-C(1B)	105.4(6)	O(3B)-C(3B)-C(6B)	109.2(9)
C(4B)-P(1B)-C(1B)	93.2(5)	O(1B)-C(3B)-C(6B)	105.0(9)
C(11B)-P(1B)-Pt(1)	117.9(4)	O(3B)-C(3B)-C(2B)	107.7(9)
C(4B)-P(1B)-Pt(1)	119.9(3)	O(1B)-C(3B)-C(2B)	110.8(9)
C(1B)-P(1B)-Pt(1)	116.2(4)	C(6B)-C(3B)-C(2B)	112.9(10)
O(2A)-C(1A)-C(2A)	105.5(9)	O(1B)-C(4B)-C(7B)	105.4(9)
O(2A)-C(1A)-C(5A)	104.8(10)	O(1B)-C(4B)-C(8B)	109.9(9)
C(2A)-C(1A)-C(5A)	115.8(10)	C(7B)-C(4B)-C(8B)	111.3(10)
O(2A)-C(1A)-P(1A)	109.6(7)	O(1B)-C(4B)-P(1B)	108.4(7)
C(2A)-C(1A)-P(1A)	109.9(9)	C(7B)-C(4B)-P(1B)	113.0(8)
C(5A)-C(1A)-P(1A)	110.8(8)	C(8B)-C(4B)-P(1B)	108.7(8)
C(1A)-C(2A)-C(3A)	112.9(10)	C(9B)-C(8B)-C(4B)	109.6(10)
O(3A)-C(3A)-O(1A)	110.5(10)	O(3B)-C(9B)-O(2B)	110.1(10)
O(3A)-C(3A)-C(6A)	110.1(10)	O(3B)-C(9B)-C(10B)	108.9(10)
O(1A)-C(3A)-C(6A)	105.3(11)	O(2B)-C(9B)-C(10B)	106.2(9)
O(3A)-C(3A)-C(2A)	106.3(10)	O(3B)-C(9B)-C(8B)	108.8(10)
O(1A)-C(3A)-C(2A)	111.0(9)	O(2B)-C(9B)-C(8B)	110.6(9)
C(6A)-C(3A)-C(2A)	113.6(11)	C(10B)-C(9B)-C(8B)	112.4(11)
O(1A)-C(4A)-C(8A)	111.4(9)	C(12B)-C(11B)-P(1B)	115.9(8)
O(1A)-C(4A)-C(7A)	107.1(10)	C(12A)-C(12B)-C(13B)	119.2(12)
C(8A)-C(4A)-C(7A)	112.2(10)	C(12A)-C(12B)-C(11B)	120.0(11)
O(1A)-C(4A)-P(1A)	107.1(8)	C(13B)-C(12B)-C(11B)	120.6(11)
C(8A)-C(4A)-P(1A)	107.9(8)	C(14B)-C(13B)-C(12B)	121.7(13)
C(7A)-C(4A)-P(1A)	111.1(8)	C(13B)-C(14B)-C(14A)	119.1(12)
C(4A)-C(8A)-C(9A)	111.0(10)	C(4A)-O(1A)-C(3A)	116.2(9)
O(2A)-C(9A)-O(3A)	110.8(10)	C(9A)-O(2A)-C(1A)	116.3(9)
O(2A)-C(9A)-C(10A)	107.5(10)	C(3A)-O(3A)-C(9A)	111.2(8)
O(3A)-C(9A)-C(10A)	105.8(9)	C(3B)-O(1B)-C(4B)	115.9(8)
O(2A)-C(9A)-C(8A)	111.2(9)	C(1B)-O(2B)-C(9B)	117.9(8)
O(3A)-C(9A)-C(8A)	107.9(10)	C(9B)-O(3B)-C(3B)	111.6(8)
C(10A)-C(9A)-C(8A)	113.6(11)	Cl(2)-C(15)-Cl(2)#1	113.5(12)
C(12A)-C(11A)-P(1A)	114.3(8)	Cl(3)-C(16)-Cl(4)	108.5(12)

Symmetry transformations used to generate equivalent atoms: #1 -x+2,y,-z+3/2

Table A.12.4 Anisotropic displacement parameters ($Å^2 \times 10^3$) for *meso/rac*-(**3.43**). The anisotropic displacement factor exponent takes the form: $-2\Pi^2[h^2a^{*2}U_{11} + ... + 2hka^*b^*U_{12}]$

Atom	U_{11}	U_{22}	U_{33}	U_{23}	U_{13}	U_{12}
Pt(1)	30(1)	27(1)	16(1)	-2(1)	-1(1)	-1(1)
P(1A)	38(2)	27(2)	14(1)	0(1)	2(1)	0(1)
P(1B)	32(2)	30(2)	11(1)	-2(1)	1(1)	1(1)
Cl(1A)	47(2)	34(2)	34(2)	-3(1)	4(1)	-8(1)
Cl(1B)	63(2)	42(2)	19(1)	-11(1)	0(1)	-11(2)
C(1A)	34(6)	29(6)	25(6)	7(4)	3(5)	6(5)
C(2A)	47(8)	34(7)	25(6)	9(5)	16(5)	7(6)
C(3A)	45(7)	50(8)	15(6)	3(5)	7(5)	-3(6)
C(4A)	38(7)	46(7)	12(5)	-1(4)	1(5)	7(6)
C(5A)	40(8)	53(8)	27(7)	9(6)	3(5)	7(6)
C(6A)	59(9)	61(9)	19(6)	-2(6)	-2(6)	-6(7)
C(7A)	44(8)	54(9)	27(7)	0(6)	-3(6)	8(7)
C(8A)	49(7)	41(7)	17(6)	5(5)	0(5)	10(6)
C(9A)	46(8)	36(7)	23(6)	11(5)	5(5)	1(6)
C(10A)	60(9)	41(8)	40(8)	7(6)	5(7)	12(7)
C(11A)	58(8)	32(7)	11(5)	-1(4)	-2(5)	3(6)
C(12A)	37(7)	33(7)	28(7)	0(5)	3(5)	3(5)
C(13A)	47(8)	27(6)	34(7)	-1(5)	13(5)	0(6)
C(14A)	44(8)	41(8)	57(10)	-7(7)	9(7)	6(7)
C(1B)	38(7)	39(7)	18(6)	-4(5)	-1(5)	7(5)
C(2B)	44(7)	41(7)	12(5)	-2(4)	-1(5)	5(6)
C(3B)	43(7)	38(7)	10(5)	-4(4)	2(5)	7(5)
C(4B)	47(7)	25(6)	15(5)	1(4)	0(5)	-8(5)
C(5B)	55(8)	62(9)	14(6)	-2(5)	-5(5)	5(7)
C(6B)	47(8)	47(8)	16(6)	4(5)	2(5)	-9(6)
C(7B)	29(6)	40(7)	36(6)	-1(5)	-3(5)	2(5)
C(8B)	28(6)	39(7)	32(7)	-8(5)	-6(5)	-1(5)
C(9B)	36(7)	43(8)	24(6)	-4(5)	-4(5)	-1(6)
C(10B)	46(8)	55(9)	25(7)	-15(6)	7(5)	3(7)
C(11B)	41(7)	39(7)	30(7)	-8(5)	5(5)	-22(6)
C(12B)	37(6)	30(6)	17(6)	-1(4)	4(5)	-6(5)
C(13B)	65(10)	34(7)	26(7)	1(5)	-8(6)	1(7)
C(14B)	54(8)	26(6)	56(9)	0(6)	-5(7)	16(6)
O(1A)	39(5)	47(5)	18(4)	3(3)	5(3)	3(4)
O(2A)	37(5)	39(5)	35(5)	7(4)	-2(4)	0(4)
O(3A)	58(6)	47(6)	24(5)	19(4)	4(4)	1(5)
O(1B)	28(4)	39(4)	12(3)	-3(3)	-1(3)	-2(4)
O(2B)	36(5)	44(5)	16(4)	-9(3)	-3(3)	-3(4)
O(3B)	47(5)	37(5)	15(4)	-6(3)	7(3)	0(4)
C(15)	44(11)	77(15)	26(10)	0	-5(8)	0
C(16)	49(12)	121(18)	230(30)	-100(20)	-60(15)	27(13)
Cl(2)	79(3)	83(3)	33(2)	-5(2)	1(2)	-13(2)
Cl(3)	142(6)	149(6)	64(4)	-8(4)	7(3)	6(5)
Cl(4)	135(6)	193(8)	88(5)	-16(5)	-18(4)	6(6)

Table A.12.5 Hydrogen coordinates (x 10^4) and isotropic displacement parameters (Å^2 x 10^3) for *meso/rac*-(**3.43**)

Atom	x	y	z	U(eq)
H(2A1)	5470	8698	7015	42
H(2A2)	6076	9399	6811	42
H(5A1)	5081	8439	5709	60
H(5A2)	5165	9344	5953	60
H(5A3)	4651	8643	6240	60
H(6A1)	7261	8434	7806	69
H(6A2)	6314	8653	7841	69
H(6A3)	6941	9320	7619	69
H(7A1)	8558	8785	6162	62
H(7A2)	8512	7887	5903	62
H(7A3)	8763	7974	6488	62
H(8A1)	7642	6901	6565	43
H(8A2)	7193	7034	6031	43
H(10A)	5643	6295	6916	70
H(10B)	6570	5994	6912	70
H(10C)	6065	6031	6393	70
H(11A)	6944	9896	6449	40
H(11B)	7669	9906	6045	40
H(13A)	5725	10656	6290	43
H(14A)	5003	11601	5812	57
H(2B1)	7833	10930	4177	39
H(2B2)	7782	10671	3590	39
H(5B1)	6464	10018	3642	65
H(5B2)	6372	10298	4222	65
H(5B3)	6273	9342	4071	65
H(6B1)	9399	11399	4091	55
H(6B2)	9168	11293	3504	55
H(6B3)	9945	10824	3731	55
H(7B1)	9868	9129	5018	52
H(7B2)	9201	8457	5179	52
H(7B3)	9120	9395	5371	52
H(8B1)	9451	8413	4171	40
H(8B2)	8557	8081	4305	40
H(10D)	8407	8504	2962	63
H(10E)	8395	7762	3367	63
H(10F)	9239	8187	3211	63
H(11C)	8095	10307	5415	44
H(11D)	7982	10822	4902	44
H(13B)	6738	11540	4740	50
H(14B)	5523	12059	5028	54
H(15A)	9851	10145	7789	59
H(15B)	10149	10145	7211	59
H(16A)	6481	2436	7619	160
H(16B)	6859	1981	8107	160

A.13 Crystal data and structure refinement for *o*-phenylene diphospha-adamantane (5.6)

This crystal structure determination was carried out by Miss H. Phetmung under the supervision of Prof. A. G. Orpen.

Identification code	rip59	
Empirical formula	$C_{16}H_{20}O_2P_2$	
Formula weight	306.26	
Temperature	173(2) K	
Wavelength	0.71073 Å	
Crystal system	Orthorhombic	
Space group	Pnma	
Unit cell dimensions	a = 17.491(3) Å	α = 90.00°
	b = 12.133(2) Å	β = 90.00°
	c = 7.347(2) Å	γ = 90.00°
Volume	1559.1(6) $Å^3$	
Z	4	
Density (calculated)	1.305 Mg/m^3	
Absorption coefficient	0.277 mm^{-1}	
F(000)	648	
Crystal size	0.30 x 0.30 x 0.20 mm	
q range for data collection	2.33° - 27.50°	
Index ranges	-11<=h<=22, -15<=k<=15, -9<=l<=9	
Reflections collected	9410	
Independent reflections	1883 [$R_{(int)}$ = 0.0596]	
Refinement method	Full-matrix least-squares on F^2	
Data/restraints/parameters	1882/0/115	
Goodness-of-fit on F^2*	1.083	
Final R indices [$I > 2\sigma(I)$]*	R_1 = 0.0466, wR_2 = 0.0906 [1501 data]	
R indices (all data)*	R_1 = 0.0649, wR_2 = 0.1008 [1883 data]	
Weighting scheme	calc $w = 1/[\sigma^2(F_o^2) + (0.0304P)^2 + 1.5904P]$	
	where $P = (\text{Max } F_o^2, 0 + 2F_c^2)/3$	
Largest diff. peak and hole	0.332 and -0.264 $e.Å^{-3}$	

*$wR_2 = [\Sigma w\Delta^2/\Sigma wF_o^4]^{0.5}$; $S = [\Sigma w\Delta^2/(N.O. - N.V.)]^{0.5}$; $\Delta = F_o^2 - F_c^2$;
$R_1 = \Sigma |F_o - F_c|/\Sigma |F_o|$; N.O. = data + restraints; N.V. = parameters

Table A.13.1 Atomic coordinates (x 10^4) and equivalent isotropic displacement parameters ($Å^2$ x 10^2) for (**5.6**). U(eq) is defined as one third of the trace of the orthogonalized U_{ij} tensor.

Atom	x	y	z	U(eq)
P(1)	2846(1)	1261(1)	9113(1)	24(1)
O(1)	4381(1)	1522(1)	9379(2)	24(1)
C(1)	1002(1)	1931(2)	12471(3)	34(1)
C(2)	1546(1)	1349(2)	11479(3)	30(1)
C(3)	2101(1)	1920(2)	10489(3)	23(1)
C(4)	3725(1)	1463(2)	10595(3)	23(1)
C(5)	4420(2)	2500	8289(4)	24(1)
C(6)	3792(2)	2500	6852(4)	28(1)
C(7)	2986(2)	2500	7655(4)	24(1)
C(8)	3718(2)	2500	11755(4)	23(1)
C(9)	3849(1)	436(2)	11734(3)	36(1)
C(10)	5213(2)	2500	7450(5)	34(1)
C(11)	2393(2)	2500	6113(5)	41(1)

Table A.13.2 Bond lengths (Å) for (**5.6**)

Atom	length(Å)	Atom	length(Å)
P(1)-C(3)	1.834(2)	C(5)-C(6)	1.523(4)
P(1)-C(7)	1.862(2)	C(6)-C(7)	1.528(4)
P(1)-C(4)	1.899(2)	C(6)-H(6A)	0.99
P(1)-P(1)#1	3.0070(11)	C(6)-H(6B)	0.99
O(1)-C(5)	1.433(2)	C(7)-C(11)	1.537(4)
O(1)-C(4)	1.457(2)	C(7)-P(1)#1	1.862(2)
C(1)-C(1)#1	1.380(5)	C(8)-C(4)#1	1.520(2)
C(1)-C(2)	1.391(3)	C(8)-H(8A)	0.99
C(1)-H(1A)	0.95	C(8)-H(8B)	0.99
C(2)-C(3)	1.396(3)	C(9)-H(9A)	0.98
C(2)-H(2A)	0.95	C(9)-H(9B)	0.98
C(3)-C(3)#1	1.407(4)	C(9)-H(9C)	0.98
C(4)-C(9)	1.516(3)	C(10)-H(10C)	0.94(4)
C(4)-C(8)	1.520(2)	C(10)-H(10A)	0.99(2)
C(5)-O(1)#1	1.433(2)	C(11)-H(11A)	0.93(4)
C(5)-C(10)	1.518(4)	C(11)-H(11B)	1.03(3)

Table A.13.3 Bond angles (°) for (**5.6**)

Atom	angle(°)	Atom	angle(°)
C(3)-P(1)-C(7)	93.36(10)	C(5)-C(6)-H(6A)	108.89(8)
C(3)-P(1)-C(4)	101.71(9)	C(7)-C(6)-H(6A)	108.89(8)
C(7)-P(1)-C(4)	96.82(10)	C(5)-C(6)-H(6B)	108.89(8)
C(3)-P(1)-P(1)#1	64.13(6)	C(7)-C(6)-H(6B)	108.89(8)
C(7)-P(1)-P(1)#1	36.16(7)	H(6A)-C(6)-H(6B)	107.7
C(4)-P(1)-P(1)#1	82.59(6)	C(6)-C(7)-C(11)	109.8(2)
C(5)-O(1)-C(4)	114.9(2)	C(6)-C(7)-P(1)#1	110.11(12)
C(1)#1-C(1)-C(2)	120.49(14)	C(11)-C(7)-P(1)#1	109.57(13)
C(1)#1-C(1)-H(1A)	119.753(6)	C(6)-C(7)-P(1)	110.11(12)
C(2)-C(1)-H(1A)	119.75(14)	C(11)-C(7)-P(1)	109.57(13)
C(1)-C(2)-C(3)	119.7(2)	P(1)#1-C(7)-P(1)	107.7(2)
C(1)-C(2)-H(2A)	120.13(14)	C(4)-C(8)-C(4)#1	111.8(2)
C(3)-C(2)-H(2A)	120.13(13)	C(4)-C(8)-H(8A)	109.26(13)
C(2)-C(3)-C(3)#1	119.75(13)	C(4)-C(8)-H(8B)	109.26(13)
C(2)-C(3)-P(1)	124.4(2)	C(4)#1-C(8)-H(8B)	109.26(13)
C(3)#1-C(3)-P(1)	115.87(6)	H(8A)-C(8)-H(8B)	107.9
O(1)-C(4)-C(9)	105.4(2)	C(4)-C(9)-H(9A)	109.47(13)
O(1)-C(4)-C(8)	108.0(2)	C(4)-C(9)-H(9B)	109.47(12)
C(9)-C(4)-C(8)	111.8(2)	H(9A)-C(9)-H(9B)	109.5
O(1)-C(4)-P(1)	107.00(13)	C(4)-C(9)-H(9C)	109.47(12)
C(9)-C(4)-P(1)	109.0(2)	H(9A)-C(9)-H(9C)	109.5
C(8)-C(4)-P(1)	115.0(2)	H(9B)-C(9)-H(9C)	109.5
O(1)-C(5)-O(1)#1	111.8(2)	C(5)-C(10)-H(10C)	107(2)
O(1)-C(5)-C(10)	105.7(2)	C(5)-C(10)-H(10A)	110.5(14)
O(1)#1-C(5)-C(10)	105.7(2)	H(10C)-C(10)-H(10A)	112(2)
O(1)-C(5)-C(6)	110.7(2)	C(7)-C(11)-H(11A)	112(2)
O(1)#1-C(5)-C(6)	110.7(2)	C(7)-C(11)-H(11B)	109(2)
C(10)-C(5)-C(6)	112.2(3)	H(11A)-C(11)-H(11B)	108(2)
C(5)-C(6)-C(7)	113.4(2)		

Symmetry transformations used to generate equivalent atoms: #1 x,-y+1/2,z

Table A.13.4 Anisotropic displacement parameters ($Å^2$ x 10^3) for (**5.6**). The anisotropic displacement factor exponent takes the form: $-2\Pi^2[h^2a^{*2}U_{11} + ... + 2hka^*b^*U_{12}]$

Atom	U_{11}	U_{22}	U_{33}	U_{23}	U_{13}	U_{12}
P(1)	20(1)	25(1)	28(1)	-6(1)	1(1)	-1(1)
O(1)	18(1)	29(1)	25(1)	1(1)	3(1)	4(1)
C(1)	19(1)	60(2)	24(1)	7(1)	1(1)	-5(1)
C(2)	21(1)	38(1)	31(1)	7(1)	-3(1)	-6(1)
C(3)	17(1)	29(1)	22(1)	1(1)	-2(1)	-1(1)
C(4)	18(1)	25(1)	25(1)	3(1)	2(1)	1(1)
C(5)	17(1)	34(2)	21(1)	0	2(1)	0
C(6)	21(1)	44(2)	18(1)	0	1(1)	0
C(7)	18(1)	39(2)	17(1)	0	-2(1)	0
C(8)	20(1)	31(2)	17(1)	0	-1(1)	0
C(9)	31(1)	31(1)	46(1)	14(1)	1(1)	4(1)
C(10)	19(2)	57(2)	27(2)	0	6(1)	0
C(11)	21(2)	76(3)	25(2)	0	-5(1)	0

Table A.13.5 Hydrogen coordinates (x 10^4) and isotropic displacement parameters ($Å^2$ x 10^3) for (**5.6**)

Atom	x	y	z	U(eq)
H(1A)	627(1)	1543(2)	13153(3)	41
H(2A)	1540(1)	566(2)	11475(3)	36
H(6A)	3853(2)	1841	6071(4)	33
H(6B)	3853(2)	3159	6071(4)	33
H(8A)	3256(2)	2500	12533(4)	27
H(8B)	4171(2)	2500	12563(4)	27
H(9A)	3909(9)	-203(3)	10931(3)	54
H(9B)	3407(4)	321(8)	12532(16)	54
H(9C)	4310(5)	526(6)	12476(16)	54
H(10C)	5564(22)	2500	8410(53)	45(11)
H(10A)	5277(14)	3144(20)	6632(33)	39(7)
H(11A)	1891(21)	2500	6549(46)	32(9)
H(11B)	2462(14)	1805(21)	5334(35)	47(8)

A.14 Crystal data and structure refinement for bicyclic diphosphine (5.7)

This crystal structure determination was carried out by Miss H. Phetmung under the supervision of Prof. A. G. Orpen.

Identification code	rip70	
Empirical formula	$C_{24}H_{32}F_6O_5P_2$	
Formula weight	576.44	
Temperature	173(2) K	
Wavelength	0.71073 Å	
Crystal system	Monoclinic	
Space group	C2/c	
Unit cell dimensions	a = 12.959(2)Å	α = 90.000°
	b = 12.429(3)Å	β = 95.783(10)°
	c = 16.461(3)Å	γ = 90.000°
Volume	2637.8(9) $Å^3$	
Z	4	
Density (calculated)	1.451 Mg/m^3	
Absorption coefficient	0.241 mm^{-1}	
F(000)	1200	
Crystal size	0.40 x 0.38 x 0.20 mm (pale yellow)	
θ range for data collection	2.28° - 27.49°	
Index ranges	-16<=h<=16, -16<=k<=16, -21<=l<=21	
Reflections collected	13019	
Independent reflections	3027 [$R_{(int)}$ = 0.0385]	
Refinement method	Full-matrix least-squares on F^2	
Data/restraints/parameters	3025/0/170	
Goodness-of-fit on F^2*	0.994	
Final R indices [$I > 2\sigma(I)$]*	R_1 = 0.0430, wR_2 = 0.1061[2464 data]	
R indices (all data)	R_1 = 0.0583, wR_2 = 0.1209[3027 data]	
Weighting scheme	calc $w = 1/[\sigma^2(F_o^2) + (0.0509P)^2 + 5.4107P]$	
	where $P = (\text{Max } F_o^2, 0 + 2F_c^2)/3$	
Largest diff. peak and hole	0.560 and -0.390 $e.Å^{-3}$	

*$wR_2 = [\Sigma w\Delta^2/\Sigma wF_o^4]^{0.5}$; $S = [\Sigma w\Delta^2/(N.O. - N.V.)]^{0.5}$; $\Delta = F_o^2 - F_c^2$;
$R_1 = \Sigma |F_o - F_c|/\Sigma |F_o|$; N.O. = data + restraints; N.V. = parameters

Table A.14.1 Atomic coordinates (x 10^4) and equivalent isotropic displacement parameters ($Å^2$ x 10^2) for (**5.7**). U(eq) is defined as one third of the trace of the orthogonalized U_{ij} tensor.

Atom	x	y	z	U(eq)
P(1)	1339(1)	10993(1)	2319(1)	27(1)
F(1)	1731(1)	12208(1)	4045(1)	50(1)
F(2)	2322(1)	10826(1)	4723(1)	52(1)
F(3)	3085(1)	11385(1)	3705(1)	52(1)
O(1)	0	9264(2)	2500	30(1)
O(2)	2040(1)	9515(1)	3381(1)	37(1)
O(4)	1240(2)	7740(1)	4098(1)	52(1)
C(1)	499(2)	14127(2)	2390(2)	42(1)
C(2)	1005(2)	13159(2)	2288(1)	34(1)
C(3)	517(2)	12176(2)	2402(1)	27(1)
C(4)	445(2)	9882(2)	1887(1)	29(1)
C(5)	1131(2)	9093(2)	1475(2)	40(1)
C(6)	1466(2)	10485(2)	3405(1)	30(1)
C(7)	413(2)	10328(2)	3744(1)	31(1)
C(8)	2148(2)	11232(2)	3968(1)	38(1)
C(11)	969(2)	6802(2)	3610(2)	46(1)
C(12)	1055(4)	5897(2)	4192(2)	80(1)
C(13)	817(3)	6358(3)	4978(2)	76(1)
C(14)	1033(3)	7523(2)	4922(2)	62(1)

Table A.14.2 Bond lengths (Å) for (**5.7**)

Atom	length(Å)	Atom	length(Å)
P(1)-C(3)	1.829(2)	C(4)-C(7)#1	1.546(3)
P(1)-C(6)	1.888(2)	C(5)-H(5A)	0.98
P(1)-C(4)	1.894(2)	C(5)-H(5B)	0.98
P(1)-P(1)#1	3.5807(11)	C(5)-H(5C)	0.98
F(1)-C(8)	1.338(3)	C(6)-C(8)	1.528(3)
F(2)-C(8)	1.339(3)	C(6)-C(7)	1.538(3)
F(3)-C(8)	1.343(3)	C(7)-C(4)#1	1.546(3)
O(1)-C(4)	1.434(2)	C(7)-H(7A)	0.99
O(1)-C(4)#1	1.434(2)	C(7)-H(7B)	0.99
O(2)-C(6)	1.419(2)	C(11)-C(12)	1.475(4)
O(2)-H(2)	0.84	C(11)-H(11A)	0.99
O(4)-C(14)	1.435(3)	C(11)-H(11B)	0.99
O(4)-C(11)	1.439(3)	C(12)-C(13)	1.476(5)
C(1)-C(1)#1	1.378(5)	C(12)-H(12A)	0.99
C(1)-C(2)	1.389(3)	C(12)-H(12B)	0.99
C(1)-H(1A)	0.95	C(13)-C(14)	1.479(4)
C(2)-C(3)	1.397(3)	C(13)-H(13A)	0.99
C(2)-H(2B)	0.95	C(13)-H(13B)	0.99
C(3)-C(3)#1	1.410(4)	C(14)-H(14A)	0.99
C(4)-C(5)	1.527(3)	C(14)-H(14B)	0.99

Table A.14.3 Bond angles (°) for (**5.7**)

Atoms	angle(°)	Atoms	angle(°)
C(3)-P(1)-C(6)	101.21(9)	C(6)-C(7)-C(4)#1	114.0(2)
C(3)-P(1)-C(4)	105.97(9)	C(6)-C(7)-H(7A)	108.76(11)
C(6)-P(1)-C(4)	95.89(9)	C(4)#1-C(7)-H(7A)	108.76(10)
C(3)-P(1)-P(1)#1	53.54(6)	C(6)-C(7)-H(7B)	108.76(11)
C(6)-P(1)-P(1)#1	80.54(6)	C(4)#1-C(7)-H(7B)	108.76(11)
C(4)-P(1)-P(1)#1	59.72(6)	H(7A)-C(7)-H(7B)	107.7
C(4)-O(1)-C(4)#1	115.2(2)	F(1)-C(8)-F(2)	106.6(2)
C(6)-O(2)-H(2)	109.47(10)	F(1)-C(8)-F(3)	106.8(2)
C(14)-O(4)-C(11)	108.5(2)	F(2)-C(8)-F(3)	106.2(2)
C(1)#1-C(1)-C(2)	119.94(13)	F(1)-C(8)-C(6)	113.2(2)
C(1)#1-C(1)-H(1A)	120.030(10)	F(2)-C(8)-C(6)	111.5(2)
C(2)-C(1)-H(1A)	120.03(13)	F(3)-C(8)-C(6)	112.1(2)
C(1)-C(2)-C(3)	121.0(2)	O(4)-C(11)-C(12)	104.8(2)
C(1)-C(2)-H(2B)	119.48(13)	O(4)-C(11)-H(11A)	110.78(13)
C(3)-C(2)-H(2B)	119.48(12)	C(12)-C(11)-H(11A)	110.8(2)
C(2)-C(3)-C(3)#1	118.98(12)	O(4)-C(11)-H(11B)	110.78(14)
C(2)-C(3)-P(1)	114.7(2)	C(12)-C(11)-H(11B)	110.8(2)
C(3)#1-C(3)-P(1)	126.26(6)	H(11A)-C(11)-H(11B)	108.9
O(1)-C(4)-C(5)	105.2(2)	C(11)-C(12)-C(13)	105.4(3)
O(1)-C(4)-C(7)#1	110.60(14)	C(11)-C(12)-H(12A)	110.7(2)
C(5)-C(4)-C(7)#1	110.1(2)	C(13)-C(12)-H(12A)	110.7(2)
O(1)-C(4)-P(1)	113.64(13)	C(11)-C(12)-H(12B)	110.7(2)
C(5)-C(4)-P(1)	105.85(14)	C(13)-C(12)-H(12B)	110.7(2)
C(7)#1-C(4)-P(1)	111.20(14)	H(12A)-C(12)-H(12B)	108.8
C(4)-C(5)-H(5A)	109.47(13)	C(12)-C(13)-C(14)	105.5(2)
C(4)-C(5)-H(5B)	109.47(12)	C(12)-C(13)-H(13A)	110.6(2)
H(5A)-C(5)-H(5B)	109.5	C(14)-C(13)-H(13A)	110.6(2)
C(4)-C(5)-H(5C)	109.47(11)	C(12)-C(13)-H(13B)	110.6(2)
H(5A)-C(5)-H(5C)	109.5	C(14)-C(13)-H(13B)	110.6(2)
H(5B)-C(5)-H(5C)	109.5	H(13A)-C(13)-H(13B)	108.8
O(2)-C(6)-C(8)	105.1(2)	O(4)-C(14)-C(13)	107.3(2)
O(2)-C(6)-C(7)	112.9(2)	O(4)-C(14)-H(14A)	110.3(2)
C(8)-C(6)-C(7)	109.7(2)	C(13)-C(14)-H(14A)	110.3(2)
O(2)-C(6)-P(1)	104.68(13)	O(4)-C(14)-H(14B)	110.3(2)
C(8)-C(6)-P(1)	111.1(2)	C(13)-C(14)-H(14B)	110.3(2)
C(7)-C(6)-P(1)	112.93(14)	H(14A)-C(14)-H(14B)	108.5

Symmetry transformations used to generate equivalent atoms: #1 -x,y,-z+1/2

Table A.14.4 Anisotropic displacement parameters ($Å^2$ x 10^3) for (**5.7**). The anisotropic displacement factor exponent takes the form: $-2\Pi^2[h^2a^{*2}U_{11} + ... + 2hka^*b^*U_{12}]$

Atom	U_{11}	U_{22}	U_{33}	U_{23}	U_{13}	U_{12}
P(1)	23(1)	30(1)	31(1)	-1(1)	9(1)	-2(1)
F(1)	57(1)	42(1)	50(1)	-13(1)	-10(1)	5(1)
F(2)	52(1)	67(1)	36(1)	7(1)	-5(1)	3(1)
F(3)	33(1)	68(1)	55(1)	-5(1)	2(1)	-14(1)
O(1)	28(1)	24(1)	40(1)	0	15(1)	0
O(2)	28(1)	34(1)	51(1)	5(1)	10(1)	9(1)
O(4)	76(1)	34(1)	48(1)	4(1)	12(1)	3(1)
C(1)	56(1)	27(1)	42(1)	3(1)	-1(1)	-7(1)
C(2)	37(1)	33(1)	33(1)	3(1)	2(1)	-7(1)
C(3)	28(1)	28(1)	26(1)	1(1)	2(1)	-1(1)
C(4)	25(1)	30(1)	33(1)	-3(1)	13(1)	-2(1)
C(5)	34(1)	39(1)	50(1)	-14(1)	17(1)	0(1)
C(6)	26(1)	30(1)	34(1)	2(1)	6(1)	5(1)
C(7)	29(1)	35(1)	30(1)	6(1)	9(1)	6(1)
C(8)	36(1)	43(1)	36(1)	2(1)	2(1)	3(1)
C(11)	51(2)	46(1)	41(1)	-2(1)	10(1)	4(1)
C(12)	145(4)	41(2)	51(2)	3(1)	-7(2)	-22(2)
C(13)	109(3)	74(2)	47(2)	10(2)	14(2)	-24(2)
C(14)	96(2)	49(2)	42(1)	-2(1)	10(2)	13(2)

Table A.14.5 Hydrogen coordinates (x 10^4) and isotropic displacement parameters ($Å^2$ x 10^3) for (**5.7**)

Atom	x	y	z	U(eq)
H(2)	1705(10)	9010(5)	3569(17)	56
H(1A)	840(2)	14789(2)	2308(2)	51
H(2B)	1694(2)	13165(2)	2138(1)	41
H(5A)	1705(8)	8860(11)	1869(3)	60
H(5B)	1409(11)	9448(5)	1012(7)	60
H(5C)	719(4)	8467(7)	1280(10)	60
H(7A)	182(2)	11029(2)	3947(1)	37
H(7B)	504(2)	9829(2)	4214(1)	37
H(11A)	1451(2)	6707(2)	3186(2)	55
H(11B)	253(2)	6862(2)	3340(2)	55
H(12A)	1764(4)	5592(2)	4240(2)	96
H(12B)	554(4)	5322(2)	4013(2)	96
H(13A)	1260(3)	6030(3)	5437(2)	91
H(13B)	81(3)	6235(3)	5063(2)	91
H(14A)	428(3)	7947(2)	5061(2)	75
H(14B)	1641(3)	7721(2)	5307(2)	75

A.15 Crystal data and structure refinement for 1,1'-ferrocene-diphospha-adamantane (5.8)

This crystal structure determination was carried out by Miss H. Phetmung under the supervision of Prof. A. G. Orpen.

Identification code	rip93s	
Empirical formula	$C_{20}H_{24}FeO_2P_2$	
Formula weight	414.18	
Temperature	173(2) K	
Wavelength	0.71073 Å	
Crystal system	Orthorhombic	
Space group	Fdd2	
Unit cell dimensions	a = 15.301(2) Å	α = 90.00°
	b = 47.793(8) Å	β = 90.00°
	c = 9.8497(13) Å	γ = 90.00°
Volume	7203(2) $Å^3$	
Z	16	
Density (calculated)	1.528 Mg/m^3	
Absorption coefficient	1.026 mm^{-1}	
F(000)	3456	
Crystal size	0.40 x 0.20 x 0.18 mm (yellow)	
q range for data collection	1.70 - 27.48°.	
Index ranges	-19<=h<=18, -61<=k<=35, -12<=l<=12	
Reflections collected	10602	
Independent reflections	4037 [$R_{(int)}$ = 0.0377]	
Refinement method	Full-matrix least-squares on F^2	
Data/restraints/parameters	4037/1/231	
Goodness-of-fit on F^2(S)*	0.934	
Final R indices [$I > 2\sigma(I)$]*	R_1 = 0.0304, wR_2 = 0.0582[3443 data]	
R indices (all data)*	R_1 = 0.0411, wR_2 = 0.0615[4037 data]	
Weighting scheme	calc $w = 1/[\sigma^2(F_o^2) + (0.0267P)^2 + 0.000P]$	
	where $P = Max(F_o^2, 0 + 2F_c^2)/3$	
Absolute structure parameter	0.025(13)	
Largest diff. peak and hole	0.287 and -0.423 e.$Å^{-3}$	

*$wR_2 = [\Sigma w\Delta^2/\Sigma wF_o^4]^{0.5}$; $S = [\Sigma w\Delta^2/(N.O. - N.V.)]^{0.5}$; $\Delta = F_o^2 - F_c^2$;
$R_1 = \Sigma |F_o - F_c|/\Sigma |F_o|$; N.O. = data + restraints; N.V. = parameters

Table A.15.1 Atomic coordinates (x 10^4) and equivalent isotropic displacement parameters ($Å^2$ x 10^2) for (**5.8**). U(eq) is defined as one third of the trace of the orthogonalized U_{ij} tensor.

Atom	x	y	z	U(eq)
Fe(1)	2307(1)	798(1)	2078(1)	19(1)
P(1)	2382(1)	317(1)	-588(1)	19(1)
P(2)	3886(1)	793(1)	-461(1)	18(1)
O(1)	2528(1)	433(1)	-3210(2)	25(1)
O(2)	3615(1)	777(1)	-3118(2)	24(1)
C(1)	1572(2)	524(1)	3210(3)	32(1)
C(2)	2102(2)	377(1)	2274(3)	26(1)
C(3)	1897(2)	471(1)	930(3)	20(1)
C(4)	1210(2)	675(1)	1077(3)	22(1)
C(5)	1021(2)	706(1)	2477(3)	31(1)
C(6)	3106(2)	1027(1)	3330(3)	27(1)
C(7)	3606(2)	866(1)	2399(3)	23(1)
C(8)	3358(2)	939(1)	1030(3)	18(1)
C(9)	2715(2)	1159(1)	1171(3)	20(1)
C(10)	2562(2)	1207(1)	2569(3)	25(1)
C(11)	2049(2)	545(1)	-2045(3)	22(1)
C(12)	3456(2)	483(1)	-3189(3)	24(1)
C(13)	3235(2)	919(1)	-1959(3)	21(1)
C(14)	3565(2)	416(1)	-572(3)	19(1)
C(15)	3891(2)	330(1)	-2005(3)	24(1)
C(16)	2252(2)	856(1)	-1949(3)	21(1)
C(17)	1089(2)	496(1)	-2403(3)	30(1)
C(18)	3797(2)	387(1)	-4537(3)	34(1)
C(19)	3408(2)	1227(1)	-2209(3)	26(1)
C(20)	4053(2)	244(1)	495(3)	28(1)

Table A.15.2 Bond lengths (Å) for (**5.8**)

Atom	length(Å)	Atom	length(Å)
Fe(1)-C(8)	2.025(3)	O(2)-C(13)	1.448(3)
Fe(1)-C(3)	2.029(3)	C(1)-C(5)	1.410(4)
Fe(1)-C(4)	2.034(3)	C(1)-C(2)	1.415(4)
Fe(1)-C(7)	2.039(3)	C(2)-C(3)	1.431(4)
Fe(1)-C(9)	2.040(3)	C(3)-C(4)	1.442(4)
Fe(1)-C(2)	2.045(3)	C(4)-C(5)	1.417(4)
Fe(1)-C(6)	2.051(3)	C(6)-C(10)	1.414(4)
Fe(1)-C(10)	2.053(3)	C(6)-C(7)	1.420(4)
Fe(1)-C(1)	2.055(3)	C(7)-C(8)	1.443(4)
Fe(1)-C(5)	2.055(3)	C(8)-C(9)	1.446(4)
P(1)-C(3)	1.823(3)	C(9)-C(10)	1.417(4)
P(1)-C(14)	1.872(2)	C(11)-C(16)	1.525(4)
P(1)-C(11)	1.870(3)	C(11)-C(17)	1.528(3)
P(2)-C(8)	1.814(3)	C(12)-C(18)	1.498(4)
P(2)-C(14)	1.872(2)	C(12)-C(15)	1.529(4)
P(2)-C(13)	1.878(3)	C(13)-C(19)	1.515(4)
O(1)-C(12)	1.439(3)	C(13)-C(16)	1.533(3)
O(1)-C(11)	1.462(3)	C(14)-C(20)	1.529(4)
O(2)-C(12)	1.430(3)	C(14)-C(15)	1.552(4)

Table A.15.3 Bond angles (°) for (**5.8**)

Atoms	angle(°)	Atoms	angle(°)
C(8)-Fe(1)-C(3)	102.57(11)	C(3)-C(2)-Fe(1)	68.8(2)
C(8)-Fe(1)-C(4)	120.29(11)	C(2)-C(3)-C(4)	106.2(2)
C(3)-Fe(1)-C(4)	41.56(11)	C(2)-C(3)-P(1)	122.9(2)
C(8)-Fe(1)-C(7)	41.60(10)	C(4)-C(3)-P(1)	130.6(2)
C(3)-Fe(1)-C(7)	120.72(11)	C(2)-C(3)-Fe(1)	70.0(2)
C(4)-Fe(1)-C(7)	157.84(10)	C(4)-C(3)-Fe(1)	69.4(2)
C(8)-Fe(1)-C(9)	41.66(11)	P(1)-C(3)-Fe(1)	129.88(14)
C(3)-Fe(1)-C(9)	120.13(11)	C(5)-C(4)-C(3)	108.6(3)
C(4)-Fe(1)-C(9)	106.55(12)	C(5)-C(4)-Fe(1)	70.5(2)
C(7)-Fe(1)-C(9)	68.56(11)	C(3)-C(4)-Fe(1)	69.0(2)
C(8)-Fe(1)-C(2)	119.80(11)	C(1)-C(5)-C(4)	108.1(3)
C(3)-Fe(1)-C(2)	41.14(11)	C(1)-C(5)-Fe(1)	70.0(2)
C(4)-Fe(1)-C(2)	68.54(11)	C(4)-C(5)-Fe(1)	68.9(2)
C(7)-Fe(1)-C(2)	107.00(11)	C(10)-C(6)-C(7)	107.8(2)
C(9)-Fe(1)-C(2)	156.88(11)	C(10)-C(6)-Fe(1)	69.9(2)
C(8)-Fe(1)-C(6)	69.91(10)	C(7)-C(6)-Fe(1)	69.2(2)
C(3)-Fe(1)-C(6)	158.40(12)	C(6)-C(7)-C(8)	109.3(2)
C(4)-Fe(1)-C(6)	159.57(11)	C(6)-C(7)-Fe(1)	70.2(2)
C(7)-Fe(1)-C(6)	40.63(10)	C(8)-C(7)-Fe(1)	68.7(2)
C(9)-Fe(1)-C(6)	68.32(11)	C(7)-C(8)-C(9)	105.4(2)
C(2)-Fe(1)-C(6)	124.00(12)	C(7)-C(8)-P(2)	123.1(2)
C(8)-Fe(1)-C(10)	69.68(11)	C(9)-C(8)-P(2)	131.2(2)
C(3)-Fe(1)-C(10)	157.60(11)	C(7)-C(8)-Fe(1)	69.7(2)
C(4)-Fe(1)-C(10)	123.13(11)	C(9)-C(8)-Fe(1)	69.71(14)
C(7)-Fe(1)-C(10)	68.06(11)	P(2)-C(8)-Fe(1)	129.66(14)
C(9)-Fe(1)-C(10)	40.50(10)	C(10)-C(9)-C(8)	109.0(3)
C(2)-Fe(1)-C(10)	160.82(11)	C(10)-C(9)-Fe(1)	70.3(2)
C(6)-Fe(1)-C(10)	40.31(11)	C(8)-C(9)-Fe(1)	68.6(2)
C(8)-Fe(1)-C(1)	157.35(12)	C(6)-C(10)-C(9)	108.5(3)
C(3)-Fe(1)-C(1)	69.03(11)	C(6)-C(10)-Fe(1)	69.8(2)
C(4)-Fe(1)-C(1)	68.07(12)	C(9)-C(10)-Fe(1)	69.3(2)
C(7)-Fe(1)-C(1)	123.48(13)	O(1)-C(11)-C(16)	107.6(2)
C(9)-Fe(1)-C(1)	160.67(12)	O(1)-C(11)-C(17)	104.2(2)
C(2)-Fe(1)-C(1)	40.38(11)	C(16)-C(11)-C(17)	111.0(2)
C(6)-Fe(1)-C(1)	109.85(12)	O(1)-C(11)-P(1)	104.7(2)
C(10)-Fe(1)-C(1)	125.67(12)	C(16)-C(11)-P(1)	117.6(2)
C(8)-Fe(1)-C(5)	158.25(11)	C(17)-C(11)-P(1)	110.5(2)
C(3)-Fe(1)-C(5)	69.27(11)	O(2)-C(12)-O(1)	109.3(2)
C(4)-Fe(1)-C(5)	40.55(11)	O(2)-C(12)-C(18)	106.6(2)
C(7)-Fe(1)-C(5)	159.78(11)	O(1)-C(12)-C(18)	106.3(2)
C(9)-Fe(1)-C(5)	123.89(12)	O(2)-C(12)-C(15)	111.0(2)
C(2)-Fe(1)-C(5)	67.96(12)	O(1)-C(12)-C(15)	111.2(2)
C(6)-Fe(1)-C(5)	124.70(11)	C(18)-C(12)-C(15)	112.1(2)
C(10)-Fe(1)-C(5)	109.88(12)	O(2)-C(13)-C(19)	104.7(2)
C(1)-Fe(1)-C(5)	40.13(12)	O(2)-C(13)-C(16)	107.9(2)
C(3)-P(1)-C(14)	106.58(13)	C(19)-C(13)-C(16)	111.2(2)
C(3)-P(1)-C(11)	106.60(12)	O(2)-C(13)-P(2)	104.9(2)
C(14)-P(1)-C(11)	97.12(12)	C(19)-C(13)-P(2)	110.2(2)
C(8)-P(2)-C(14)	107.47(12)	C(16)-C(13)-P(2)	116.9(2)
C(8)-P(2)-C(13)	106.12(11)	C(20)-C(14)-C(15)	109.0(2)
C(14)-P(2)-C(13)	97.05(12)	C(20)-C(14)-P(1)	110.0(2)
C(12)-O(1)-C(11)	115.0(2)	C(15)-C(14)-P(1)	103.6(2)

Atoms	angle(°)	Atoms	angle(°)
C(12)-O(2)-C(13)	115.4(2)	C(20)-C(14)-P(2)	110.5(2)
C(5)-C(1)-C(2)	108.4(3)	C(15)-C(14)-P(2)	103.0(2)
C(5)-C(1)-Fe(1)	69.9(2)	P(1)-C(14)-P(2)	119.75(12)
C(2)-C(1)-Fe(1)	69.4(2)	C(12)-C(15)-C(14)	115.3(2)
C(1)-C(2)-C(3)	108.8(3)	C(11)-C(16)-C(13)	113.0(2)
C(1)-C(2)-Fe(1)	70.2(2)		

Table A.15.4 Anisotropic displacement parameters ($Å^2$ x 10^3) for (**5.8**). The anisotropic displacement factor exponent takes the form:

$-2\Pi^2[h^2a^{*2}U_{11} + ... + 2hka^*b^*U_{12}]$

Atom	U_{11}	U_{22}	U_{33}	U_{23}	U_{13}	U_{12}
Fe(1)	19(1)	20(1)	19(1)	-2(1)	4(1)	-5(1)
P(1)	19(1)	17(1)	22(1)	-2(1)	4(1)	-3(1)
P(2)	16(1)	19(1)	19(1)	-1(1)	2(1)	-2(1)
O(1)	25(1)	31(1)	19(1)	-7(1)	2(1)	-7(1)
O(2)	29(1)	23(1)	21(1)	-2(1)	8(1)	-6(1)
C(1)	39(2)	35(2)	24(2)	-1(1)	14(1)	-19(2)
C(2)	30(2)	20(1)	26(2)	4(1)	-1(1)	-8(1)
C(3)	18(1)	19(1)	23(2)	-1(1)	5(1)	-7(1)
C(4)	14(1)	23(2)	28(2)	-5(1)	4(1)	-4(1)
C(5)	23(1)	35(2)	34(2)	-10(1)	11(1)	-12(1)
C(6)	27(2)	34(2)	19(2)	-6(1)	1(1)	-11(1)
C(7)	20(1)	28(2)	20(2)	1(1)	-3(1)	-8(1)
C(8)	18(1)	18(1)	19(2)	-2(1)	1(1)	-6(1)
C(9)	20(1)	19(1)	21(2)	-2(1)	3(1)	-4(1)
C(10)	26(1)	23(2)	26(2)	-9(1)	7(1)	-9(1)
C(11)	21(1)	24(2)	23(2)	-4(1)	-2(1)	-1(1)
C(12)	22(1)	24(1)	25(2)	-7(1)	6(1)	-6(1)
C(13)	24(1)	21(2)	18(1)	-1(1)	0(1)	-2(1)
C(14)	15(1)	17(1)	25(2)	1(1)	1(1)	0(1)
C(15)	21(1)	18(1)	32(2)	-5(1)	7(1)	-2(1)
C(16)	24(1)	22(2)	16(1)	1(1)	-2(1)	2(1)
C(17)	23(1)	42(2)	26(2)	-7(1)	-3(1)	-6(1)
C(18)	35(2)	38(2)	28(2)	-13(1)	13(1)	-13(2)
C(19)	37(2)	21(2)	20(2)	4(1)	4(1)	-2(1)
C(20)	26(2)	21(2)	36(2)	3(1)	-3(1)	6(1)

Table A.15.5 Hydrogen coordinates (x 10^4) and isotropic displacement parameters (Å^2 x 10^3) for **(5.8)**

Atom	x	y	z	U(eq)
H(1A)	1590(2)	504(1)	4220(3)	39
H(2A)	2557(2)	235(1)	2513(3)	31
H(4A)	920(2)	779(1)	319(3)	26
H(5A)	581(2)	837(1)	2877(3)	37
H(6A)	3131(2)	1014(1)	4342(3)	32
H(7A)	4043(2)	720(1)	2652(3)	27
H(9A)	2412(2)	1256(1)	405(3)	24
H(10A)	2131(2)	1343(1)	2953(3)	30
H(15A)	4528(2)	363(1)	-2053(3)	29
H(15B)	3793(2)	126(1)	-2120(3)	29
H(16A)	1994(2)	931(1)	-1102(3)	25
H(16B)	1973(2)	954(1)	-2722(3)	25
H(17A)	960(3)	583(3)	-3282(9)	45
H(17B)	718(2)	580(3)	-1702(10)	45
H(17C)	974(3)	295(1)	-2455(19)	45
H(18A)	3469(9)	478(3)	-5266(3)	51
H(18B)	3729(12)	183(1)	-4611(9)	51
H(18C)	4417(4)	435(4)	-4614(9)	51
H(19A)	3131(10)	1283(1)	-3062(9)	39
H(19B)	4040(2)	1258(1)	-2267(18)	39
H(19C)	3166(10)	1337(1)	-1459(9)	39
H(20A)	3918(9)	45(1)	370(11)	42
H(20B)	3869(9)	303(3)	1404(3)	42
H(20C)	4683(2)	273(3)	394(12)	42

A.16 Crystal data and structure refinement for *o*-xylene-diphospha-adamantane (5.9)

This crystal structure determination was carried out by Dr. J. Charmant.

Identification code	scraptox	
Empirical formula	$C_{18}H_{24}O_2P_2$	
Formula weight	334.31	
Temperature	163(2) K	
Wavelength	0.71073 Å	
Crystal system	Triclinic	
Space group	P-1	
Unit cell dimensions	a = 7.5421(14) Å	α = 84.301(3)°
	b = 9.3297(17) Å	β = 74.501(3)°
	c = 12.780(2) Å	γ = 80.573(3)°
Volume	853.4(3) $Å^3$	
Z	2	
Density (calculated)	1.301 Mg/m^3	
Absorption coefficient	0.259 mm^{-1}	
F(000)	356	
Crystal size	0.4 x 0.4 x 0.3 mm	
θ range for data collection	1.66 to 27.62°	
Index ranges	-9<=h<=9, -11<=k<=12, -16<=l<=16	
Reflections collected	8929	
Independent reflections	3887 [R_{int} = 0.0516]	
Completeness to θ = 27.62°	98.1 %	
Absorption correction	Empirical	
Max. and min. transmission	0.973 and 0.827	
Refinement method	Full-matrix least-squares on F^2	
Data/restraints/parameters	3887/0/203	
Goodness-of-fit on F^2	S = 1.038	
R indices [3293 reflections, $I > 2\sigma(I)$]	R_1 = 0.0347, wR_2 = 0.0877	
R indices (for all 3887 data)	R_1 = 0.0437, wR_2 = 0.0923	
Weighting scheme	$w^{-1} = \sigma^2(F_o^2) + (aP)^2 + (bP)$, where $P = [\max(F_o^2, 0) + 2F_c^2]/3$ a = ?, b = ?	
Largest diff. peak and hole	0.385 and -0.284 $eÅ^{-3}$	

Table A.16.1 Atomic coordinates (x 10^4) and equivalent isotropic displacement parameters ($Å^2$ x 10^2) for (**5.9**). U(eq) is defined as one third of the trace of the orthogonalized U_{ij} tensor.

Atom	x	y	z	U(eq)
P(1)	3263(1)	8424(1)	6894(1)	21(1)
P(1A)	-243(1)	6691(1)	7462(1)	24(1)
C(5)	1816(2)	9333(2)	8161(1)	22(1)
C(10)	2388(2)	10821(2)	8159(1)	28(1)
C(6)	1754(2)	7075(2)	9268(1)	24(1)
C(11)	2216(2)	6439(2)	10313(1)	31(1)
C(5A)	-971(2)	7956(2)	8606(1)	24(1)
C(10A)	-3077(2)	8120(2)	9034(1)	35(1)
C(9)	-295(2)	9440(2)	8375(1)	24(1)
C(7)	2712(2)	6109(2)	8317(1)	25(1)
C(8)	2315(2)	6663(2)	7205(1)	22(1)
C(12)	3400(2)	5548(2)	6371(1)	30(1)
C(4)	2205(2)	9455(2)	5821(1)	24(1)
C(4A)	-997(2)	7854(2)	6336(1)	28(1)
C(3)	1933(2)	8511(2)	5003(1)	24(1)
C(2)	3210(2)	8380(2)	3992(1)	29(1)
C(1)	3002(2)	7501(2)	3227(1)	34(1)
C(1A)	1499(3)	6741(2)	3471(1)	36(1)
C(2A)	213(2)	6866(2)	4474(1)	32(1)
C(3A)	401(2)	7740(2)	5253(1)	26(1)
O(1)	2350(1)	8479(1)	9068(1)	23(1)
O(2)	-223(1)	7204(1)	9480(1)	25(1)

Table A.16.2 Bond Lengths (Å) for (**5.9**)

Atoms	length(Å)	Atoms	length(Å)
P(1)-C(8)	1.8635(15)	C(5A)-O(2)	1.4521(17)
P(1)-C(4)	1.8734(15)	C(5A)-C(10A)	1.523(2)
P(1)-C(5)	1.8863(15)	C(5A)-C(9)	1.528(2)
P(1A)-C(8)	1.8648(15)	C(7)-C(8)	1.552(2)
P(1A)-C(4A)	1.8696(16)	C(8)-C(12)	1.537(2)
P(1A)-C(5A)	1.8800(16)	C(4)-C(3)	1.506(2)
C(5)-O(1)	1.4502(17)	C(4A)-C(3A)	1.500(2)
C(5)-C(10)	1.520(2)	C(3)-C(2)	1.393(2)
C(5)-C(9)	1.5292(19)	C(3)-C(3A)	1.408(2)
C(6)-O(2)	1.4292(17)	C(2)-C(1)	1.391(2)
C(6)-O(1)	1.4315(17)	C(1)-C(1A)	1.384(2)
C(6)-C(11)	1.511(2)	C(1A)-C(2A)	1.387(3)
C(6)-C(7)	1.531(2)	C(2A)- C(3A)	1.398(2)

Table A.16.3 Bond angles (°) for (**5.9**)

Atoms	angle(°)	Atoms	angle(°)
C(8)-P(1)-C(4)	106.91(6)	C(9)-C(5A)-P(1A)	117.03(10)
C(8)-P(1)-C(5)	97.01(6)	C(5A)-C(9)-C(5)	112.87(12)
C(4)-P(1)-C(5)	101.79(7)	C(6)-C(7)-C(8)	115.86(12)
C(8)-P(1A)-C(4A)	107.24(7)	C(12)-C(8)-C(7)	107.55(12)
C(8)-P(1A)-C(5A)	97.11(6)	C(12)-C(8)-P(1)	110.96(10)
C(4A)-P(1A)-C(5A)	102.17(7)	C(7)-C(8)-P(1)	103.81(9)
O(1)-C(5)-C(10)	105.96(11)	C(12)-C(8)-P(1A)	111.24(10)
O(1)-C(5)-C(9)	107.42(11)	C(7)-C(8)-P(1A)	103.61(9)
C(10)-C(5)-C(9)	111.01(12)	P(1)-C(8)-P(1A)	118.57(8)
O(1)-C(5)-P(1)	106.29(9)	C(3)-C(4)-P(1)	114.10(10)
C(10)-C(5)-P(1)	108.81(10)	C(3A)-C(4A)-P(1A)	114.07(10)
C(9)-C(5)-P(1)	116.71(10)	C(2)-C(3)-C(3A)	119.27(14)
O(2)-C(6)-O(1)	110.80(11)	C(2)-C(3)-C(4)	120.18(13)
O(2)-C(6)-C(11)	105.69(11)	C(3A)-C(3)-C(4)	120.55(13)
O(1)-C(6)-C(11)	106.19(12)	C(1)-C(2)-C(3)	121.28(15)
O(2)-C(6)-C(7)	110.98(11)	C(1A)-C(1)-C(2)	119.60(16)
O(1)-C(6)-C(7)	111.09(12)	C(1)-C(1A)-C(2A)	119.72(15)
C(11)-C(6)-C(7)	111.87(12)	C(1A)-C(2A)-C(3A)	121.51(15)
O(2)-C(5A)-C(10A)	105.99(12)	C(2A)-C(3A)-C(3)	118.62(15)
O(2)-C(5A)-C(9)	107.40(11)	C(2A)-C(3A)-C(4A)	120.75(14)
C(10A)-C(5A)-C(9)	111.06(13)	C(3)-C(3A)-C(4A)	120.63(13)
O(2)-C(5A)-P(1A)	106.00(9)	C(6)-O(1)-C(5)	114.08(10)
C(10A)-C(5A)-P(1A)	108.68(11)	C(6)-O(2)-C(5A)	114.16(10)

Table A.16.4 Anisotropic displacement parameters ($Å^2$ x 10^3) for (**5.9**). The anisotropic displacement factor exponent takes the form:

$-2\Pi^2[h^2a^{*2}U_{11} + ... + 2hka^*b^*U_{12}]$

Atom	U_{11}	U_{22}	U_{33}	U_{23}	U_{13}	U_{12}
P(1)	20(1)	23(1)	21(1)	-1(1)	-5(1)	-5(1)
P(1A)	24(1)	23(1)	26(1)	2(1)	-9(1)	-8(1)
C(5)	24(1)	23(1)	21(1)	-1(1)	-7(1)	-3(1)
C(10)	35(1)	25(1)	27(1)	-3(1)	-9(1)	-8(1)
C(6)	20(1)	25(1)	25(1)	1(1)	-6(1)	-4(1)
C(11)	32(1)	36(1)	24(1)	5(1)	-9(1)	-6(1)
C(5A)	20(1)	28(1)	24(1)	2(1)	-6(1)	-3(1)
C(10A)	20(1)	45(1)	39(1)	0(1)	-5(1)	-5(1)
C(9)	22(1)	24(1)	25(1)	-2(1)	-5(1)	0(1)
C(7)	24(1)	23(1)	26(1)	2(1)	-8(1)	-1(1)
C(8)	23(1)	20(1)	24(1)	0(1)	-7(1)	-2(1)
C(12)	35(1)	24(1)	30(1)	-5(1)	-9(1)	2(1)
C(4)	29(1)	21(1)	24(1)	2(1)	-9(1)	-7(1)
C(4A)	25(1)	31(1)	31(1)	3(1)	-13(1)	-8(1)
C(3)	30(1)	20(1)	24(1)	2(1)	-13(1)	-4(1)
C(2)	35(1)	27(1)	26(1)	2(1)	-11(1)	-6(1)
C(1)	48(1)	28(1)	25(1)	-1(1)	-10(1)	-3(1)
C(1A)	59(1)	24(1)	31(1)	-1(1)	-23(1)	-8(1)

Atom	U_{11}	U_{22}	U_{33}	U_{23}	U_{13}	U_{12}
C(2A)	44(1)	24(1)	36(1)	4(1)	-23(1)	-10(1)
C(3A)	31(1)	22(1)	28(1)	5(1)	-16(1)	-5(1)
O(1)	25(1)	25(1)	21(1)	2(1)	-8(1)	-6(1)
O(2)	20(1)	32(1)	23(1)	3(1)	-4(1)	-6(1)

Table A.16.5 Hydrogen coordinates (x 10^4) and isotropic displacement parameters ($Å^2$ x 10^3) for **(5.9)**

Atom	x	y	z	U(eq)
H(10C)	1703	11276	8837	43
H(10A)	2104	11435	7540	43
H(10B)	3726	10712	8098	43
H(11A)	3565	6318	10216	46
H(11C)	1780	5491	10506	46
H(11B)	1602	7097	10897	46
H(10E)	-3457	7163	9282	52
H(10D)	-3657	8544	8452	52
H(10F)	-3472	8760	9643	52
H(9B)	-897	10043	9004	29
H(9A)	-682	9937	7733	29
H(7B)	2327	5132	8511	29
H(7A)	4071	5995	8230	29
H(12A)	4733	5474	6315	45
H(12B)	3165	5863	5660	45
H(12C)	2995	4595	6607	45
H(4B)	984	9996	6180	29
H(4A)	3013	10178	5432	29
H(4AA)	-2172	7576	6269	33
H(4AB)	-1257	8881	6532	33
H(2)	4242	8901	3821	35
H(1)	3887	7423	2541	41
H(1A)	1348	6137	2954	43
H(2A)	-819	6345	4634	38

A.17 Crystal data and structure refinement for binuclear gold complex (5.17)

This crystal structure determination was carried out by Miss H. Phetmung, under the supervision of Prof. A. G. Orpen.

Identification code	rip112s	
Empirical formula	$C_{16}H_{20}Au_2Cl_2O_2P_2$	
Formula weight	771.09	
Temperature	173(2) K	
Wavelength	0.71073Å	
Crystal system	Triclinic	
Space group	$P\bar{1}$.	
Unit cell dimensions	a = 7.934(2) Å	α = 85.449(13)°
	b = 8.2681(12) Å	β = 87.77(2)°.
	c = 15.118(2) Å	γ = 76.846(12)°.
Volume	962.4(3) $Å^3$	
Z	2	
Density (calculated)	2.661 Mg/m^3	
Absorption coefficient	15.677 mm^{-1}	
F(000)	708	
Crystal size	0.28 x 0.20 x 0.18 mm (colourless,block)	
q range for data collection	1.35 - 27.48°.	
Index ranges	-10<=h<=10, -10<=k<=10, -19<=l<=19	
Reflections collected	9647	
Independent reflections	4344 [R(int) = 0.0244]	
Refinement method	Full-matrix least-squares on F^2	
Data/restraints/parameters	4343/0/222	
Goodness-of-fit on F^2*	0.854	
Final R indices [$I > 2\sigma(I)$]*	R_1 = 0.0203, wR_2 = 0.0458	
R indices (all data)	R_1 = 0.0281, wR_2 = 0.0598	
Weighting scheme	calc $w = 1/[[\sigma^2(F_o^2)+(0.0258P)^2+0.0000P]$	
	where $P = (\text{Max } F_o^2,0 + 2F_c^2)/3$	
Extinction coefficient	0.00330(13)	
Largest diff. peak and hole	1.247 and -0.672 $e.Å^{-3}$	

*$wR_2 = [\Sigma w\Delta^2/\Sigma wF_o^4]^{0.5}$; $S = [\Sigma w\Delta^2/(N.O. - N.V.)]^{0.5}$; $\Delta = F_o^2 - F_c^2$;
$R_1 = \Sigma |F_o - F_c|/\Sigma |F_o|$; N.O. = data + restraints; N.V. = parameters

Table A.17.1 Atomic coordinates (x 10^4) and equivalent isotropic displacement parameters ($Å^2$ x 10^2) for (**5.17**). U(eq) is defined as one third of the trace of the orthogonalized U_{ij} tensor.

Atom	x	y	z	U(eq)
Au(1)	2543(1)	596(1)	8670(1)	17(1)
Au(2)	3976(1)	8037(1)	7212(1)	17(1)
Cl(1)	3344(2)	-1744(2)	9614(1)	26(1)
Cl(2)	6277(2)	9274(2)	7034(1)	26(1)
P(1)	1736(2)	3041(2)	7898(1)	15(1)
P(2)	2209(2)	6297(2)	7321(1)	14(1)
O(1)	2017(4)	2490(4)	6165(2)	16(1)
O(2)	2409(4)	5175(4)	5665(2)	15(1)
C(1)	328(6)	4684(6)	8456(3)	16(1)
C(2)	548(6)	6302(6)	8180(3)	16(1)
C(3)	-521(6)	7683(6)	8527(3)	21(1)
C(4)	-1869(6)	7490(7)	9101(3)	24(1)
C(5)	-2113(6)	5928(7)	9359(3)	23(1)
C(6)	-1007(6)	4517(7)	9051(3)	21(1)
C(11)	1108(6)	6004(6)	6275(3)	14(1)
C(12)	3267(6)	3495(6)	5950(3)	16(1)
C(13)	687(6)	3140(6)	6795(3)	15(1)
C(14)	3456(6)	4161(5)	7566(3)	14(1)
C(15)	4416(6)	3485(6)	6728(3)	17(1)
C(16)	-205(6)	4921(6)	6469(3)	16(1)
C(17)	315(6)	7688(6)	5824(3)	21(1)
C(18)	4292(7)	2748(6)	5161(3)	22(1)
C(19)	-549(6)	1978(6)	6855(3)	20(1)
C(20)	4719(6)	4042(6)	8324(3)	22(1)

Table A.17.2 Bond Lengths (Å) for (**5.17**)

Atom	length(Å)	Atom	length(Å)
Au(1)-P(1)	2.2258(13)	O(2)-C(11)	1.446(5)
Au(1)-Cl(1)	2.2920(13)	C(1)-C(6)	1.387(6)
Au(1)-Au(2)#1	3.1749(6)	C(1)-C(2)	1.417(6)
Au(2)-P(2)	2.2193(12)	C(2)-C(3)	1.385(6)
Au(2)-Cl(2)	2.2841(13)	C(3)-C(4)	1.380(7)
Au(2)-Au(1)#2	3.1748(6)	C(4)-C(5)	1.373(7)
P(1)-C(1)	1.795(5)	C(5)-C(6)	1.392(7)
P(1)-C(14)	1.850(4)	C(11)-C(17)	1.511(6)
P(1)-C(13)	1.880(5)	C(11)-C(16)	1.527(6)
P(2)-C(2)	1.813(5)	C(12)-C(18)	1.510(6)
P(2)-C(14)	1.835(5)	C(12)-C(15)	1.514(6)
P(2)-C(11)	1.893(5)	C(13)-C(19)	1.517(6)
O(1)-C(13)	1.433(5)	C(13)-C(16)	1.533(6)
O(1)-C(12)	1.444(5)	C(14)-C(15)	1.530(6)
O(2)-C(12)	1.440(5)	C(14)-C(20)	1.533(6)

Table A.17.3 Bond angles (°) for (**5.17**)

Atom	angle(°)	Atom	angle(°)
P(1)-Au(1)-Cl(1)	173.13(4)	C(4)-C(5)-C(6)	120.7(5)
P(1)-Au(1)-Au(2)#1	104.37(3)	C(1)-C(6)-C(5)	119.9(5)
Cl(1)-Au(1)-Au(2)#1	82.32(4)	O(2)-C(11)-C(17)	106.5(4)
P(2)-Au(2)-Cl(2)	166.47(5)	O(2)-C(11)-C(16)	107.9(3)
P(2)-Au(2)-Au(1)#2	104.30(3)	C(17)-C(11)-C(16)	112.7(4)
Cl(2)-Au(2)-Au(1)#2	86.75(4)	O(2)-C(11)-P(2)	108.6(3)
C(1)-P(1)-C(14)	97.4(2)	C(17)-C(11)-P(2)	109.4(3)
C(1)-P(1)-C(13)	103.3(2)	C(16)-C(11)-P(2)	111.5(3)
C(14)-P(1)-C(13)	99.4(2)	O(2)-C(12)-O(1)	110.6(4)
C(1)-P(1)-Au(1)	116.8(2)	O(2)-C(12)-C(18)	107.0(4)
C(14)-P(1)-Au(1)	116.9(2)	O(1)-C(12)-C(18)	105.3(4)
C(13)-P(1)-Au(1)	119.4(2)	O(2)-C(12)-C(15)	110.6(4)
C(2)-P(2)-C(14)	97.8(2)	O(1)-C(12)-C(15)	111.4(4)
C(2)-P(2)-C(11)	103.8(2)	C(18)-C(12)-C(15)	111.8(4)
C(14)-P(2)-C(11)	99.7(2)	O(1)-C(13)-C(19)	106.2(4)
C(2)-P(2)-Au(2)	124.2(2)	O(1)-C(13)-C(16)	108.9(4)
C(14)-P(2)-Au(2)	109.7(2)	C(19)-C(13)-C(16)	112.1(4)
C(11)-P(2)-Au(2)	117.4(2)	O(1)-C(13)-P(1)	107.6(3)
C(13)-O(1)-C(12)	115.4(3)	C(19)-C(13)-P(1)	109.2(3)
C(12)-O(2)-C(11)	115.5(3)	C(16)-C(13)-P(1)	112.5(3)
C(6)-C(1)-C(2)	118.9(4)	C(15)-C(14)-C(20)	110.8(4)
C(6)-C(1)-P(1)	126.4(4)	C(15)-C(14)-P(2)	110.1(3)
C(2)-C(1)-P(1)	114.4(3)	C(20)-C(14)-P(2)	112.1(3)
C(3)-C(2)-C(1)	120.0(4)	C(15)-C(14)-P(1)	110.5(3)
C(3)-C(2)-P(2)	127.0(4)	C(20)-C(14)-P(1)	110.9(3)
C(1)-C(2)-P(2)	112.9(3)	P(2)-C(14)-P(1)	102.1(2)
C(4)-C(3)-C(2)	120.0(5)	C(12)-C(15)-C(14)	114.7(4)
C(5)-C(4)-C(3)	120.3(5)	C(11)-C(16)-C(13)	111.3(4)

Symmetry transformations used to generate equivalent atoms: #1 x,y-1,z #2 x,y+1,z

Table A.17.4 Anisotropic displacement parameters ($Å^2$ x 10^3) for (**5.17**). The anisotropic displacement factor exponent takes the form:

$-2\Pi^2[h^2a^{*2}U_{11} + ... + 2hka^*b^*U_{12}]$

Atom	U_{11}	U_{22}	U_{33}	U_{23}	U_{13}	U_{12}
Au(1)	20(1)	16(1)	16(1)	1(1)	0(1)	-5(1)
Au(2)	17(1)	16(1)	18(1)	-2(1)	1(1)	-6(1)
Cl(1)	31(1)	22(1)	24(1)	7(1)	-3(1)	-5(1)
Cl(2)	19(1)	21(1)	39(1)	-1(1)	1(1)	-8(1)
P(1)	16(1)	16(1)	14(1)	0(1)	1(1)	-6(1)
P(2)	15(1)	15(1)	14(1)	-2(1)	1(1)	-5(1)
O(1)	18(2)	16(2)	17(2)	-7(1)	4(1)	-6(1)
O(2)	16(2)	17(2)	12(2)	-2(1)	4(1)	-3(1)
C(1)	15(2)	22(2)	13(2)	-4(2)	-3(2)	-4(2)
C(2)	14(2)	21(2)	13(2)	-2(2)	-1(2)	-5(2)

Atom	U_{11}	U_{22}	U_{33}	U_{23}	U_{13}	U_{12}
C(3)	18(2)	25(3)	19(3)	-3(2)	-2(2)	-4(2)
C(4)	19(3)	32(3)	18(3)	-8(2)	0(2)	-2(2)
C(5)	15(2)	39(3)	13(2)	-1(2)	2(2)	-4(2)
C(6)	19(2)	32(3)	13(2)	-2(2)	0(2)	-10(2)
C(11)	14(2)	16(2)	13(2)	-1(2)	1(2)	-3(2)
C(12)	17(2)	15(2)	16(2)	0(2)	2(2)	-4(2)
C(13)	16(2)	17(2)	12(2)	0(2)	0(2)	-5(2)
C(14)	12(2)	16(2)	15(2)	0(2)	1(2)	-3(2)
C(15)	18(2)	16(2)	18(2)	-3(2)	0(2)	-4(2)
C(16)	14(2)	20(2)	14(2)	-4(2)	0(2)	-4(2)
C(17)	22(3)	19(2)	19(3)	0(2)	-2(2)	-3(2)
C(18)	27(3)	21(3)	17(3)	-4(2)	1(2)	-3(2)
C(19)	18(2)	23(3)	22(3)	-1(2)	-2(2)	-11(2)
C(20)	20(3)	31(3)	18(3)	-4(2)	-3(2)	-7(2)

Table A.17.5 Hydrogen coordinates (x 10^4) and isotropic displacement parameters ($Å^2$ x 10^3) for (**5.17**)

Atom	x	y	z	U(eq)
H(3A)	-327(6)	8762(6)	8371(3)	25
H(4A)	-2632(6)	8443(7)	9318(3)	28
H(5A)	-3047(6)	5810(7)	9753(3)	27
H(6A)	-1167(6)	3441(7)	9248(3)	25
H(15A)	5274(6)	4156(6)	6545(3)	20
H(15B)	5063(6)	2327(6)	6874(3)	20
H(16A)	-844(6)	4893(6)	5923(3)	19
H(16B)	-1052(6)	5414(6)	6926(3)	19
H(17A)	-277(36)	7539(6)	5290(12)	31
H(17B)	1228(8)	8285(17)	5659(19)	31
H(17C)	-520(30)	8331(16)	6231(8)	31
H(18A)	3506(9)	2768(37)	4674(8)	33
H(18B)	4884(34)	1595(14)	5327(7)	33
H(18C)	5149(29)	3397(25)	4970(14)	33
H(19A)	-1148(31)	2074(30)	6291(8)	30
H(19B)	-1401(26)	2282(26)	7335(14)	30
H(19C)	102(8)	829(7)	6976(21)	30
H(20A)	5588(26)	4683(34)	8142(9)	34
H(20B)	5295(32)	2874(8)	8462(15)	34
H(20C)	4080(9)	4494(38)	8851(7)	34

A.18 Crystal data and structure refinement for diphospa-chelate platinum complex (5.18)

This crystal structure determination was carried out by Miss H. Phetmung, under the supervision of Prof. A. G. Orpen.

Identification code	rip189s
Empirical formula	$C_{23}H_{40}Cl_4O_2P_2Pt$
Formula weight	747.38
Temperature	293(2) K
Wavelength	0.71073 Å
Crystal system	Triclinic
Space group	$P\bar{1}$
Unit cell dimensions	a = 8.9144(4) Å α = 111.2070(10)° b = 12.3303(6) Å β = 105.6450(10)° c = 14.0416(6) Å γ = 91.1460(10)° Volume1373.65(11) Å^3
Z	2
Density (calculated)	1.807 Mg/m^3
Absorption coefficient	5.633 mm^{-1}
F(000)	740
Crystal size	0.32 x 0.26 x 0.14 mm(yellow)
θ range for data collection	1.63 - 25.00°
Index ranges	-11<=h<=11, -16<=k<=15, -18<=l<=18
Reflections collected	11922
Independent reflections	4820 [R(int) = 0.0278]
Refinement method	Full-matrix least-squares on F^2
Data/restraints/parameters	4820/0/293
Goodness-of-fit on F^2	0.959
Final R indices [$I > 2\sigma(I)$]*	R_1 = 0.0201, wR_2 = 0.0430[4265 data]
R indices (all data)*(S)	R_1 = 0.0253, wR_2 = 0.0437[4820 data]
Weighting scheme	calc w = $1/[\sigma^2(F_o^2) + (0.0202P)^2 + 0.000P]$ where P= (Max F_o^2,0 + $2F_c^2$)/3
Largest diff. peak and hole	0.774 and -0.599 e.Å^{-3}

*$wR_2 = [\Sigma w\Delta^2/\Sigma wF_o^4]^{0.5}$; $S = [\Sigma w\Delta^2/(N.O. - N.V.)]^{0.5}$; $\Delta = F_o^2 - F_c^2$;
$R_1 = \Sigma |F_o - F_c|/\Sigma |F_o|$; N.O. = data + restraints; N.V. = parameters

Table A.18.1 Atomic coordinates (x 10^4) and equivalent isotropic displacement parameters ($Å^2$ x 10^2) for (**5.18**). U(eq) is defined as one third of the trace of the orthogonalized U_{ij} tensor.

Atom	x	y	z	U(eq)
Pt(1)	3971(1)	13256(1)	3345(1)	16(1)
Cl(2)	2490(1)	12646(1)	4269(1)	26(1)
Cl(1)	2088(1)	14447(1)	2868(1)	22(1)
P(2)	5767(1)	12048(1)	3423(1)	17(1)
P(1)	5798(1)	13618(1)	2630(1)	17(1)
O(2)	6740(3)	10555(2)	1754(2)	21(1)
O(1)	6870(3)	12035(2)	1047(2)	20(1)
C(11)	5433(4)	12439(3)	1247(3)	19(1)
C(12)	7736(4)	11471(3)	1725(3)	21(1)
C(13)	5308(4)	10897(3)	2016(3)	19(1)
C(14)	7368(4)	13007(3)	3402(3)	18(1)
C(15)	8522(4)	12375(3)	2838(3)	20(1)
C(16)	4429(4)	11392(3)	1202(3)	20(1)
C(17)	4638(4)	12855(3)	364(3)	23(1)
C(18)	8939(4)	10872(3)	1207(3)	29(1)
C(19)	4351(4)	9793(3)	1898(3)	26(1)
C(20)	8201(4)	13942(3)	4498(3)	24(1)
C(21)	6305(4)	11344(3)	4387(3)	19(1)
C(22)	7666(4)	10600(3)	4263(3)	23(1)
C(23)	7893(4)	9942(3)	5011(3)	24(1)
C(24)	8237(4)	10789(3)	6178(3)	29(1)
C(25)	6953(4)	11572(3)	6319(3)	26(1)
C(26)	6653(4)	12221(3)	5557(3)	23(1)
C(31)	6543(4)	15087(3)	2782(3)	19(1)
C(32)	8031(4)	15111(3)	2435(3)	25(1)
C(33)	8703(4)	16374(3)	2705(3)	29(1)
C(34)	7482(4)	16999(3)	2204(3)	30(1)
C(35)	6005(4)	16969(3)	2537(3)	26(1)
C(36)	5315(4)	15714(3)	2267(3)	24(1)
Cl(4)	-1879(1)	14030(1)	-589(1)	48(1)
Cl(3)	119(2)	12180(1)	-687(1)	55(1)
C(40)	-682(5)	13301(4)	133(3)	37(1)

Table A.18.2 Bond lengths (Å) for (**5.18**)

Atoms	length(Å)	Atoms	length(Å)
Pt(1)-P(2)	2.2172(9)	C(13)-C(19)	1.524(5)
Pt(1)-P(1)	2.2446(9)	C(13)-C(16)	1.527(5)
Pt(1)-Cl(2)	2.3627(9)	C(14)-C(20)	1.522(5)
Pt(1)-Cl(1)	2.3715(8)	C(14)-C(15)	1.523(5)
P(2)-C(21)	1.826(3)	C(21)-C(22)	1.545(5)
P(2)-C(14)	1.848(4)	C(21)-C(26)	1.546(5)
P(2)-C(13)	1.896(3)	C(22)-C(23)	1.520(5)
P(2)-P(1)	2.5619(13)	C(23)-C(24)	1.533(5)
P(1)-C(31)	1.834(3)	C(24)-C(25)	1.519(5)

Atoms	length(Å)	Atoms	length(Å)
P(1)-C(14)	1.875(3)	C(25)-C(26)	1.527(5)
P(1)-C(11)	1.894(3)	C(31)-C(36)	1.528(5)
O(2)-C(12)	1.442(4)	C(31)-C(32)	1.534(5)
O(2)-C(13)	1.451(4)	C(32)-C(33)	1.529(5)
O(1)-C(11)	1.445(4)	C(33)-C(34)	1.513(5)
O(1)-C(12)	1.446(4)	C(34)-C(35)	1.515(5)
C(11)-C(17)	1.518(5)	C(35)-C(36)	1.526(5)
C(11)-C(16)	1.528(5)	Cl(4)-C(40)	1.757(4)
C(12)-C(18)	1.512(5)	Cl(3)-C(40)	1.755(4)
C(12)-C(15)	1.514(5)		

Table A.18.3 Bond angles (°) for **(5.18)**

Atoms	angle(°)	Atoms	angle(°)
P(2)-Pt(1)-P(1)	70.08(3)	O(1)-C(12)-C(18)	106.5(3)
P(2)-Pt(1)-Cl(2)	97.20(3)	O(2)-C(12)-C(15)	111.3(3)
P(1)-Pt(1)-Cl(2)	166.75(3)	O(1)-C(12)-C(15)	110.1(3)
P(2)-Pt(1)-Cl(1)	167.14(3)	C(18)-C(12)-C(15)	111.1(3)
P(1)-Pt(1)-Cl(1)	100.38(3)	O(2)-C(13)-C(19)	107.3(3)
Cl(2)-Pt(1)-Cl(1)	92.75(3)	O(2)-C(13)-C(16)	106.7(3)
C(21)-P(2)-C(14)	115.9(2)	C(19)-C(13)-C(16)	110.3(3)
C(21)-P(2)-C(13)	109.5(2)	O(2)-C(13)-P(2)	111.0(2)
C(14)-P(2)-C(13)	99.3(2)	C(19)-C(13)-P(2)	111.1(2)
C(21)-P(2)-Pt(1)	126.66(12)	C(16)-C(13)-P(2)	110.2(2)
C(14)-P(2)-Pt(1)	96.06(11)	C(20)-C(14)-C(15)	112.1(3)
C(13)-P(2)-Pt(1)	105.61(11)	C(20)-C(14)-P(2)	113.0(3)
C(21)-P(2)-P(1)	158.67(12)	C(15)-C(14)-P(2)	115.5(2)
C(14)-P(2)-P(1)	46.97(10)	C(20)-C(14)-P(1)	110.3(2)
C(13)-P(2)-P(1)	88.06(11)	C(15)-C(14)-P(1)	116.9(2)
Pt(1)-P(2)-P(1)	55.46(3)	P(2)-C(14)-P(1)	86.95(14)
C(31)-P(1)-C(14)	109.9(2)	C(12)-C(15)-C(14)	113.6(3)
C(31)-P(1)-C(11)	115.3(2)	C(13)-C(16)-C(11)	110.9(3)
C(14)-P(1)-C(11)	99.1(2)	C(22)-C(21)-C(26)	110.4(3)
C(31)-P(1)-Pt(1)	124.29(12)	C(22)-C(21)-P(2)	114.0(2)
C(14)-P(1)-Pt(1)	94.37(11)	C(26)-C(21)-P(2)	112.7(2)
C(11)-P(1)-Pt(1)	108.82(12)	C(23)-C(22)-C(21)	109.7(3)
C(31)-P(1)-P(2)	149.25(12)	C(22)-C(23)-C(24)	111.3(3)
C(14)-P(1)-P(2)	46.08(11)	C(25)-C(24)-C(23)	111.2(3)
C(11)-P(1)-P(2)	90.52(11)	C(24)-C(25)-C(26)	112.6(3)
Pt(1)-P(1)-P(2)	54.46(3)	C(25)-C(26)-C(21)	110.4(3)
C(12)-O(2)-C(13)	115.4(2)	C(36)-C(31)-C(32)	110.9(3)
C(11)-O(1)-C(12)	116.2(3)	C(36)-C(31)-P(1)	114.4(2)
O(1)-C(11)-C(17)	106.7(3)	C(32)-C(31)-P(1)	113.3(2)
O(1)-C(11)-C(16)	107.1(3)	C(33)-C(32)-C(31)	110.7(3)
C(17)-C(11)-C(16)	111.2(3)	C(34)-C(33)-C(32)	110.8(3)
O(1)-C(11)-P(1)	112.2(2)	C(33)-C(34)-C(35)	111.5(3)
C(17)-C(11)-P(1)	112.6(2)	C(34)-C(35)-C(36)	111.5(3)
C(16)-C(11)-P(1)	106.9(2)	C(35)-C(36)-C(31)	110.2(3)
O(2)-C(12)-O(1)	111.5(3)	Cl(3)-C(40)-Cl(4)	111.8(2)
O(2)-C(12)-C(18)	106.2(3)		

Table A.18.4 Anisotropic displacement parameters ($Å^2$ x 10^3) for **(5.18)**. The anisotropic displacement factor exponent takes the form:

$-2\Pi^2[h^2a^{*2}U_{11} + ... + 2hka^*b^*U_{12}]$

Atom	U_{11}	U_{22}	U_{33}	U_{23}	U_{13}	U_{12}
Pt(1)	14(1)	17(1)	17(1)	6(1)	4(1)	2(1)
Cl(2)	18(1)	37(1)	30(1)	19(1)	10(1)	3(1)
Cl(1)	17(1)	26(1)	27(1)	12(1)	8(1)	9(1)
P(2)	15(1)	17(1)	17(1)	5(1)	4(1)	1(1)
P(1)	16(1)	16(1)	18(1)	6(1)	4(1)	3(1)
O(2)	22(1)	17(1)	27(1)	6(1)	13(1)	5(1)
O(1)	20(1)	21(1)	21(1)	7(1)	10(1)	5(1)
C(11)	17(2)	21(2)	18(2)	4(2)	6(2)	4(2)
C(12)	17(2)	22(2)	28(2)	12(2)	8(2)	5(2)
C(13)	19(2)	16(2)	19(2)	3(2)	7(2)	2(2)
C(14)	15(2)	17(2)	22(2)	10(2)	4(2)	2(1)
C(15)	16(2)	21(2)	26(2)	11(2)	8(2)	4(2)
C(16)	21(2)	19(2)	16(2)	3(2)	4(2)	1(2)
C(17)	25(2)	21(2)	21(2)	8(2)	4(2)	4(2)
C(18)	24(2)	34(2)	34(2)	14(2)	15(2)	9(2)
C(19)	26(2)	23(2)	25(2)	7(2)	5(2)	-2(2)
C(20)	22(2)	23(2)	22(2)	9(2)	0(2)	-2(2)
C(21)	18(2)	20(2)	19(2)	8(2)	5(2)	1(2)
C(22)	21(2)	24(2)	24(2)	10(2)	6(2)	5(2)
C(23)	22(2)	22(2)	33(2)	16(2)	7(2)	5(2)
C(24)	29(2)	32(2)	28(2)	17(2)	2(2)	0(2)
C(25)	28(2)	28(2)	19(2)	9(2)	4(2)	-3(2)
C(26)	23(2)	21(2)	23(2)	4(2)	6(2)	4(2)
C(31)	19(2)	19(2)	22(2)	9(2)	7(2)	1(2)
C(32)	17(2)	27(2)	35(2)	14(2)	8(2)	7(2)
C(33)	20(2)	30(2)	39(2)	18(2)	7(2)	2(2)
C(34)	31(2)	25(2)	36(2)	17(2)	7(2)	-2(2)
C(35)	25(2)	24(2)	32(2)	13(2)	11(2)	5(2)
C(36)	21(2)	23(2)	30(2)	10(2)	11(2)	5(2)
Cl(4)	42(1)	55(1)	46(1)	24(1)	3(1)	10(1)
Cl(3)	57(1)	56(1)	59(1)	18(1)	34(1)	21(1)
C(40)	39(3)	40(3)	37(2)	17(2)	14(2)	10(2)

Table A.18.5 Hydrogen coordinates (x 10^4) and isotropic displacement parameters (Å^2 x 10^3) for **(5.18)**

Atom	x	y	z	U(eq)
H(15A)	9225(4)	12950(3)	2790(3)	24
H(15B)	9153(4)	11989(3)	3267(3)	24
H(16A)	3461(4)	11636(3)	1351(3)	24
H(16B)	4159(4)	10786(3)	489(3)	24
H(17A)	5362(9)	13418(15)	331(12)	35
H(17B)	3736(16)	13214(18)	510(10)	35
H(17C)	4312(24)	12198(4)	-308(4)	35
H(18A)	9663(17)	11452(4)	1197(17)	44
H(18B)	8416(5)	10341(16)	488(7)	44
H(18C)	9501(20)	10443(17)	1608(11)	44
H(19A)	4980(10)	9424(11)	2334(14)	39
H(19B)	4037(23)	9260(9)	1163(4)	39
H(19C)	3435(15)	9999(4)	2123(17)	39
H(20A)	7442(5)	14255(14)	4861(8)	35
H(20B)	8755(22)	14562(10)	4415(3)	35
H(20C)	8933(20)	13601(5)	4910(7)	35
H(21A)	5383(4)	10799(3)	4246(3)	23
H(22A)	7428(4)	10045(3)	3529(3)	28
H(22B)	8626(4)	11106(3)	4430(3)	28
H(23A)	8759(4)	9486(3)	4937(3)	29
H(23B)	6952(4)	9403(3)	4812(3)	29
H(24A)	8315(4)	10343(3)	6631(3)	35
H(24B)	9236(4)	11272(3)	6401(3)	35
H(25A)	7251(4)	12140(3)	7050(3)	31
H(25B)	5989(4)	11096(3)	6197(3)	31
H(26A)	7567(4)	12779(3)	5738(3)	28
H(26B)	5766(4)	12653(3)	5632(3)	28
H(31A)	6859(4)	15558(3)	3552(3)	23
H(32A)	8811(4)	14740(3)	2796(3)	30
H(32B)	7781(4)	14672(3)	1670(3)	30
H(33A)	9049(4)	16791(3)	3476(3)	34
H(33B)	9607(4)	16370(3)	2445(3)	34
H(34A)	7218(4)	16629(3)	1431(3)	35
H(34B)	7916(4)	17809(3)	2417(3)	35
H(35A)	5232(4)	17344(3)	2175(3)	31
H(35B)	6249(4)	17408(3)	3301(3)	31
H(36A)	4972(4)	15294(3)	1497(3)	29
H(36B)	4408(4)	15725(3)	2525(3)	29
H(40A)	163(5)	13863(4)	703(3)	45
H(40B)	-1299(5)	12968(4)	458(3)	45

References

1 *Comprehensive Organometallic Chemistry*, ed. E. W. Abel, F. G. A. Stone and G. Wilkinson, Elsevier Science Ltd., Oxford, 1982.

2 C. A. McAuliffe, in *Comprehensive Coordination Chemistry*, ed. G. Wilkinson, R. P. Gillard and J. A. McCleverty, Pergamon Press, Oxford, 1987, vol. 2, p. 992.

3 *Homogeneous Catalysis with Metal Phosphine Complexes*, ed. L. H. Pignolet, Plenum Press, New York, 1983.

4 *Transition Metal Complexes of Phosphorus, Arsenic and Antimony Ligands*, ed. C. A. McAuliffe, Macmillan, London and Basingstoke, 1973.

5 A. Baeyer, *Chem. Ber.*, 1885, **18**, 2269.

6 A. W. Hofmann, *Chem. Ber.*, 1872, **5**, 704.

7 F. Kehrmann, *Chem. Ber.*, 1888, **21**, 3315.

8 V. Meyer, *Chem. Ber.*, 1894, **25**, 510.

9 E. Mohr, *J. Prakt. Chem.*, 1918, **98**, 315.

10 H. Sachse, *Chem. Ber.*, 1890, **23**, 1363.

11 R. Wegschneider, *Monatsch. Chem.*, 1895, **16**, 75.

12 C. K. Ingold, *J. Chem. Soc.*, 1921, **305**, 951.

13 B. Capon and S. P. McManus, in *Neighbouring Group Participation*, Plenum Press, New York and London, 1965, vol. 1.

14 E. L. Eliel, in *Stereochemistry of Carbon Compouds*, McGraw-Hill, New York, 1962.

15 E. L. Eliel, N. L. Allinger, S. J. Angyll and G. A. Morrison, in *Conformational Analysis*, Interscience, New York, 1965.

16 G. S. Hammond, in *Steric Effects in Organic Chemistry*, ed. M. S. Newman, Wiley, New York, 1956, p. 468.

17 N. L. Allinger and V. Zalkow, *J. Org. Chem.*, 1960, **25**, 701.

18 L. Anschutz, *Angew. Chem.*, 1928, **41**, 691.

19 *Steric Effects in Organic Chemistry*, ed. M. S. Newman, Wiley, New York, 1956.

20 H. S. Mosher and T. T. Tidwell, *J. Chem. Educ.*, 1990, **67**, 9.

21 B. L. Shaw, *J. Organomet. Chem.*, 1980, **200**, 307.

22 A. Bright, B. E. Mann, C. Masters, B. L. Shaw, R. M. Slade and R. E. Stainbank, *J. Chem. Soc.*, 1971, **A**, 1826.

23 J. M. Jenkins and B. L. Shaw, *Proc. Chem. Soc.*, 1968, 279.

24 C. A. Tolman, W. C. Seidel and L. W. Gosser, *J. Am. Chem. Soc.*, 1974, **96**, 53.

25 C. A. Tolman, *Chem. Rev.*, 1977, **77**, 313.

26 T. Yoshida, T. Okano, D. L. Thorn, T. H. Tulip, S. Otsuka and J. A. Ibers, *J. Organomet. Chem.*, 1979, **181**, 183.

27 H. L. M. van Gaal and F. L. A. van den Bekerom, *J. Organomet. Chem.*, 1977, **134**, 237.

28 S. Otsuka, T. Yoshida, M. Matsumoto and K. Nakatsu, *J. Am. Chem. Soc.*, 1976, **98**, 5850.

29 B. E. Mann and A. Musco, *J. Chem. Soc., Dalton Trans.*, 1975, 1673.

30 M. Matsumoto, H. Yoshiska, K. Nakatsu, T. Yoshida and S. Otsuka, *J. Am. Chem. Soc.*, 1974, **96**, 3322.

31 M. Green, J. A. Howard, J. L. Spencer and F. G. A. Stone, *J. Chem. Soc., Chem. Commun.*, 1975, 3.

32 A. Immirzi, A. Musco, G. Carturan and U. Belluco, *Inorg. Chim. Acta.*, 1975, **12**, L23.

33 B. L. Shaw and M. F. Uttley, *J. Chem. Soc., Chem. Commun.*, 1974, 918.

34 C. J. Moulton and B. L. Shaw, *J. Chem. Soc., Chem. Commun.*, 1976, 365.

35 T. Yoshida, T. Yamagata, T. H. Tulip, J. A. Ibers and S. Otsuka, *J. Am. Chem. Soc.*, 1978, **100**, 2063.

36 W. Clegg, G. R. Eastham, M. R. J. Elsegood, R. P. Tooze, X. L. Wang and K. Whiston, *J. Chem. Soc., Chem. Commun.*, 1999, 1877.

37 R. P. Tooze, G. R. Eastham, K. Whiston and X. L. Wang, *World. Pat.* 19 434, 1996, to ICI

38 E. Drent and E. Kragtwijk, *Eur. Pat.* 495 548, 1992, to Shell

39 H. D. Empsall, E. M. Hyde, E. Mentzer, B. L. Shaw and M. F. Uttley, *J. Chem. Soc., Dalton Trans.*, 1976, 2069.

40 H. D. Empsall, E. Mentzer and B. L. Shaw, *J. Chem. Soc., Chem. Commun.*, 1975, 861.

41 H. D. Empsall, E. M. Hyde and B. L. Shaw, *J. Chem. Soc., Dalton Trans.*, 1975, 1690.

42 R. Mason, K. M. Thomas, H. D. Empsall, S. R. Fletcher, P. N. Heys, E. M. Hyde, C. E. Jones and B. L. Shaw, *J. Chem. Soc., Chem. Commun.*, 1974, 612.

43 B. L. Shaw, *J. Organomet. Chem.*, 1975, **94**, 251.

44 C. Masters and B. L. Shaw, *J. Chem. Soc.*, 1971, **A**, 3679.

45 C. Masters, B. L. Shaw and R. E. Stainbank, *J. Chem. Soc., Dalton Trans.*, 1972, 664.

46 D. F. Gill and B. L. Shaw, *Inorg. Chim. Acta.*, 1979, **32**, 19.

47 F. G. Moers and J. P. Langhart, *Rec. Trav. Chim. Pays-Bas*, 1972, **91**, 591.

48 D. F. Gill, B. E. Mann and B. L. Shaw, *J. Chem. Soc., Dalton Trans.*, 1973, 311.

49 R. Mason, K. M. Thomas, D. F. Gill and B. L. Shaw, *J. Organomet. Chem.*, 1972, **40**, C67.

50 J. Dehand and M. Pfeffer, *Coord. Chem. Rev.*, 1976, **18**, 327.

51 M. I. Bruce, *Angew. Chem., Int. Ed. Engl.*, 1977, **16**, 73.

52 G. W. Parshall, *Acc. Chem. Res.*, 1970, **3**, 139.

53 N. A. Al-Salem, H. D. Empsall, R. Markham, B. L. Shaw and B. Weeks, *J. Chem. Soc., Dalton Trans.*, 1979, 1972.

54 A. J. Cheney, W. S. McDonald, K. H. P. O'Flynn, B. L. Shaw and B. L. Turtle, *J. Chem. Soc., Chem. Commun.*, 1973, 128.

55 C. Crocker, R. J. Errington, W. S. McDonald, K. J. Odell, B. L. Shaw and R. J. Goodfellow, *J. Chem. Soc., Chem. Commun.*, 1979, 498.

56 C. Crocker, R. J. Errington, R. Markham, C. J. Moulton, K. J. Odell and B. L. Shaw, *J. Am. Chem. Soc.*, 1980, **102**, 4373.

57 H. D. Empsall, E. M. Hyde, D. Pawson and B. L. Shaw, *J. Chem. Soc., Dalton Trans.*, 1977, 1292.

58 C. E. Jones, B. L. Shaw and B. L. Turtle, *J. Chem. Soc., Dalton Trans.*, 1974, 992.

59 R. Mason, M. Textor, N. A. Al-Salem and B. L. Shaw, *J. Chem. Soc., Chem. Commun.*, 1976, 292.

60 A. J. Cheney, B. E. Mann, B. L. Shaw and R. M. Slade, *J. Chem. Soc., Chem. Commun.*, 1970, 1176.

61 J. C. Chottard, E. Mulliez, J. P. Girault and D. Munsay, *J. Chem. Soc., Chem. Commun.*, 1974, 780.

62 N. W. Alcock, J. M. Brown and J. C. Jeffery, *J. Chem. Soc., Dalton Trans.*, 1977, 588.

63 N. W. Alcock, J. M. Brown and J. C. Jeffery, *J. Chem. Soc., Dalton Trans.*, 1976, 583.

64 A. J. Pryde, B. L. Shaw and B. Weeks, *J. Chem. Soc., Chem. Commun.*, 1973, 947.

65 S. Masamune, G. S. Bates and J. W. Corcoran, *Angew. Chem., Int. Ed. Engl.*, 1977, **16**, 585.

66 C. A. Tolman, *J. Am. Chem. Soc.*, 1970, **92**, 2953.

67 E. C. Alyea, G. Ferguson and A. Somogyvani, *Inorg. Chem.*, 1982, **21**, 1369.

68 G. Ferguson, P. J. Roberts, E. C. Alyea and M. Khan, *Inorg. Chem.*, 1978, **17**, 2965.

69 A. Immirzi and A. Musco, *Inorg. Chim. Acta.*, 1977, **25**, L41.

70 J. D. Smith and J. D. Oliver, *Inorg. Chem.*, 1978, **17**, 2585.

71 T. L. Brown, *Inorg. Chem.*, 1992, **31**, 1286.

72 M.-G. Choi and T. L. Brown, *Inorg. Chim. Acta.*, 1992, **198**, 823.

73 A. Rodger and B. F. G. Johnson, *Inorg. Chim. Acta.*, 1992, **191**, 109.

74 H. C. Clark and M. J. Hampden-Smith, *Coord. Chem. Rev.*, 1987, **79**, 229.

75 D. White and N. J. Coville, *Adv. Organomet. Chem.*, 1994, **36**, 95.

76 W. Strohmeier and F. J. Muller, *Chem. Ber.*, 1967, **100**, 2812.

77 F. A. Cotton and G. Wilkinson, *Advanced Inorganic Chemistry*, Wiley, New York, 1988, p. 64.

78 A. G. Orpen and N. G. Connelly, *J. Chem. Soc., Chem. Commun.*, 1985, 1310.

79 B. J. Dunne, R. B. Morris and A. G. Orpen, *J. Chem. Soc., Dalton Trans.*, 1991, 653.

80 A. T. Hutton, B. Shabanzadeh and B. L. Shaw, *J. Chem. Soc., Chem. Commun.*, 1982, 1345.

81 C. Crocker, H. D. Empsall, R. J. Errington, E. M. Hyde, W. S. McDonald, R. Markham, M. C. Norton, B. L. Shaw and B. Weeks, *J. Chem. Soc., Dalton Trans.*, 1982, 1217.

82 J. R. Briggs, A. G. Constable, W. S. McDonald and B. L. Shaw, *J. Chem. Soc., Dalton Trans.*, 1982, 1225.

83 R. J. Errington, W. S. McDonald and B. L. Shaw, *J. Chem. Soc., Dalton Trans.*, 1982, 1829.

84 C. Crocker, R. J. Errington, R. Markham, C. J. Moulton and B. L. Shaw, *J. Chem. Soc., Dalton Trans.*, 1982, 387.

85 B. L. Shaw, *Advances in Chemistry Series*, 1982, 101.

86 A. R. H. Bottomley, C. Crocker and B. L. Shaw, *J. Organomet. Chem.*, 1983, **250**, 617.

87 K. Jonas and G. Wilke, *Angew. Chem., Int. Ed. Engl.*, 1970, **9**, 312.

88 M. Green, J. A. K. Howard, J. Proud, J. L. Spencer and F. G. A. Stone, *J. Chem. Soc., Chem. Commun.*, 1976, 671.

89 M. Ciriano, M. Green, J. A. K. Howard, J. Proud, J. L. Spencer, F. G. A. Stone and C. A. Tsipis, *J. Chem. Soc., Dalton Trans.*, 1978, 801.

90 T. H. Tulip, T. Yamagata, T. Yoshida, R. D. Wilson, J. A. Ibers and S. Otsuka, *Inorg. Chem.*, 1979, **18**, 2239.

91 P. W. Frost, J. A. K. Howard, J. L. Spencer, D. G. Turner and D. Gregson, *J. Chem. Soc., Chem. Commun.*, 1981, 1104.

92 D. Gregson, J. A. K. Howard, M. Murray and J. L. Spencer, *J. Chem. Soc., Chem. Commun.*, 1981, 716.

93 R. J. Goodfellow, E. M. Hamon, J. A. K. Howard, J. L. Spencer and D. G. Turner, *J. Chem. Soc., Chem. Commun.*, 1984, 1604.

94 M. Brookhart, M. L. H. Green and L.-L. Wong, *Prog. Inorg. Chem.*, 1988, **36**, 1.

95 M. Brookhart and M. L. H. Green, *J. Organomet. Chem.*, 1983, **250**, 395.

96 N. Carr, B. J. Dunne, A. G. Orpen and J. L. Spencer, *J. Chem. Soc., Chem. Commun.*, 1988, 926.

97 N. Carr, B. J. Dunne, L. Mole, A. G. Orpen and J. L. Spencer, *J. Chem. Soc., Dalton Trans.*, 1991, 863.

98 F. M. Conroylewis, L. Mole, A. D. Redhouse, S. A. Litster and J. L. Spencer, *J. Chem. Soc., Chem. Commun.*, 1991, 1601.

99 L. Mole, J. L. Spencer, N. Carr and A. G. Orpen, *Organometallics*, 1991, **10**, 49.

100 J. L. Spencer and G. S. Mhinzi, *J. Chem. Soc., Dalton Trans.*, 1995, 3819.

101 N. Carr, L. Mole, A. G. Orpen and J. L. Spencer, *J. Chem. Soc., Dalton Trans.*, 1992, 2653.

102 L. E. Crascall, S. A. Litster, A. D. Redhouse and J. L. Spencer, *J. Organomet. Chem.*, 1990, **394**, C35.

103 L. E. Crascall and J. L. Spencer, *J. Chem. Soc., Dalton Trans.*, 1992, 3445.

104 L. E. Crascall and J. L. Spencer, *J. Chem. Soc., Dalton Trans.*, 1995, 2391.

105 G. S. Mhinzi, L. E. Crascall and J. L. Spencer, *Inorg. Chim. Acta.*, 1997, **265**, 83.

106 D. J. Schwartz and R. A. Anderson, *J. Am. Chem. Soc.*, 1995, **117**, 4014.

107 M. D. Fryzuk, B. R. Lloyd, G. K. B. Clentsmith and S. J. Rettig, *J. Am. Chem. Soc.*, 1994, **116**, 3804.

108 M. D. Fryzuk, B. R. Lloyd, G. K. B. Clentsmith and S. J. Rettig, *J. Am. Chem. Soc.*, 1991, **113**, 4332.

109 L. Mole, J. L. Spencer, S. A. Litster, A. D. Redhouse, N. Carr and A. G. Orpen, *J. Chem. Soc., Dalton Trans.*, 1996, 2315.

110 M. E. van der Boom, H. B. Kraatz, Y. Ben-David and D. Milstein, *J. Chem. Soc., Chem. Commun.*, 1996, 2167.

111 M. E. van der Boom, H.-B. Kraatz, L. Hassner, Y. Ben-David and D. Milstein, *Organometallics*, 1999, **18**, 3873.

112 M. Gozin, M. Aizenberg, S. Y. Liou, A. Weisman, Y. Ben-David and D. Milstein, *Nature*, 1994, **370**, 42.

113 M. E. van der Boom, S. Y. Liou, L. J. W. Shimon, Y. Ben-David and D. Milstein, *Organometallics*, 1996, **15**, 2562.

114 M. E. van der Boom, J. Ott and D. Milstein, *Organometallics*, 1998, **17**, 4263.

115 M. H. P. Rietveld, D. M. Grove and G. van Koten, *New J. Chem.*, 1997, **21**, 751.

116 M. Gandelman, A. Vigalok, L. J. W. Shimon and D. Milstein, *Organometallics*, 1997, **16**, 3981.

117 M. E. van der Boom, S.-Y. Liou, Y. Ben-David, J. W. Shimon and D. Milstein, *J. Am. Chem. Soc.*, 1998, **120**, 6531.

118 M. E. van der Boom, S. Y. Liou, Y. Ben-David, A. Vigalok and D. Milstein, *Angew. Chem., Int. Ed. Engl.*, 1997, **36**, 625.

119 R. F. Heck, in *Comprehensive Organic Synthesis*, ed. B. M. Trost and I. Fleming, Pergamon Press, Oxford and New York, 1991, vol. 4, p. 833.

120 R. F. Heck, in *Palladium Reagents in Organic Synthesis*, Academic Press, London, 1985.

121 M. Ohff, A. Ohff, M. E. van der Boom and D. Milstein, *J. Am. Chem. Soc.*, 1997, **119**, 11687.

122 J. P. Wolfe, S. Wagaw and S. L. Buchwald, *J. Am. Chem. Soc.*, 1996, **118**, 7215.

123 J. P. Wolfe, S. Wagaw, J.-F. Marcoux and S. L. Buchwald, *Acc. Chem. Res.*, 1998, **31**, 805.

124 A. S. Guram, R. A. Rennels and S. L. Buchwald, *Angew. Chem., Int. Ed. Engl.*, 1995, **34**, 1348.

125 J. Louie and J. F. Hartwig, *Tetrahedron Lett.*, 1995, **36**, 3609.

126 M. S. Driver and J. F. Hartwig, *J. Am. Chem. Soc.*, 1996, **118**, 7217.

127 J. F. Hartwig, *Angew. Chem., Int. Ed. Engl.*, 1998, **37**, 2047.

128 Y. P. Hong, C. H. Senanayake, T. Xiang, C. P. Vandenbossche, G. J. Tanoury, R. P. Bakale and S. A. Wald, *Tetrahedron Lett.*, 1998, **39**, 3121.

129 Y. P. Hong, G. J. Tanoury, H. S. Wilkinson, R. P. Bakale, S. A. Wald and C. H. Senanayake, *Tetrahedron Lett.*, 1997, **38**, 5663.

130 F. E. Goodson and J. F. Hartwig, *Macromolecules*, 1998, **31**, 1700.

131 F. E. Goodson, S. I. Hauck and J. F. Hartwig, *J. Am. Chem. Soc.*, 1999, **121**, 7527.

132 J. P. Sadighi, R. A. Singer and S. L. Buchwald, *J. Am. Chem. Soc.*, 1998, **120**, 4960.

133 G. E. Greco, A. I. Popa and R. R. Schrock, *Organometallics*, 1998, **17**, 5591.

134 J. Louie, F. Paul and J. F. Hartwig, *Organometallics*, 1996, **15**, 2794.

135 M. Kosugi, M. Kameyama and T. Migita, *Chem. Lett.*, 1983, 927.

136 M. Kosugi, M. Kameyama and T. Migita, *Nippon Kagaku Kaishi*, 1985, **3**, 547.

137 A. S. Guram and S. L. Buchwald, *J. Am. Chem. Soc.*, 1994, **116**, 7901.

138 J. F. Hartwig and F. Paul, *J. Am. Chem. Soc.*, 1995, **117**, 5373.

139 B. C. Hamann and J. F. Hartwig, *J. Am. Chem. Soc.*, 1998, **120**, 3694.

140 B. C. Hamann and J. F. Hartwig, *J. Am. Chem. Soc.*, 1998, **120**, 7369.

141 M. Nishiyama, T. Yamamoto and Y. Koie, *Tetrahedron Lett.*, 1998, **39**, 617.

142 J. F. Hartwig, M. Kawatsura, S. I. Hauck, K. H. Shaughnessy and L. M. Alcazar-Roman, *J. Org. Chem.*, 1999, **64**, 5575.

143 M. Kawatsura and J. F. Hartwig, *J. Am. Chem. Soc.*, 1999, **121**, 1473.

144 K. H. Shaughnessy, P. Kim and J. F. Hartwig, *J. Am. Chem. Soc.*, 1999, **121**, 2123.

145 G. Mann, C. Incarvito, A. L. Rheingold and J. F. Hartwig, *J. Am. Chem. Soc.*, 1999, **121**, 3224.

146 T. Satoh, J. Inoh, Y. Kawamura, M. Miura and M. Nomura, *Bull. Chem. Soc. Jpn.*, 1998, **71**, 2239.

147 D. D. Hennings, S. Iwasa and V. H. Rawal, *J. Org. Chem.*, 1997, **62**, 2.

148 T. Satoh, Y. Kawamura, M. Miura and M. Nomura, *Angew. Chem. Int. Ed.*, 1997, **36**, 1740.

149 B. Windmuller, O. Nurnberg, J. Wolf and H. Werner, *European Journal of Inorganic Chemistry*, 1999, 613.

150 H. Werner, J. Wolf, R. Zolk and U. Schubert, *Angew. Chem., Int. Ed. Engl.*, 1983, **22**, 981.

151 J. Wolf, H. Werner, O. Serhadli and M. L. Ziegler, *Angew. Chem., Int. Ed. Engl.*, 1983, **22**, 414.

152 H. Werner, J. Wolf, U. Schubert and K. Ackermann, *J. Organomet. Chem.*, 1983, **243**, C63.

153 H. Werner, J. Wolf and A. Hohn, *J. Organomet. Chem.*, 1985, **287**, 395.

154 F. J. G. Alonso, A. Hohn, J. Wolf, H. Otto and H. Werner, *Angew. Chem., Int. Ed. Engl.*, 1985, **24**, 406.

155 H. Werner, L. Hofmann, J. Wolf and G. Muller, *J. Organomet. Chem.*, 1985, **280**, C55.

156 H. Werner, J. Wolf, U. Schubert and K. Ackermann, *J. Organomet. Chem.*, 1986, **317**, 327.

157 H. Otto, F. J. G. Alonso and H. Werner, *J. Organomet. Chem.*, 1986, **306**, C13.

158 H. Werner, J. Wolf, F. J. G. Alonso, M. L. Ziegler and O. Serhadli, *J. Organomet. Chem.*, 1987, **336**, 397.

159 J. Wolf and H. Werner, *J. Organomet. Chem.*, 1987, **336**, 413.

160 J. Wolf and H. Werner, *Organometallics*, 1987, **6**, 1164.

161 H. Werner, F. J. G. Alonso, H. Otto, K. Peters and H. G. Vonschnering, *Chem. Ber.*, 1988, **121**, 1565.

162 H. Werner, L. Hofmann, W. Paul and U. Schubert, *Organometallics*, 1988, **7**, 1106.

163 A. Hohn and H. Werner, *Chem. Ber.*, 1988, **121**, 881.

164 H. Werner, F. J. G. Alonso, H. Otto and J. Wolf, *Z. Naturforsch., B: Chem. Sci.*, 1988, **43**, 722.

165 J. Wolf, R. Zolk, U. Schubert and H. Werner, *J. Organomet. Chem.*, 1988, **340**, 161.

166 H. Werner, J. Wolf, G. Muller and C. Kruger, *J. Organomet. Chem.*, 1988, **342**, 381.

167 H. Werner, A. Hampp, K. Peters, E. M. Peters, L. Walz and H. G. Vonschnering, *Z. Naturforsch., B: Chem. Sci.*, 1990, **45**, 1548.

168 C. Cauletti, F. Grandinetti, G. Granozzi, M. Casarin, H. Werner, J. Wolf, A. Hohn and F. J. G. Alonso, *J. Organomet. Chem.*, 1990, **382**, 445.

169 U. Brekau and H. Werner, *Organometallics*, 1990, **9**, 1067.

170 M. Schafer, J. Wolf and H. Werner, *J. Chem. Soc., Chem. Commun.*, 1991, 1341.

171 H. Werner, O. Schippel, J. Wolf and M. Schulz, *J. Organomet. Chem.*, 1991, **417**, 149.

172 H. Werner, U. Brekau and M. Dziallas, *J. Organomet. Chem.*, 1991, **406**, 237.

173 T. Rappert, O. Nurnberg, N. Mahr, J. Wolf and H. Werner, *Organometallics*, 1992, **11**, 4156.

174 H. Werner, U. Brekau, O. Nurnberg and B. Zeier, *J. Organomet. Chem.*, 1992, **440**, 389.

175 H. Werner, A. Hampp and B. Windmuller, *J. Organomet. Chem.*, 1992, **435**, 169.

176 T. Dirnberger and H. Werner, *Chem. Ber.*, 1992, **125**, 2007.

201 H. Werner, R. Wiedemann, N. Mahr, P. Steinert and J. Wolf, *Chem. -Eur. J.*, 1996, **2**, 561.

202 R. Wiedemann, J. Wolf and H. Werner, *Chem. Ber.*, 1996, **129**, 29.

203 H. Werner, S. Poelsma, M. E. Schneider, B. Windmuller and D. Barth, *Chem. Ber.*, 1996, **129**, 647.

204 O. Gevert, J. Wolf and H. Werner, *Organometallics*, 1996, **15**, 2806.

205 R. Wiedemann, P. Steinert, O. Gevert and H. Werner, *J. Am. Chem. Soc.*, 1996, **118**, 2495.

206 H. Werner, P. Schwab, E. Bleuel, N. Mahr, P. Steinert and J. Wolf, *Chem. -Eur. J.*, 1997, **3**, 1375.

207 M. Manger, J. Wolf, M. Laubender, M. Teichert, D. Stalke and H. Werner, *Chem. -Eur. J.*, 1997, **3**, 1442.

208 H. Werner, *J. Chem. Soc., Chem. Commun.*, 1997, 903.

209 H. Werner, O. Gevert and P. Haquette, *Organometallics*, 1997, **16**, 803.

210 R. Wiedemann, R. Fleischer, D. Stalke and H. Werner, *Organometallics*, 1997, **16**, 866.

211 H. Werner, M. Bosch, M. E. Schneider, C. Hahn, F. Kukla, M. Manger, B. Windmuller, B. Weberndorfer and M. Laubender, *J. Chem. Soc., Dalton Trans.*, 1998, 3549.

212 H. Werner, M. Manger, M. Laubender, M. Teichert and D. Stalke, *J. Organomet. Chem.*, 1998, **569**, 189.

213 H. Werner, P. Bachmann, M. Laubender and O. Gevert, *Eur. J. Inorg. Chem.*, 1998, 1217.

214 M. Manger, J. Wolf, M. Teichert, D. Stalke and H. Werner, *Organometallics*, 1998, **17**, 3210.

215 I. Kovacik, O. Gevert, H. Werner, M. Schmittel and R. Sollner, *Inorg. Chim. Acta.*, 1998, **276**, 435.

216 E. Bleuel and H. Werner, *C. R. Acad. Sci., Ser. IIc: Chim.*, 1999, **2**, 341.

217 M. Bosch, M. Laubender, B. Weberndorfer and H. Werner, *Chem. -Eur. J.*, 1999, **5**, 2203.

218 J. Wolf, M. Manger, U. Schmidt, G. Fries, D. Barth, B. Weberndorfer, D. A. Vicic, W. D. Jones and H. Werner, *J. Chem. Soc., Dalton Trans.*, 1999, 1867.

219 U. Herber, B. Weberndorfer and H. Werner, *Angew. Chem., Int. Ed. Engl.*, 1999, **38**, 1609.

220 J. GilRubio, B. Weberndorfer and H. Werner, *J. Chem. Soc., Dalton Trans.*, 1999, 1437.

221 H. Werner and A. Hohn, *Z. Naturforsch., B: Chem. Sci.*, 1984, **39**, 1505.

222 H. Werner and A. Hohn, *J. Organomet. Chem.*, 1984, **272**, 105.

223 H. Werner, A. Hohn and M. Dziallas, *Angew. Chem., Int. Ed. Engl.*, 1986, **25**, 1090.

224 H. Werner, T. Dirnberger and A. Hohn, *Chem. Ber.*, 1991, **124**, 1957.

225 H. Werner, A. Hohn and M. Schulz, *J. Chem. Soc., Dalton Trans.*, 1991, 777.

226 M. Schulz and H. Werner, *Organometallics*, 1992, **11**, 2790.

227 M. A. Esteruelas, J. Herrero, A. M. Lopez, L. A. Oro, M. Schulz and H. Werner, *Inorg. Chem.*, 1992, **31**, 4013.

228 M. A. Esteruelas, O. Nurnberg, M. Olivan, L. A. Oro and H. Werner, *Organometallics*, 1993, **12**, 3264.

229 M. A. Esteruelas, A. M. Lopez, L. A. Oro, A. Perez, M. Schulz and H. Werner, *Organometallics*, 1993, **12**, 1823.

230 L. Brandt, J. Wolf and H. Werner, *J. Organomet. Chem.*, 1993, **444**, 235.

231 H. Werner, M. Schulz, M. A. Esteruelas and L. A. Oro, *J. Organomet. Chem.*, 1993, **445**, 261.

232 M. Schulz and H. Werner, *J. Organomet. Chem.*, 1994, **470**, 243.

233 P. Steinert and H. Werner, *Organometallics*, 1994, **13**, 2677.

234 R. W. Lass, P. Steinert, J. Wolf and H. Werner, *Chem. -Eur. J.*, 1996, **2**, 19.

235 P. Steinert and H. Werner, *Chem. Ber.*, 1997, **130**, 1591.

236 K. Ilg and H. Werner, *Organometallics*, 1999, **18**, 5426.

237 E. Sola, J. Navarro, J. A. Lopez, F. J. Lahoz, L. A. Oro and H. Werner, *Organometallics*, 1999, **18**, 3534.

238 D. A. Ortmann, B. Weberndorfer, J. Schoneboom and H. Werner, *Organometallics*, 1999, **18**, 952.

239 A. Albinati, V. I. Bakhmutov, K. G. Caulton, E. Clot, J. Eckert, O. Eisenstein, D. G. Gusev, V. V. Grushin, B. E. Hauger, W. T. Klooster, T. F. Koetzle, R. K. McMullan, T. J. Oloughlin, M. Pelissier, J. S. Ricci, M. P. Sigalas and A. B. Vymenits, *J. Am. Chem. Soc.*, 1993, **115**, 7300.

240 B. Hauger and K. G. Caulton, *J. Organomet. Chem.*, 1993, **450**, 253.

241 B. E. Hauger, D. Gusev and K. G. Caulton, *J. Am. Chem. Soc.*, 1994, **116**, 208.

242 A. C. Cooper and K. G. Caulton, *Inorg. Chim. Acta.*, 1996, **251**, 41.

243 A. C. Cooper, W. E. Streib, O. Eisenstein and K. G. Caulton, *J. Am. Chem. Soc.*, 1997, **119**, 9069.

244 A. C. Cooper, J. C. Huffman and K. G. Caulton, *Organometallics*, 1997, **16**, 1974.

245 A. C. Cooper, K. Folting, J. C. Huffman and K. G. Caulton, *Organometallics*, 1997, **16**, 505.

246 A. C. Cooper and K. G. Caulton, *Inorg. Chem.*, 1998, **37**, 5938.

247 A. C. Cooper, J. C. Bollinger, J. C. Huffman and K. G. Caulton, *New J. Chem.*, 1998, **22**, 473.

248 A. C. Cooper, O. Eisenstein and K. G. Caulton, *New J. Chem.*, 1998, **22**, 307.

249 A. C. Cooper, J. C. Huffman and K. G. Caulton, *Inorg. Chim. Acta.*, 1998, **270**, 261.

250 A. C. Cooper, E. Clot, J. C. Huffman, W. E. Streib, F. Maseras, O. Eisenstein and K. G. Caulton, *J. Am. Chem. Soc.*, 1999, **121**, 97.

251 B. Rybtchinski and D. Milstein, *J. Am. Chem. Soc.*, 1999, **121**, 4258.

252 M. E. vanderBoom, C. L. Higgitt and D. Milstein, *Organometallics*, 1999, **18**, 2413.

253 M. E. vanderBoom, Y. BenDavid and D. Milstein, *J. Am. Chem. Soc.*, 1999, **121**, 6652.

254 A. Vigalok, B. Rybtchinski, L. J. W. Shimon, Y. BenDavid and D. Milstein, *Organometallics*, 1999, **18**, 895.

255 M. E. vanderBoom, S. Y. Liou, Y. BenDavid, M. Gozin and D. Milstein, *J. Am. Chem. Soc.*, 1998, **120**, 13415.

256 A. Vigalok, O. Uzan, L. J. W. Shimon, Y. BenDavid, J. M. L. Martin and D. Milstein, *J. Am. Chem. Soc.*, 1998, **120**, 12539.

257 M. E. vanderBoom, Y. BenDavid and D. Milstein, *J. Chem. Soc., Chem. Commun.*, 1998, 917.

258 S. Y. Lieu, E. Milko and D. Milstein, *J. Chem. Soc., Chem. Commun.*, 1998, 687.

259 A. Vigalok, L. J. W. Shimon and D. Milstein, *J. Am. Chem. Soc.*, 1998, **120**, 477.

260 A. Vigalok, Y. BenDavid and D. Milstein, *Organometallics*, 1996, **15**, 1839.

261 B. Rybtchinski, A. Vigalok, Y. BenDavid and D. Milstein, *J. Am. Chem. Soc.*, 1996, **118**, 12406.

262 A. Vigalok, L. J. W. Shimon and D. Milstein, *J. Chem. Soc., Chem. Commun.*, 1996, 1673.

263 A. Vigalok, H. B. Kraatz, L. Konstantinovsky and D. Milstein, *Chem. -Eur. J.*, 1997, **3**, 253.

264 B. Rybtchinski, Y. BenDavid and D. Milstein, *Organometallics*, 1997, **16**, 3786.

265 B. Rybtchinski and D. Milstein, *Angew. Chem., Int. Ed. Engl.*, 1999, **38**, 870.

266 H. Werner and J. Gotzig, *J. Organomet. Chem.*, 1985, **284**, 73.

267 H. Werner, M. A. Esteruelas and H. Otto, *Organometallics*, 1986, **5**, 2295.

268 M. A. Esteruelas and H. Werner, *J. Organomet. Chem.*, 1986, **303**, 221.

269 M. A. Esteruelas, E. Sola, L. A. Oro, H. Werner and U. Meyer, *J. Mol. Cat.*, 1988, **45**, 1.

270 H. Werner, U. Meyer, M. A. Esteruelas, E. Sola and L. A. Oro, *J. Organomet. Chem.*, 1989, **366**, 187.

271 M. A. Esteruelas, E. Sola, L. A. Oro, H. Werner and U. Meyer, *J. Mol. Cat.*, 1989, **53**, 43.

272 M. A. Esteruelas, M. P. Garcia, A. M. Lopez, L. A. Oro, N. Ruiz, C. Schlunken, C. Valero and H. Werner, *Inorg. Chem.*, 1992, **31**, 5580.

273 H. Werner, T. Daniel, W. Knaup and O. Nurnberg, *J. Organomet. Chem.*, 1993, **462**, 309.

274 M. A. Tena, O. Nurnberg and H. Werner, *Chem. Ber.*, 1993, **126**, 1597.

275 J. Bank, O. Gevert, W. Wolfsberger and H. Werner, *Organometallics*, 1995, **14**, 4972.

276 T. Braun, O. Gevert and H. Werner, *J. Am. Chem. Soc.*, 1995, **117**, 7291.

277 H. Werner, M. A. Tena, N. Mahr, K. Peters and H. G. Vonschnering, *Chem. Ber.*, 1995, **128**, 41.

278 T. Braun, P. Steinert and H. Werner, *J. Organomet. Chem.*, 1995, **488**, 169.

279 R. Flugel, B. Windmuller, O. Gevert and H. Werner, *Chem. Ber.*, 1996, **129**, 1007.

280 J. Bank, P. Steinert, B. Windmuller, W. Wolfsberger and H. Werner, *J. Chem. Soc., Dalton Trans.*, 1996, 1153.

281 C. Grunwald, O. Gevert, J. Wolf, P. GonzalezHerrero and H. Werner, *Organometallics*, 1996, **15**, 1960.

282 M. Martin, O. Gevert and H. Werner, *J. Chem. Soc., Dalton Trans.*, 1996, 2275.

283 W. Stuer, J. Wolf, H. Werner, P. Schwab and M. Schulz, *Angew. Chem., Int. Ed. Engl.*, 1998, **37**, 3421.

284 J. Wolf, W. Stuer, C. Grunwald, O. Gevert, M. Laubender and H. Werner, *Eur. J. Inorg. Chem.*, 1998, 1827.

285 J. Wolf, W. Stuer, C. Grunwald, H. Werner, P. Schwab and M. Schulz, *Angew. Chem., Int. Ed. Engl.*, 1998, **37**, 1124.

286 H. Werner, J. Bank, P. Steinert and W. Wolfsberger, *Z. Anorg. Allg. Chem.*, 1999, **625**, 2178.

287 H. Werner, W. Stuer, B. Weberndorfer and J. Wolf, *Eur. J. Inorg. Chem.*, 1999, 1707.

288 J. N. Coalter, J. C. Bollinger, J. C. Huffman, U. WernerZwanziger, K. G. Caulton, E. R. Davidson, H. Gerard, E. Clot and O. Eisenstein, *New J. Chem.*, 2000, **24**, 9.

289 M. A. Esteruelas, E. Sola, L. A. Oro, U. Meyer and H. Werner, *Angew. Chem., Int. Ed. Engl.*, 1988, **27**, 1563.

290 A. Andriollo, M. A. Esteruelas, U. Meyer, L. A. Oro, R. A. Sanchezdelgado, E. Sola, C. Valero and H. Werner, *J. Am. Chem. Soc.*, 1989, **111**, 7431.

291 K. Roder and H. Werner, *J. Organomet. Chem.*, 1989, **367**, 321.

292 H. Werner, R. Weinand, W. Knaup, K. Peters and H. G. Vonschnering, *Organometallics*, 1991, **10**, 3967.

293 H. Werner, W. Knaup and M. Schulz, *Chem. Ber.*, 1991, **124**, 1121.

294 H. Werner, S. Stahl and W. Kohlmann, *J. Organomet. Chem.*, 1991, **409**, 285.

295 H. Werner, A. Michenfelder and M. Schulz, *Angew. Chem., Int. Ed. Engl.*, 1991, **30**, 596.

296 W. Knaup and H. Werner, *J. Organomet. Chem.*, 1991, **411**, 471.

297 M. Aracama, M. A. Esteruelas, F. J. Lahoz, J. A. Lopez, U. Meyer, L. A. Oro and H. Werner, *Inorg. Chem.*, 1991, **30**, 288.

298 M. A. Esteruelas, C. Valero, L. A. Oro, U. Meyer and H. Werner, *Inorg. Chem.*, 1991, **30**, 1159.

299 T. Daniel and H. Werner, *Z. Naturforsch., B: Chem. Sci.*, 1992, **47**, 1707.

300 H. Werner, B. Weber, O. Nurnberg and J. Wolf, *Angew. Chem., Int. Ed. Engl.*, 1992, **31**, 1025.

301 M. A. Esteruelas, F. J. Lahoz, J. A. Lopez, L. A. Oro, C. Schlunken, C. Valero and H. Werner, *Organometallics*, 1992, **11**, 2034.

302 C. Schlunken and H. Werner, *J. Organomet. Chem.*, 1993, **454**, 243.

303 T. Daniel, N. Mahr and H. Werner, *Chem. Ber.*, 1993, **126**, 1403.

304 B. Weber, P. Steinert, B. Windmuller, J. Wolf and H. Werner, *J. Chem. Soc., Chem. Commun.*, 1994, 2595.

305 H. Werner, T. Daniel, T. Braun and O. Nurnberg, *J. Organomet. Chem.*, 1994, **480**, 145.

306 T. Daniel and H. Werner, *J. Chem. Soc., Dalton Trans.*, 1994, 221.

307 H. Werner, G. Henig, U. Wecker, N. Mahr, K. Peters and H. G. vonSchnering, *Chem. Ber.*, 1995, **128**, 1175.

308 H. Werner, R. Flugel, B. Windmuller, A. Michenfelder and J. Wolf, *Organometallics*, 1995, **14**, 612.

309 H. Werner, T. Daniel, M. Muller and N. Mahr, *J. Organomet. Chem.*, 1996, **512**, 197.

310 H. Werner, W. Stuer, M. Laubender, C. Lehmann and R. HerbstIrmer, *Organometallics*, 1997, **16**, 2236.

311 G. Henig and H. Werner, *Z. Naturforsch., B: Chem. Sci.*, 1998, **53**, 540.

312 H. Werner, W. Stuer, J. Wolf, M. Laubender, B. Weberndorfer, R. HerbstIrmer and C. Lehmann, *Eur. J. Inorg. Chem.*, 1999, 1889.

313 H. Werner, S. Jung, B. Weberndorfer and J. Wolf, *Eur. J. Inorg. Chem.*, 1999, 951.

314 H. Werner, G. Henig, B. Windmuller, O. Gevert, C. Lehmann and R. HerbstIrmer, *Organometallics*, 1999, **18**, 1185.

315 J. T. Poulton, K. Folting, W. E. Streib and K. G. Caulton, *Inorg. Chem.*, 1992, **31**, 3190.

316 R. H. Heyn, J. C. Huffman and K. G. Caulton, *New J. Chem.*, 1993, **17**, 797.

317 J. T. Poulton, M. P. Sigalas, O. Eisenstein and K. G. Caulton, *Inorg. Chem.*, 1993, **32**, 5490.

318 T. J. Johnson, P. S. Coan and K. G. Caulton, *Inorg. Chem.*, 1993, **32**, 4594.

319 W. E. Streib, A. A. Zlota and K. G. Caulton, *Bulletin of the Polish Academy of Sciences-Chemistry*, 1994, **42**, 197.

320 J. T. Poulton, M. P. Sigalas, K. Folting, W. E. Streib, O. Eisenstein and K. G. Caulton, *Inorg. Chem.*, 1994, **33**, 1476.

321 J. T. Poulton, B. E. Hauger, R. L. Kuhlman and K. G. Caulton, *Inorg. Chem.*, 1994, **33**, 3325.

322 M. Ogasawara, S. A. Macgregor, W. E. Streib, K. Folting, O. Eisenstein and K. G. Caulton, *J. Am. Chem. Soc.*, 1995, **117**, 8869.

323 T. J. Johnson, K. Folting, W. E. Streib, J. D. Martin, J. C. Huffman, S. A. Jackson, O. Eisenstein and K. G. Caulton, *Inorg. Chem.*, 1995, **34**, 488.

324 A. Pedersen, M. Tilset, K. Folting and K. G. Caulton, *Organometallics*, 1995, **14**, 875.

325 J. U. Notheis, R. H. Heyn and K. G. Caulton, *Inorg. Chim. Acta.*, 1995, **229**, 187.

326 M. Ogasawara, F. Maseras, N. Gallego-Planas, W. E. Streib, O. Eisenstein and K. G. Caulton, *Inorg. Chem.*, 1996, **35**, 7468.

327 M. Ogasawara, S. A. Macgregor, W. E. Streib, K. Folting, O. Eisenstein and K. G. Caulton, *J. Am. Chem. Soc.*, 1996, **118**, 10189.

328 D. G. Gusev, T. T. Nadasdi and K. G. Caulton, *Inorg. Chem.*, 1996, **35**, 6772.

329 C. B. Li, M. Ogasawara, S. P. Nolan and K. G. Caulton, *Organometallics*, 1996, **15**, 4900.

330 D. J. Huang, K. Folting and K. G. Caulton, *Inorg. Chem.*, 1996, **35**, 7035.

331 D. J. Huang, W. E. Streib, O. Eisenstein and K. G. Caulton, *Angew. Chem., Int. Ed. Engl.*, 1997, **36**, 2004.

332 R. H. Heyn, S. A. Macgregor, T. T. Nadasdi, M. Ogasawara, O. Eisenstein and K. G. Caulton, *Inorg. Chim. Acta.*, 1997, **259**, 5.

333 D. J. Huang, J. C. Huffman, J. C. Bollinger, O. Eisenstein and K. G. Caulton, *J. Am. Chem. Soc.*, 1997, **119**, 7398.

334 M. Olivan, A. V. Marchenko, J. N. Coalter and K. G. Caulton, *J. Am. Chem. Soc.*, 1997, **119**, 8389.

335 M. Ogasawara, D. J. Huang, W. E. Streib, J. C. Huffman, N. Gallego-Planas, F. Maseras, O. Eisenstein and K. G. Caulton, *J. Am. Chem. Soc.*, 1997, **119**, 8642.

336 C. B. Li, M. Olivan, S. P. Nolan and K. G. Caulton, *Organometallics*, 1997, **16**, 4223.

337 M. Olivan and K. G. Caulton, *J. Chem. Soc., Chem. Commun.*, 1997, 1733.

338 M. Ogasawara, F. Maseras, N. Gallego-Planas, K. Kawamura, K. Ito, K. Toyota, W. E. Streib, S. Komiya, O. Eisenstein and K. G. Caulton, *Organometallics*, 1997, **16**, 1979.

339 M. Olivan, O. Eisenstein and K. G. Caulton, *Organometallics*, 1997, **16**, 2227.

340 D. J. Huang, R. H. Heyn, J. C. Bollinger and K. G. Caulton, *Organometallics*, 1997, **16**, 292.

341 D. Huang, G. J. Spivak and K. G. Caulton, *New J. Chem.*, 1998, **22**, 1023.

342 D. J. Huang, M. Olivan, J. C. Huffman, O. Eisenstein and K. G. Caulton, *Organometallics*, 1998, **17**, 4700.

343 J. N. Coalter, G. J. Spivak, H. Gerard, E. Clot, E. R. Davidson, O. Eisenstein and K. G. Caulton, *J. Am. Chem. Soc.*, 1998, **120**, 9388.

344 M. Olivan, E. Clot, O. Eisenstein and K. G. Caulton, *Organometallics*, 1998, **17**, 3091.

345 M. Olivan, E. Clot, O. Eisenstein and K. G. Caulton, *Organometallics*, 1998, **17**, 897.

346 D. J. Huang, H. Gerard, E. Clot, V. Young, W. E. Streib, O. Eisenstein and K. G. Caulton, *Organometallics*, 1999, **18**, 5441.

347 D. J. Huang, K. Folting and K. G. Caulton, *J. Am. Chem. Soc.*, 1999, **121**, 10318.

348 T. Gottschalk-Gaudig, K. Folting and K. G. Caulton, *Inorg. Chem.*, 1999, **38**, 5241.

349 D. J. Huang, W. E. Streib, J. C. Bollinger, K. G. Caulton, R. F. Winter and T. Scheiring, *J. Am. Chem. Soc.*, 1999, **121**, 8087.

350 T. GottschalkGaudig, J. C. Huffman, K. G. Caulton, H. Gerard and O. Eisenstein, *J. Am. Chem. Soc.*, 1999, **121**, 3242.

351 M. Olivan and K. G. Caulton, *Inorg. Chem.*, 1999, **38**, 566.

352 K. T. Smith, M. Tilset, R. Kuhlman and K. G. Caulton, *J. Am. Chem. Soc.*, 1995, **117**, 9473.

353 R. Kuhlman, W. E. Streib and K. G. Caulton, *Inorg. Chem.*, 1995, **34**, 1788.

354 D. G. Gusev, R. Kuhlman, J. R. Rambo, H. Berke, O. Eisenstein and K. G. Caulton, *J. Am. Chem. Soc.*, 1995, **117**, 281.

355 D. G. Gusev, R. L. Kuhlman, K. B. Renkema, O. Eisenstein and K. G. Caulton, *Inorg. Chem.*, 1996, **35**, 6775.

356 R. Kuhlman, W. E. Streib, J. C. Huffman and K. G. Caulton, *J. Am. Chem. Soc.*, 1996, **118**, 6934.

357 R. Kuhlman, E. Clot, C. Leforestier, W. E. Streib, O. Eisenstein and K. G. Caulton, *J. Am. Chem. Soc.*, 1997, **119**, 10153.

358 R. Kuhlman, D. G. Gusev, I. L. Eremenko, H. Berke, J. C. Huffman and K. G. Caulton, *J. Organomet. Chem.*, 1997, **536**, 139.

359 D. V. Yandulov, K. G. Caulton, N. V. Belkova, E. S. Shubina, L. M. Epstein, D. V. Khoroshun, D. G. Musaev and K. Morokuma, *J. Am. Chem. Soc.*, 1998, **120**, 12553.

360 G. J. Spivak and K. G. Caulton, *Organometallics*, 1998, **17**, 5260.

361 D. V. Yandulov, W. E. Streib and K. G. Caulton, *Inorg. Chim. Acta.*, 1998, **280**, 125.

362 G. J. Spivak, J. N. Coalter, M. Olivan, O. Eisenstein and K. G. Caulton, *Organometallics*, 1998, **17**, 999.

363 K. B. Renkema, R. Bosque, W. E. Streib, F. Maseras, O. Eisenstein and K. G. Caulton, *J. Am. Chem. Soc.*, 1999, **121**, 10895.

364 K. B. Renkema and K. G. Caulton, *New J. Chem.*, 1999, **23**, 1027.

365 K. B. Renkema, J. C. Huffman and K. G. Caulton, *Polyhedron*, 1999, **18**, 2575.

366 J. Espuelas, M. A. Esteruelas, F. J. Lahoz, L. A. Oro and C. Valero, *Organometallics*, 1993, **12**, 663.

367 M. P. Garcia, A. M. Lopez, M. A. Esteruelas, F. J. Lahoz and L. A. Oro, *J. Organomet. Chem.*, 1990, **388**, 365.

368 M. A. Esteruelas, M. P. Garcia, A. M. Lopez and L. A. Oro, *Organometallics*, 1991, **10**, 127.

369 M. A. Esteruelas, M. P. Garcia, A. M. Lopez and L. A. Oro, *Organometallics*, 1992, **11**, 702.

370 M. A. Esteruelas, L. A. Oro and C. Valero, *Organometallics*, 1991, **10**, 462.

371 C. Bianchini, A. Meli, M. Peruzzini, P. Frediani, C. Bohanna and M. A. Esteruelas, *Organometallics*, 1992, **11**, 138.

372 K. B. Renkema, M. Ogasawara, W. E. Streib, J. C. Huffman and K. G. Caulton, *Inorg. Chim. Acta.*, 1999, **291**, 226.

373 M. Epstein and S. A. Buckler, *J. Am. Chem. Soc.*, 1961, **83**, 3279.

374 M. Epstein and S. A. Buckler, *U.S. Pat.* 3 050 531, 1962, to American Cyanamid Co.

375 V. Gee, Ph.D. Thesis, University of Bristol, 1997.

376 J. H. Downing, Ph.D. Thesis, University of Bristol, 1992.

377 V. Gee, A. G. Orpen, H. Phetmung, P. G. Pringle and R. I. Pugh, *J. Chem. Soc., Chem. Commun.*, 1999, 901.

378 G. Bekiaris, E. Lork, W. Offermann and G. V. Roschenthaler, *Chem. Ber.*, 1997, **130**, 1547.

379 G. Bekiaris and G. V. Roschenthaler, *Heteroat. Chem.*, 1998, **9**, 173.

380 O. Casher, D. O'Hagan, R. C. A., H. S. Rzepa and N. A. Zaidi, *J. Chem. Soc., Chem. Commun.*, 1993, 1337.

381 M. Harada, Y. Kai, N. Yasuoka and N. Kasai, *Bull. Chem. Soc. Jpn.*, 1979, **52**, 390.

382 P. H. M. Budzelaar, E. Drent and P. G. Pringle, *Eur. Pat.* 97 302 079, 1996, to Shell

383 J. C. L. J. Suykerbuyk, E. Drent and P. G. Pringle, *World Pat.* 42 717, 1997, to Shell

384 P. G. Pringle, D. G. Brewin, M. B. Smith and K. Worboys, in *Aqueous Organometallic Chemistry and Catalysis*, Exxon Research and Engineering Co., Netherlands, 1995, p. 111.

385 C. N. Robinson and R. C. Lewis, *J. Heterocyclic Chem.*, 1973, **10**, 395.

386 E. P. Kyba, S.-T. Liu and R. L. Harris, *Organometallics*, 1983, **2**, 1877.

387 K. Bourumeau, A.-C. Gaumont and J.-M. Denis, *J. Organomet. Chem.*, 1997, **529**, 205.

388 M. J. Burk and M. F. Gross, *Tetrahedron Lett.*, 1994, **35**, 4963.

389 K. L. Mason, Ph.D. Thesis, University of Bristol, 1997.

390 M. D. Rausch and C. J. Ciappenelli, *J. Organomet. Chem.*, 1967, **10**, 127.

391 N. Weferling, *Z. anorg. allg. chem.*, 1987, **548**, 55.

392 H. Goldwhite and B. C. Saunders, *J. Chem. Soc.*, 1955, 2040.

393 V. G. Gee and P. G. Pringle, *unpublished results*.

394 W. H. Pirkle and D. J. Hoover, *Top. Stereochem.*, 1982, **13**, 263.

395 S. Otsuka, A. Nakamura, T. Kano and K. Tani, *J. Am. Chem. Soc.*, 1971, **93**, 4301.

396 S. B. Wild, *Coord. Chem. Rev.*, 1997, **166**, 291.

397 E. Drent, *Pure Appl. Chem.*, 1990, **62**, 661.

398 E. Drent, *UK Pat.* 2 183 631, 1985, to Shell

399 E. Drent, *Eur. Pat.* 220 767, 1985, to Shell

400 E. Drent and P. H. M. Budzelaar, *J. Organomet. Chem.*, 2000, **593-594**, 211.

401 F. Garbassi, A. Sommazzi, L. Meda, G. Mestroni and A. Sciutto, *Polymer*, 1998, **39**, 1503.

402 E. Drent and P. H. M. Budzelaar, *Chem. Rev.*, 1996, **96**, 663.

403 E. Drent, in *Applied Homogeneous Catalysis with Organometallic Compounds*, ed. B. Cornils and W. A. Herman, VCH, New York, 1996.

404 G. R. Eastham, B. T. Heaton, J. A. Iggo, R. P. Tooze, R. Whyman and S. Zacchini, *J. Chem. Soc., Chem. Commun.*, 2000, 609.

405 Y. Koide, S. G. Bott and A. R. Barron, *Organometallics*, 1996, **15**, 2213.

406 W. G. Reman, G. B. J. De Boer, S. A. J. Van Langen and A. Nahuijsen, *Eur. Pat.* 411 721, 1989, to Shell

407 P. W. Mul and J. F. K. Buijink, *unpublished results*.

408 E. Drent, P. G. Pringle and R. I. Pugh, *patent pending*.

409 R. H. Mitchell and F. Sondheimer, *Tetrahedron*, 1968, **24**, 1397.

410 R. E. Beyler and L. H. Sarrett, *J. Am. Chem. Soc.*, 1952, **74**, 1411.

411 K. Moedritzer and R. R. Irani, *J. Inorg. Nucl. Chem.*, 1961, **22**, 297.

412 L. Maier, *Helv. Chim. Acta*, 1966, **49**, 842.

413 J. X. Dermott, J. F. White and G. M. Whitesides, *J. Am. Chem. Soc.*, 1976, **98**, 6521.

414 E. G. Cox, H. Saenger and W. Warplaw, *J. Chem. Soc.*, 1934, 182.

415 L. E. Crascall and J. L. Spencer, *Inorg. Synth.*, 1990, **28**, 126.

416 M. S. Kharasch, R. C. Seyler and F. R. Mayo, *J. Am. Chem. Soc.*, 1938, **60**, 882.

417 R. Cramer, *Inorg. Synth.*, 1979, **19**, 218.

418 R. Uson, A. Laguna and J. Vicente, *J. Organomet. Chem.*, 1977, **131**, 471.